Hungarian University of Agriculture and Life Sciences

Institute of Food Science and Technology

Department of Food Chemistry and Analysis

Doctoral (PhD) thesis

METABOLOMIC PROFILING OF MEDICINAL PLANTS AND RELATED FOOD PRODUCTS USING COUPLED MASS SPECTROMETRY METHODS

Katalin Nagy

Budapest

2026

Doctoral School:

Name: Doctoral School of Agricultural and Food Sciences

Discipline: Food Science

Head of Doctoral School: Dr. Melinda Kovács
Professor, PhD
MATE, Institute of Physiology and Nutrition

Supervisors: Dr. Zsuzsanna Jókai-Szatura
Associate professor, PhD
MATE, Institute of Food Science and Technology
Department of Food Chemistry and Analysis

Dr. Tibor Janda
Scientific advisor, DSc
HUN-REN Centre for Agricultural Research
Agricultural Institute
Department of Plant Physiology and Metabolomics

.....	.....	.....
Approval of the Head of School	Approval of Supervisor	Approval of Supervisor

TABLE OF CONTENTS

LIST OF ABBREVIATIONS

ANN	artificial neural network
ANOVA	analysis of variance
CE	capillary electrophoresis
CCS	collision cross section
DAD	diode array detector
DW	dry weight
EEA	European Economic Area
EMA	European Medicines Agency
FI-ICR	Fourier transform ion cyclotron resonance
FLD	fluorescence detector
FW	fresh weight
GC/GLC	gas chromatography/ gas liquid chromatography
HACCP	Hazard Analysis and Critical Control Points
HMPC	Committee on Herbal Medicinal Products
HPLC	high-performance liquid chromatography
HPTLC	high-performance thin-layer chromatography
HR	high resolution
IMS	ion mobility spectrometry
LED	light-emitting diode
LOD	limit of detection
LOQ	limit of quantification
MS	mass spectrometry
NCI	National Cancer Institute
NMR	nuclear magnetic resonance spectroscopy
PC	paper chromatography
PCA	principal component analysis
PLS-DA	partial least squares discriminant analysis
PPFD	photosynthetic photon flux density
R_F	retention factor
S/N	signal-to-noise ratio
TIC	total ion chromatogram
TLC	thin layer chromatography
UPLC-ESI-IMS-QTOF-MS	ultrahigh-performance liquid chromatography coupled with electrospray ionization ion mobility spectrometry quadrupole time-of-flight mass spectrometry
UV	ultraviolet radiation
VIP	variable importance of projection
WHO	World Health Organization

1. INTRODUCTION

Only about 69,000 of the more than 391,000 plant species that exist worldwide have been the focus of scientific research (Kattge et al., 2011; RBG Kew, 2016). Plants produce a broad range of secondary metabolites in addition to the basic metabolic pathways necessary for growth and development. The synthesis of secondary bioactive molecules may seem random from a phylogenetic standpoint, but these metabolites have prominent and distinct roles that we might have not been precisely aware of yet. Generally, these compounds are important for defense mechanisms, pollinator and seed disperser attraction, and interspecies communication, even though they are not necessary for the plant's fundamental physiological processes. For instance, flavonoids function as antioxidants that reduce photooxidative stress (Fini et al., 2011), terpenoids are involved in signaling (Rider et al., 2005) and allelopathic interactions (Fernandez et al., 2016; Fischer et al., 1994), and alkaloids offer chemical defenses against pathogens and herbivores (Adler and Kittelson, 2004; Baldwin, 1988; Manson et al., 2010). Many of these secondary metabolites are bioactive compounds that have toxicological or pharmacological impacts on both humans and animals. Bioactive plant compounds can affect health when ingested or absorbed through the skin, although they are not necessary for nutrition like vitamins and minerals are.

Scientific knowledge of the connection between diet and health has progressed dramatically over the last forty years. It is now clear that diet affects almost all physiological systems, including fetal development, gene expression, hormone regulation, and long-term disease risk, whereas nutrition research previously concentrated mostly on preventing deficiency diseases through essential nutrients (Gupta and Gupta, 2014). The health impacts of dietary toxins and non-nutrient bioactive substances are also being highlighted by growing data. Thus, the idea that "we are what we eat" is supported by contemporary nutritional science, which emphasizes the necessity of identification and characterization the actual plant-derived compounds that cause physiological and biological effects. The distinction between nutrition and medicine has become hazier as interest in the medicinal potential of bioactive plant compounds has grown. More than 100 plant-based compounds have been shown to have potential medical uses (Wilson, 1988), many of them have their roots in traditional medicine. Powders or extracts from medicinal plants were historically the main active ingredients in pharmaceutical medicines until the early 20th century (Bernhoft, 2010). Moreover, special attention should be paid to the Traditional Chinese Medicines with more than 20,000 ingredients listed, most of which are plant derived (Zhang et al., 2022).

For a large portion of the world's population, traditional medicine is still the mainstay of healthcare. The World Health Organization (WHO) reports that about 80% of the world's

population, especially in developing nations, still rely on plant-based medicines for their primary healthcare needs, and that about 25% of all medical prescriptions are based on substances derived from plants or their synthetic analogues (Gurib-Fakim, 2006). This persistent reliance underscores the medicinal plants' cultural and historical significance as well as their ongoing value as sources of pharmacologically active chemicals in contemporary medicine.

The considerable variation in plant quality makes it difficult to manage the quality of raw plant materials and the products that are developed from them. Many nations have put in place mechanisms to control the quality of herbal medicines in order to address this problem. Legally permitted medications must pass identification and purity tests, include standardized amounts of important bioactive ingredients, and adhere to microbiological safety and plant conservation regulations. Establishing unambiguous rules and regulations is crucial, and national and international organizations like the EMA (European Medicines Agency, 2010) and WHO (World Health Organization, 2007) are currently working on developing a common set of rules. The Committee on Herbal Medicinal Products (HMPC) was established in 2004 under Directive 2001/83/EC, as amended by Directive 2004/24/EC (European Parliament & Council, 2004a). Its primary function is to develop community herbal monographs and documentation supporting the inclusion of traditional herbal medicinal products on the community list, which is formally adopted by the European Commission. While community monographs are not legally binding, they must be taken into account during product registration. In contrast, the community list is binding across EU and EEA (European Economic Area) member states, granting automatic registration to compliant traditional herbal medicines that meet established quality standards. Also, Directive 2004/24/EC stipulates that products should comply with quality standards in relevant European Pharmacopoeia monographs or those in the pharmacopoeia of a Member State.

Herbal plant quality issues also come into play when we consider herbs as food ingredients. In this case, Regulation (EC) No 178/2002 (the General Food Law) (European Parliament & Council, 2002), and Regulation (EC) No 852/2004 on the hygiene of foodstuffs (European Parliament & Council, 2004b) serve as the main legal basis. The former regulation mandates that all food put on the market be safe and that traceability be established, and the latter requires food business operators to put in place, also implement and maintain procedures based on the principles of Hazard Analysis and Critical Control Points (HACCP) (Codex Alimentarius Commission, 2003). The HACCP system should be modified to account for the unique risks and properties of plant raw materials when employing herbs as food components.

The natural consequence of complying with these regulations and also to meet the consumer’s demand in food properties must be the standardization of plant cultivation conditions in order to

ensure consistent raw material quality. This task is exponentially more difficult in the case of plants that are harvested in the wild, which is true of most of our medicinal plants. At the same time, even with adequate quality assurance, thousands of secondary metabolites can be present in plants in a wide range of concentrations and with a wide range of chemical properties, that can also be altered with different production technologies, making any qualitative or quantitative analysis of them a challenge for analysts.

In this current work I attempted to investigate the qualitative and quantitative composition of various medicinal plants, contributing to further scientifically based decisions on the use of these plants. Furthermore, I attempted to improve both the quality of the plant material and the production technology used to manufacture a plant derived beverage product.

2. AIMS

The population may have different attitudes towards medicinal plants: they may regard them as a food source or as medicine. However, regardless of their use, there is a common need for more accurate knowledge about the composition of medicinal plants and plant-based products, the consequences of the effects to which the plants are exposed, and the results of the production technology used.

In my research, the first aim was to find cultivation/lighting conditions that increase the yield of high-value chemicals by examining how LED light spectrum alterations impact the metabolic profile of a medicinal plant (Ouzounis et al., 2015; Zhiponova et al., 2025). The target species was *Catharanthus roseus* (Madagascar periwinkle), which is an important herb historically and medicinally as well, since it contains indole alkaloids used in cancer treatment (Goswami et al., 2024). I used targeted and untargeted metabolomics approaches (using ultrahigh-performance liquid chromatography coupled with electrospray ionization ion mobility spectrometry quadrupole time-of-flight mass spectrometry, or UPLC-ESI-IMS-QTOF-MS), in order to measure and compare the accumulation of pharmaceutically valuable alkaloids (particularly dimer alkaloids like vinblastine and vincristine) and related metabolites in the leaves of the plant when grown under various LED light compositions.

My second aim was to conduct metabolomic fingerprinting during a food production technology which uses a medicinal plant. For this purpose, I chose *Taraxacum officinale* (dandelion) and the marketed liqueur product that is made from the flowers of the plant. Since dandelion is consumed in a variety of ways, including as an edible plant and herb, its composition is significant from both a plant biological and nutritional perspective. In addition, during the development of the analytical methods (Brezo-Borjan and Švarc-Gajić, 2024; Khan et al., 2018), the volume of material obtained from the plant had to be maximized in order to achieve the highest possible concentration of the final extracts (Chen et al., 2020; Liu et al., 2020). The actual objectives were to learn more about the secondary metabolites contained in dandelion plants and to investigate how their metabolomic profile varies in a liqueur made from dandelion flowers. Additionally, we made an effort to monitor the changes that took place throughout the liqueur's maturation process.

3. LITERATURE OVERVIEW

3.1. Metabolomics approaches on the characterization of medicinal plants and derived products

It is noteworthy that despite the enormous progress made in the field of phytochemistry, only a relatively small proportion of the plant world has been subjected to thorough chemical analysis. Prior to the 1990s, the majority of therapeutic candidates came from natural sources; however, synthetic compounds have gained prominence since then.

Phytochemistry, often known as plant chemistry, has emerged as a separate field that is closely related to both plant biochemistry and natural product organic chemistry. It addresses the vast array of organic compounds that plants biosynthesize or uptake, as well as their chemical structures, biosynthesis, turnover, metabolism, their natural distribution and biological role. Techniques for separating, purifying, and identifying the numerous compounds found in plants are required to implement the processes mentioned above. Therefore, the effective application of established protocols and the continuous development of new methods to address emerging unresolved issues are closely linked to the advancement of our knowledge of phytochemistry. The limited amount of test material that can be obtained from medicinal plants in some cases, on which the above-mentioned test steps must be performed, also poses a major challenge for researchers.

The development of quick, reproducible, and robust methods to screen plants for specific compounds, primarily using chromatographic techniques, has greatly aided phytochemical advancement. According to Harborne (1984), the separation and purification of plant constituents is mainly carried out using one or other, or a combination, of four chromatographic techniques: paper chromatography (PC), thin layer chromatography (TLC), gas liquid chromatography (GLC) and high performance liquid chromatography (HPLC). Over the past forty years, the available techniques have expanded and refined, and the role of PC and TLC has also changed. PC has become almost completely obsolete; according to the Scopus database, 63% of the publications regarding the topic were published between 1965 and 1975. TLC is now used mainly in preparative laboratories for rapid testing, with its automated and high-performance version playing a relatively minor role in analytics (HPTLC) (Kowalska and Sajewicz, 2022). Currently, a number of integrated technologies and methodologies (with or without a hyphenation to chromatography), such as non-destructive NMR (nuclear magnetic resonance spectroscopy), mass spectrometry (MS) based techniques like GC–MS (gas chromatography–MS), LC–MS (liquid chromatography–MS), CE–MS (capillary electrophoresis–MS), and FI-ICR–MS (Fourier transform ion cyclotron

resonance–MS), enable large-scale analysis of highly complex mixtures (Hong et al., 2016). However, the basic principle still applies today: the choice of technique depends largely on the general purpose of the analysis ("fit-for-purpose"), the financial limitations ("value-for-money"), the sample preparation chosen for the set of metabolites to be screened, the solubility properties and the volatility of the compounds to be separated (if applicable).

Previously, the identification of plant components used to be based on traditional qualitative analytical tools. Once a plant compound has been extracted and purified, it was vital to define the chemical class it belongs to before determining which specific substance it is. The compound's response to color tests, solubility, R_F (retention factor) characteristics on PC or TLC, and UV spectral features typically revealed its class. Additionally, biochemical studies could also be very helpful. Plant compounds should be accurately identified by measuring their physical and spectral characteristics and comparing the results with known information. Initial identification data were provided by physical characteristics such R_F values, melting and boiling points, and optical rotation. Spectral analyses, such as UV, IR, NMR, and later on, MS spectroscopy, provided more conclusive characterization (Shriner et al., 2004). When authentic reference materials were available, identification was verified by direct comparison; if not, literature data may have been utilized. In most cases, complete characterization of new compounds could be accomplished by combining these physical and spectral datasets.

Since its increasingly widespread introduction in the 1960s, mass spectrometry has developed into a key method in the study of natural products because of its great sensitivity and capacity for identification and quantification (McLafferty, 2011). Since the introduction of the first high resolution (HR) quadrupole time-of-flight (QTOF) devices during the late 1990's, it could also offer precise molecular mass measurement and distinctive fragmentation patterns that support compound identification with just microgram amounts of sample (Chernushevich et al., 2001). The high accuracy of modern, HR-MS instruments [that could be linked to the merchandising of the first Orbitrap and internal mass calibration assisted QTOF mass spectrometers in 2005 (Eliuk and Makarov, 2015)] has enabled the determination of a compound's exact molecular formula, rendering traditional elemental analysis largely unnecessary. The implementation of the ion mobility spectrometry (IMS) into MS instruments with the launch of the first commercial traveling wave IMS-QTOF system in 2006 could be regarded as the latest important instrumental leap to consider in plant metabolomics (Dodds and Baker, 2019). Afterwards, although the resolution and mass accuracy parameters of the state-of-the-art instruments have been upgraded several folds, the main emphasis has been put on the development of high data throughput software tools, which are

usually assisted by multivariate statistical approaches and at least entry-level artificial intelligence toolkits such as artificial neural networks (ANN).

There are several approaches available for establishing the most comprehensive metabolomic fingerprint of plant samples by combining the various methods for creating a metabolomic profile with MS setup. The following are the most common methods aimed at the secondary metabolite set:

(i) Authentic standards - Running targeted searches on authentic standard sets.

(ii) Literature - Search for metabolites formerly reported for the plant species or plant genus.

(iii) Major compounds - Semi-targeted or untargeted identification of major components based on high intensity GC-HRMS, LC-HRMS or UV/VIS peaks.

(iv) Statistics - Running multivariate statistical analysis, then focusing on the largest discriminating features (molecular entities) between predefined groups, with an intention to identify them.

The primary drawback of targeted metabolic profiling techniques that are based on authentic standards (i.e., a commercially available or in-house synthesized form of the analyte with the highest available structure matching and purity), is that they can analyze compounds that are either commercially available or have already been identified and deeply characterized by orthogonal techniques including HR-MS and NMR. This is because targeted analyses require authentic reference compounds for the identification and quantification of the measured compound. Therefore, one of the main obstacles in metabolomics research is the structural elucidation of an unknown analyte that does not match any of the commercially accessible reference molecules. Higher-dimension NMR techniques, which can be considered the ultimate reference methods, enable the true *de novo* determination of the final structure and stereochemistry of a small molecule; however, this method requires demanding sample purification and enrichment steps for most test samples, which makes it considerably more difficult to identify metabolites in complex mixtures. Due to the challenges associated with compound identification, a hierarchical annotation system was established for MS-based metabolomics, defining distinct levels of confidence in compound identification.

Çiçek et al. (2024) proposed the latest classification of identification confidence levels. This system is ranging from level A to level F and is meant to account for the unusual chemical complexity of plant metabolites, which sometimes contain multiple stereocenters and numerous isomeric possibilities, a feature hardly seen in mammalian metabolomics or environmental studies. Level A demands full structural elucidation utilizing highly orthogonal techniques such as high-resolution MS/MS, multidimensional NMR spectroscopy, and, where appropriate, X-ray

crystallography, supported by chiroptical measurements and classical chemical approaches. Critically, level A identification also demands the exclusion of all potential isomers, including enantiomers. Level B (B1 and B2) identification softens the criterion for full stereochemical confirmation, allowing for one or more chiral centers to remain unresolved. Level C relates to tentative identification based on authentic standards and is typically the greatest practically available confidence level in routine phytochemical investigations, particularly for complex metabolites. Level D identification is based mostly on analytical databases (spectral libraries), requiring a match of retention time, MS and MS/MS data. Achieving level A identification is exceptionally demanding. It requires sufficient sample amounts to permit NMR or X-ray analysis, as well as access to all relevant stereoisomers or the ability to experimentally distinguish between them. For highly complicated natural products, such as multiple glycosylated flavonoids or diterpenoids, level A is sometimes attainable only when repeating the original structural characterization of a known chemical. Consequently, most published identifications in plant metabolomics correspond to levels C or D, representing tentative assignments based on standards or library matches. Due to the strict nature of the classification, it is not yet possible to assess layered identification without an authentic standard. Taking into account the identification potential of additional orthogonal techniques (e.g., ion mobility data), further intermediate identification levels could be defined, thereby refining the assessment of the work of those involved in the earliest stages of untargeted analysis.

The use of plant-based active ingredients in drug research has persisted despite the latter's successes in synthetic drug development. Screening assays have been and still are used to find possible novel active substances. The objective is obvious: to choose species from the >391,000 plants mentioned above that have not yet been investigated or are worth re-examining, that show promise from a pharmacological and therapeutic perspective, and that can be suggested for additional phytochemical, pharmacological, preclinical, and clinical testing. The selection and gathering of plant material and the isolation of active substances with complicated chemical structures are frequently major drawbacks, despite the benefits of plant-based chemicals, such as increased structural richness and more targeted effects.

Thanks mostly to a program started by the US National Cancer Institute (NCI), extensive screening for anticancer activity of plants, microbes, and marine organisms started in the late 1950s (National Cancer Institute (U.S.), 1977). Assuming that tumor-inhibiting compounds can be found anywhere in the plant and animal kingdom and that their synthesis is frequently unique to a single genus or even a single species, this set of experiments was based on random selection. Random screening programs were only used for diseases with an urgent medical need, such as cancer,

because they were very expensive. The NCI gathered plant samples from 60 nations between 1960 and 1982 and examined 114,000 extracts from 35,000 different species. The 1980s saw an increase in screening efforts due to worries that many of these important natural sources would be irreversibly destroyed by human activity and environmental pollution. Although camptothecin (1966) and taxol (1971) were isolated as a result of the NCI program, screening programs carried out parallel revealed the components of *C. roseus*, vinblastine and vincristine (Svoboda et al., 1959).

New biologically active substances can be identified through two main screening approaches: phytochemical and biological testing. Phytochemical screening focuses on detecting known or novel metabolites to expand knowledge of plant chemical diversity. In contrast, biological screening evaluates plant extracts for new biological activities or active constituents, while also assessing potential toxicity.

Over the past two to three decades, advances in separation techniques and the emergence of new methods have made it quicker and easier to analyze the chemical composition of plant extracts. In plant research, metabolomics has emerged as a crucial method for chemical fingerprinting and compositional analysis. The thorough mapping of metabolites in biological systems is now more feasible than ever because of important developments in analytical equipment and data processing. Metabolomics is a particularly useful technology in medicinal plant research because it makes it possible to understand the molecular basis behind the benefits of traditional treatments that have been empirically seen. This method aids in the creation of more accurate, scientifically supported medicinal and nutritional uses of plants by describing the metabolomic profile.

3.2. *Catharanthus roseus* (L.) G. Don

Madagascar periwinkle (see Figure 1), or *Catharanthus roseus* (L.) G. Don, is an evergreen perennial plant, semi-shrub, or herbaceous species that belongs to the *Apocynaceae* family. It was formerly known as *Vinca rosea*. Although it is indigenous to Madagascar, it has spread over many tropical and subtropical areas, becoming the only species of the eight belonging to the *Catharanthus* genus found worldwide. It has gained popularity as an ornamental plant all over the world because of its long flowering period and adaptability (Nejat et al., 2015). The plant has opposite glossy, green leaf pairs. In addition to its naturally occurring pink and white flower

variations, many hybrids, including blush pink with red eye, crimson, and white with red eye, are commercially available as seeds (Wilson, 1988).

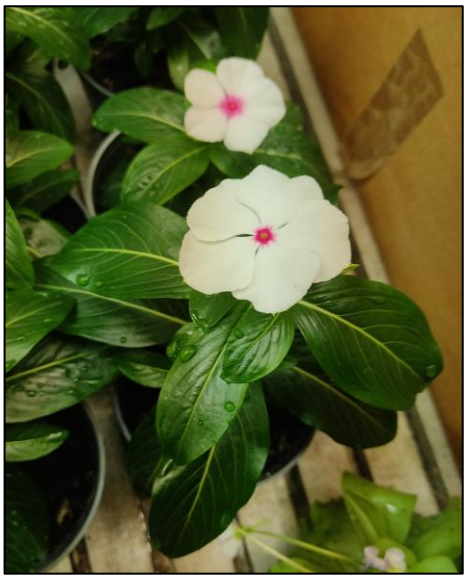

Figure 1. *Catharanthus roseus* (L.) G. Don *(Photo by the author)*

Based on its usage in traditional medicine, Madagascar periwinkle gained recognition in scientific research in the late 1950s, when Svoboda et al. (1959) included it in a comprehensive screening program of *Apocynaceae* plants intended to detect hypoglycemic components. Certain fractions of the plant extract had delayed toxic effects in experimental animals, while no compounds affecting blood glucose levels or carbohydrate metabolism were discovered. Numerous indole alkaloids with notable pharmacological activity were eventually found as a result of the research being turned toward the isolation of alkaloid fractions causing the reported toxicity.

Nearly 200 monoterpenoid indole alkaloids have now been found among the secondary metabolites of *C. roseus* thanks to extensive phytochemical and metabolomic research (De Luca et al., 2014). However, a complete picture of the plant's metabolomic and regulatory processes is hampered by the fact that the entire biosynthesis pathways of these complex molecules are still only partially understood, with numerous important enzymes remaining unidentified.

C. roseus has been included in comprehensive screening programs intended to find plant-derived bioactive chemicals for medicinal uses since its rediscovery in the middle of the 20th century. Vincristine sulfate and vinblastine sulfate, two potent anticancer drugs, were developed as a result of this research (Yaniv and Bachrach, 2005). These vinca alkaloids are essential parts of combination chemotherapy treatments for diseases such acute leukemia, lung cancer, Hodgkin's disease, and choriocarcinoma (Vici et al., 2002). However, the plant's restricted worldwide availability limits the industrial-scale production of vinblastine and vincristine, which as a result fetch extraordinarily high market prices of roughly $2 million/kg and $15 million/kg, respectively (Kumar et al., 2022).

3.2.1. The alkaloids of *C. roseus*

The condensation reaction of secologanin, which is obtained from geraniol via the monoterpene pathway, and tryptamine, which is formed from L-tryptophan, with the aid of the enzyme strictosidine synthase (EC 3.5.99.13), forms strictosidine as the first step in the

biosynthesis of indole alkaloids (see Figure 2). Numerous alkaloids identified from plant samples are produced during the complicated synthesis route, many of which have well-known biological effects. The most important dimer alkaloids in medicine are formed by the reaction between catharanthine and vindoline to form 3',4'-anhydrovinblastine, which is the bottleneck reaction of the synthesis pathway. Although a peroxidase that can catalyze this reaction has been discovered (Sottomayor et al., 1998), the precise nature of this enzyme-catalyzed reaction is yet unknown.

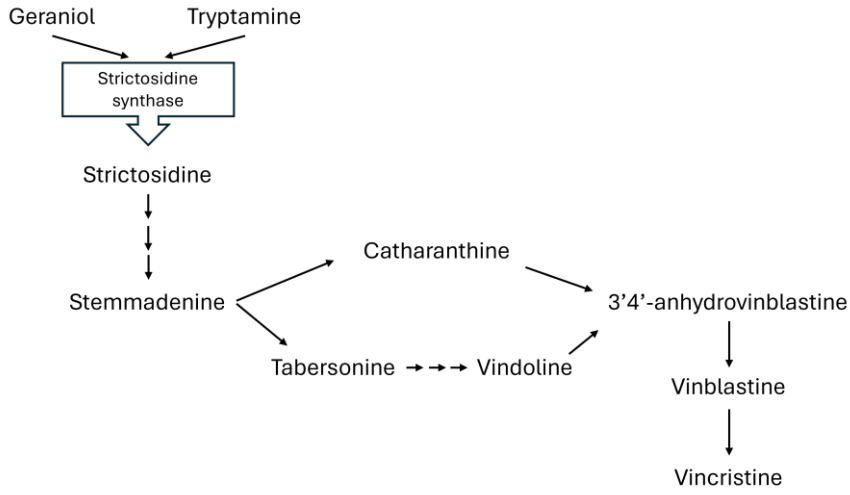

Figure 2. Schematic diagram of the bisindol alkaloid’s synthesis route (KEGG Indole alkaloid biosynthesis - Reference pathway)

The two main dimer alkaloids of periwinkle that have anticancer properties are vinblastine and vincristine, which represent the currently known end of the synthesis pathway. For patients with advanced Hodgkin's disease who were resistant to alkylating agents and unable to receive radiation therapy, it was found that vinblastine was an effective medication (Sohier et al., 1968). Vincristine has antitumor effects in leukemia and several types of childhood tumors. Both vinblastine and vincristine play a significant role in disrupting the microtubule dynamics of tumor cells, inhibiting the chromatin filaments that pull toward their respective poles, thereby inhibiting mitosis during metaphase, which leads to cell death. In addition, vincristine also inhibits microtubule polymerization, inducing cell cycle arrest and apoptosis in the G2/M phase (Al-Amin et al., 2022). In addition to dimer alkaloids, intermediates and other branches of the biosynthetic pathway are also considered useful (health promoting or medically important) bioactive compounds. While serpentine has a relaxing effect (Moreno et al., 1995), ajmaline, which is derived from catenamine, is also used to treat high blood pressure and other circulatory disorders (Van Der Heijden et al., 1989).

Vinblastine and vincristine are frequently referred to as bisindoles because they have two distinct indole units in their structure: the velbanamine or cleavamine part (upper unit) and the vindoline part (lower unit) (see Figure 3). Vinblastine and vincristine are obvious starting points for preparative chemists who have attempted to design more potent but less toxic semi-synthetic analogues. Looking at the molecular effects and structures of the approved derivatives that have entered production, it is clear that relatively small structural changes lead to significantly different oncological and toxicological profiles.

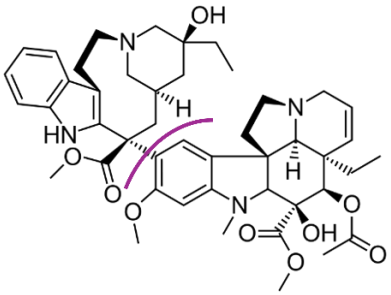

vinblastine

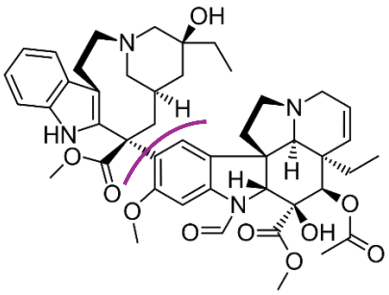

vincristine

Figure 3. Structure of the major dimeric alkaloids of periwinkle. The link of the velbanamine and vindoline molecular entities are marked in purple.

For instance, vinflunine, a fluorinated derivative, is used to treat bladder cancer; vinorelbine, a derivative of vinblastine that differs from the parent molecule by just one hydroxyl group in its structure, is used to treat breast cancer and non-small cell lung cancer (Béni et al., 2012).

3.2.2. Production of bisindol alkaloids

The plant material contains bisindol alkaloids in very low concentrations: the concentration of vinblastine and vincristine in field grown leaves are generally in the $mg \cdot kg^{-1}$ range (Banyal et al., 2023; Mujib et al., 2017; Salama et al., 2020). Their extraction is often unprofitable, involving the processing of large quantities of plant material and time-consuming and costly purification steps. The primary reasons for beginning to synthesize these chemicals *via* different methods were the dimer alkaloids' low yield [0.0001-0.0005% leaf DW (Sharma et al., 2022)] and high cost. An obvious solution is to produce the compounds using cell and tissue cultures, but even the biosynthesis of one of their monomers, vindoline, requires cell differentiation. Accordingly, dimeric alkaloids can only be produced from differentiated callus cultures or organ cultures (Van Der Heijden et al., 1989).

Apart from plant extraction, other feasible options include total synthesis of the compounds and semi-synthetic production of dimeric alkaloids from monomers (Rahman (Ed.), 1994). However, the complex bisindole structure of dimer alkaloids (the C-C bond connecting the velbanamine moiety to vindoline) and their possible isomers had to be taken into account. While vindoline occurs together with vinblastine in the leaves of periwinkle, the velbanamine moiety cannot be detected separately in the plant, and experiments aimed at synthesizing vinblastine or vincristine must necessarily include the production of this interesting indole system, which carries a nine-atom, nitrogen-containing ring. In semi-synthetic production, the dimers are most often produced by the oxidative coupling of monomer precursors. For this purpose, vindoline is extracted from periwinkle leaves, while catharanthine can be obtained from the roots of the plant or from *in vitro* cultures (Mishra et al., 2001).

Since the procedure of extracting alkaloids from grown plants is still crucial, we can endeavor to apply agrotechnological solutions to enhance the useful metabolites of periwinkle. This requires understanding how biosynthesis is regulated during plant development and where it takes place in plant cells. Tabersonine accumulation can be observed in seedlings grown in the dark (since the enzymes necessary for its production are present in all parts of the plant), as well as the restriction of vindoline and its precursors to the cotyledons (DeLuca et al., 1986). While tabersonine and catharanthine are found in all tissues of the plant, vindoline and the dimer alkaloids formed from it are restricted to the aerial parts of the plant and their appearance is developmentally regulated. The formation of the main leaf alkaloids requires the participation of at least two cell types in the plants and the intercellular translocation of an intermediate. The genes involved in strictosidine formation are expressed only in the epidermis of the aerial tissues and in the cells of the root apical meristem, while the enzymes required for the last two steps of vindoline biosynthesis (deacetoxivindoline 4-hydroxylase and deacetylvindoline 4-O-acetyltransferase) occur exclusively in the laticifers and idioblasts of the aerial tissues (Schröder et al., 1999).

The 2-C-methyl-D-erythritol-4-phosphate pathway (KEGG Terpenoid backbone biosynthesis pathway), which provides the carbon skeletons necessary for secologanin biosynthesis, and geraniol 10-hydroxylase, which is involved in the first step of this pathway, have been localized in biochemically specialized internal phloem parenchyma cells. In contrast, loganic acid O-methyltransferase and secologanin synthase, which catalyze the terminal reactions of secologanin biosynthesis, are expressed exclusively in the epidermis of young leaves and stems. This suggests that an as yet uncharacterized intermediate is transported between the internal phloem parenchyma and epidermal cells for the formation of the secologanin molecule at the appropriate location (Roepke et al., 2010).

The concentration of vindoline, catharanthine, and 3',4'-anhydrovinblastine in the leaves of the plant is age-dependent. During the ripening process of the leaves, the concentration of catharanthine and vindoline decreases, while the concentration of 3',4'-anhydrovinblastine increases (Moreno et al., 1995). It is important to note that transport mechanisms directed towards alkaloid biosynthesis are linked in the leaf epidermis to enable the selection of catharanthine into the surface wax, while vindoline accumulates in special idioblast/laticifer cells found in the leaf. This spatial separation of monomeric alkaloids provides a clear explanation for the low levels of dimeric alkaloids found in periwinkle (Roepke et al., 2010).

Various stress factors affecting plants can influence their alkaloid content. According to Frischknecht et al. (1987), in healthy, non-stressed plants, the youngest part of the shoot tip contained more than 3% alkaloids; moving down the shoot, the alkaloid content of successive leaf pairs decreased. Drought had little effect on the concentration of alkaloids within the plant. Wound stress increased the alkaloid content in the shoot by 100%, but wounding did not increase alkaloid accumulation in non-growing tissues.

The generation of alkaloids by the plant is also influenced by lighting. Treatment with UV-A and UV-B radiation can increase the accumulation of alkaloids, including dimers (Fukuyama et al., 2017; Zhong et al., 2021), but UV irradiation can cause unpredictable physiological effects. Treating the plant with LED light, which has been utilized for roughly ten years to create the appropriate amount of active compounds (Fukuyama et al., 2013), is one possible answer.

3.3. *Taraxacum officinale* (L.) Weber ex F.H. Wigg

Plants in the genus *Taraxacum*, which is a member of the *Asteraceae* family and *Cichorioideae* subfamily, have long been utilized for their medicinal properties. Dandelion (see Figure 4), *Taraxacum officinale* (L.) Weber ex F.H. Wigg, is widely distributed throughout the northern hemisphere and is listed in both the European Pharmacopoeia (*European pharmacopoeia*, 2022) and plant monographs (European Medicines Agency, 2020; World Health Organization, 2007) because of its widespread use in folk medicine. Related species, including *T. mongolicum* and *T. sinicum*, are native to China and the Korean Peninsula.

Figure 4. *Taraxacum officinale* (L.) Weber ex F.H. Wigg (*Source: https://unsplash.com*)

As *T. officinale* is a common weed, and its collection in the wild is as common as its cultivation, making it difficult to identify its main suppliers. However, according to Bisset (1994), Hungary was one of the main suppliers of dandelion in the 1990s.

Dandelion drug (*Taraxaci herba cum radice*) has a variety of use in traditional medicine. It is well recognized for its "blood-purifying" qualities and is used as a tonic, laxative, and galactagogue. Among the several conditions it is used to treat include boils, sores, diabetes, fever, eye irritation, insomnia, sore throat, lung abscesses, jaundice, and urinary tract infections. Additionally, it is also applied to treat dermatitis, rheumatism, arthritis, and other skin conditions (Bisset et al., 1994; Gruszecki et al., 2024; Schütz et al., 2006). *T. officinale* drug is a mild choleretic, diuretic, and appetite-stimulating bitter that can be used as an adjuvant in cases of incomplete fat digestion, liver and gallbladder diseases, and digestive symptoms (Bisset et al., 1994; Schütz et al., 2006). Additionally, upper respiratory tract infections have been treated with dandelion flower infusions and syrups (Bylka et al., 2010). These diverse effects are mainly believed to be caused by the presence of various sesquiterpenes and polyphenolic compounds. The plant may be a valuable source of bioactive components and natural antioxidants (Hu and Kitts, 2003; Kisiel and Barszcz, 2000).

Though to differing degrees, the effort of putting many folk medicine applications on a scientific foundation is still in progress. It was discovered that the dandelion aqueous extract had a protective effect on acute liver inflammation (Park et al., 2010), acute anti-inflammatory activity on cholecystokinin-induced acute pancreatitis (Seo, 2005), and a significant action on sodium dichromate-induced hepatotoxicity, oxidative stress, and genotoxicity (Hfaiedh et al., 2016). Additionally, it has the potential to treat endogenous and/or exogenous-originated kidney toxicity in rats (Karakuş et al., 2017) as well as chemically induced or viral hepatitis (Park et al., 2007). The effects of numerous bioactive metabolites found in dandelions have also been studied individually. In Swiss albino mice under chronic stress, Kour and Bani (2011) reported that chicoric acid at a dose of 1 $mg \cdot kg^{-1}$ had a substantial antidepressant and stress-reducing effect. Chicoric acid also possesses antioxidant and anti-adhesive qualities and according to to a human blood test by Lis et al. (2019), it does not exhibit cytotoxic side effects against platelets. By secreting interleukin (IL)-1β and tumor necrosis factor-α (TNF-α), the dandelion extract induced apoptosis in human Hep G2 cells (Koo et al., 2004). Additionally, based on experiments conducted on the lung adenocarcinoma cell line A549 (Man et al., 2022), it may inhibit tumor cell growth, disrupt cell membrane stability, and reduce cell adhesion – all of which are important aspects of its anti-cancer effect. According to *in vitro* experiments (Hu and Kitts, 2003), luteolin and luteolin 7-O-glucoside are primarily responsible for the antioxidant and cytotoxic properties of dandelion

flowers. Luteolin and luteolin 7-O-glucoside reduce the generation of nitric oxide and prostaglandin E2 in LPS-activated RAW 264.7 macrophage cells by blocking inducible nitric oxide synthase (iNOS) and cyclooxygenase-2 (COX-2) (Hu and Kitts, 2004). The advantages of employing these bioactive compounds in medicine, such as their potential to lessen reliance on expensive, high-tech, or chemical-based therapies frequently employed in Western medicine, are supported by ongoing research.

In addition to its medicinal applications, *T. officinale* can be recommended as a food source (Escudero et al., 2003). Its roots, leaves, and flowers are used to make a range of culinary products. While the roots are roasted and used as a coffee substitute, young leaves are eaten raw in salads (Hadjichambis et al., 2008). Additionally, a wide range of culinary products, including cheese, gelatins, baked goods, frozen dairy desserts, alcoholic beverages, soft drinks, and candies, use dandelion extracts as flavoring ingredients (Cacak-Pietrzak et al., 2021; Gatto et al., 2011). Dried dandelion flowers are available as a dietary supplement (Wappel and Schulte, 2004) for turtles, rabbits and horses due to their high polyphenol content, and adding dandelion extract to feed can improve the antioxidant capacity and non-specific immunity of common carp (Chen et al., 2023).

Like most herbs used in traditional medicine, *T. officinale*'s health benefits are empirically proven, but surprisingly little is known about the bioactive components and mechanisms underlying its effects. However, *T. officinale* is the only species within the genus that has been researched in terms of its biochemical and nutritional composition in relation to its economic relevance. This is mainly because it is widely distributed around the world, incorporated into various ethnobotanical activities, and commonly found in pasturelands used for cattle grazing (Martinez et al., 2015; Zhang et al., 2024). Despite all these advantages, only a few scientific publications discussed the chemical composition of dandelion, as Williams et al. pointed out in 1996. In their study, Schütz et al. (2006) reported a lack of data from human or clinical studies, while Martinez et al. (2015) cited the low level of interest in clinical studies related to the topic as the reason for this phenomenon. Clare et al. carried out a pilot study in 2009 to look into the diuretic effect of dandelion over the course of a one-day period. An ethanolic extract of fresh leaves (1 $g \cdot mL^{-1}$) increased the frequency of urination and the amount of fluid excreted in healthy individuals, according to the results. Also, there were attempts to conduct clinical trials, for example to prove the effectiveness of the natural dandelion product in treating obesity in premenopausal women or treating vesicular hand eczema with the ingestion of dandelion juice (Clinical Trials 1.; Clinical Trials 2.).

T. officinale has been recognized as a useful bioindicator plant due to its capacity to absorb and store toxic metals. According to Bini et al. (2012), dandelions can tolerate and accumulate

high levels of metals like lead (up to 200 $mg \cdot kg^{-1}$) and zinc (up to 160 $mg \cdot kg^{-1}$), especially in leaves and roots, with minimal visible damage. Their ability to uptake and move essential metals like zinc and iron throughout the plant makes them promising for phytoremediation and erosion control, offering a low-cost and effective solution. However, growing in toxic metal contaminated soils raises health concerns due to the plant's role in the food and pharmaceutical industries. Also, dandelion can be used as a bioindicator for the genotoxicity of nebulized dispersions of ZnO and CuO nanoparticles as representative atmospheric nanostructured pollutants (Abrica-González et al., 2023).

3.3.1. The secondary metabolites of *T. officinale*

Our understanding of the dandelion plant's secondary metabolites has grown significantly during the last 20 years. Terpenes, flavonoids, and phenolic compounds are the most studied and discovered compounds, making about 45% of the relevant literature (Martinez et al., 2015). More than 200 small molecular secondary metabolites have been found in dandelions or in various plant tissues, according to the literature (see App. A2: Table 2., based on the research of Budzianowski, 1997; Bylka et al., 2010; Choi et al., 2018; Grauso et al., 2019; Hänsel et al., 1980; Hu and Kitts, 2003; Jedrejek et al., 2019; Jedrejek and Pawelec, 2024; Jung et al., 2011; Kamal et al., 2022; O. Kenny et al., 2015; Owen Kenny et al., 2015; Kikuchi et al., 2016; Kisiel and Barszcz, 2000; Kristó et al., 2002; Lis et al., 2020; López-García et al., 2013; Melendez-Martinez et al., 2006; Miłek et al., 2019; Pedneault et al., 2002; Saeki et al., 2013; Schütz et al., 2005; Sergio et al., 2020; Tsagkaris et al., 2022 and Zou et al., 2023), and this number only rises when we consider reports of related species in the *Taraxacum* genus. The plant's flowers and the essential oil that was extracted from them have been found to contain a variety of aliphatic hydrocarbons, alcohols, aldehydes, and organic acids. However, the flowers, as well as the much more studied leaves and roots, contain a variety of terpenoids, phenolic acids, flavonoids, and their derivatives. These three metabolite groups comprise over half of all metabolites discovered so far. Interestingly, Williams et al. (1996) found that dandelion flowers contained free luteolin and chrysoeriol in addition to high concentrations of yellow carotenoids. These flavonoids are presumed to contribute to the plant's protection against ultraviolet radiation. In comparison to outdoor cultivation, Pedneault et al. (2002) examined the effects of greenhouse hydroponic cultivation on the levels of caffeic acid, chicoric acid, and chlorogenic acid in dandelions. According to their research, plants grown in the field had far higher concentrations of these phenolic compounds (31.2 $mg \cdot g^{-1}$ DW) than plants produced hydroponically in greenhouse (5.0 $mg \cdot g^{-1}$ DW). The authors hypothesized that exposure

to UV-B radiation may be the cause of the increased phenolic acid accumulation in field-grown *T. officinale*.

However, when it comes to dandelion – (or any herbal –) based products and dishes, it's crucial to consider the impact of the technologies and cooking methods employed during production, as these can have a significant impact on the quantitative and qualitative composition of the particular product to be consumed (Sergio et al., 2020). Based on the health promoting properties of some compounds found in dandelion, alcoholic extracts made from dandelions can be used to produce new food or medicinal products, provided that the tradition of folk medicine production is followed. There is a lack of trustworthy quantitative data that is verified by authentic standards and occasionally contradicts one another. For instance, Hu and Kitts (2004) found 0.85±0.09 $\mu g \cdot mg^{-1}$ caffeic acid in the flowers' aqueous extract and 7.26±0.03 $\mu g \cdot mg^{-1}$ in the ethyl acetate extract (related to unspecified dry material content), although López-García et al. (2013) detected no caffeic acid in the dandelion flowers they studied. There are also significant differences between the reported concentrations of compounds. Hu and Kitts (2004) were unable to detect luteolin in the aqueous extract of dandelion flowers, but the ethyl acetate extract yielded a luteolin concentration of 25.20±0.56 $\mu g \cdot mg^{-1}$ (related to unspecified dry material content), while Miłek et al. (2019) found that the acetone extract of the flower contained 11.87±1.19 $mg \cdot g^{-1}$ DW luteolin. The scarcity of consistent and comparable data, coupled with the consequent under-regulation of this field, underscores the need for further research to support the evidence-based utilization of dandelion and other common plants rich in bioactive compounds that remain largely overlooked in everyday practice.

3.4. Plant cultivation under controlled conditions

In addition to natural diversity among individual plants, cultivation practices and environmental conditions have a significant impact on plant traits, including alterations in their metabolomic pathways. Many plants, particularly herbs and legumes, are cultivated in controlled environments to attain optimal quality and output. Environmental parameters (temperature, light, humidity) may all be fixed or changed adequately in these artificial environments to suit the unique requirements of different plant species. LED technology is frequently used in modern indoor cultivation systems to give the ideal light intensity and spectral composition for plant growth and development (Darko et al., 2014; Olle and Viršile, 2013; Singh et al., 2015). Targeted secondary metabolite production can be promoted by modifying plant biosynthesis pathways with LED lighting assistance. This method may be more ecologically friendly than conventional chemical synthesis and provides a workable substitute for creating chemicals that are challenging to

synthesize. In order to increase the production of valuable plant-derived substances, this method has been widely used in horticulture, the food industry, and more recently, the pharmaceutical sector (Darko et al., 2022; Kubica et al., 2020).

Researchers have been using LED lights to increase the stability of *C. roseus*'s vinca alkaloid output for almost a decade. The main goal of these investigations was to increase the production of vinblastine precursors, vindoline and catharanthine, by optimizing light conditions. Red light significantly increased plant growth, however under various lighting conditions, Fukuyama et al. (2013) did not see a significant rise in vindoline or catharanthine levels. They subsequently found that the optimal red light intensities for producing these precursors per plant were 150-300 $\mu mol \cdot m^{-2} \cdot s^{-1}$ (Fukuyama et al., 2015). Red light, however, did not increase vinblastine production. To resolve this, increased exposure to UV-A light was demonstrated to elevate vinblastine levels in *C. roseus* leaves in the plants grown under red light (Fukuyama et al., 2017), whereas UV-B exposure similarly enhanced alkaloid accumulation (Zhong et al., 2021). Despite these benefits, UV treatment may induce unwanted physiological alterations, including diminished internode length, indicating that gentler, less stressful approaches to enhance vinca alkaloid content may be more desirable (Chen and Chen, 2013).

3.5. Metabolomics of *C. roseus* alkaloids and *T. officinale* secondary metabolites

During structural determination for small molecule secondary metabolites, including alkaloids, NMR and MS are key techniques. Together, NMR and MS often enable the unambiguous determination of the structure of an unknown compound, even if only small quantities are present. In Hungary, Richter Gedeon Plc. is a leader not only in the research of the two main alkaloids of periwinkle, but also in the structural determination of by-products and metabolites generated during the production of active pharmaceutical ingredients (Dubrovay et al., 2013; Háda et al., 2013).

Although both NMR and MS techniques have advanced significantly in recent decades, their limitations should not be overlooked. NMR analysis still requires at least 1-3 mg of sufficiently pure (>95%) extracted/produced compound, which is extremely difficult to collect in the case of for example, surrogating contaminants in the order of $\mu g \cdot kg^{-1}$ concentrations during the production of active pharmaceutical ingredients, or relatively less abundant (“minor”) components found in similar concentrations in plants. Without independent NMR-based identification, GC/LC-HRMS techniques are suitable "only" for the tentative identification of compounds, based on accurate

mass measurement and fragmentation pattern analysis. In addition, both NMR spectrum interpretation and MS fragment spectrum analyses typically require researcher-level expertise and cannot be fully automated, meaning that human errors cannot be ruled out. With the advancement of analytical techniques and instruments, new publications continue to appear to this day, targeting the determination of metabolites from their original plant matrix (Hisiger and Jolicoeur, 2007; Jedrejek and Pawelec, 2024; Kenny et al., 2014; Lourenço et al., 2022). Compared to gas chromatography and capillary electrophoresis techniques, HPLC combined with a diode array detector (DAD), fluorescence detector (FLD), or mass spectrometry (MS) is the most commonly used method when it comes to involatile compounds. The latter is considered a fundamental technique, given that no authentic standards are available for most of the secondary metabolites (Kulagina et al., 2022).

For the detection and identification of secondary plant metabolites without authentic standards, high-resolution mass spectrometry systems coupled with liquid chromatography (LC-ESI-/Q/TOF-MS, LC-ESI-Orbitrap-MS) offer an adequate alternative that is even suitable for retrospective analysis. After quadrupole–time-of-flight (QTOF) mass spectrometers became commercially available 30 years ago (Chernushevich et al., 2001), the analytical community quickly embraced them as powerful, robust instruments with unique features. ESI-QTOF systems can be viewed either as an ESI-TOF augmented with a quadrupole and collision cell, or as a triple quadrupole instrument in which the third quadrupole is replaced by a TOF analyzer. In both cases, the resulting tandem mass spectrometer provides high sensitivity, high mass resolution, and high mass accuracy in MS (and partly in MS/MS) modes. The excellent full-scan sensitivity of TOFMS over a broad mass range, made possible by parallel detection, is one of its main advantages in both modes. In addition, the examination of the isotopologue profile of unknown components, together with their accurate mass determination, reduces the uncertainty of spectral analysis, enabling the determination of the metabolic profile of the plant. Also, the accurate mass spectral data can be analyzed retrospectively for newly emerging substances of interest.

Analytes are separated by liquid chromatography and assigned by their measured *m/z* and retention time parameters (together often referred to as molecular features) in a standard LC–MS procedure. High selectivity and reproducibility in mass accuracy are provided by HRMS; nonetheless, interferences and chromatographic instability can make the identification based only on retention time and *m/z* problematic in complicated matrices or in the presence of numerous background signals (matrix ions). Therefore, separation and identification certainty can be enhanced by an extra orthogonal property that separates ions with identical retention durations and closely spaced *m/z* values. This attribute is achieved by ion mobility, which makes it possible to

quantify a molecule's collision cross section (CCS) under specific circumstances. The ion mobility device in the Vion IMS QTOF system (see Figure 5) is situated between the StepWave and the quadrupole, where ions are segregated according to their gas phase dimensions and reported as drift time or CCS.

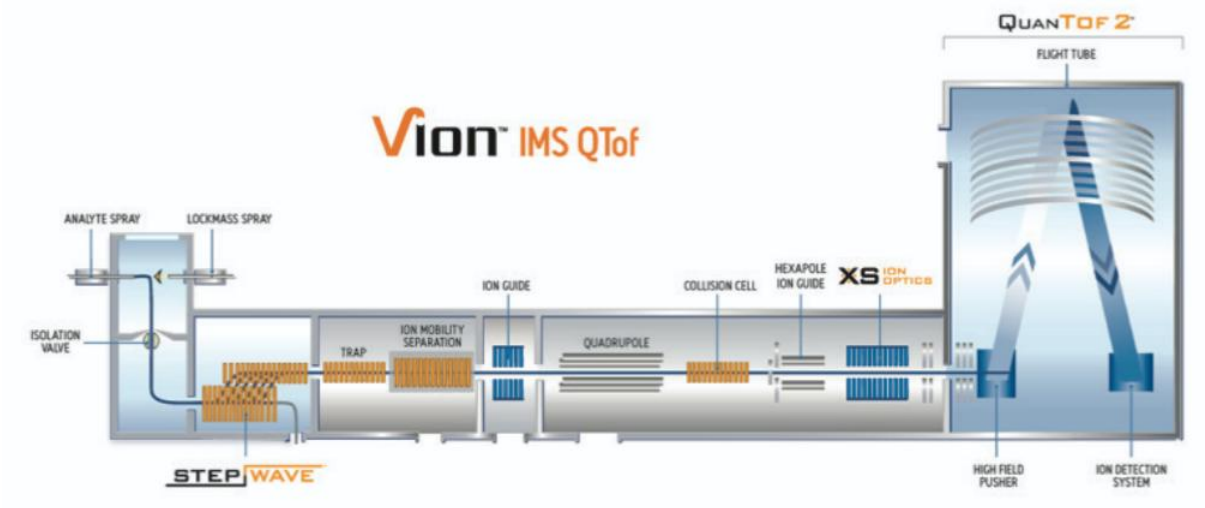

Figure 5. System diagram of Vion IMS QTof platform *(Source: www.waters.com)*

By employing less selective sample preparation to look at a wide variety of substances at once, applying untargeted analysis on LC-HRMS instruments provides a more thorough approach. However, compared to the few hours usually needed for targeted analysis, the resulting enormous data sets require considerable processing, frequently requiring weeks or months for evaluation. Because of this, untargeted methodologies are currently mostly employed in research and development. Untargeted analysis can produce rich insights, allowing the detection of particular differences and the finding of distinguishing traits between samples, despite being time-consuming and requiring a high level of analytical skills.

Determining the concentration levels of vinca alkaloids in *C. roseus,* in related pharmaceutical products, and in human serum samples is crucial from a clinical perspective, also it shouldn't be overlooked in the case of dandelion, regards to its medicinal and food industry uses. Triple quadrupole LC-ESI-MS instruments in multiple reaction monitoring (MRM) mode or HR-MS instruments in MRM or single ion monitoring (SIM) modes can be used to quantitatively determine target analytes in very low concentrations for which authentic standards are commercially available; however, additional members of the biosynthetic pathway can only be determined with some degree of uncertainty and quantified to another component (semi-quantitative approach) (Ferreres et al., 2010; Kumar et al., 2018). Since there is no single group of compounds in

dandelion that is attributed with any strong medicinal properties, the goal in this case is to map the metabolome as completely as possible. In contrast, the vinca alkaloid metabolome has been the subject of relatively few papers to far (Al-Amin et al., 2022; Jeong and Lim, 2018; Yu et al., 2022), and none of them have attempted to cover the most important, related alkaloid biosynthetic pathway.

4. MATERIALS AND METHODS

4.1. Plant materials and growth conditions of *C. roseus*

A total of 300 seedlings, raised from seeds (source: Rédei Kertimag Zrt., Réde, Hungary; undisclosed cultivar), were cultivated for two months in a PGR-15 growth chamber (Conviron Ltd., Winnipeg, Canada) under controlled conditions: 26/20°C day/night temperature, light intensity of 300 µmol $m^{-2} \cdot s^{-1}$ supplied by metal halide lamps with 16/8 h photoperiod, and relative humidity sustained at 70–75%.

Following two months of initial growth, the seedlings were transferred to LED chambers and subjected to various light treatments (as shown in Table 1) for a period of two weeks.

Table 1. Experimental settings of the LED treatment

No.	Type	SUM PPFD* (µmol $m^{-2} \cdot s^{-1}$)	Blue %	Green %	Red %	Far-red %
1	High blue	350	43	15	41	1
2	High red	350	11	15	73	1
3	High far-red	350	20	15	44	21
4	Medium light (control)	350	20	15	64	1
5	Low light	115	20	15	64	1

* Photosynthetic photon flux density

For each lighting condition, 12 seedlings were selected, as illustrated in Figure 6. After the two-week exposure, five plants from each LED group were chosen for vinca alkaloid analysis. From each plant, four fully developed leaves were collected from the top of the plant. The leaf samples were immediately frozen in liquid nitrogen and stored at –80 °C until further processing.

Figure 6. *C. roseus* plants during the LED treatment (No. 5 low light on the left side and No. 1 high blue to the right). *(Photo by the author)*

4.2. Plant materials and product samples of *T. officinale*

Dried dandelion leaf-root drug (*Taraxaci herba cum radice*) was purchased from a local market (Mecsek-Drog Kft., Pécsvárad, Hungary). The drug contained the dried roots and rosettes since it was collected before the flowering period. Dandelion flowers were collected in Gyömrő, Hungary (47°25'05.5"N 19°23'54.8"E) in spring 2023. The freshly collected flowers were mechanically cleaned and frozen at -80°C until sample preparation.

The dandelion liqueur products were made from the flowers collected in Gyömrő. The liqueur was produced by macerating fresh dandelion flowers in ethanol (40 V/V%) at room temperature in the dark, which is then aged for two months before being bottled and commercialized. The leaf-root drug and liqueur samples were stored in a dark and dry place until analysis.

A test batch was used to examine extraction optimization and monitor maturation. The extraction solvent in this case was ethanol (70 V/V%). This test batch was sampled weekly over a period of two months.

4.3. Chemicals and reagents

As for authentic standards to measure periwinkle samples, vincristine sulfate (≥ 99 %) and vinblastine sulfate (≥ 97 %) were purchased from the Merck-Sigma group (Darmstadt, Germany). 63 authentic standards were used for the identification, quantitation and semi-quantitation of the dandelion samples. For the details of the authentic standards and the stock solutions, see A8: App. Table 5.

Sample preparations was carried out with UPLC gradient grade ethanol, methanol and HPLC grade n-hexane, all obtained from VWR (Radnor, PA, USA). Deionized water (18.2 MΩ·cm) was obtained from a Millipore purification system (Merck-Millipore; Darmstadt, Germany). For the LC-MS analyses, UPLC-MS-grade acetonitrile and MS-grade formic acid were used (VWR).

4.4. Sample preparation for *C. roseus* samples

Leaf samples were powdered in liquid nitrogen using a mortar and pestle. 0.2 g portions of the powdered sample were weighed, and extraction was carried out twice using 1.0 mL of a methanol–water mixture (2:1, V/V) for 2 minutes each in a 1600 MiniG® Automated Tissue Homogenizer and Cell Lyser (SPEX; Rickmansworth, UK) at 1250 rpm. The extracts were then centrifuged at 16,500 *g* for 10 minutes at 4 °C, and the supernatants were collected. These were mixed and subjected to liquid-liquid partitioning by adding 1.0 mL of n-hexane to remove carotenoids. Prior to LC-MS analysis, the methanol–water phase was filtered using a 0.22 µm PTFE syringe filter. Following filtering, 0.5 mL of the filtered sample was diluted either two-fold (using 0.5 mL of Milli-Q water containing 0.2% formic acid) or ten-fold (using 4.5 mL of Milli-Q water containing 0.11% formic acid). The diluted samples were filtered using 0.22 µm hydrophilic PTFE syringe filters before injection.

4.5. Sample preparation for *T. officinale* samples

Dried leaf-root drug samples were ground by an electric grinder. Fresh flower samples were powdered in liquid nitrogen in a mortar with a pestle. In both cases, 0.5 g sized subsamples were weighed and vortexed with 8.0 mL ethanol (80 V/V%). The extraction was performed using an ultrasonic bath for 1 hour, followed by shaking for 3 min in the 1600 MiniG® at 1250 rpm. After centrifugation (20 min, 4 °C, 8000 *g*), the supernatants were evaporated. The evaporation residues were taken up in 0.8 mL of methanol and complemented to 2.0 mL final volume with MQ water containing 0.1 V/V% formic acid. After centrifugation (10 min, 4 °C, 16,000 *g*), the supernatants were filtered through a 0.22 µm pore sized PTFE syringe filter.

The liqueur samples were diluted four-fold with MQ water containing 0.4 V/V% formic acid, then were filtered through a 0.22 µm PTFE syringe filter. Ten-fold dilutions were conducted for the quantification of caftaric acid, chicoric acid, chlorogenic acid, luteolin, luteolin 7-O-glucoside and caffeoylsucrose. Each sample group was measured in seven replicates.

The test batch samples obtained were analyzed in three technical replicates using the same sample preparation method as for the original liqueur sample.

4.6. Metabolomics and multivariate statistical analysis

A Vion ESI-IMS-QTOF-MS instrument (Waters; Milford, MA, USA) and equipped with a Z-spray ion source was connected to a Waters Acquity I-Class ultra-performance liquid chromatography (UPLC) system with a PDA detector to perform the analyses. A BEH-C_{18} reversed-phase UPLC column (100 mm × 2.1 mm, 1.7 µm; Waters) kept at 40 °C was used for the separation. Both acetonitrile and water with 0.1% formic acid (V/V) were used for gradient elution. The injected sample volume was 1 µL. Tables 2 and 3 include the related instrumental parameters.

Table 2. UPLC gradient conditions for *C. roseus* and *T. officinale* analyses

C. roseus analysis

Gradient conditions			
Eluent 'A': water with 0.1 % V/V formic acid Eluent 'B': acetonitrile with 0.1 % V/V formic acid			
Time (min)	Flow rate ($ml \cdot min^{-1}$)	A%	B%
0.0	0.4	95	5
0.5	0.4	95	5
8.0	0.4	82	18
12.0	0.4	60	40
15.0	0.4	20	80
16.0	0.4	0	100
18.0	0.4	0	100
19.0	0.4	95	5
22.0	0.4	95	5

T. officinale analysis

Gradient conditions			
Eluent 'A': water with 0.1 % V/V formic acid Eluent 'B': acetonitrile with 0.1 % V/V formic acid			
Time (min)	Flow rate ($ml \cdot min^{-1}$)	A%	B%
0.0	0.4	96	4
0.5	0.4	96	4
15.0	0.4	85	15
18.0	0.4	60	40
20.0	0.4	0	100
21.0	0.4	0	100
21.5	0.4	96	4
23.0	0.4	96	4

Table 3. ESI-IMS-QTOF-MS parameters applied for the analyses

	***C. roseus* analysis**	***T. officinale analysis***
Detector 1	PDA - 220-600 nm; 20 scans/s at 2.4 nm resolution	PDA - 220-550 nm; 20 scans/s at 1.2 nm resolution
Detector 2	Vion IMS QTOF MS with ESI ion source	
Resolution	> 40 000 (calculated for leucine enkephalin)	
Capillary voltage	0.5 kV	
Polarity	negative and positive	
Source temperature	120°C	
Desolvation temperature	550°C	
Nebulizer gas	6.5 bar N_2	
Cone gas voltage	30 V	
Desolvation gas flow	1000 L h^{-1} N_2	
Cone gas flow	150 L h^{-1} N_2	100 L h^{-1} N_2
Collision gas flow	0.15 ml min^{-1} Ar 5.0	
IMS	ON	
MS scan	*m/z* 90 – 2000	
MS scan time	0.4 s	
Lock mass	ON	
MS/MS scan	*m/z* 50 – 2000	
MS/MS collision energy	individually optimized	
MS^E low collision energy	6.0 eV	
MS^E high collision energy ramp	20.0-30.0 eV	10.0-40.0 eV

In the case of *C. roseus* measurements, a validation study that included evaluations of specificity/selectivity, linearity, accuracy, analytical range, the limits of detection (LOD) and quantification (LOQ), and the matrix effect was conducted to show the method's applicability.

Authentic standards of vinblastine and vincristine were utilized to set up the calibration for the measurement of the samples using the standard addition method. Since the concentration of 3',4'-anhydrovinblastine was determined using the authentic vinblastine standard, this method can be considered semi-quantitative for this compound.

For *T. officinale* samples, standard addition method with authentic standards was used for the quantification (for 30 identified compounds). The concentration of further 38 compounds was determined in relation to the most suitable authentic standard, which can therefore be regarded as a semi-quantitative approach. The list of compounds semi-quantified with the authentic standards is presented in Table 4.

Table 4. Compounds quantified using the semi-quantitative method in dandelion samples and the authentic standards used for this purpose

Identified compound	Authentic standard used for semi-quantification
1-Caffeyllaminaribiose	Caffeic acid
Caffeic acid derivative_1	
Caffeic acid glucoside_1	
Caffeic acid glucoside_2	
Caffeic acid sulfate_1	
Caffeic acid sulfate_2	
Caffeic acid derivative_2	
Caffeoylglycerol	
Caffeoylsucrose	
Dicaffeoylquinic acid_1	Chlorogenic acid
Dicaffeoylquinic acid_2	
Apigenin derivative	Apigenin
Schaftoside isomer_1	
Schaftoside isomer_2	
Chicoric acid derivative	Chicoric acid
Chrysoeriol	Hesperetin
Chrysoeriol rutinoside	
Esculetin sulfate	Esculetin
Isorhamnetin 3-glucoside	Isorhamnetin 3-rutinoside
Isorhamnetin disaccharide 1	
Isorhamnetin disaccharide 2	
Luteolin/kaempferol glycoside	Luteolin 7-O-glucoside
Luteolin/kaempferol rutinoside	
Luteolin/kaempferol dihexoside_1	
Luteolin/kaempferol dihexoside_2	
Luteolin/kaempferol dihexoside_3	
Quercetin rutinoside	Quercetin 3,4'-diglucoside
Quercetin derivative_1 (pentose+hexose moiety)	

Identified compound	Authentic standard used for semi-quantification
Quercetin derivative_2 (pentose+hexose moiety)	Quercetin 3,4'-diglucoside
Quercetin derivative_3 (pentose+hexose moiety)	
Quercetin derivative_4	
Quercetin dihexoside_1	
Quercetin dihexoside_2	
Quercetin dihexoside_3	
Quercetin glucoside	
Quercetin pentoside_1	
Quercetin pentoside_2	
Quercetin hexosyl derivative	

Only normalized intensity values (to compensate for differences arising from different sample preparation methods) were indicated for the remaining 16 components. The analytical range for the standard addition process was 25–1000 $\mu g \cdot L^{-1}$. The limit of quantification (LOQ) values of the compounds were defined as a signal-to-noise (S/N) ratio of 10:1 and the LOQ concentrations were equated accordingly (see Table 5). For compounds determined by the semi-quantitative approach, the LOQ value of the authentic standard used for quantification is indicated.

Table 5. LOQ values of the authentic standards

Authentic standard	LOQ [$\mu g \cdot L^{-1}$]
Apigenin	20.56
Caffeic acid	16.08
Caftaric acid	22.37
Chicoric acid	0.56
Chlorogenic acid	1.01
Chryptochlorogenic acid	26.68
Chrysin	2.60
Daidzein	1.31
Daphnetin	19.56
Eriodictyol	1.06
Esculetin	3.09
Esculin	5.02
Ethyl caffeate	26.21
Ferulic acid	22.47

Authentic standard	LOQ [µg·L^{-1}]
Fraxin	1.02
Hesperidin	1.00
Isorhamnetin 3-rutinoside	0.77
Kaempferol 3-O-rutinoside	0.11
Luteolin	0.02
Luteolin 7-O-glucoside	0.01
Naringenin	0.74
Neochlorogenic acid	24.33
Phlorizin	2.74
Quercetin 3,4'-diglucoside	2.51
Quercitrin	1.04
Robinin	1.04
Rosmarinic acid	10.61
Rutin	1.32
Sebacic acid	4.81
Umbelliferone	4.56

Data processing and multivariate statistical analyses were performed using UNIFI (version 1.9.4; Waters), Waters Connect (version 3.4.0.19; Waters), Progenesis QI (for Principle Component Analysis /PCA/; Version 27.26.1020; Nonlinear Dynamics, Quayside, Newcastle Upon Tyne, UK), EZinfo (for Partial Least Squares Discriminant Analysis /PLS-DA/, S-plot and variable importance of projections /VIP/ analyses; version 3.0.3; UMetrics AB, Umeei, Sweden), R (version 4.1.2; R Core Team; Vienna, Austria) and IBM SPSS (v29) software packages. The data are expressed as the mean ± standard deviation (S.D.).

In the case of periwinkle samples, the height of the plants ($n = 12$ in each experimental group) was compared by one-way ANOVA. The model residuals were tested for normality and homogeneity of variances by Shapiro-Wilk's and Levene's tests, respectively ($p > 0.05$). The effect of LED parameters on vinca alkaloids and metabolites was tested by one-way MANOVA. During this process, vinblastine was transformed by 1/sqrt(x) to ensure the distribution requirement. The normality of the residuals was accepted according to Shapiro-Wilk's test ($p > 0.05$). The homogeneity of variances was checked by Levene's test; it was violated in cases of catharanthine and vincristine. With a significant overall MANOVA result, one-way ANOVA tests were run with Bonferroni's correction to avoid familywise error rate inflation. In cases where a significant factor

effect was detected, pairwise comparisons were made using Games-Howell's post hoc test, which can manage the homoscedasticity violation.

In the case of dandelion samples, one-way ANOVA with Welch correction was used to compare the mean values of the samples of the leaf-root drug, the flowers, and the liqueur samples as the three levels of the independent factor variable. When ANOVA yielded a significant result ($p < 0.05$), the Games-Howell post hoc test was employed to separate the homogeneous groups of means.

The maturation process was analyzed by repeated measures of ANOVA, considering the initial, the fourth, and the seventh time points of measurement. The within-subject effects were tested using Greenhouse-Geisser Type I error correction. The estimated marginal means were then compared across the three time points using Sidak's confidence interval adjustment.

The normality requirements were tested for all models by means of the Shapiro-Wilk test ($p > 0.05$).

5. RESULTS AND DISCUSSION

5.1. Results regarding *C. roseus*

5.1.1. Plant morphology

The main indicator of phenotypic variations in the response to light conditions was considered to be plant height. Plants exposed to strong far-red irradiation (group No. 3) were considerably higher than those in the other groups, as shown in Figure 7, although a one-way ANOVA revealed that the impact was not significant ($F(4;55)=2.12$, $p = 0.09$). The effect of far-red light, which can encourage stem elongation in plants through a process known as shadow avoidance syndrome (Tan et al., 2022), is generally consistent with higher plant length. This observation cannot be directly collated with former studies on *C. roseus* (Fukuyama et al., 2015, 2013).

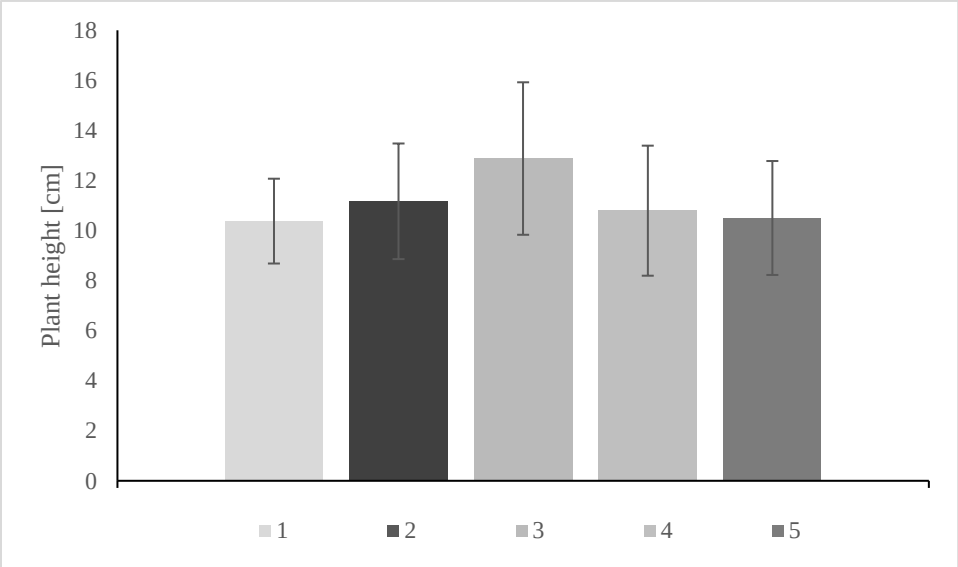

Figure 7. Plant heights after two weeks of treatment. [1 – high blue, 2 – high red, 3 – high far-red, 4 – medium light (control), 5 – low light]. Error bars represent ± 1 SD, n = 12.

5.1.2. Metabolomic profiling

A dataset of 64 vinca analytes with their elemental composition (also referred to as chemical formula or molecular formula) and accurate mass information was set up (App. A2: Table 1.), together with the favored ionization mode. Based on this list, the full scan UPLC-ESI-QTOF-MS spectra were screened for indole alkaloids, their metabolites, and precursors. Apart from vincristine and vinblastine, the other compounds were tentatively identified

with the help of their HR-MS and HR-MS/MS spectra and retention time order. Finally, 14 compounds of the related pathway could be assigned from the 64 targeted analytes (Table 6) on the basis of authentic standards (vinblastine, vincristine), of the reference MS/MS spectra from the MoNA database (catharanthine, deacetylvindoline, loganic acid, strictosidine, vindoline, vindolinine) and of the studies of Kumar et al. (2016) (serpentine), Abouzeid et al. (2017) (vincadifformine), Wang et al. (2022) (alstonine), Pan et al. (2019) (3',4'-anhydrovinblastine, secologanin), Eng et al. (2022) and Ferreres et al. (2010) (19-*S*-vindolinine).

Other than chromatography and MS data, the compounds' VIP scores were also given in Table 6. A VIP score quantifies how important a variable is in a PLS-DA model by summarizing its overall contribution to group discrimination. As a rule of thumb, in the case of LC-MS measurements, VIP > 2 values are considered to be significant in distinguishing the groups.

Table 6. List of the identified compounds of the indole alkaloid biosynthesis pathway in *C. roseus* leaves. (*) VIP scores of alstonine and serpentine could not be determined because of their partially resolved chromatographic elution. (#) Not analyzed in the positive ion mode.

No.	Component name	Elemental composition (neutral)	Detected as	Theoretical *m/z*	Experimental *m/z*	Difference, ppm	Rt, min	VIP (group #1 vs. #4)
1	19-S-vindolinine	C21H24N2O2	$[M+H]^+$	337.1911	337.1916	1.48	7.06	3.0
2	3',4'-Anhydrovinblastine	C46H56N4O8	$[M+2H]^{++}$	397.2122	397.2129	1.76	11.74	32.3
3	Alstonine	C21H20N2O3	$[M+H]^+$	349.1547	349.1554	2.00	10.65	-*
4	Catharanthine	C21H24N2O2	$[M+H]^+$	337.1911	337.1909	-0.59	10.41	< 2
5	Deacetylvindoline	C23H30N2O5	$[M+H]^+$	415.2228	415.2231	0.72	10.13	5.3
6	Loganic acid	C16H24O10	$[M-H]^-$	375.1297	375.1301	1.07	3.17	#
7	Secologanin	C17H24O10	$[M+Na]^+$	411.1262	411.1267	1.22	6.64	6.6
8	Serpentine	C21H20N2O3	$[M+H]^+$	349.1547	349.1543	-1.15	10.46	-*
9	Strictosidine	C27H34N2O9	$[M+H]^+$	531.2337	531.2339	0.38	9.63	< 2
10	Vinblastine	C46H58N4O9	$[M+2H]^{++}$	406.2175	406.2176	0.25	11.12	6.6
11	Vincadifformine	C21H26N2O2	$[M+H]^+$	339.2067	339.2070	0.88	10.55	< 2
12	Vincristine	C46H56N4O10	$[M+2H]^{++}$	413.2071	413.2076	1.21	10.72	2.9
13	Vindoline	C25H32N2O6	$[M+H]^+$	457.2333	457.2327	-1.31	11.25	2.6
14	Vindolinine	C21H24N2O2	$[M+H]^+$	337.1911	337.1915	1.19	8.01	< 2

The discovery of numerous vincristine isomers made the use of the authentic standard of vincristine crucial (see Figure 8 for the extracted ion chromatogram of the accurate mass of vincristine). Therefore, the resolution of isomers from the authentic compound with the help of UPLC was a key feature for the accurate quantification of vincristine.

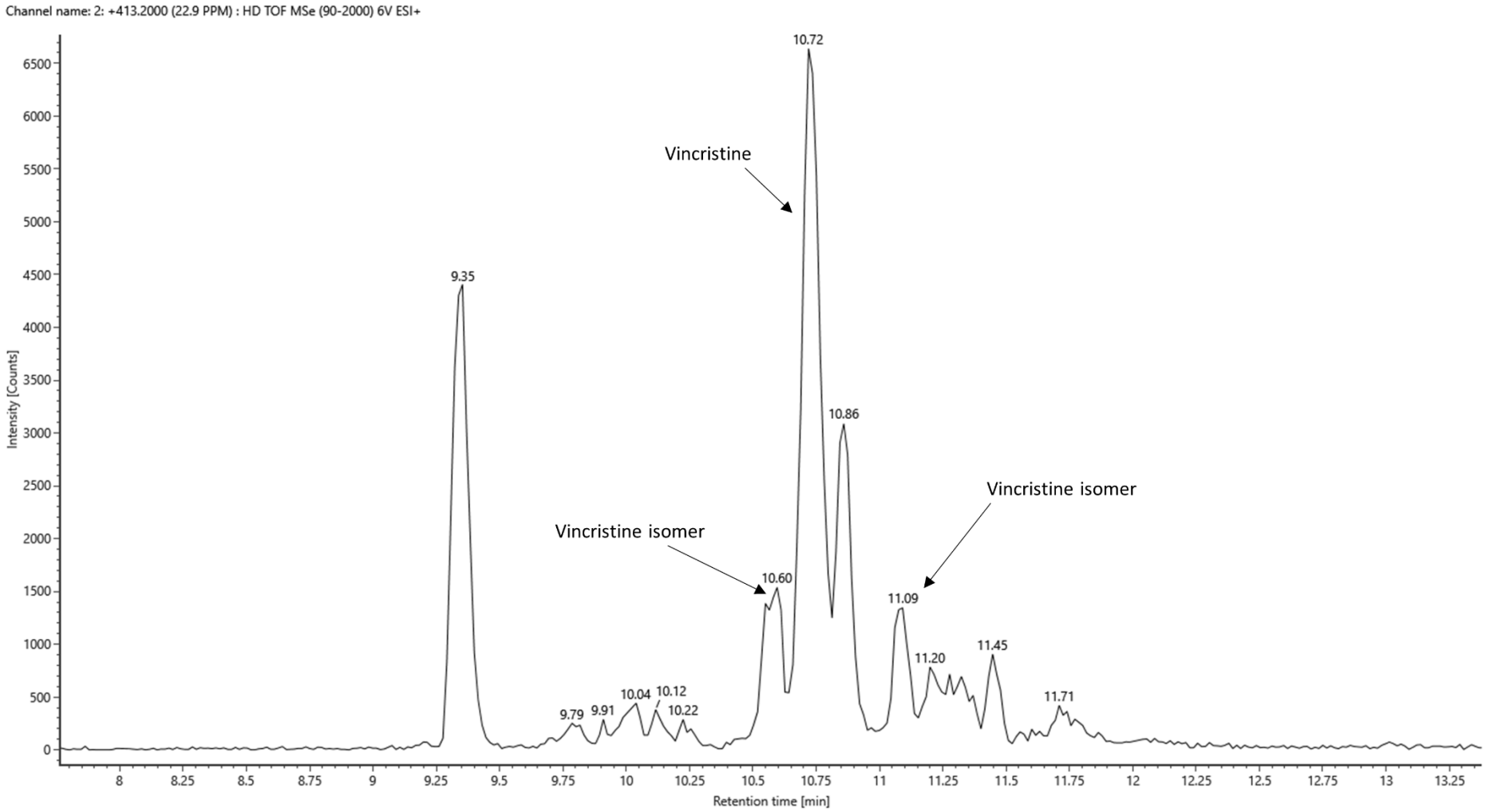

Figure 8. Extracted ion chromatogram of vincristine (from *C. roseus* leaf sample – blue light treatment), detected as $[M+2\ H]^{++}$ in the positive ESI mode. The retention time of the analyte (Rt = 10.72 min) was validated with the use of an authentic standard.

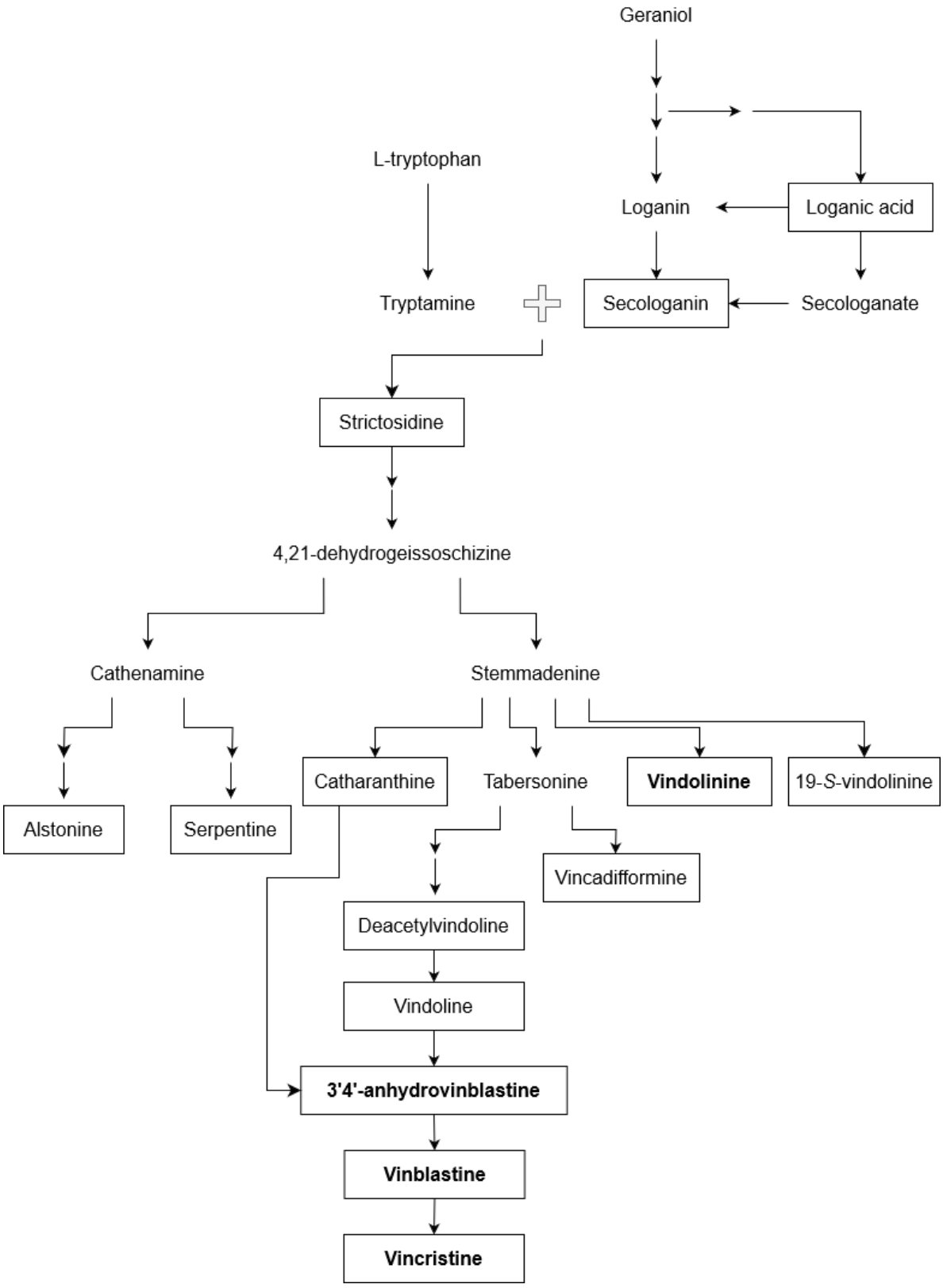

Figure 9. Schematic diagram of the indole alkaloid biosynthesis pathway (Eng et al., 2022; KEGG Indole alkaloid biosynthesis - Reference pathway). The framed components could be identified in the analyzed samples. The components that showed significantly higher abundance as a result of the high blue LED treatment are marked in bold.

Appendices 4. (App. Figure 1), 5. and 6. (App. Figure 2) also presents the extracted ion chromatograms and all full scan MS spectra of the 14 analytes assigned in the study that are shown framed in Figure 9. Some of the metabolites of the indole alkaloid pathway (see the unframed compounds) could not be unambiguously detected in any of the samples, because of either inadequate retention on the applied C_{18} column, low concentration hampering high quality MS/MS acquisition, or the lack of authentic standards that would have been required to assign the target analytes among the series of isomers.

5.1.3. Quantification and statistics

For both vinblastine and vincristine, the performance characteristics were examined using both the standard addition method and external calibration (Table 7). For external calibration, the analytical range was 10–250 $\mu g \cdot L^{-1}$; for the standard addition procedure, it was 25–100 $\mu g \cdot L^{-1}$. Both vincristine and vinblastine showed signal enhancement (Table 7) however the calculated matrix effect never exceeded 10%. Therefore, standard addition was eventually addressed for the more accurate quantification, even though external calibration would still have been an appropriate option.

Table 7. Performance characteristics of the UPLC-MS/MS method.

		Regression equation		**LOD [$\mu g \cdot L^{-1}$]**	**LOQ [$\mu g \cdot L^{-1}$]**	**Matrix effect**
Vinblastine	External calibration	$y = 3.6459x$	$R^2 = 0.9991$	5	10	8.1%
	Standard addition	$y = 4.0083x + 182.33$	$R^2 = 0.9944$	10	25	
Vincristine	External calibration	$y = 3.3054x$	$R^2 = 0.9998$	5	10	10.0%
	Standard addition	$y = 3.6450x + 294.39$	$R^2 = 0.9954$	10	25	

Two primary statistical analyses were conducted to establish the light dependence of the production of recognized or assigned indole alkaloids. Initially, the target analyte abundances were used to calculate the overall MANOVA, and the outcome was significant (the unexplained variance rate: Wilk's lambda < 0.001, $p < 0.001$). For loganic acid, 3',4'-anhydrovinblastine, vinblastine, vincristine, vindolinine, and 19-*S*-vindolinine, the subsequent univariate ANOVA

tests with Bonferroni's correction showed a significant factor effect ($F(4;20) > 6.01$, $p < 0.01$). The factor effect was insignificant for strictosidine, deacetylvindoline, and vincadifformine ($F(4;20) < 2.96$, $p > 0.4$), but it was slightly significant for vindoline, catharanthine, and secologanin with F(1:20) values between 3.3 and 4.9 (Bonferroni's: $0.05 < p < 0.1$).

Ultimately, the findings of the five different light treatments were directly comparable according to Games-Howell's pairwise comparison (App. A7: Table 3). The two primary precursors of 3',4'-anhydrovinblastine, catharanthine and vindoline, did not exhibit significant changes at any light intensity or spectral combination, despite the fact that the amount of 3',4'-anhydrovinblastine was significantly higher under blue light and at low light intensity than at other spectral combinations (App. A7: Table 3, App. A7: Figure 4).

Fukuyama et al. (2015) investigated how red light intensity affected the accumulation of vindoline and catharanthine and they discovered that the highest concentration of alkaloids was observed at low light intensity of 150 $\mu mol \cdot m^{-2} \cdot s^{-1}$ as opposed to 300 or 600 $\mu mol \cdot m^{-2} \cdot s^{-1}$. This outcome is consistent with our discovery that alkaloids accumulated more at lower light intensities. However, a highly significant effect was induced when blue light was used.

When a large proportion of blue light was employed, the concentrations of vinblastine, vincristine, and 3',4'-anhydrovinblastine were significantly higher (group No. 1). When compared to other spectrum combinations, it produced an impressive 15-fold increase in the concentration of these important vinca alkaloids. This increase was as significant as the findings of Yu et al. (Yu et al., 2015) under UV-B treatment or Fukuyama et al. (Fukuyama et al., 2017) under UV-A treatment.

Although not to the same degree as under UV-A irradiation, blue light also increased the vinblastine content in the latter study. The authors recommended using UV light only briefly prior to harvest because UV treatments have negative effects on the growth. Our experiment showed that blue light used for two weeks can also be as effective as UV treatment. These findings confirmed that the short wavelength of light can likewise stimulate the synthesis of these alkaloids, in line with previous results (Li et al., 2022; Ouzounis et al., 2015).

To match the dynamic range of the UPLC-ESI-QTOF-MS setup, multivariate statistical analyses were performed for both the two-fold and ten-fold diluted samples. In both cases, the PCA analysis was able to successfully separate group No. 1 (see Figures 10 and 11); but, group No. 4 (the control group) could not be clearly distinguished from the other experimental groups. To emphasize the metabolic changes generated by blue light, VIP scores for the modeling coefficients of PLS-DA were determined.

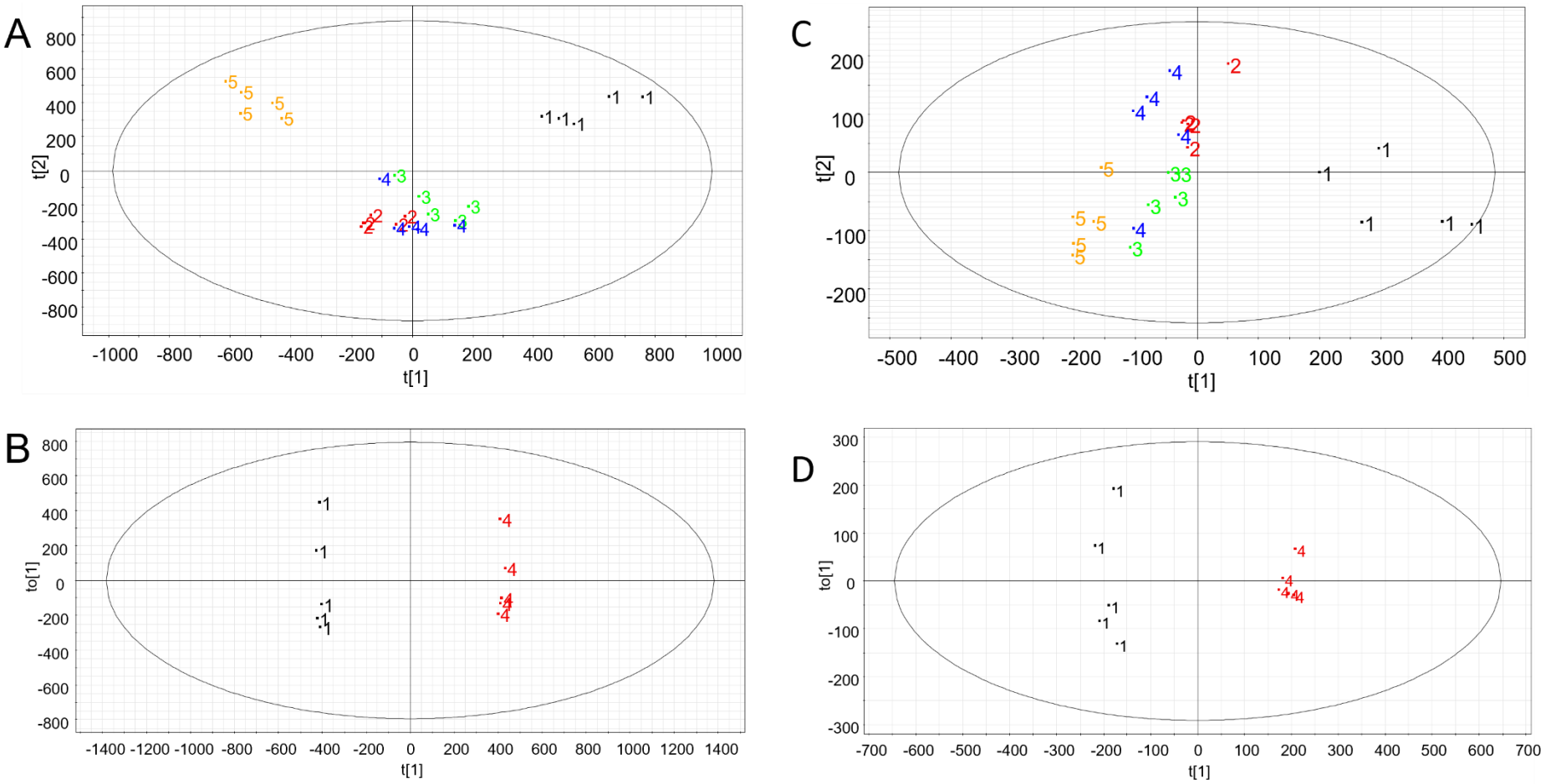

Figure 10. Multivariate statistical analyses of the two-fold (A, B) and ten-fold (C, D) diluted dandelion sample extracts. A, C – PCA; B, D – PLS-DA

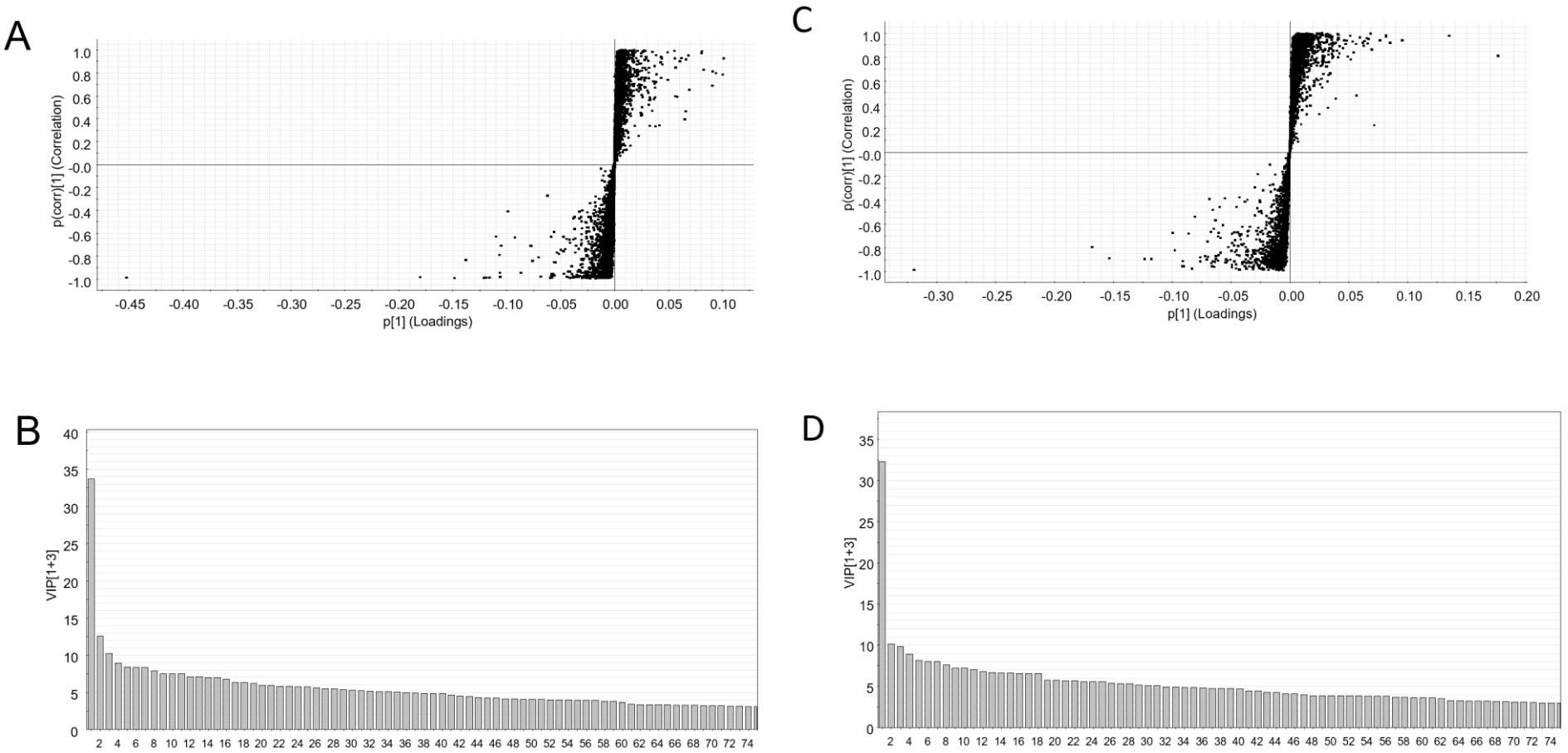

Figure 11. Multivariate statistical analyses of the two-fold (A, B) and ten-fold (C, D) diluted dandelion sample extracts. A, C – S-plot; B, D –VIP scores

Experimental groups Nos. 1 and 4 (high blue and control conditions, respectively) were included in the PLS-DA, S-plot, and VIP scores due to the ANOVA results and the higher abundance of key compounds in these groups. In these, 4858 molecular entities (molecular features) were encountered in the positive ion mode analysis, out of which the entities with a VIP score > 2 were regarded as the most contributory variables; finally 165 entities exceeded this limit. The two most significant vinca alkaloids (vinblastine and vincristine) as well as their direct precursors – catharanthine, vindoline, and, lastly, 3',4'-anhydrovinblastine – which had the highest VIP score (32.3) of the 165 metabolites (see Table 8) – proved to be highly discriminative in group No. 1 (high blue) when compared to the control group (group No. 4).

The results showed that among the metabolites that were particularly activated by high blue light exposure, the important metabolites of the vinca alkaloid pathway were highly represented. These VIP scores should anyhow be regarded in the view of the Games-Howell's post hoc test results to match the discriminative power with the abundance/concentration data; accordingly, the high blue LED application was finally responsible for the significant enrichment of four vinca alkaloids, that is, vinblastine, vincristine, 3',4'-anhydrovinblastine and vindolinine (App. A7: Table 3). Table 8 and Figure 12 show the final concentration ranges (961 mg·kg^{-1} DW, 33.8 mg·kg^{-1} DW, and 11.7 mg·kg^{-1} DW for 3',4'-anhydrovinblastine, vinblastine, and vincristine, respectively). The concentration of vinblastine in the high blue light group exceeds some of the recently published levels in screening studies (13.1 mg·kg^{-1} DW) (Mujib et al. 2022) and even after UV-A irradiation (2–30 mg·kg^{-1} DW) (Fukuyama et al., 2017). This is also true for vincristine (4.22 mg·kg^{-1} DW) (Mujib et al. 2022). However, the concentration levels reported in the literature cannot always be directly compared with our study in a straightforward manner due to either different production schemes (e.g., callus culture) or different analytical approaches.

Table 8. Average concentrations of 3’,4’-anhydrovinblastine, vinblastine and vincristine in the five experimental groups

	Concentration (mg·kg^{-1} DW) (± 1 SD)		
Group No.	3’,4’-anhydrovinblastine	Vinblastine	Vincristine
1	961 ± 137	33.8 ± 4.71	11.7 ± 0.85
2	69.9 ± 8.50	2.68 ± 0.26	0.59 ± 0.11
3	123 ± 28.8	4.38 ± 0.85	0.92 ± 0.13
4	83.0 ± 15.7	3.66 ± 0.46	0.78 ± 0.12
5	337 ± 119	15.1 ± 4.51	4.44 ± 1.50

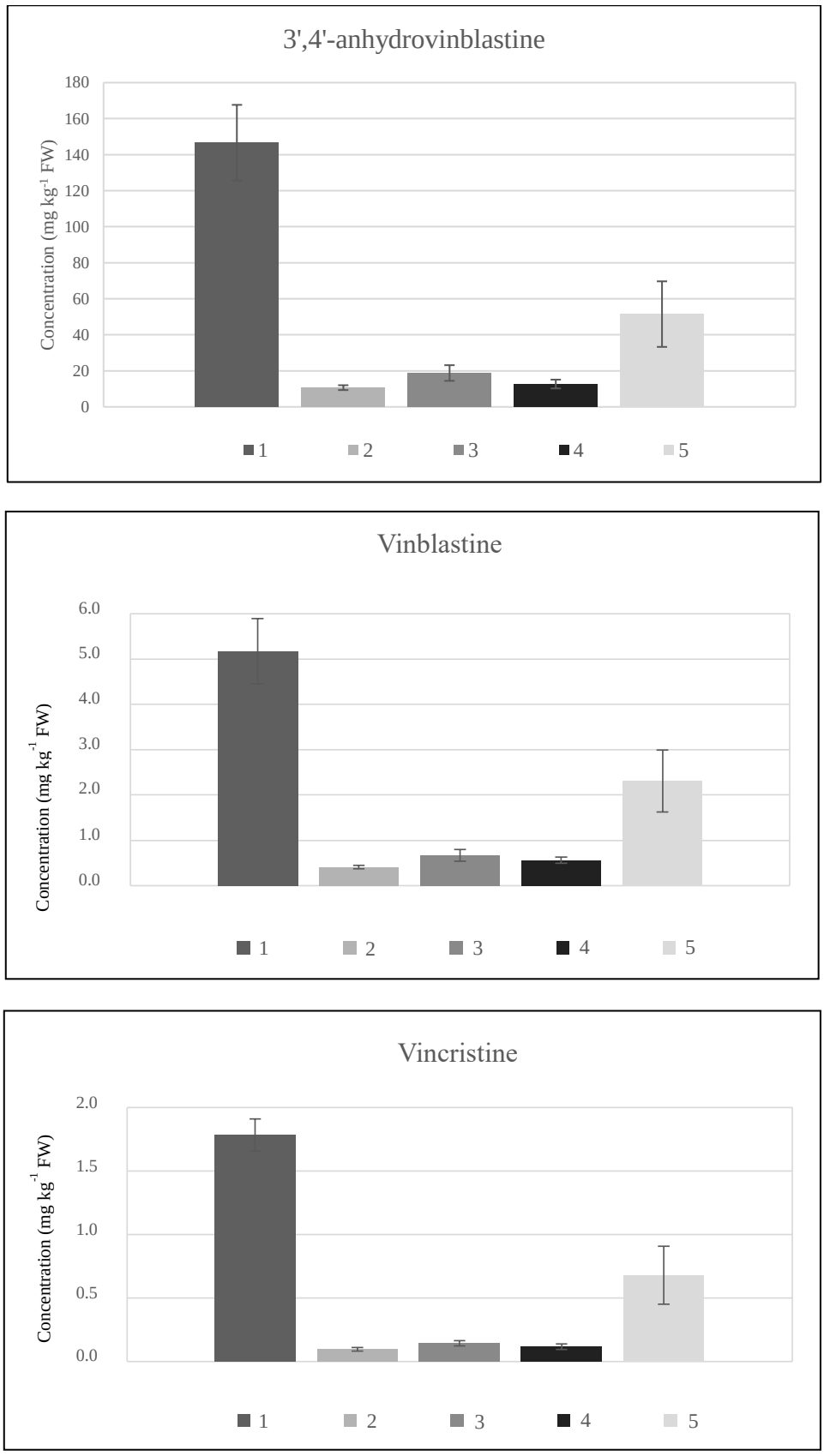

Figure 12. Concentrations of 3',4'-anhydrovinblastine, vinblastine and vincristine in the five experimental groups [1 – high blue, 2 – high red, 3 – high far-red, 4 – medium light (control), 5 – low light]. Error bars represent +/- 1 SD.

The light-dependent regulation of the synthesis of indole alkaloids is poorly understood. Comparing etiolated and light-treated *C. roseus* seedlings, Vazquez-Folta and Luca (1998) demonstrated the participation of photoreversible phytochromes in the regulation of the enzymes responsible of vindoline biosynthesis at gene expression level. Red light treatment promoted, while far-red light reversed these effects. Some transcriptional factors, like GATA and PIF were identified in the regulatory pathway responsible for the vindoline and vinblastine synthesis, but the blue-light-induced accumulation of these metabolites is not yet known.

Yu et al. (2015) reported that while the majority of the structural genes in the alkaloid biosynthesis pathway were upregulated, UV-B radiation also increased the indol alkaloids in *C. roseus*. It is possible that UV and/or blue light photoreceptors are also engaged in these processes, even though a thorough analysis has not yet been done. Our results confirmed this hypothesis, but more research is needed to identify the blue-light-mediated photoreceptors implicated in the production of vinblastine and vindoline. This is especially important as the dimerization (formation) of 3',4'-anhydrovinblastine is often regarded as a bottleneck in the synthesis (and evidently, when aiming at the high production yield) of vinblastine and vincristine (Asano et al., 2016), and our experiments revealed this bottleneck might be eliminated by the application of blue light irradiation.

5.2. Results regarding *T. officinale*

5.2.1. Metabolomic profiling

Given the production process of dandelion liqueur, liquid chromatography considered the most suitable analytical technique for assessing both the qualitative and quantitative composition of metabolites extracted from the flowers and for comparison with the raw plant material. The bioactive secondary metabolites of dandelion are predominantly organic acids, flavonoids, and terpenoids (see App. A2: Table 2), which are particularly suitable to analysis by reversed-phase UPLC methods.

At first look, the total ion chromatograms of the measurements performed in ESI "-" mode revealed the anticipated differences in the metabolite profile of dandelion leaf-root drug, flowers, and flower-based liqueur (Figure 13). The accumulation and detection of different metabolites in the various plant parts is the primary cause of the differences. Additionally, the production method has a significant impact on the composition of the liqueur product: the average intensity of the compounds is one or even several orders of magnitude lower than that of the plant parts, and the chromatogram of the liqueur shows surprisingly few detectable peaks.

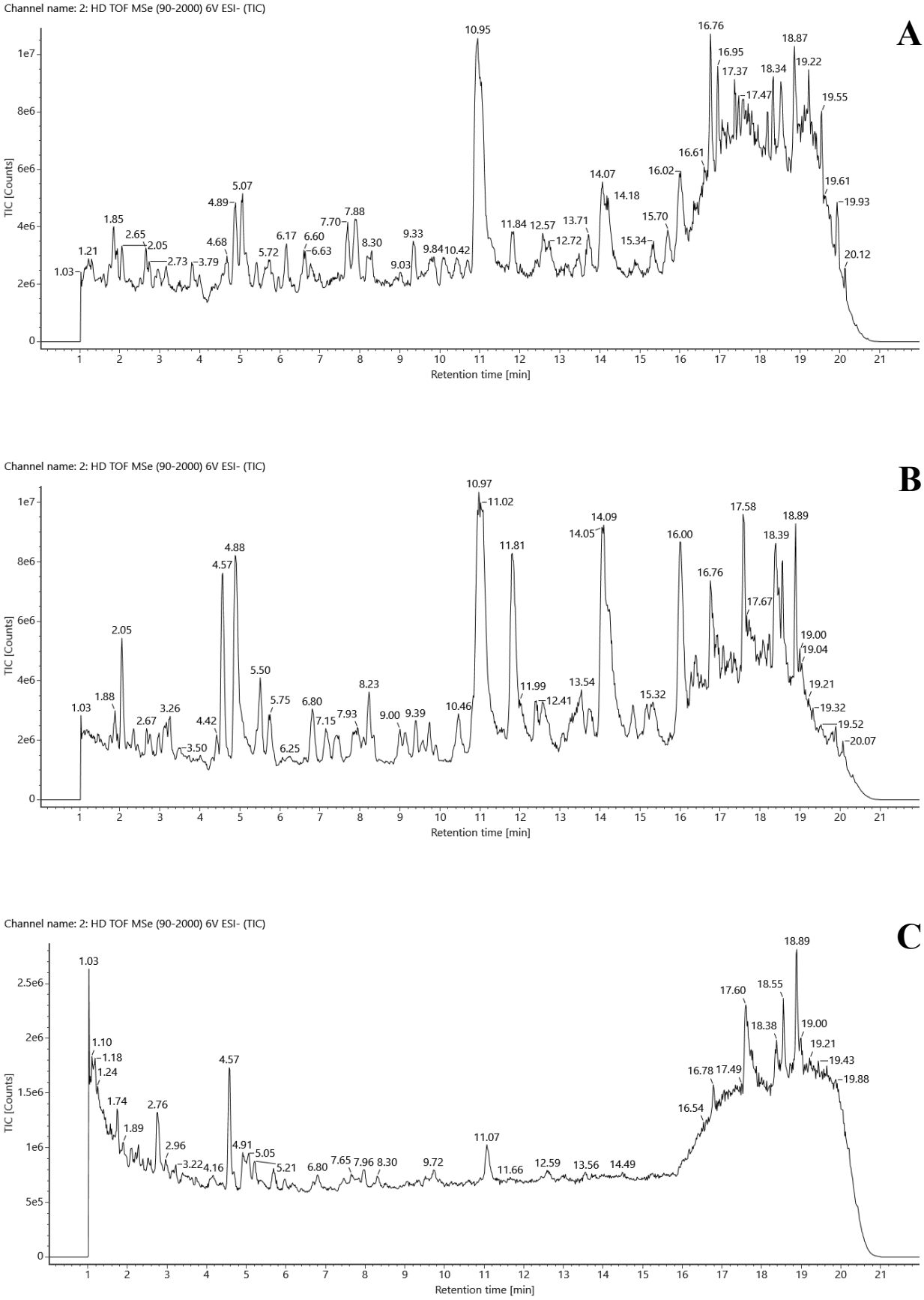

Figure 13. Typical total ion chromatograms (TICs) of dandelion leaf-root drug (A), dandelion flowers (B), and dandelion liqueur (C) in the negative ion mode

This is explained by the use of a low recovery extraction technique (mechanically unassisted maceration) during production. A tangible way to interpret the differences between sample groups is to identify as many secondary metabolites as possible, thus providing a snapshot of the biochemical processes that took place in different parts of the plant, as well as which metabolites from the flowers made it into the liqueur product and what transformations they may have undergone during its maturation process.

Detailed analysis was performed for all four approaches described in Chapter 3.1., A3. and App. A6: Figure 3 contain the chromatographic, ion mobility and MS data of the components identified to any degree in any of the examined sample groups (except for the fragmentation patterns of daphnetin and ferulic acid, as the low-mass fragments of these two components cannot be detected at adequate quality). By running the available standard set of 63 compounds used for plant metabolite profiling, I could identify and quantify 30 compounds (see App. A8: Table 5). Subsequently, the list of potential target compounds was determined using the methods described above. A total of 84 components were identified – of which 54 were tentative –, on the basis of authentic standards, of the reference MS/MS spectra from the MoNA, MassBank and LIPID MAPS® databases, and of the studies listed (Commisso et al., 2019; Fan et al., 2020; Gidda et al., 2003; Marinaccio et al., 2025; Piazzon et al., 2012; Plazonić et al., 2009; Wu et al., 2016; Yang et al., 2017; Zuo et al., 2020) in App. A2: Table 2 and A3. The degree of identification according to Çiçek et al. (2024) is also included.

Here, it should be highlighted that the selectivity parameters of the validation process in the case of analytes identified without authentic standards cannot be compared to the cases when the ISO/IEC 17025:2017 (International Organization for Standardization, 2017) standard is regarded as a reference. For tentatively identified compounds where even the MS/MS data might also be missing, selectivity is limited to some of the reproducible but highly instrumental setup dependent data such as retention time (=a function of the actual LC system and chromatographic column), ESI adducts (=a function of the actual chromatographic eluents, the ion source and its settings), ion mobility data (=recorded with an inherent standard deviation of +/- 1%), and MS/MS data (=a function of vendor-dependent default instrumental characteristics and actual settings). All these cannot exclude the possibility of not only the co-eluting stereoisomers but simpler isomers (e.g., whether any of the hexoside moieties is galactose or glucose) too. Hence, the use of the degree of identification (analytical confidence level, which is not meant here as a statistical term) is the only straight way to characterize selectivity.

When referring to the four approaches listed in section 3.1., I could identify 35% of the 84 compounds using authentic standards; 11% was based on literature data, 34% were regarded as

major compounds, while multivariate statistical analysis drew my attention to the remaining 20%, respectively. Overall, it can be said that the standards at my disposal were important starting points for further investigations, because they included several secondary metabolites that are characteristic of dandelion, and also the information obtained during their investigation contributed greatly to the identification of their derivatives.

Twenty components were identified from a large family of compounds derived from caffeic acid using the fragmentation pattern of caffeic acid in negative mode (Figures 14 and 15).

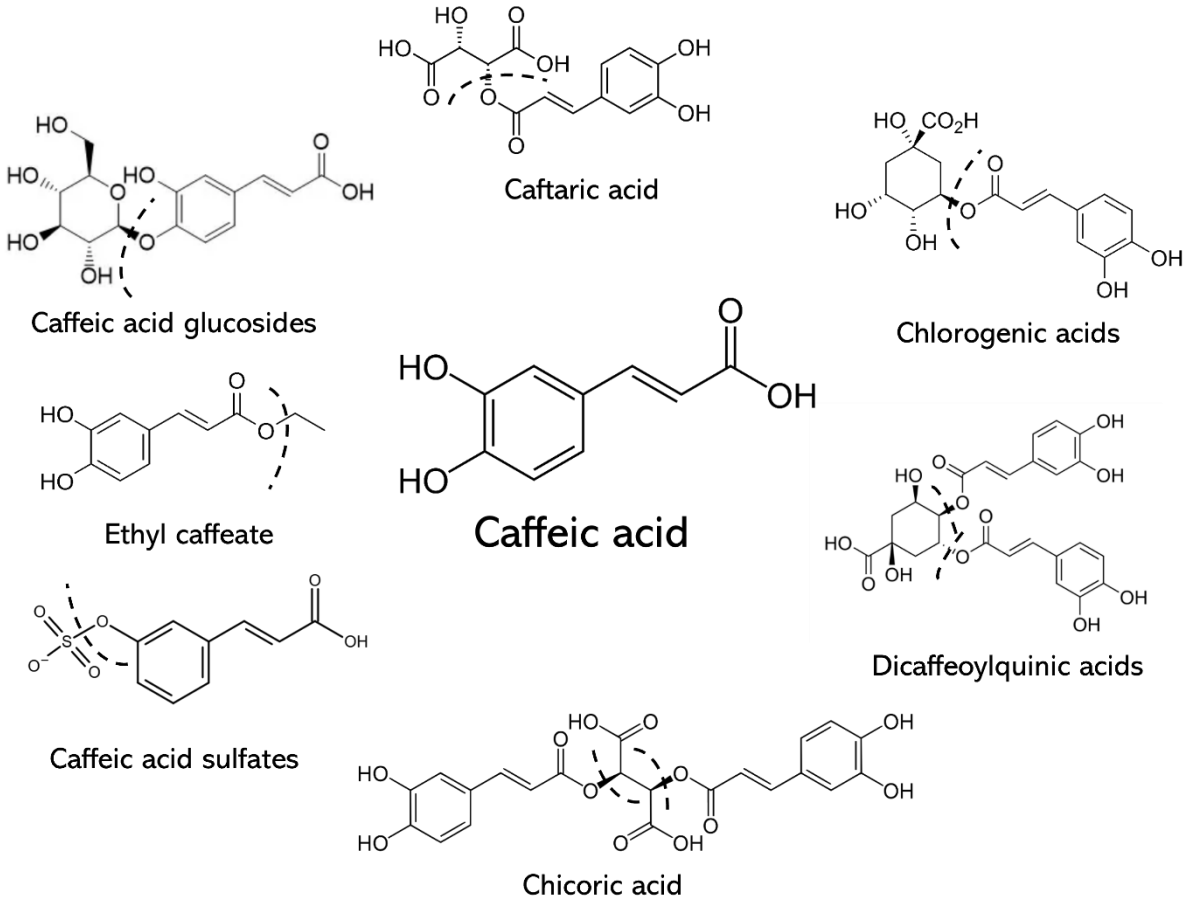

Figure 14. The formula of caffeic acid and a few derivatives identified in the dandelion samples. The caffeic acid fragment appearing in the compounds is marked.

To identify the derivatives, it was necessary to analyze characteristic fragment ions of other parts of the molecules or losses occurring during fragmentation, such as the hexose loss ($C_6H_{10}O_5$, $\Delta m/z$ = 162.0528) found in the fragmentation pattern of caffeoyl glucosides, the SO_3 loss ($\Delta m/z$ = 79.9568) in the caffeic acid sulfates, the fragment derived from the tartaric acid part ($C_4H_5O_6^-$, m/z = 149.0092) of chicoric acid and caftaric acid, or the quinic acid fragment ($C_7H_{11}O_6^-$, m/z = 191.0561) found among the fragments of chlorogenic acid derivatives. No

corresponding MS/MS spectrum was found for the caffeic acid derivative with the molecular formula C21H28O14 (compound no.12), but the analysis of its fragment pattern suggested that a caffeoyl glucoside moiety is linked to a hexose (the neutral loss was observed), so this component was tentatively identified as caffeoylsucrose.

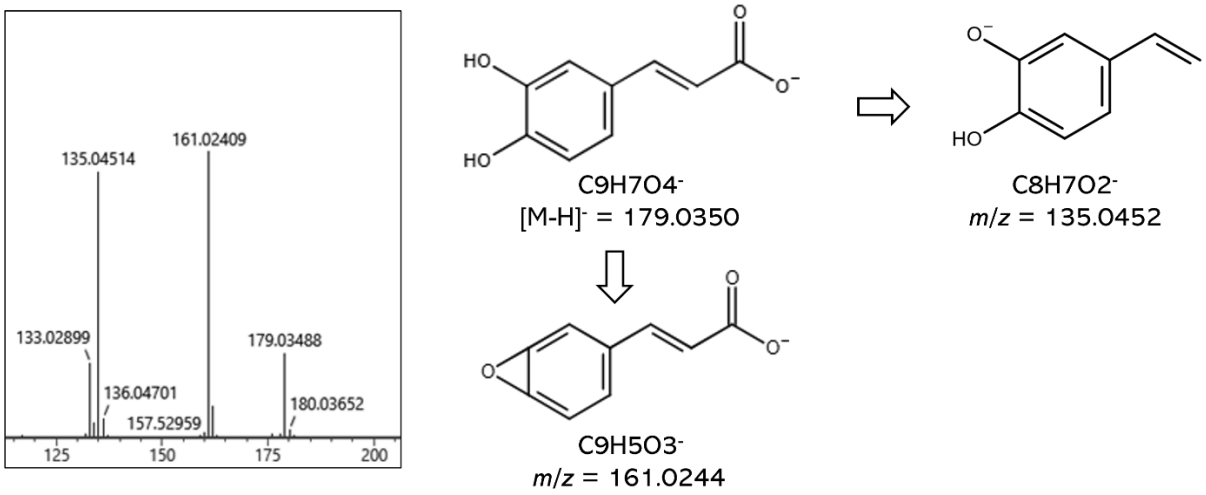

Figure 15. The proposed fragmentation pattern of caffeic acid in the negative ion mode. The insert shows the MS/MS spectrum (ESI '-' mode) of caffeic acid from the leaf-root drug sample.

Another family of molecules occurring in large quantities in dandelion is the flavonoids. The general chemical structure of flavonoids is a 15-carbon skeleton consisting of a heterocyclic ring (C) and two phenyl rings (A and B). Flavonoid compounds frequently undergo retro Diels-Alder (RDA) reactions in MS/MS under high-energy collisions (Śliwka-Kaszyńska et al., 2022), which cause a cleavage in the C-ring's C–C bond and produce distinctive diagnostic fragment ions (Figure 16).

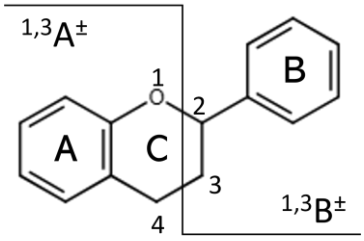

Figure 16. The structure of the flavonoid skeleton and the 1,3-cleavage caused by the retro Diels-Alder (RDA) reaction.

These ions offer important information about the type and position of substituents on the A- and B-rings. The most prominent fragmentations involve cleavage between the heterocyclic oxygen atom and the second carbon atom and after the third carbon atom, resulting in structurally informative $^{1,3}A^{\pm}$ ions and the corresponding $^{1,3}B^{\pm}$ ions. The characteristic fragments were observed in the MS/MS spectra of three flavonoids, luteolin [$^{1,3}A^{\pm}$ ion: $C7H3O4^-$ (*m/z* = 151.0037), $^{1,3}B^{\pm}$ ion: $C8H5O2^-$ (*m/z* = 133.0295)], naringenin [$^{1,3}A^{\pm}$ ion: $C7H3O4^-$ (*m/z* = 151.0037), $^{1,3}B^{\pm}$ ion: $C8H7O^-$ (*m/z* = 119.0502)], and apigenin [$^{1,3}A^{\pm}$ ion: $C7H3O4^-$ (*m/z* = 151.0037), $^{1,3}B^{\pm}$ ion: $C8H5O^-$ (*m/z* = 117.0346)], but they had little identification potential because they appeared with too low intensity in the fragmentation pattern of derivatives during even high-energy fragmentation. For the same reason, it has become difficult to distinguish between different glycosylated flavonoid derivatives in which the aglycones are isomers – this problem has arisen primarily in the determination of luteolin and kaempferol derivatives. Dandelion contains large amounts of luteolin and its glycosylated forms (Williams et al., 1996), so it can be assumed that the components found are luteolin derivatives. As regards kaempferol derivatives, I could detect kaempferol 3-O-rutinoside in small quantities using the authentic standard, so it cannot be excluded that kaempferol derivatives may also be present in the samples.

Among the flavonoids, various quercetin and isorhamnetin (3-methylquercetin) derivatives were well represented, with a total of 21 compounds identified. The identification of quercetin glycosides is aided by the characteristic, intense fragment signal of the aglycone, which also often contains the negatively charged ion of the stabilized ring form, and, with low intensity, the $1,3A^{\pm}$ ion (*m/z* = 151.0026) from the RDA reaction as well as other characteristic fragments (see Figure 17 and App. A6: Figure 3). In the case of isorhamnetin derivatives, CH3 loss ($\Delta m/z$ =15.0235) resulting from the detachment of the methyl group can be noticeable. The different sugar losses provided information for distinguishing between the various glycosylated derivatives [pentose loss: C5H8O4 ($\Delta m/z$ = 132.0423), hexose loss: C6H10O5 ($\Delta m/z$ = 162.0528), rhamnose loss: C6H10O4 ($\Delta m/z$ = 146.0579), dihexoside loss: C12H20O10 ($\Delta m/z$ = 324.1057) and rutinose loss: C12H20O9 ($\Delta m/z$ = 308.1107)]. However, due to the large number of possible isomers, other orthogonal techniques or the use of authentic standards would be required for higher-level identification of these compounds.

According to the literature, various long-chain carboxylic acids and their hydroxylated derivatives have been detected in different parts of the dandelion plant (see App. A2: Table 2). Hydroxylated derivatives from this compound group can be measured using RP-HPLC technique, and due to their relatively apolar nature, their appearance can be expected at a longer retention time.

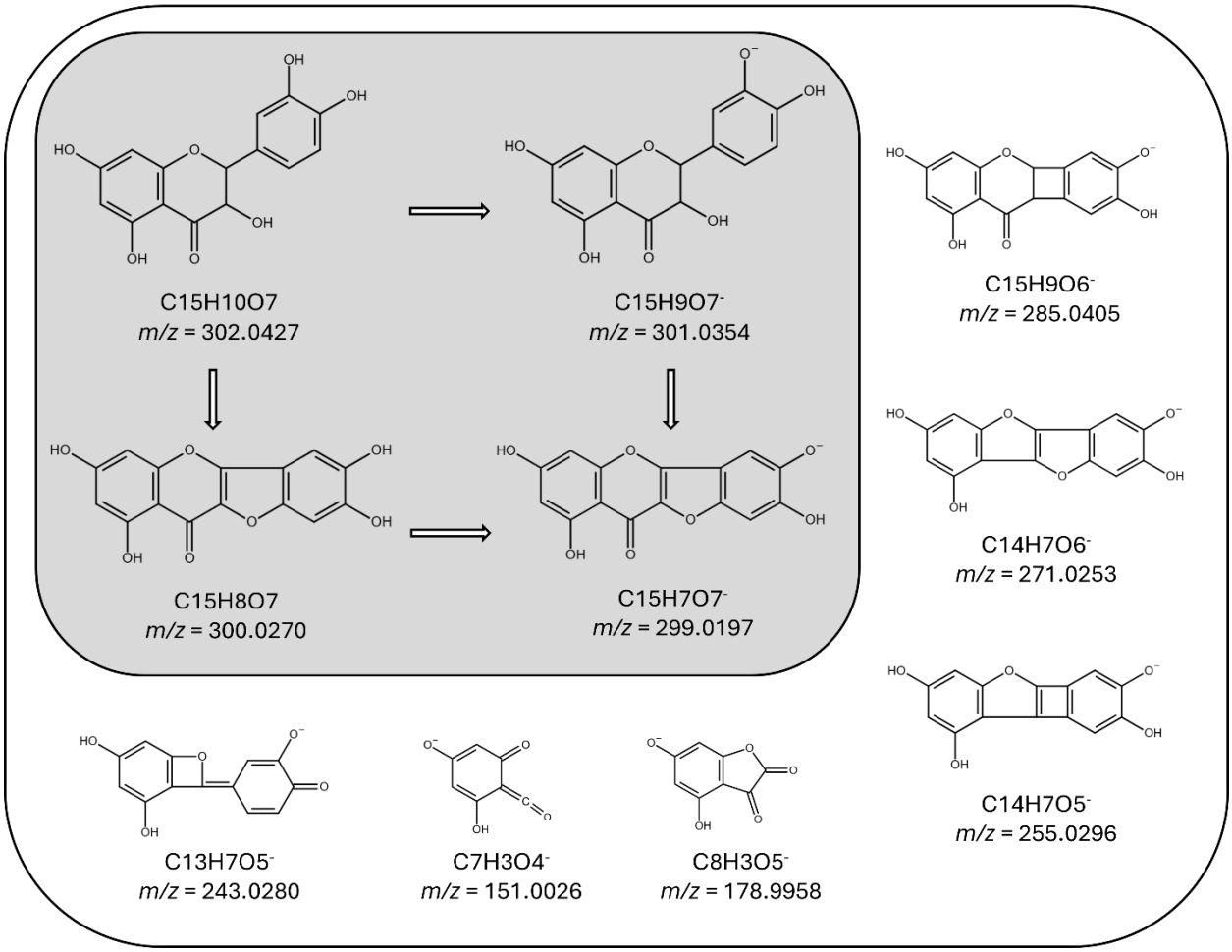

Figure 17. The proposed fragmentation pathway of quercetin.

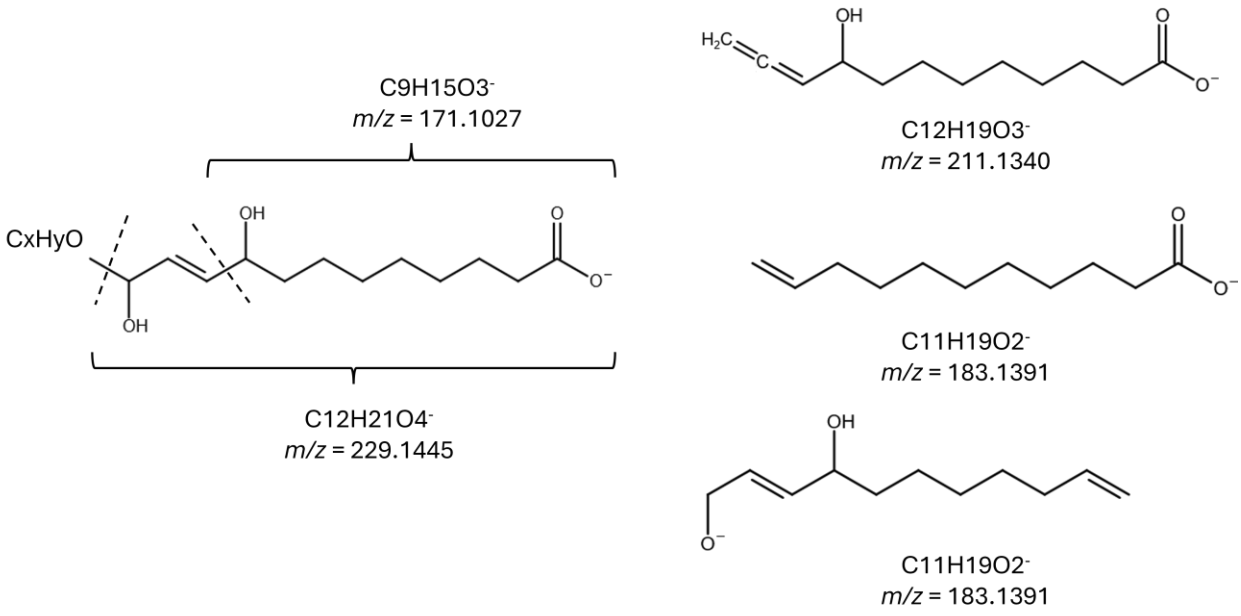

Figure 18. The proposed fragment structures of the tentatively identified hydroxylated fatty acids (compounds no. 79 and 80). CxHyO: no.79. – C6H10O; no.80. – C6H12O

I could tentatively identify five different hydroxylated fatty acids, all of which have a C18 carbon chain and differ only in the number and location of hydroxyl groups and double bonds in their structure. Four of them share a common fragment, ($C_9H_{15}O_3^-$, *m/z* = 171.1027), which appears in all four fragmentation patterns. In addition, three further fragments match in the fragment patterns of compounds no. 79 and 80, indicating even closer structural similarity (see Figure 18). The structure of the five hydroxylated fatty acids was proposed using LIPID MAPS®, without complete stereochemical identification.

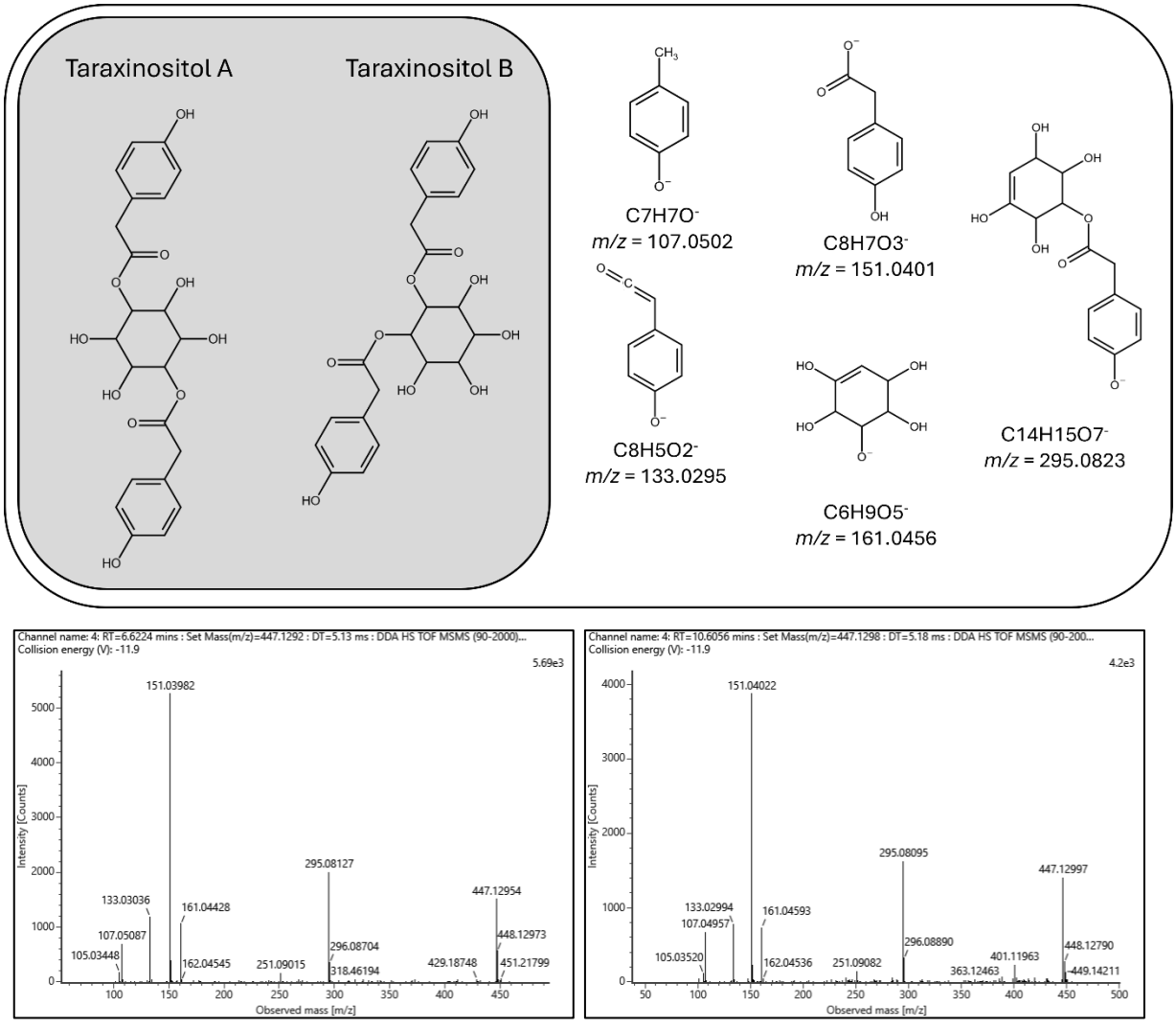

Figure 19. The structural formulas, the proposed fragment structures and the MS/MS fragment spectra of taraxinositol A and B.

Taraxinositol A and taraxinositol B are two compounds that have been reported from the root of *T. coreanum* (Mo et al., 2017). However, their presence in *T. officinale* has not yet been demonstrated, nor has their fragmentation pattern been published. During this study I could

tentatively identify both compounds in plant samples, record their MS/MS spectra, and propose the structure of their characteristic fragments (see Figure 19).

The results obtained were compared with the list of compounds formerly reported in the literature (App. A2: Table 2). Partial identifications with low identification levels that appeared in some of the publications could not be considered here; finally, 24 compounds were found (see Table 9), that had not previously been reported with a high level of identification in *T. officinale*, 13 of which were identified using authentic standards.

Table 9. List of compounds that have been reported for the first time in dandelion-related samples

New identified compound	Sample that contains it
Protocatechuoylglucose_1	leaf-root drug, flowers, liqueur
Caffeic acid sulfate_1	liqueur
Protocatechuoylglucose_2	leaf-root drug, flowers, liqueur
Esculetin sulfate	liqueur
Caffeic acid sulfate_2	leaf-root drug, liqueur
Caffeoylsucrose	leaf-root drug, flowers, liqueur
1-caffeyllaminaribiose	leaf-root drug, flowers, liqueur
Daphnetin*	leaf-root drug, liqueur
12-Hydroxyjasmonate sulfate_1	leaf-root drug, flowers, liqueur
Taraxinositol A	leaf-root drug, flowers, liqueur
Taraxinositol B	leaf-root drug, flowers, liqueur
Fraxin*	flowers
12-Hydroxyjasmonate sulfate_2	flowers
Robinin*	leaf-root drug
Kaempferol 3-O-rutinoside*	leaf-root drug, flowers, liqueur
Quercitrin*	leaf-root drug, flowers, liqueur
Isorhamnetin 3-rutinoside*	leaf-root drug, flowers, liqueur
Rosmarinic acid*	leaf-root drug
Hesperidin*	leaf-root drug, liqueur
Phlorizin*	leaf-root drug, flowers
Sebacic acid*	leaf-root drug, liqueur
Ethyl caffeate*	leaf-root drug, flowers, liqueur
Naringenin*	leaf-root drug, flowers, liqueur
Chrysin*	flowers, liqueur

*identified with authentic standards

5.2.2. Compound distribution in the plant and liqueur samples

Lima et al. (2025) examined the polyphenol content of jaboticaba [*Plinia cauliflora* (Mart.) Kausel] dry wine, liqueur, sweet wine, and juice products. The differences in ion intensity results between the juice and liqueur samples showed that the fermentation process and alcohol concentration facilitate a more effective transfer of metabolites from jabuticaba fruit to the beverage. Myrtle [*Myrtus communis* (L.)] liqueurs' phenolic components alter significantly with time, as Vacca et al. (2003) showed in a one-year follow-up study. Exposure to air accelerates these changes, causing the product's proanthocyanidins and flavans to rapidly decline and the anthocyanins to disappear after just four months. Falcone et al. (2025) examined great yellow gentian [*Gentiana lutea* (L.)] and liqueur made from its roots, pointing to changes in the metabolomic profile, primarily the absence of gentiopicroside and amarogentin in the product. These former findings highlighted the trends that could be expected from the dandelion samples, as well as the complexity of evaluating the data in this current study.

Quantitative analysis of the samples was performed (see Table 10). Most of the components first identified in this actual study in *T. officinale* clearly fit into the molecular groups described above. These include caffeic acid derivatives (caffeic acid sulfates, caffeoyl-dihexosides, ethyl caffeate), coumarin derivatives (esculetin sulfate, daphnetin, fraxin), and products of the flavonoid biosynthesis pathway and their derivatives (e.g., robinin, quercitrin). Of particular interest are taraxinositol A and B, which are present in all samples and have so far only been found in *T. coreanum*. Most of the newly reported compounds are abundant in all parts of the plant, and most of them could also be detected in the liqueur samples as well. However, fraxin and crysin were only found in flower samples, while robinin and hesperidin were only found in the leaf-root drug. It is also important to highlight the four sulfated derivatives of caffeic acid and esculetin, which I probably would not have identified by examining the plant samples alone, either because of the matrix-effect or their low concentration; however, their greater presence in the liqueur samples drew my attention to them.

Comparing the results with data from the literature (App. A2: Table 2), several compounds have been detected in dandelion flowers that had previously only been identified in the roots or leaves of the plant (Hu and Kitts, 2003; Schütz et al., 2006; Williams et al., 1996) (e.g., cryptochlorogenic acid, esculetin, esculin, ferulic acid, dicaffeoylquinic acids). This is probably due to the fact that dandelion flowers have been studied in far fewer publications than roots and leaves were. The exceptions are daidzein and umbelliferone, which have so far only been identified in roots (Liu et al., 2020; Schütz et al., 2006), but I only found them in flower samples. Previous studies (Lis et al., 2020; Miłek et al., 2019; Williams et al., 1996) have only reported chrysoeriol

in its free form in flowers, but I could also detect it in low concentrations in leaf-root drug samples. In the case of flavonoid derivatives, it is more difficult to determine how many of the detected compounds have already been reported, due to their low level of identification. Our results suggest that, compared to previously published compounds, there are many more glycosylated derivatives in all plant parts. Another important result is that, in spite of the two hydroxylated fatty acid components previously detected in dandelion, we identified three additional compounds in the samples.

Numerous differences were observed between the drug and the flower samples in terms of the detected metabolites and their absolute or relative quantity. In general, most of the well-described, known compounds reported in the literature are present in high concentrations in the leaves and roots of the plant and are either completely absent from the flowers or present in much lower concentrations (e.g., chlorogenic acids, rosmarinic acid, luteolin 7-O-glucoside). The exception to this is chicoric acid, which was found in concentrations two and a half-fold higher in the flowers than in the leaf-root drug. In contrast, chrysoeriol met the expectations of the literature, being present in two orders of magnitude higher concentrations in the flower samples than in the leaf-root drug.

The comparison of the flower and liqueur samples shows important characteristics. There are compounds that are either missing from both groups (e.g., quercetin 3,4´-diglucoside, robinin) or being present in both. In the latter case, the concentration of the compound may be lower in the liqueur than in the flowers, but reverse concentration ratios could also be observed. The lower concentration of a component in liqueur can be explained by insufficient extraction or enzymatic degradation processes that occur during maturation. The reverse situation occurs when a compound detected in higher concentrations in the liqueur can be produced during maturation through the degradation of another compound. An example of this is the change in the concentration ratios of esculetin and its derivatives. Esculin, the glycosylated derivative of esculetin, is only present in the flowers, not in the liqueur samples, because it probably decomposed during the maturing process and released the esculetin aglycone. However, based on an approximate material balance, it can be concluded that the liqueur had a significantly higher esculetin content (53.93±1.02 $mg \cdot L^{-1}$) than could have been derived from the esculin content of the flowers and the initially free esculetin (less than 2.5 $mg \cdot kg^{-1}$ DW in total). This suggests that there may be other, as yet unidentified esculetin derivatives present in the flowers; also, esculetin could be derived from the umbelliferone and caffeoyl-CoA content during the maturation process.

Table 10. Quantitative analysis of the 84 identified compounds within the three sample groups. A complete quantitative analysis was performed on the compounds of Section A. The concentrations of the compounds in section B were determined by semi-quantitative analysis (see details in the chapter Metabolomics and multivariate statistical analysis). For the compounds in section C, only normalized intensity values are shown. Mean values ± 1 SD are given (n=7). Capital letters indicate Games-Howell post hoc test results.

	Section A	**Leaf-root drug**		**Flowers**		**Liqueur product**	
No.	**Compound**	**Concentration [mg·kg^{-1} DW]**	**Games-Howell score**	**Concentration [mg·kg^{-1} DW]**	**Games-Howell score**	**Concentration [mg·L^{-1}]**	**Games-Howell score**
9	Neochlorogenic acid	313.3±39.1	C	4.87±0.92	A	21.10±1.02	B
11	Esculin	2.06±0.08		2.20±0.34		<LOQ	
14	Esculetin	68.19±2.63	C	0.93±0.18	A	53.93±1.02	B
15	Caffeic acid	545.0±18.0	C	7.84±1.48	A	57.34±3.08	B
17	Chryptochlorogenic acid	264.1±14.3	B	<LOQ		22.05±3.42	A
18	Daphnetin	0.68±0.07	B	<LOQ		0.45±0.07	A
21	Fraxin	<LOQ		0.24±0.05		<LOQ	
31	Umbelliferone	<LOQ		2.81±0.43	B	0.21±0.01	A
34	Ferulic acid	168.3±13.3	B	<LOQ		17.16±1.25	A
35	Quercetin 3,4'-diglucoside	0.41±0.06		<LOQ		<LOQ	
46	Robinin	0.51±0.12		<LOQ		<LOQ	
48	Rutin	348.9±65.3	C	17.95±4.51	B	0.08±0.00	A
56	Kaempferol 3-O-rutinoside	3.52±0.18	B	4.45±0.73	C	0.01±0.00	A
58	Quercitrin	2.98±0.48	B	3.39±0.66	B	0.02±0.00	A

No.	Compound	Concentration [mg·kg^{-1} DW]	Games-Howell score	Concentration [mg·kg^{-1} DW]	Games-Howell score	Concentration [mg·L^{-1}]	Games-Howell score
60	Isorhamnetin 3-rutinoside	0.74±0.07	B	1.04±0.17	C	0.12±0.02	A
63	Rosmarinic acid	79.58±17.31		<LOQ		<LOQ	
65	Hesperidin	0.21±0.04	B	<LOQ		0.07±0.01	A
68	Phlorizin	0.75±0.15	A	2.41±0.64	B	<LOQ	
70	Daidzein	<LOQ		0.09±0.01		<LOQ	
71	Eriodictyol	<LOQ		4.47±0.89	B	0.20±0.02	A
72	Sebacic acid	9.41±1.10	B	<LOQ		0.22±0.03	A
74	Ethyl caffeate	1.12±0.21	B	0.17±0.04	A	4.99±0.13	C
75	Naringenin	0.23±0.04	B	4.19±0.76	C	0.04±0.00	A
76	Apigenin	1.44±0.14	B	8.96±0.54	C	0.19±0.01	A
81	Chrysin	<LOQ		0.19±0.04	B	0.01±0.00	A
No.	**Compound**	**Concentration [g·kg^{-1} DW]**	**Games-Howell score**	**Concentration [g·kg^{-1} DW]**	**Games-Howell score**	**Concentration [g·L^{-1}]**	**Games-Howell score**
8	Caftaric acid	72.79±4.68	C	0.07±0.02	A	2.79±0.29	B
13	Chlorogenic acid	4.07±0.18	C	0.48±0.02	B	0.04±0.01	A
42	Chicoric acid	1.03±0.12	B	2.51±0.54	C	0.25±0.02	A
51	Luteolin 7-O-glucoside	1.17±0.03	C	0.58±0.07	B	0.001±0.000	A
73	Luteolin	0.17±0.01	B	0.23±0.05	C	0.04±0.00	A

	Section B	Leaf-root drug		Flowers		Liqueur product	
No.	**Compound**	**Concentration [mg·kg^{-1} DW]**	**Games-Howell score**	**Concentration [mg·kg^{-1} DW]**	**Games-Howell score**	**Concentration [mg·L^{-1}]**	**Games-Howell score**
1	Caffeic acid glucoside_1	119.0±5.8		<LOQ		<LOQ	
2	Caffeic acid derivative_1	<LOQ		<LOQ		19.53±0.98	
3	Caffeic acid glucoside_2	221.7±12.8		<LOQ		<LOQ	
5	Caffeic acid sulfate_1	<LOQ		<LOQ		29.79±5.15	
7	Esculetin sulfate	<LOQ		<LOQ		2.72±0.67	
10	Caffeic acid sulfate_2	1.80±0.38		<LOQ		20.27±2.11	
16	1-caffeyllaminaribiose	92.01±6.47	C	14.40±2.51	B	0.42±0.10	A
23	Caffeoylglycerol	138.6±5.9	C	1.28±0.23	B	0.28±0.02	A
24	Quercetin dihexoside_1	8.64±0.55	B	5.39±0.87	A	<LOQ	
26	Quercetin derivative_1 (pentose+hexose moiety)	112.0±3.5	B	0.31±0.08	A	<LOQ	
27	Chicoric acid derivative	830.2±145.6	B	242.9±58.7	A	<LOQ	
28	Quercetin dihexoside_2	10.64±0.70		<LOQ		<LOQ	
32	Quercetin dihexoside_3	<LOQ		1.66±0.28		<LOQ	
33	Quercetin derivative_2 (pentose+hexose moiety)	62.88±2.24		<LOQ		<LOQ	
36	Schaftoside isomer_1	10.00±0.55	B	<LOQ		0.07±0.00	A
37	Quercetin hexosyl derivative	10.14±0.91	B	<LOQ		0.07±0.00	A

No.	Compound	Concentration [mg·kg^{-1} DW]	Games-Howell score	Concentration [mg·kg^{-1} DW]	Games-Howell score	Concentration [mg·L^{-1}]	Games-Howell score
38	Luteolin/kaempferol dihexoside_1	5.90±0.52	B	36.82±7.67	C	0.02±0.00	A
39	Quercetin derivative_3 (pentose+hexose moiety)	7.46±0.51		<LOQ		<LOQ	
41	Quercetin rutinoside	0.30±0.06	A	13.29±1.88	B	<LOQ	
43	Schaftoside isomer_2	11.64±0.70	B	<LOQ		0.07±0.00	A
44	Luteolin/kaempferol dihexoside_2	48.73±7.70	B	560.6±113.3	C	0.04±0.00	A
45	Luteolin/kaempferol dihexoside_3	11.03±1.04	A	27.62±5.41	B	<LOQ	
47	Quercetin pentoside_1	42.36±1.35		<LOQ		<LOQ	
49	Quercetin glucoside	28.91±1.87	B	28.17±5.16	B	0.03±0.00	A
50	Isorhamnetin disaccharide 1	2.77±0.25	B	83.91±21.60	C	1.76±0.03	A
52	Luteolin/kaempferol rutinoside	84.05±11.36	B	189.3±35.6	C	0.19±0.02	A
53	Isorhamnetin disaccharide 2	0.69±0.06	B	22.69±4.07	C	0.44±0.01	A
54	Quercetin pentoside_2	19.97±0.85		<LOQ		<LOQ	
55	Quercetin derivative_4	12.39±0.90		10.86+±2.04		<LOQ	
57	Apigenin derivative	25.13±0.96	C	7.00±1.19	B	0.39±0.01	A

No.	Compound	Concentration [mg·kg^{-1} DW]	Games-Howell score	Concentration [mg·kg^{-1} DW]	Games-Howell score	Concentration [mg·L^{-1}]	Games-Howell score
59	Dicaffeoylquinic acid_1	166.1±15.7	B	278.6±64.0	C	2.56±0.17	A
61	Isorhamnetin 3-glucoside	1.35±0.11	B	49.08±11.95	C	0.18±0.01	A
62	Caffeic acid derivative_2	167.6±14.2		<LOQ		<LOQ	
64	Chrysoeriol rutinoside	8.29±0.60		<LOQ		<LOQ	
66	Dicaffeoylquinic acid_2	96.55±4.97	C	9.10±1.42	B	3.91±0.49	A
67	Luteolin/kaempferol glycoside	3.16±0.28	A	61.98±9.53	B	<LOQ	
77	Chrysoeriol	1.97±0.19	A	212.4±22.1	C	4.60±0.15	B
No.	**Compound**	**Concentration [g·kg^{-1} DW]**	**Games-Howell score**	**Concentration [g·kg^{-1} DW]**	**Games-Howell score**	**Concentration [g·L^{-1}]**	**Games-Howell score**
12	Caffeoylsucrose	0.11±0.01	A	5.34±0.81	C	0.24±0.01	B

	Section C	**Leaf-root drug**		**Flowers**		**Liqueur product**	
No.	**Compound**	**Normalized detector counts [cps]**	**Games-Howell score**	**Normalized detector counts [cps]**	**Games-Howell score**	**Normalized detector counts [cps]**	**Games-Howell score**
4	Protocatechuoylglucose_1	972±167	B	1209±279	B	2±0	A
6	Protocatechuoylglucose_2	2528±296	C	1625±293	B	9±1	A
19	12-Hydroxyjasmonate sulfate_1	1009±26	C	299±58	B	11±0	A
20	Taraxinositol A/B	1143±44	B	10524±2271	C	1±0	A

No.	Compound	Normalized detector counts [cps]	Games-Howell score	Normalized detector counts [cps]	Games-Howell score	Normalized detector counts [cps]	Games-Howell score
22	12-Hydroxyjasmonate sulfate_2	n.d.		4536±915		n.d.	
25	Pyroglutamylisoleucine	106±9	C	8±2	A	90±2	B
29	Unknown1	788±97	C	32±8	B	2±0	A
30	Unknown2	1189±63	C	787±126	B	83±2	A
40	Taraxinositol B/A	1353±297	B	2870±646	C	5±0	A
69	Abscisic acid glucose ester	1322±68	B	1465±439	B	12±1	A
78	Unknown3	2010±170	B	84396±5639	C	954±83	A
79	9,12,13-trihydroxy-10E,15Z-octadecadienoic acid	8086±231	B	18446±4137	C	966±46	A
80	9,12,13-trihydroxy-10E-octadecenoic acid	6399±172	B	25627±5059	C	1319±15	A
82	9,10-dihydroxy-12Z-octadecenoic acid	1261±52	C	692±84	B	23±1	A
83	Hydroxyoctadecatrienoic acid derivative	1870±78	C	337±72	B	11±1	A
84	9-hydroxy-10E,12Z-octadecadienoic acid	741±121	C	342±79	B	3±1	A

<LOQ – Detector count lower than the detector count corresponding to the LOQ concentration specified for the authentic standard

n.d. - The data evaluation software cannot distinguish the received signal from noise; in the absence of an authentic standard, no LOQ concentration value is assigned to it.

Furthermore, a new compound – formerly not identified in dandelion – appeared in the liqueur, the sulfated form of esculetin, which appears to be a product of the maturation process. In addition, it can be seen that there are compounds that were still present in the flowers but could not be detected in the liqueur (e.g., daidzein, esculin, fraxin), but there are also reverse cases where compounds appeared in the liqueur (chryptochlorogenic acid, daphnetin, caffeic acid sulfates).

5.2.3. Quantitative analysis of the maturation process

The quantified results from the batch sample monitored over two months of aging are shown in App. A7: Table 4. As expected with such a complex matrix and process, it is not possible to draw clear conclusions for all compounds regarding the transformations that occurred during maturation and how the background processes are reflected in the concentration ratios obtained. Looking at the previously identified major molecular families, the maturation process is clearly evident in the case of esculetin derivatives (see Figure 20).

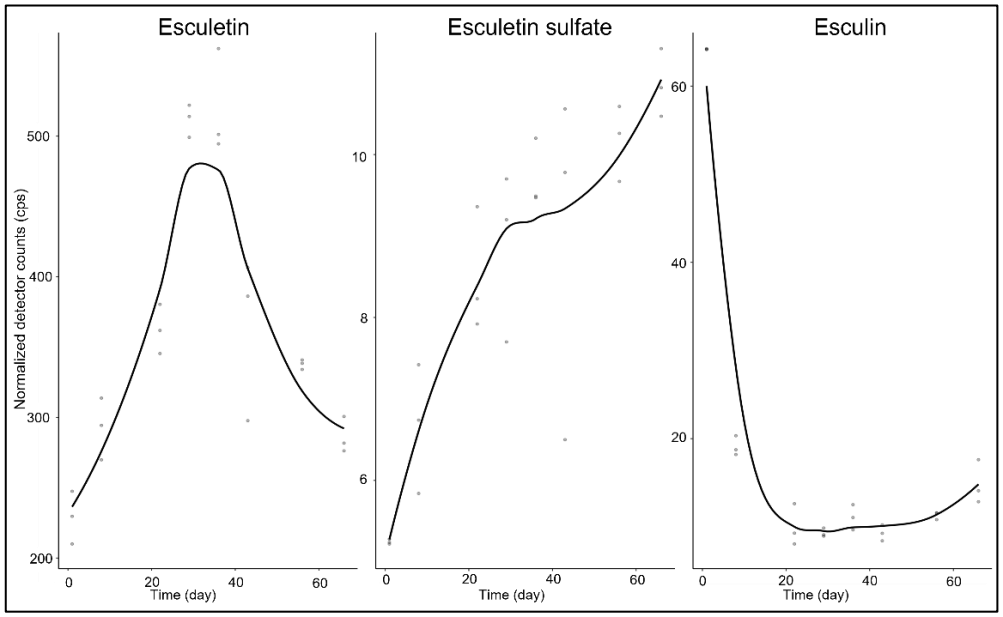

Figure 20. Trends in intensity changes in esculetin derivatives during the maturation process of dandelion liqueur.

The concentration of esculin decreases throughout the maturation process, presumably due to the release of esculetin aglycone as a result of enzymatic reactions. Furthermore, the appearance of esculetin sulfate and a continuous increase in its concentration can be observed during the process. However, the change in the amount of esculetin in the liqueur should not be overlooked, as a sharp decline can be observed after an initial increase. Based on this, it can be assumed that the background processes also caused the degradation of esculetin over time.

Similar results can be seen for both caffeic acid derivatives and quercetin derivatives (see Figures 21 and 22). For some compounds, an increase in concentration can be observed during the first month of aging, partly due to slow extraction process and partly due to the release of these compounds from other ones in the system. However, during the second month, with a few exceptions, there is an almost uniform decrease in the amount of secondary metabolites. These results somewhat contradict the fact that during long maturation processes, glycosylated forms released are enriched with biologically more active aglycones - the extraction and maturation process clearly appears to reach a maximum after about one month, when the amount of active metabolites in the product can be maximized. It is important to note that these products are likely to lose some of their bioactive compound content even when bottled, especially during improper and long-term storage.

In order to provide a simplified description of the compound concentration curves, App. A7: Table 4 contains a maturation profile dataset, on the basis of the ANOVA / Greenhouse-Geisser Type I error correction / Sidak's confidence interval calculation. In case the concentration of the given analyte in the 7th week of maturation was significantly lower or higher than after the 1st week sampling without a significant increase or decrease at the 4th week, a "D" or "R" code (standing for decrease and rising, respectively) was used. In case the concentration detected at the 4th week was significantly lower or higher than the concentration values detected for the 1st week and the 7th week, a "V" or "P" code (standing for valleying or peaking, respectively) was used. An "S" code (standing for stable) was applied if there was no significant difference between any of the pairwise settings (that is, 1st week vs. 4th week and 4th week vs. 7th week). This characterization could be carried out for 67 of the identified/assigned compounds, out of which 32 showed a significant decrease in concentration, 16 showed rising, 13 could be considered stable, while five compounds had a peak and one compound had a valley in concentration. For an additional set of seven compounds, where the concentration values dropped under the relevant LOQ to the last weeks of the maturation process (thus hampering the multivariate statistical analyses), a "D" code was noted.

Comparing the extract of the maturation process with the finished liqueur, it cannot be clearly determined that switching to ethanol (70 V/V%) clearly increases extraction efficiency. The compounds appeared in varying concentrations in the liqueur and in the test batch made with ethanol (70 V/V%), depending on their polarity and physical properties [e.g. caffeic acid: 57.34±3.08 mg·L^{-1} (liqueur) vs. 8.40±0.24 mg·L^{-1} (test batch); chicoric acid: 0.25±0.02 g·L^{-1} (liqueur) vs. 1.28±0.04 g·L^{-1} (test batch)].

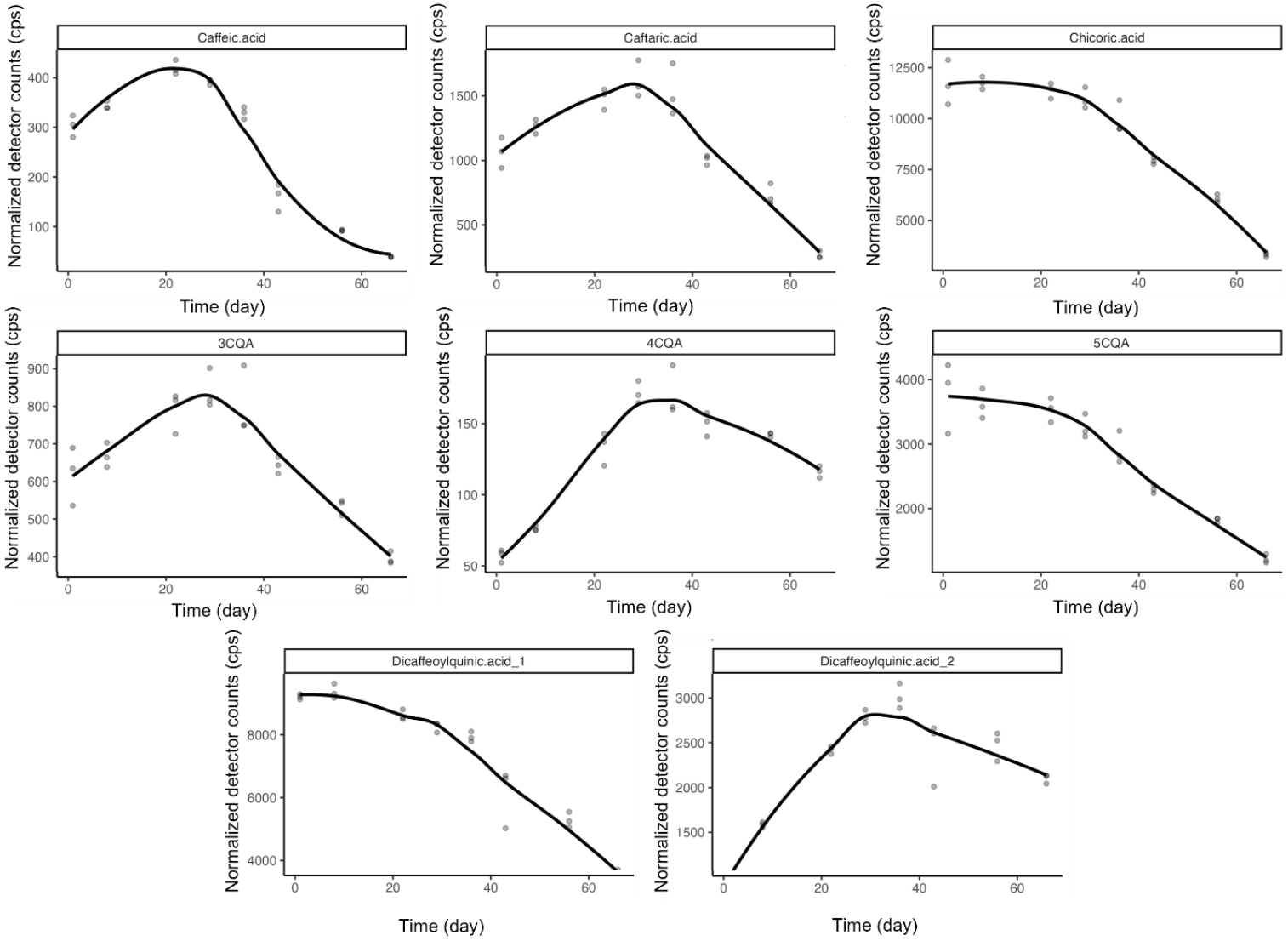

Figure 21. Trends in intensity changes in caffeic acid derivatives during the maturation process of dandelion liqueur.

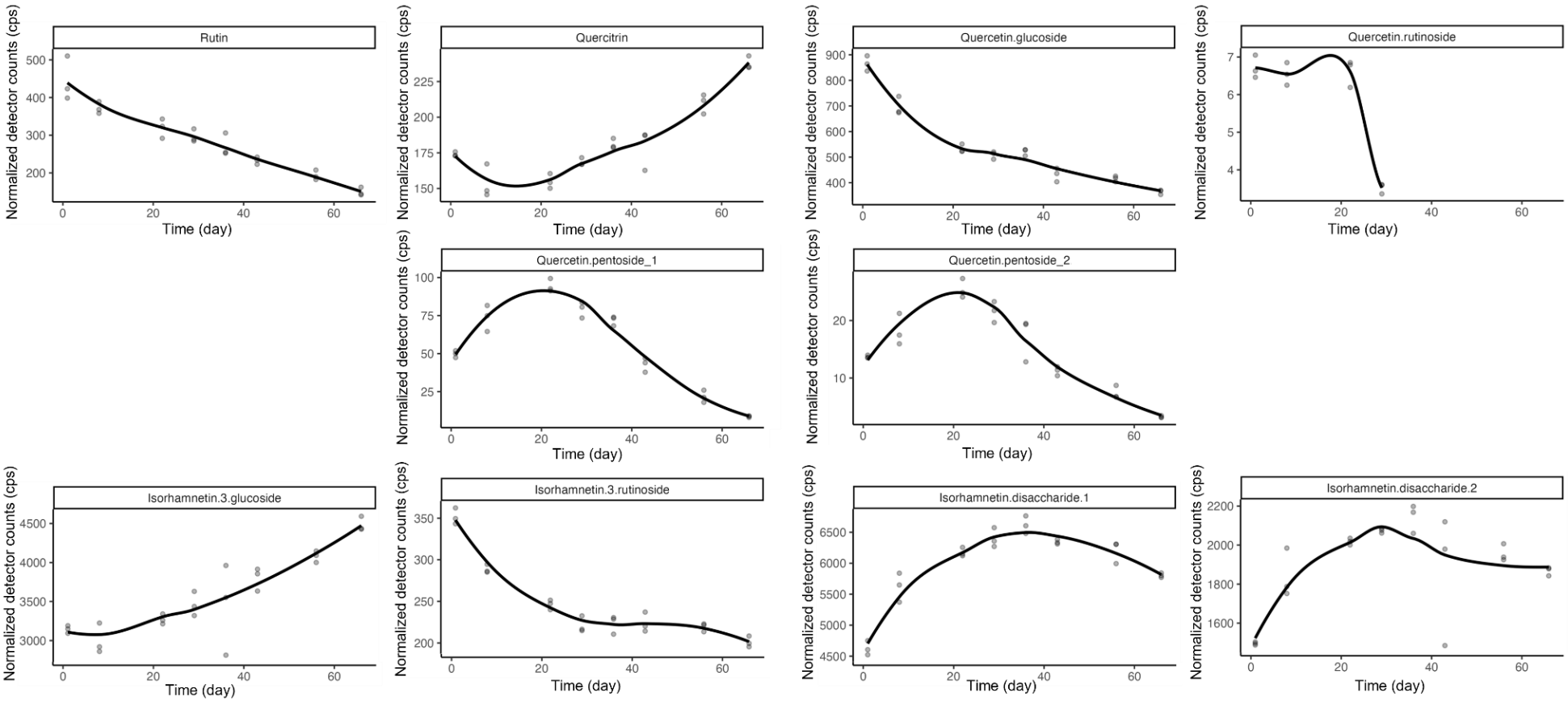

Figure 22. Trends in intensity changes in quercetin derivatives during the maturation process of dandelion liqueur

6. CONCLUSIONS AND RECOMMENDATIONS

A set of experiments conducted under various LED illumination conditions have comprehensively examined the biosynthesis of indole alkaloids in *C. roseus* plants. The UPLC-ESI-IMS-QTOF-MS setup allowed for the assignment of 14 analytes from the metabolites of the related pathway, and the concentrations of three alkaloids – vinblastine, vincristine, and 3',4'-anhydrovinblastine – were quantified. The use of high blue light ratio increased the concentration of these important vinca alkaloids significantly, by up to 15-fold, while none of the experimental settings led to a significant increase in plant height. Taking into account the large-scale availability of LED based plant growth devices in vertical (indoor) farming systems, our results indicate that looking for the applications of tuned spectral illumination is a viable research direction in the field of plant-derived active pharmaceutical ingredients (APIs).

Keeping reproducible quality of liqueurs or any kind of plant-based products is a common challenge because of the natural variability of plant metabolites. This especially relates to the secondary metabolites whose composition and relative/absolute concentration highly influence sensory attributes. Our study on the comprehensive metabolomic fingerprinting of various plant parts of *T. officinale* and its flower-based liqueur highlights the complexity of the extracted metabolites and their decomposition/build-up during the maceration process. Our observation on compounds formerly disregarded (e.g., taraxinositol A and B) or undetected (such as the sulfated derivatives of caffeic acid and esculetin that could be considered as either liqueur or maceration process-specific metabolites) in dandelion samples calls attention to the need of untargeted metabolomics: for example, the large amount of caffeoyl sucrose present in the flower samples (5.34 ± 0.81 g·kg^{-1} DW) points to the possibility that producers might not have been aware of even some of the major plant metabolites. Also, based on monitoring the liqueur maturation process, the complexity of extraction and enzymatic processes does not allow for a clear prediction of the optimal technological approach; however, in this actual case, the concentration of most compounds reached its local maximum after one month. Clearly, such a product-oriented untargeted metabolomics approach should have its practical place in the quality control of food products of plant origin, especially in the higher priced (inclusive) brands.

Further experiments should be considered in the following areas:

- To confirm the effects of light spectrum on alkaloid production in *C. roseus* plants, conduct extensive research in controlled vertical farm settings under production-relevant settings.

- Extend the number of identified metabolites by working with more authentic standards – collaborate with organic chemistry research groups to synthesize standard materials that are not commercially available – for both *C. roseus* and *T. officinale*.
- To capture genetic and environmental diversity, conduct comprehensive metabolomic investigations of *T. officinale* from various geographic origins.
- Determine and confirm which compounds are principally responsible for the therapeutic benefits of the dandelion plant. Establish standardized analytical techniques and concentration thresholds for inclusion in pharmacopoeias or food-quality documentations.

7. NEW SCIENTIFIC RESULTS

1. I developed a comprehensive targeted and untargeted metabolomic analysis using UPLC–ESI–IMS–QTOF–MS for the simultaneous identification and measurement of vinca alkaloids in *Catharanthus roseus* leaves. I identified 14 alkaloid compounds in total, vinblastine and vincristine confirmed by authentic standards, and 12 other was tentatively identified based on retention time order, accurate mass and fragmentation spectra.

2. I demonstrated that the concentration of pharmaceutically important bisindol alkaloids could be significantly (up to 15-fold) increased by exposing the *C. roseus* plant to blue LED illumination without requiring UV stress.

3. I established a comprehensive metabolomic profile of *Taraxacum officinale*, covering the leaf–root drug, flowers, and a commercially available dandelion flower–based liqueur. I identified 84 compounds, out of which 24 were first reported, which considerably increased the species' known metabolome.

4. I tentatively identified taraxinositol A and B for the first time in *T. officinale*, reported their ESI ‘-‘ MS/MS fragmentation spectra together with their possible fragmentation patterns.

5. I described the maturation process of a dandelion flower-derived liqueur through the UPLC–ESI–IMS–QTOF–MS based monitoring of 60 known and 24 formerly unreported secondary metabolites. I described a complex accumulation/decomposition pattern for all the 84 compounds for a period of two months and I could suggest an optimal maturation period of one month for this food product.

8. SUMMARY

This work used advanced coupled mass spectrometry techniques to investigate two complimentary aspects of metabolomic profiling in medicinal plants and plant-derived food products. The first part concentrated on *Catharanthus roseus*, with the goal of improving lighting conditions for increased production of alkaloids with therapeutic value. The second part examined *Taraxacum officinale*, evaluating the metabolomic fingerprinting of various plant parts and how it changed during the maturation of a liqueur made from dandelion flowers.

Without genetic alteration or stress induction, regulated LED lighting for *C. roseus* provides a viable biotechnological approach to increase yields of pharmaceutically significant vinca alkaloids. The findings also support *T. officinale*'s pharmacological significance and its potential as a bioactive component in foods and beverages by offering one of the most extensive metabolomic dataset to date.

Overall, the results show how metabolomic profiling can help standardization and quality control in pharmaceutical and food applications by bridging the fields of plant physiology, food science, and applied pharmacognosy. The findings collectively demonstrate the power of integrated targeted and untargeted metabolomic approaches in elucidating the chemical diversity and dynamic biosynthesis of plants.

APPENDICES

A1: Bibliography

Abouzeid, S., Beutling, U., Surup, F., Abdel Bar, F.M., Amer, M.M., Badria, F.A., Yahyazadeh, M., Brönstrup, M., Selmar, D., 2017. Treatment of *Vinca minor* Leaves with Methyl Jasmonate Extensively Alters the Pattern and Composition of Indole Alkaloids. J. Nat. Prod. 80, 2905–2909. https://doi.org/10.1021/acs.jnatprod.7b00424

Abrica-González, P., Gómez-Arroyo, S., Jazcilevich-Diamant, A., Sotelo-López, A., Flores-Márquez, A.R., Cortés-Eslava, J., 2023. Evaluation of Toxicological Effects of ZnO and CuO Nanoparticles with Taraxacum officinale as Bioindicator. Water Air Soil Pollut 234, 443. https://doi.org/10.1007/s11270-023-06432-3

Adler, L.S., Kittelson, P.M., 2004. Variation in Lupinus arboreus alkaloid profiles and relationships with multiple herbivores. Biochemical Systematics and Ecology 32, 371–390. https://doi.org/10.1016/j.bse.2003.11.002

Al-Amin, M., Eltayeb, N.M., Rahiman, S.S.F., Khairuddean, M., Salhimi, S.M., 2022. UPLC-ESI-QTOF-MS/MS and 1H-NMR identification of alkaloids in potent fraction of Catharanthus roseus leaves inhibits migration and invasion of MDA-MB-231 cells. Biologia 77, 3291–3303. https://doi.org/10.1007/s11756-022-01185-6

Asano, M., Harada, K., Umeno, A., Hirata, K., 2016. Optimization of 3', 4'-Anhydrovinblastine Synthesis *in vitro* Using Crude Extracts of *Catharanthus roseus* Irradiated with Near-Ultraviolet Light. Natural Product Communications 11, 1934578X1601100814. https://doi.org/10.1177/1934578X1601100814

Baldwin, I.T., 1988. The alkaloidal responses of wild tobacco to real and simulated herbivory. Oecologia 77, 378–381. https://doi.org/10.1007/BF00378046

Banyal, A., Tiwari, S., Sharma, A., Chanana, I., Patel, S.K.S., Kulshrestha, S., Kumar, P., 2023. Vinca alkaloids as a potential cancer therapeutics: recent update and future challenges. 3 Biotech 13, 211. https://doi.org/10.1007/s13205-023-03636-6

Béni, Z., Háda, V., Dubrovay, Z., Szántay, C., 2012. Structure elucidation of indole–indoline type alkaloids: A retrospective account from the point of view of current NMR and MS technology. Journal of Pharmaceutical and Biomedical Analysis 69, 106–124. https://doi.org/10.1016/j.jpba.2012.02.015

Bernhoft, A., 2010. Bioactive compounds in plants: benefits and risks for man and animals : proceedings from a symposium held in Norwegian Academy of Science and Letters, Oslo, 13-14 November 2008, Berit Smestad Paulsen: Highlights through the history of plant medicine. Novus Forlag, Oslo.

Bini, C., Wahsha, M., Fontana, S., Maleci, L., 2012. Effects of heavy metals on morphological characteristics of Taraxacum officinale Web growing on mine soils in NE Italy. Journal of Geochemical Exploration 123, 101–108. https://doi.org/10.1016/j.gexplo.2012.07.009

Bisset, N.G., Wichtl, M., Czygan, F.-C. (Eds.), 1994. Herbal drugs and phytopharmaceuticals: a handbook for practice on a scientific basis. Medpharm Scientific Publ, Stuttgart.

Brezo-Borjan, T., Švarc-Gajić, J., 2024. Subcritical water extraction of dandelion (*Taraxacum officinale* L.) flowers: Influence of temperature on polyphenols content and antioxidant activity. Food & Feed Res 51, 219–227. https://doi.org/10.5937/ffr0-53875

Budzianowski, J., 1997. Coumarins, Caffeoyltartaric Acids and their Artifactual Methyl Esters from *Taraxacum officinale* Leaves. Planta Med 63, 288–288. https://doi.org/10.1055/s-2006-957681

Bylka, W., Matlawska, I., Frański, R., 2010. Essential oil composition of Taraxacum officinale. Acta Physiol Plant 32, 231–234. https://doi.org/10.1007/s11738-009-0381-5

Cacak-Pietrzak, G., Dziki, D., Gawlik-Dziki, U., Sułek, A., Kalisz, S., Sujka, K., 2021. Effect of the Addition of Dried Dandelion Roots (Taraxacum officinale F. H. Wigg.) on Wheat

Dough and Bread Properties. Molecules 26, 7564. https://doi.org/10.3390/molecules26247564
Chen, Q., Chen, Z., 2013. Analysis of Catharanthus Alkaloids, in: Ramawat, K.G., Mérillon, J.-M. (Eds.), Natural Products. Springer Berlin Heidelberg, Berlin, Heidelberg, pp. 1121–1132. https://doi.org/10.1007/978-3-642-22144-6_33
Chen, W., Xia, B., Zou, Y., Xiang, Y., Shen, Z., Xue, S., 2023. Protective effect of dietary dandelion (Taraxacum officinale) extract on common carp under acute ammonia stress. Aquaculture Reports 30, 101609. https://doi.org/10.1016/j.aqrep.2023.101609
Chen, X., Ji, H., Zhang, C., Liu, A., 2020. Optimization of extraction process from *Taraxacum officinale* polysaccharide and its purification, structural characterization, antioxidant and anti-tumor activity. Food Measure 14, 194–206. https://doi.org/10.1007/s11694-019-00281-7
Chernushevich, I.V., Loboda, A.V., Thomson, B.A., 2001. An introduction to quadrupole–time-of-flight mass spectrometry. J. Mass Spectrom. 36, 849–865. https://doi.org/10.1002/jms.207
Choi, J., Yoon, K.D., Kim, J., 2018. Chemical constituents from Taraxacum officinale and their α-glucosidase inhibitory activities. Bioorganic & Medicinal Chemistry Letters 28, 476–481. https://doi.org/10.1016/j.bmcl.2017.12.014
Çiçek, S.S., Mangoni, A., Hanschen, F.S., Agerbirk, N., Zidorn, C., 2024. Essentials in the acquisition, interpretation, and reporting of plant metabolite profiles. Phytochemistry 220, 114004. https://doi.org/10.1016/j.phytochem.2024.114004
Clare, B.A., Conroy, R.S., Spelman, K., 2009. The Diuretic Effect in Human Subjects of an Extract of *Taraxacum officinale* Folium over a Single Day. The Journal of Alternative and Complementary Medicine 15, 929–934. https://doi.org/10.1089/acm.2008.0152
Clinical Trials 1., https://clinicaltrials.gov/study/NCT06625736?term=dandelion&rank=1 (accessed 11.4.25).
Clinical Trials 2., https://clinicaltrials.gov/study/NCT00442091?term=dandelion&rank=2 (accessed 11.4.25).
Codex Alimentarius Commission, 2003. Hazard analysis and critical control point (HACCP) system and guidelines for its application. (CAC/RCP 1-1969, Rev. 4–2003). FAO/WHO.
Commisso, M., Negri, S., Bianconi, M., Gambini, S., Avesani, S., Ceoldo, S., Avesani, L., Guzzo, F., 2019. Untargeted and Targeted Metabolomics and Tryptophan Decarboxylase In Vivo Characterization Provide Novel Insight on the Development of Kiwifruits (Actinidia deliciosa). IJMS 20, 897. https://doi.org/10.3390/ijms20040897
Darko, E., Hamow, K.A., Marček, T., Dernovics, M., Ahres, M., Galiba, G., 2022. Modulated Light Dependence of Growth, Flowering, and the Accumulation of Secondary Metabolites in Chilli. Front. Plant Sci. 13, 801656. https://doi.org/10.3389/fpls.2022.801656
Darko, E., Heydarizadeh, P., Schoefs, B., Sabzalian, M.R., 2014. Photosynthesis under artificial light: the shift in primary and secondary metabolism. Phil. Trans. R. Soc. B 369, 20130243. https://doi.org/10.1098/rstb.2013.0243
De Luca, V., Salim, V., Thamm, A., Masada, S.A., Yu, F., 2014. Making iridoids/secoiridoids and monoterpenoid indole alkaloids: progress on pathway elucidation. Current Opinion in Plant Biology 19, 35–42. https://doi.org/10.1016/j.pbi.2014.03.006
DeLuca, V., Balsevich, J., Tyler, R.T., Eilert, U., Panchuk, B.D., Kurz, W.G.W., 1986. Biosynthesis of Indole Alkaloids: Developmental Regulation of the Biosynthetic Pathway from Tabersonine to Vindoline in Catharanthus roseus. Journal of Plant Physiology 125, 147–156. https://doi.org/10.1016/S0176-1617(86)80252-8
Dodds, J.N., Baker, E.S., 2019. Ion Mobility Spectrometry: Fundamental Concepts, Instrumentation, Applications, and the Road Ahead. J. Am. Soc. Mass Spectrom. 30, 2185–2195. https://doi.org/10.1007/s13361-019-02288-2

Dubrovay, Z., Háda, V., Béni, Z., Szántay, C., 2013. NMR and mass spectrometric characterization of vinblastine, vincristine and some new related impurities – Part I. Journal of Pharmaceutical and Biomedical Analysis 84, 293–308. https://doi.org/10.1016/j.jpba.2012.08.019

Eliuk, S., Makarov, A., 2015. Evolution of Orbitrap Mass Spectrometry Instrumentation. Annual Rev. Anal. Chem. 8, 61–80. https://doi.org/10.1146/annurev-anchem-071114-040325

Eng, J.G.M., Shahsavarani, M., Smith, D.P., Hájíček, J., De Luca, V., Qu, Y., 2022. A Catharanthus roseus Fe(II)/α-ketoglutarate-dependent dioxygenase catalyzes a redox-neutral reaction responsible for vindolinine biosynthesis. Nat Commun 13, 3335. https://doi.org/10.1038/s41467-022-31100-1

Escudero, N.L., De Arellano, M.L., Fernández, S., Albarracín, G., Mucciarelli, S., 2003. Taraxacum officinale as a food source. Plant Foods Hum Nutr 58, 1–10. https://doi.org/10.1023/B:QUAL.0000040365.90180.b3

European Medicines Agency, 2020. European Union herbal monograph.

European Medicines Agency, 2010. Guideline on declaration of herbal substances and herbal preparations in herbal medicinal products/traditional herbal medicinal products 18.

European Parliament & Council, 2004a. Directive 2004/24/EC of the European Parliament and of the Council of 31 March 2004 amending, as regards traditional herbal medicinal products, Directive 2001/83/EC on the Community code relating to medicinal products for human use. Official Journal of the European Union, L 136, 85–90.

European Parliament & Council, 2004b. Regulation (EC) No 852/2004 of 29 April 2004 on the hygiene of foodstuffs. Official Journal of the European Union, L 139, 1–54.

European Parliament & Council, 2002. Regulation (EC) No 178/2002 of 28 January 2002 laying down the general principles and requirements of food law, establishing the European Food Safety Authority and laying down procedures in matters of food safety. Official Journal of the European Union, L 31, 1–24.

European pharmacopoeia, Eleventh edition. ed, 2022. . Council of Europe : European Directorate for the Quality of Medicines and Healthcare, Strasbourg.

Falcone, G., Di Matteo, G., Mannina, L., Cellini, F., Menghini, L., Carradori, S., Al-Samydai, A., Chiavaroli, A., Di Simone, S.C., Ferrante, C., 2025. Phytochemical profiling and anti-inflammatory activity of Gentiana lutea roots from Pollino National Park. Journal of Ethnopharmacology 353, 120430. https://doi.org/10.1016/j.jep.2025.120430

Fan, J., Xiao, D., Zhang, L., Edirisinghe, I., Burton-Freeman, B., Sandhu, A.K., 2020. Pharmacokinetic Characterization of (Poly)phenolic Metabolites in Human Plasma and Urine after Acute and Short-Term Daily Consumption of Mango Pulp. Molecules 25, 5522. https://doi.org/10.3390/molecules25235522

Fernandez, C., Monnier, Y., Santonja, M., Gallet, C., Weston, L.A., Prévosto, B., Saunier, A., Baldy, V., Bousquet-Mélou, A., 2016. The Impact of Competition and Allelopathy on the Trade-Off between Plant Defense and Growth in Two Contrasting Tree Species. Front. Plant Sci. 7. https://doi.org/10.3389/fpls.2016.00594

Ferreres, F., Pereira, D.M., Valentão, P., Oliveira, J.M.A., Faria, J., Gaspar, L., Sottomayor, M., Andrade, P.B., 2010. Simple and reproducible HPLC–DAD–ESI-MS/MS analysis of alkaloids in Catharanthus roseus roots. Journal of Pharmaceutical and Biomedical Analysis 51, 65–69. https://doi.org/10.1016/j.jpba.2009.08.005

Fini, A., Brunetti, C., Di Ferdinando, M., Ferrini, F., Tattini, M., 2011. Stress-induced flavonoid biosynthesis and the antioxidant machinery of plants. Plant Signaling & Behavior 6, 709–711. https://doi.org/10.4161/psb.6.5.15069

Fischer, N.H., Williamson, G.B., Weidenhamer, J.D., Richardson, D.R., 1994. In search of allelopathy in the Florida scrub: The role of terpenoids. J Chem Ecol 20, 1355–1380. https://doi.org/10.1007/BF02059812

Frischknecht, P.M., Bättig, M., Baumann, T.W., 1987. Effect of drought and wounding stress on indole alkaloid formation in Catharanthus roseus. Phytochemistry 26, 707–710. https://doi.org/10.1016/S0031-9422(00)84769-X

Fukuyama, T., Ohashi-Kaneko, K., Hirata, K., Muraoka, M., Watanabe, H., 2017. Effects of Ultraviolet A Supplemented with Red Light Irradiation on Vinblastine Production in *Catharanthus roseus*. ecb 55, 65–69. https://doi.org/10.2525/ecb.55.65

Fukuyama, T., Ohashi-Kaneko, K., Ono, E., Watanabe, H., 2013. Growth and alkaloid yields of Catharanthus roseus (L.) G. Don cultured under red and blue LEDs. Journal of Science and High Technology in Agriculture 25, 175–182. https://doi.org/10.2525/shita.25.175

Fukuyama, T., Ohashi-Kaneko, K., Watanabe, H., 2015. Estimation of Optimal Red Light Intensity for Production of the Pharmaceutical Drug Components, Vindoline and Catharanthine, Contained in *Catharanthus roseus* (L.) G. Don. ecb 53, 217–220. https://doi.org/10.2525/ecb.53.217

Gatto, M.A., Ippolito, A., Linsalata, V., Cascarano, N.A., Nigro, F., Vanadia, S., Di Venere, D., 2011. Activity of extracts from wild edible herbs against postharvest fungal diseases of fruit and vegetables. Postharvest Biology and Technology 61, 72–82. https://doi.org/10.1016/j.postharvbio.2011.02.005

Gidda, S.K., Miersch, O., Levitin, A., Schmidt, J., Wasternack, C., Varin, L., 2003. Biochemical and Molecular Characterization of a Hydroxyjasmonate Sulfotransferase from Arabidopsis thaliana. Journal of Biological Chemistry 278, 17895–17900. https://doi.org/10.1074/jbc.M211943200

Goswami, S., Ali, A., Prasad, M.E., Singh, P., 2024. Pharmacological significance of Catharanthus roseus in cancer management: A review. Pharmacological Research - Modern Chinese Medicine 11, 100444. https://doi.org/10.1016/j.prmcm.2024.100444

Grauso, L., Emrick, S., Bonanomi, G., Lanzotti, V., 2019. Metabolomics of the alimurgic plants *Taraxacum officinale*, *Papaver rhoeas* and *Urtica dioica* by combined NMR and GC–MS analysis. Phytochemical Analysis 30, 535–546. https://doi.org/10.1002/pca.2845

Gruszecki, R., Walasek-Janusz, M., Caruso, G., Pokluda, R., Tallarita, A.V., Golubkina, N., Sękara, A., 2024. Multilateral Use of Dandelion in Folk Medicine of Central-Eastern Europe. Plants 14, 84. https://doi.org/10.3390/plants14010084

Gupta, U.C., Gupta, S.C., 2014. Sources and Deficiency Diseases of Mineral Nutrients in Human Health and Nutrition: A Review. Pedosphere 24, 13–38. https://doi.org/10.1016/S1002-0160(13)60077-6

Gurib-Fakim, A., 2006. Medicinal plants: Traditions of yesterday and drugs of tomorrow. Molecular Aspects of Medicine 27, 1–93. https://doi.org/10.1016/j.mam.2005.07.008

Háda, V., Dubrovay, Z., Lakó-Futó, Á., Galambos, J., Gulyás, Z., Aranyi, A., Szántay, C., 2013. NMR and mass spectrometric characterization of vinblastine, vincristine and some new related impurities—Part II. Journal of Pharmaceutical and Biomedical Analysis 84, 309–322. https://doi.org/10.1016/j.jpba.2012.09.008

Hadjichambis, A.Ch., Paraskeva-Hadjichambi, D., Della, A., Elena Giusti, M., De Pasquale, C., Lenzarini, C., Censorii, E., Reyes Gonzales-Tejero, M., Patricia Sanchez-Rojas, C., Ramiro-Gutierrez, J.M., Skoula, M., Johnson, C., Sarpaki, A., Hmamouchi, M., Jorhi, S., El-Demerdash, M., El-Zayat, M., Pieroni, A., 2008. Wild and semi-domesticated food plant consumption in seven circum-Mediterranean areas. International Journal of Food Sciences and Nutrition 59, 383–414. https://doi.org/10.1080/09637480701566495

Hänsel, R., Kartarahardja, M., Huang, J.-T., Bohlmann, F., 1980. Sesquiterpenlacton-β-d-glucopyranoside sowie ein neues eudesmanolid aus Taraxacum officinale. Phytochemistry 19, 857–861. https://doi.org/10.1016/0031-9422(80)85126-0

Harborne, J.B., 1984. Methods of Plant Analysis, in: Phytochemical Methods. Springer Netherlands, Dordrecht, pp. 1–36. https://doi.org/10.1007/978-94-009-5570-7_1

Hfaiedh, M., Brahmi, D., Zourgui, L., 2016. Hepatoprotective effect of *T araxacum officinale* leaf extract on sodium dichromate-induced liver injury in rats: Hepatoprotective effect of

TOE on sodium dichromate-induced liver injury in rats. Environ. Toxicol. 31, 339–349. https://doi.org/10.1002/tox.22048
Hisiger, S., Jolicoeur, M., 2007. Analysis of Catharanthus roseus alkaloids by HPLC. Phytochem Rev 6, 207–234. https://doi.org/10.1007/s11101-006-9036-y
Hong, J., Yang, L., Zhang, D., Shi, J., 2016. Plant Metabolomics: An Indispensable System Biology Tool for Plant Science. IJMS 17, 767. https://doi.org/10.3390/ijms17060767
Hu, C., Kitts, D.D., 2004. Luteolin and luteolin-7-O-glucoside from dandelion flower suppress iNOS and COX-2 in RAW264.7 cells. Mol Cell Biochem 265, 107–113. https://doi.org/10.1023/B:MCBI.0000044364.73144.fe
Hu, C., Kitts, D.D., 2003. Antioxidant, Prooxidant, and Cytotoxic Activities of Solvent-Fractionated Dandelion (*Taraxacum officinale*) Flower Extracts in Vitro. J. Agric. Food Chem. 51, 301–310. https://doi.org/10.1021/jf0258858
International Organization for Standardization, 2017. ISO/IEC 17025:2017—General requirements for the competence of testing and calibration laboratories.
Jedrejek, D., Lis, B., Rolnik, A., Stochmal, A., Olas, B., 2019. Comparative phytochemical, cytotoxicity, antioxidant and haemostatic studies of Taraxacum officinale root preparations. Food and Chemical Toxicology 126, 233–247. https://doi.org/10.1016/j.fct.2019.02.017
Jedrejek, D., Pawelec, S., 2024. Comprehensive Qualitative and Quantitative Analysis of Flavonoids in Dandelion (*Taraxacum officinale*) Flowers and Food Products. J. Agric. Food Chem. 72, 17368–17376. https://doi.org/10.1021/acs.jafc.4c03108
Jeong, W.T., Lim, H.B., 2018. A UPLC-ESI-Q-TOF method for rapid and reliable identification and quantification of major indole alkaloids in Catharanthus roseus. Journal of Chromatography B 1080, 27–36. https://doi.org/10.1016/j.jchromb.2018.02.018
Jung, Y., Ahn, Y.G., Kim, H.K., Moon, B.C., Lee, A.Y., Ryu, D.H., Hwang, G.-S., 2011. Characterization of dandelion species using 1H NMR- and GC-MS-based metabolite profiling. Analyst 136, 4222. https://doi.org/10.1039/c1an15403f
Kamal, F.Z., Lefter, R., Mihai, C.-T., Farah, H., Ciobica, A., Ali, A., Radu, I., Mavroudis, I., Ech-Chahad, A., 2022. Chemical Composition, Antioxidant and Antiproliferative Activities of Taraxacum officinale Essential Oil. Molecules 27, 6477. https://doi.org/10.3390/molecules27196477
Karakuş, A., Değer, Y., Yıldırım, S., 2017. Protective effect of *Silybum marianum* and *Taraxacum officinale* extracts against oxidative kidney injuries induced by carbon tetrachloride in rats. Renal Failure 39, 1–6. https://doi.org/10.1080/0886022X.2016.1244070
Kattge, J., Díaz, S., Lavorel, S., Prentice, I.C., Leadley, P., Bönisch, G., Garnier, E., Westoby, M., Reich, P.B., Wright, I.J., Cornelissen, J.H.C., Violle, C., Harrison, S.P., Van Bodegom, P.M., Reichstein, M., Enquist, B.J., Soudzilovskaia, N.A., Ackerly, D.D., Anand, M., Atkin, O., Bahn, M., Baker, T.R., Baldocchi, D., Bekker, R., Blanco, C.C., Blonder, B., Bond, W.J., Bradstock, R., Bunker, D.E., Casanoves, F., Cavender-Bares, J., Chambers, J.Q., Chapin Iii, F.S., Chave, J., Coomes, D., Cornwell, W.K., Craine, J.M., Dobrin, B.H., Duarte, L., Durka, W., Elser, J., Esser, G., Estiarte, M., Fagan, W.F., Fang, J., Fernández-Méndez, F., Fidelis, A., Finegan, B., Flores, O., Ford, H., Frank, D., Freschet, G.T., Fyllas, N.M., Gallagher, R.V., Green, W.A., Gutierrez, A.G., Hickler, T., Higgins, S.I., Hodgson, J.G., Jalili, A., Jansen, S., Joly, C.A., Kerkhoff, A.J., Kirkup, D., Kitajima, K., Kleyer, M., Klotz, S., Knops, J.M.H., Kramer, K., Kühn, I., Kurokawa, H., Laughlin, D., Lee, T.D., Leishman, M., Lens, F., Lenz, T., Lewis, S.L., Lloyd, J., Llusià, J., Louault, F., Ma, S., Mahecha, M.D., Manning, P., Massad, T., Medlyn, B.E., Messier, J., Moles, A.T., Müller, S.C., Nadrowski, K., Naeem, S., Niinemets, Ü., Nöllert, S., Nüske, A., Ogaya, R., Oleksyn, J., Onipchenko, V.G., Onoda, Y., Ordoñez, J., Overbeck, G., Ozinga, W.A., Patiño, S., Paula, S., Pausas, J.G., Peñuelas, J., Phillips, O.L., Pillar, V., Poorter, H., Poorter, L., Poschlod, P., Prinzing, A., Proulx, R., Rammig, A., Reinsch,

S., Reu, B., Sack, L., Salgado-Negret, B., Sardans, J., Shiodera, S., Shipley, B., Siefert, A., Sosinski, E., Soussana, J. -F., Swaine, E., Swenson, N., Thompson, K., Thornton, P., Waldram, M., Weiher, E., White, M., White, S., Wright, S.J., Yguel, B., Zaehle, S., Zanne, A.E., Wirth, C., 2011. TRY – a global database of plant traits. Global Change Biology 17, 2905–2935. https://doi.org/10.1111/j.1365-2486.2011.02451.x

KEGG Indole alkaloid biosynthesis - Reference pathway, n.d. URL https://www.kegg.jp/pathway/map00901 (accessed 11.4.25).

KEGG Terpenoid backbone biosynthesis pathway, n.d. URL https://www.kegg.jp/entry/ko00900 (accessed 11.4.25).

Kenny, O., Brunton, N.P., Walsh, D., Hewage, C.M., McLoughlin, P., Smyth, T.J., 2015. Characterisation of Antimicrobial Extracts from Dandelion Root (*Taraxacum officinale*) Using LC-SPE-NMR. Phytotherapy Research 29, 526–532. https://doi.org/10.1002/ptr.5276

Kenny, Owen, Smyth, T.J., Hewage, C.M., Brunton, N.P., 2015. Quantitative UPLC - MS / MS analysis of chlorogenic acid derivatives in antioxidant fractionates from dandelion (*Taraxacum officinale*) root. Int J of Food Sci Tech 50, 766–773. https://doi.org/10.1111/ijfs.12668

Kenny, O., Smyth, T.J., Hewage, C.M., Brunton, N.P., McLoughlin, P., 2014. 4-Hydroxyphenylacetic acid derivatives of inositol from dandelion (Taraxacum officinale) root characterised using LC–SPE–NMR and LC–MS techniques. Phytochemistry 98, 197–203. https://doi.org/10.1016/j.phytochem.2013.11.022

Khan, A., Arif, K., Munir, B., Kiran, S., Jalal, F., Qureshi, N., Hassan, S., Soomro, G., Nazir, A., Ghaffar, A., Tahir, M., Iqbal, M., 2018. Estimating Total Phenolics in *Taraxacum officinale* (L.) Extracts. Pol. J. Environ. Stud. 28, 497–501. https://doi.org/10.15244/pjoes/78435

Kikuchi, T., Tanaka, A., Uriuda, M., Yamada, T., Tanaka, R., 2016. Three Novel Triterpenoids from Taraxacum officinale Roots. Molecules 21, 1121. https://doi.org/10.3390/molecules21091121

Kisiel, W., Barszcz, B., 2000. Further sesquiterpenoids and phenolics from Taraxacum officinale. Fitoterapia 71, 269–273. https://doi.org/10.1016/S0367-326X(99)00158-6

Koo, H.-N., Hong, S.-H., Song, B.-K., Kim, C.-H., Yoo, Y.-H., Kim, H.-M., 2004. Taraxacum officinale induces cytotoxicity through TNF-α and IL-1α secretion in Hep G2 cells. Life Sciences 74, 1149–1157. https://doi.org/10.1016/j.lfs.2003.07.030

Kour, K., Bani, S., 2011. Chicoric acid regulates behavioral and biochemical alterations induced by chronic stress in experimental Swiss albino mice. Pharmacology Biochemistry and Behavior 99, 342–348. https://doi.org/10.1016/j.pbb.2011.05.008

Kowalska, T., Sajewicz, M., 2022. Thin-Layer Chromatography (TLC) in the Screening of Botanicals–Its Versatile Potential and Selected Applications. Molecules 27, 6607. https://doi.org/10.3390/molecules27196607

Kristó, Sz.T., Ganzler, K., Apáti, P., Szőke, É., Kéry, Á., 2002. Analysis of antioxidant flavonoids from asteraceae and moraceae plants by capillary electrophoresis. Chromatographia 56, S121–S126. https://doi.org/10.1007/BF02494124

Kubica, P., Szopa, A., Prokopiuk, B., Komsta, Ł., Pawłowska, B., Ekiert, H., 2020. The influence of light quality on the production of bioactive metabolites – verbascoside, isoverbascoside and phenolic acids and the content of photosynthetic pigments in biomass of Verbena officinalis L. cultured in vitro. Journal of Photochemistry and Photobiology B: Biology 203, 111768. https://doi.org/10.1016/j.jphotobiol.2019.111768

Kulagina, N., Méteignier, L.-V., Papon, N., O'Connor, S.E., Courdavault, V., 2022. More than a Catharanthus plant: A multicellular and pluri-organelle alkaloid-producing factory. Current Opinion in Plant Biology 67, 102200. https://doi.org/10.1016/j.pbi.2022.102200

Kumar, S., Singh, A., Bajpai, V., Srivastava, M., Singh, B.P., Kumar, B., 2016. Structural characterization of monoterpene indole alkaloids in ethanolic extracts of Rauwolfia

species by liquid chromatography with quadrupole time-of-flight mass spectrometry. Journal of Pharmaceutical Analysis 6, 363–373. https://doi.org/10.1016/j.jpha.2016.04.008
Kumar, S., Singh, A., Kumar, B., Singh, B., Bahadur, L., Lal, M., 2018. Simultaneous quantitative determination of bioactive terpene indole alkaloids in ethanolic extracts of Catharanthus roseus (L.) G. Don by ultra high performance liquid chromatography–tandem mass spectrometry. Journal of Pharmaceutical and Biomedical Analysis 151, 32–41. https://doi.org/10.1016/j.jpba.2017.12.040
Kumar, S., Singh, B., Singh, R., 2022. Catharanthus roseus (L.) G. Don: A review of its ethnobotany, phytochemistry, ethnopharmacology and toxicities. Journal of Ethnopharmacology 284, 114647. https://doi.org/10.1016/j.jep.2021.114647
Li, Q., Xu, J., Yang, L., Sun, Y., Zhou, X., Zheng, Y., Zhang, Y., Cai, Y., 2022. LED Light Quality Affect Growth, Alkaloids Contents, and Expressions of Amaryllidaceae Alkaloids Biosynthetic Pathway Genes in Lycoris longituba. J Plant Growth Regul 41, 257–270. https://doi.org/10.1007/s00344-021-10298-2
Lima, N.M., Santos, G.F., De Jesus A. S. Andrade, T., Dias, L.S., Silva, P.A., Castro, S.B.R., Carli, A.P., Alves, C.C.S., Lima, G.S., Vaz, B.G., 2025. Metabolic signatures by LC-HRMS/MS of jabuticaba (Plinia cauliflora) juice, liqueur, and wines reveal the wealthiest sources of bioactive metabolites. Talanta 287, 127602. https://doi.org/10.1016/j.talanta.2025.127602
LIPID MAPS®, n.d. . A free, open access lipidomics resource. URL https://www.lipidmaps.org/ (accessed 8.22.25).
Lis, B., Jedrejek, D., Moldoch, J., Stochmal, A., Olas, B., 2019. The anti-oxidative and hemostasis-related multifunctionality of L-chicoric acid, the main component of dandelion: An in vitro study of its cellular safety, antioxidant and anti-platelet properties, and effect on coagulation. Journal of Functional Foods 62, 103524. https://doi.org/10.1016/j.jff.2019.103524
Lis, B., Jedrejek, D., Rywaniak, J., Soluch, A., Stochmal, A., Olas, B., 2020. Flavonoid Preparations from *Taraxacum officinale* L. Fruits—A Phytochemical, Antioxidant and Hemostasis Studies. Molecules 25, 5402. https://doi.org/10.3390/molecules25225402
Liu, N., Song, M., Wang, N., Wang, Y., Wang, R., An, X., Qi, J., 2020. The effects of solid-state fermentation on the content, composition and *in vitro* antioxidant activity of flavonoids from dandelion. PLoS ONE 15, e0239076. https://doi.org/10.1371/journal.pone.0239076
López-García, J., Kuceková, Z., Humpolíček, P., Mlček, J., Sáha, P., 2013. Polyphenolic Extracts of Edible Flowers Incorporated onto Atelocollagen Matrices and Their Effect on Cell Viability. Molecules 18, 13435–13445. https://doi.org/10.3390/molecules181113435
Lourenço, M.S.C., Prada, J.E.C., Heuvelink, E., Carvalho, S.M.P., 2022. Production of *Catharanthus roseus* in vertical farming systems: dynamic analyses of plant morphological responses of nine cultivars to N-UV supplementation. Acta Hortic. 217–224. https://doi.org/10.17660/ActaHortic.2022.1337.29
Man, J., Wu, L., Han, P., Hao, Y., Li, J., Gao, Z., Wang, J., Yang, W., Tian, Y., 2022. Revealing the metabolic mechanism of dandelion extract against A549 cells using UPLC-QTOF MS. Biomedical Chromatography 36, e5272. https://doi.org/10.1002/bmc.5272
Manson, J.S., Otterstatter, M.C., Thomson, J.D., 2010. Consumption of a nectar alkaloid reduces pathogen load in bumble bees. Oecologia 162, 81–89. https://doi.org/10.1007/s00442-009-1431-9
Marinaccio, L., Gentile, G., Llorent-Martínez, E.J., Zengin, G., Masci, D., Flamminii, F., Stefanucci, A., Mollica, A., 2025. Valorization of grape pomace extracts against cranberry, elderberry, rose hip berry, goji berry and raisin extracts: Phytochemical profile and in vitro biological activity. Food Chemistry 463, 141323. https://doi.org/10.1016/j.foodchem.2024.141323

Martinez, M., Poirrier, P., Chamy, R., Prüfer, D., Schulze-Gronover, C., Jorquera, L., Ruiz, G., 2015. Taraxacum officinale and related species—An ethnopharmacological review and its potential as a commercial medicinal plant. Journal of Ethnopharmacology 169, 244–262. https://doi.org/10.1016/j.jep.2015.03.067

MassBank, n.d. . High Quality Mass Spectral Database. URL https://massbank.eu/MassBank/ (accessed 8.22.25).

McLafferty, F.W., 2011. A Century of Progress in Molecular Mass Spectrometry. Annual Rev. Anal. Chem. 4, 1–22. https://doi.org/10.1146/annurev-anchem-061010-114018

Melendez-Martinez, A., Britton, G., Vicario, I., Heredia, F., 2006. HPLC analysis of geometrical isomers of lutein epoxide isolated from dandelion (Taraxacum officinale F. Weber ex Wiggers). Phytochemistry 67, 771–777. https://doi.org/10.1016/j.phytochem.2006.02.002

Miłek, M., Marcinčáková, D., Legáth, J., 2019. Polyphenols Content, Antioxidant Activity, and Cytotoxicity Assessment of *Taraxacum officinale* Extracts Prepared through the Micelle-Mediated Extraction Method. Molecules 24, 1025. https://doi.org/10.3390/molecules24061025

Mishra, P., Uniyal, G.C., Sharma, S., Kumar, S., 2001. Pattern of diversity for morphological and alkaloid yield related traits among the periwinkle Catharanthus roseus accessions collected from in and around Indian subcontinent. Genetic Resources and Crop Evolution 48, 273–286. https://doi.org/10.1023/A:1011218329118

Mo, E., Ahn, J., Jo, Y., Kim, S., Hwang, B., Lee, M., 2017. Inositol Derivatives and Phenolic Compounds from the Roots of Taraxacum coreanum. Molecules 22, 1349. https://doi.org/10.3390/molecules22081349

MoNA, n.d. . MassBank of North America. URL https://mona.fiehnlab.ucdavis.edu/ (accessed 8.22.25).

Moreno, P.R.H., Van Der Heijden, R., Verpoorte, R., 1995. Cell and tissue cultures of Catharanthus roseus: A literature survey: II. Updating from 1988 to 1993. Plant Cell Tiss Organ Cult 42, 1–25. https://doi.org/10.1007/BF00037677

Mujib, A., Fatima, S., Malik, M.Q., 2022. Cryo-derived plants through embryogenesis showed same levels of vinblastine and vincristine (anticancer) in Catharanthus roseus and had normal genome size. Sci Rep 12, 16635. https://doi.org/10.1038/s41598-022-20993-z

Mujib, A., Gupta, D., Tonk, D., 2017. Catharanthus roseus plant extracts (cultivated in vitro and ex vitro) protect Wistar rats against chemically induced liver carcinogenesis. Phytothérapie. https://doi.org/10.1007/s10298-017-1127-y

National Cancer Institute (U.S.), 1977. National Cancer Institute Monograph, 45. edition. ed. DHEW publication.

Nejat, N., Valdiani, A., Cahill, D., Tan, Y.-H., Maziah, M., Abiri, R., 2015. Ornamental Exterior versus Therapeutic Interior of Madagascar Periwinkle (*Catharanthus roseus*): The Two Faces of a Versatile Herb. The Scientific World Journal 2015, 982412. https://doi.org/10.1155/2015/982412

Olle, M., Viršile, A., 2013. The effects of light-emitting diode lighting on greenhouse plant growth and quality. AFSci 22, 223–234. https://doi.org/10.23986/afsci.7897

Ouzounis, T., Rosenqvist, E., Ottosen, C.-O., 2015. Spectral Effects of Artificial Light on Plant Physiology and Secondary Metabolism: A Review. horts 50, 1128–1135. https://doi.org/10.21273/HORTSCI.50.8.1128

Pan, Q., Wang, C., Xiong, Z., Wang, H., Fu, X., Shen, Q., Peng, B., Ma, Y., Sun, X., Tang, K., 2019. CrERF5, an AP2/ERF Transcription Factor, Positively Regulates the Biosynthesis of Bisindole Alkaloids and Their Precursors in Catharanthus roseus. Front. Plant Sci. 10, 931. https://doi.org/10.3389/fpls.2019.00931

Park, C.M., Youn, H.J., Chang, H.K., Song, Y.S., 2010. TOP1 and 2, polysaccharides from Taraxacum officinale, attenuate CCl4-induced hepatic damage through the modulation of NF-κB and its regulatory mediators. Food and Chemical Toxicology 48, 1255–1261. https://doi.org/10.1016/j.fct.2010.02.019

Park, J., Kim, J., Park, C., Noh, K., Song, Y., 2007. Hepatoprotective activity of Taraxacum Officinale Water Extract against D-galactosamine-induced hepatitis in rats. The FASEB Journal 21. https://doi.org/10.1096/fasebj.21.6.A1088-d

Pedneault, K., Léonhart, S., Gosselin, A., Papadopoulos, A.P., Dorais, M., Angers, P., 2002. Variations in concentration of active compounds in four hydroponically- and field- grown medicinal plant species. Acta Hortic. 255–262. https://doi.org/10.17660/ActaHortic.2002.580.34

Piazzon, A., Vrhovsek, U., Masuero, D., Mattivi, F., Mandoj, F., Nardini, M., 2012. Antioxidant Activity of Phenolic Acids and Their Metabolites: Synthesis and Antioxidant Properties of the Sulfate Derivatives of Ferulic and Caffeic Acids and of the Acyl Glucuronide of Ferulic Acid. J. Agric. Food Chem. 60, 12312–12323. https://doi.org/10.1021/jf304076z

Plazonić, A., Bucar, F., Maleš, Ž., Mornar, A., Nigović, B., Kujundžić, N., 2009. Identification and Quantification of Flavonoids and Phenolic Acids in Burr Parsley (Caucalis platycarpos L.), Using High-Performance Liquid Chromatography with Diode Array Detection and Electrospray Ionization Mass Spectrometry. Molecules 14, 2466–2490. https://doi.org/10.3390/molecules14072466

Rahman (Ed.), A.-U., 1994. Synthetic Approaches to Vinblastine and Vincristine - Anticancer Alkaloids of Catharanthus Roseus, in: Studies in Natural Products Chemistry. Elsevier, pp. 805–877. https://doi.org/10.1016/B978-0-444-81780-8.50028-4

RBG Kew, 2016. State of the world's plants. Royal Botanic Gardens, Kew.

Rider, C.V., Gorr, T.A., Olmstead, A.W., Wasilak, B.A., LeBlanc, G.A., 2005. Stress signaling: coregulation of hemoglobin and male sex determination through a terpenoid signaling pathway in a crustacean. Journal of Experimental Biology 208, 15–23. https://doi.org/10.1242/jeb.01343

Roepke, J., Salim, V., Wu, M., Thamm, A.M.K., Murata, J., Ploss, K., Boland, W., De Luca, V., 2010. Vinca drug components accumulate exclusively in leaf exudates of Madagascar periwinkle. Proc. Natl. Acad. Sci. U.S.A. 107, 15287–15292. https://doi.org/10.1073/pnas.0911451107

Saeki, D., Yamada, T., In, Y., Kajimoto, T., Tanaka, R., Iizuka, Y., Nakane, T., Takano, A., Masuda, K., 2013. Officinatrione: an unusual (17S)-17,18-seco-lupane skeleton, and four novel lupane-type triterpenoids from the roots of Taraxacum officinale. Tetrahedron 69, 1583–1589. https://doi.org/10.1016/j.tet.2012.12.001

Salama, I.M., Eliwa, N.E., Mohamed, M.H., 2020. Effect of UV-A on vincristine biosynthesis and related peroxidase isozyme changes in Catharanthus roseus. Journal of Radiation Research and Applied Sciences 13, 808–814. https://doi.org/10.1080/16878507.2020.1777658

Schröder, G., Unterbusch, E., Kaltenbach, M., Schmidt, J., Strack, D., De Luca, V., Schröder, J., 1999. Light-induced cytochrome P450-dependent enzyme in indole alkaloid biosynthesis: tabersonine 16-hydroxylase. FEBS Letters 458, 97–102. https://doi.org/10.1016/S0014-5793(99)01138-2

Schütz, K., Carle, R., Schieber, A., 2006. Taraxacum—A review on its phytochemical and pharmacological profile. Journal of Ethnopharmacology 107, 313–323. https://doi.org/10.1016/j.jep.2006.07.021

Schütz, K., Kammerer, D.R., Carle, R., Schieber, A., 2005. Characterization of phenolic acids and flavonoids in dandelion (*Taraxacum officinale* WEB. ex WIGG.) root and herb by high-performance liquid chromatography/electrospray ionization mass spectrometry. Rapid Comm Mass Spectrometry 19, 179–186. https://doi.org/10.1002/rcm.1767

Seo, S.-W., 2005. *Taraxacum officinale* protects against cholecystokinin-induced acute pancreatitis in rats. WJG 11, 597. https://doi.org/10.3748/wjg.v11.i4.597

Sergio, L., Boari, F., Pieralice, M., Linsalata, V., Cantore, V., Di Venere, D., 2020. Bioactive Phenolics and Antioxidant Capacity of Some Wild Edible Greens as Affected by Different Cooking Treatments. Foods 9, 1320. https://doi.org/10.3390/foods9091320

Sharma, A., Tiwari, P., Arora, R., Sankaranarayanan, A., 2022. Madagascar periwinkle alkaloids: Biosynthesis, ethnobotanical attributes, and pharmacological functions. South African Journal of Botany 151, 108–115. https://doi.org/10.1016/j.sajb.2022.09.039
Shriner, R.L., Fuson, R.C., Curtin, D.Y., Morrill, T.C., 2004. The systematic identification of organic compounds, 8th ed. J. Wiley & sons, Hoboken (N.J.).
Singh, D., Basu, C., Meinhardt-Wollweber, M., Roth, B., 2015. LEDs for energy efficient greenhouse lighting. Renewable and Sustainable Energy Reviews 49, 139–147. https://doi.org/10.1016/j.rser.2015.04.117
Śliwka-Kaszyńska, M., Anusiewicz, I., Skurski, P., 2022. The Mechanism of a Retro-Diels–Alder Fragmentation of Luteolin: Theoretical Studies Supported by Electrospray Ionization Tandem Mass Spectrometry Results. Molecules 27, 1032. https://doi.org/10.3390/molecules27031032
Sohier, W.D., Wong, R.K.L., Aisenberg, A.C., 1968. Vinblastine in the treatment of advanced Hodgkin's disease. Cancer 22, 467–472. https://doi.org/10.1002/1097-0142(196808)22:2%253C467::AID-CNCR2820220226%253E3.0.CO;2-A
Sottomayor, M., López-Serrano, M., DiCosmo, F., Ros Barceló, A., 1998. Purification and characterization of α-3′,4′-anhydrovinblastine synthase (peroxidase-like) from *Catharanthus roseus* (L.) G. Don. FEBS Letters 428, 299–303. https://doi.org/10.1016/S0014-5793(98)00551-1
Svoboda, G.H., Neuss, N., Gorman, M., 1959. Alkaloids of Vinca rosea Linn. (Catharanthus roseus G. Don.) V.**Organic Chemical Development and Lilly Research Laboratories, Eli Lilly and Co., Indianapolis, Ind. Journal of the American Pharmaceutical Association (Scientific ed.) 48, 659–666. https://doi.org/10.1002/jps.3030481115
Tan, T., Li, S., Fan, Y., Wang, Z., Ali Raza, M., Shafiq, I., Wang, B., Wu, X., Yong, T., Wang, X., Wu, Y., Yang, F., Yang, W., 2022. Far-red light: A regulator of plant morphology and photosynthetic capacity. The Crop Journal 10, 300–309. https://doi.org/10.1016/j.cj.2021.06.007
Tsagkaris, A.S., Louckova, A., Jaegerova, T., Tokarova, V., Hajslova, J., 2022. The In Vitro Inhibitory Effect of Selected Asteraceae Plants on Pancreatic Lipase Followed by Phenolic Content Identification through Liquid Chromatography High Resolution Mass Spectrometry (LC-HRMS). IJMS 23, 11204. https://doi.org/10.3390/ijms231911204
Vacca, V., Piga, A., Del Caro, A., Fenu, P.A.M., Agabbio, M., 2003. Changes in phenolic compounds, colour and antioxidant activity in industrial red myrtle liqueurs during storage. Nahrung 47, 442–447. https://doi.org/10.1002/food.200390098
Van Der Heijden, R., Verpoorte, R., Ten Hoopen, H.J.G., 1989. Cell and tissue cultures ofCatharanthus roseus (L.) G. Don: a literature survey. Plant Cell Tiss Organ Cult 18, 231–280. https://doi.org/10.1007/BF00043397
Vazquez-Flota, F.A., De Luca, V., 1998. Developmental and Light Regulation of Desacetoxyvindoline 4-Hydroxylase in *Catharanthus roseus* (L.) G. Don.1. Plant Physiology 117, 1351–1361. https://doi.org/10.1104/pp.117.4.1351
Vici, P., Colucci, G., Gebbia, V., Amodio, A., Giotta, F., Belli, F., Conti, F., Gebbia, N., Pezzella, G., Valerio, M.R., Brandi, M., Pisconti, S., Durini, E., Giannarelli, D., Lopez, M., 2002. First-Line Treatment With Epirubicin and Vinorelbine in Metastatic Breast Cancer. JCO 20, 2689–2694. https://doi.org/10.1200/JCO.2002.06.039
Wang, Z., Xiao, Y., Wu, S., Chen, J., Li, A., Tatsis, E.C., 2022. Deciphering and reprogramming the cyclization regioselectivity in bifurcation of indole alkaloid biosynthesis. Chem. Sci. 13, 12389–12395. https://doi.org/10.1039/D2SC03612F
Wappel, S.M., Schulte, M.S., 2004. Turtle care and husbandry. Veterinary Clinics of North America: Exotic Animal Practice 7, 447–472. https://doi.org/10.1016/j.cvex.2004.03.002
Williams, C.A., Goldstone, F., Greenham, J., 1996. Flavonoids, cinnamic acids and coumarins from the different tissues and medicinal preparations of Taraxacum officinale. Phytochemistry 42, 121–127. https://doi.org/10.1016/0031-9422(95)00865-9

Wilson, E.O. (Ed.), 1988. Biodiversity. National Academies Press, Washington, D.C. https://doi.org/10.17226/989
World Health Organization, 2007. WHO guidelines on good manufacturing practices (GMP) for herbal medicines 72.
Wu, G., Johnson, S.K., Bornman, J.F., Bennett, S.J., Clarke, M.W., Singh, V., Fang, Z., 2016. Growth temperature and genotype both play important roles in sorghum grain phenolic composition. Sci Rep 6, 21835. https://doi.org/10.1038/srep21835
Yang, Z.-W., Xu, F., Liu, X., Cao, Y., Tang, Q., Chen, Q.-Y., Shang, M.-Y., Liu, G.-X., Wang, X., Cai, S.-Q., 2017. An untargeted metabolomics approach to determine component differences and variation in their *in vivo* distribution between Kuqin and Ziqin, two commercial specifications of Scutellaria Radix. RSC Adv. 7, 54682–54695. https://doi.org/10.1039/C7RA10705F
Yaniv, Z., Bachrach, U. (Eds.), 2005. Handbook of Medicinal Plants. CRC Press. https://doi.org/10.1201/9781482278026
Yu, B., Liu, Y., Liu, J., Guo, X., Tang, Z., 2022. Integrated Analyses of Metabolomic Profiling and Associated Gene Expression of Catharanthus roseus Seedling Reveal the Metabolic Alternations of Primary Metabolites and Flavonoids During the Apical Hook Opening Phase. J Plant Growth Regul 41, 2093–2107. https://doi.org/10.1007/s00344-021-10374-7
Yu, R., Zhu, J., Wang, M., Wen, W., 2015. Biosynthesis and regulation of terpenoid indole alkaloids in Catharanthus roseus. Phcog Rev 9, 24. https://doi.org/10.4103/0973-7847.156323
Zhang, L.-X., Dong, J., Wei, H., Shi, S.-H., Lu, A.-P., Deng, G.-M., Cao, D.-S., 2022. TCMSID: a simplified integrated database for drug discovery from traditional chinese medicine. J Cheminform 14, 89. https://doi.org/10.1186/s13321-022-00670-z
Zhang, Y., Mgeni, M., Xiu, Z., Chen, Y., Chen, J., Sun, Y., 2024. Effects of Dandelion Extract on Promoting Production Performance and Reducing Mammary Oxidative Stress in Dairy Cows Fed High-Concentrate Diet. IJMS 25, 6075. https://doi.org/10.3390/ijms25116075
Zhiponova, M., Zehirov, G., Rusanov, K., Rusanova, M., Stefanova, M., Ganeva, T., Paunov, M., Ganeva, V., Mishev, K., Dobrev, P.I., Vaculíková, R., Motyka, V., Yordanova, Z., Chaneva, G., Vassileva, V., 2025. Blue–Red LED Light Modulates Morphophysiological and Metabolic Responses in the Medicinal Plant Nepeta nuda. Plants 14, 2285. https://doi.org/10.3390/plants14152285
Zhong, Z., Liu, S., Han, S., Li, Y., Tao, M., Liu, A., He, Q., Chen, S., Dufresne, C., Zhu, W., Tian, J., 2021. Integrative omic analysis reveals the improvement of alkaloid accumulation by ultraviolet-B radiation and its upstream regulation in Catharanthus roseus. Industrial Crops and Products 166, 113448. https://doi.org/10.1016/j.indcrop.2021.113448
Zou, H., Ben, T., Wu, P., Waterhouse, G.I.N., Chen, Y., 2023. Effective anti-inflammatory phenolic compounds from dandelion: identification and mechanistic insights using UHPLC-ESI-MS/MS, fluorescence quenching and anisotropy, molecular docking and dynamics simulation. Food Science and Human Wellness 12, 2184–2194. https://doi.org/10.1016/j.fshw.2023.03.031
Zuo, J., Zhang, W., Jian, H., Bou-Chacra, N., Löbenberg, R., 2020. Esculetin as bioactive marker: towards a rational scientific approach for the treatment of hyperuricemia using Traditional Chinese Medicine. Braz. J. Pharm. Sci. 56, e17827. https://doi.org/10.1590/s2175-97902019000417827

A2: Literature overviews for metabolomic profiling

App. Table 1. List of vinca alkaloids and metabolically-related compounds

Compound	Neutral formula	Neutral monoisotopic mass	Characteristic adduct in ESI-MS
(3R)-3-Hydroxy-1,2-didehydro-2,3-dihydrotabersonine	C21H24N2O3	352.1787	-
(3R)-3-Hydroxy-16-methoxy-1,2-didehydro-2,3-dihydrotabersonine	C22H26N2O4	382.1893	-
(3R)-3-Hydroxy-2,3-dihydrotabersonine	C21H26N2O3	354.1943	-
(S)-8-Oxocitronellyl enol	C10H16O2	168.1150	-
10-Deoxygeniposidic acid	C16H22O9	358.1264	-
16-Hydroxytabersonine	C21H24N2O3	352.1787	$[M+H]^+$
16-Methoxy-2,3-dihydro-3-hydroxytabersonine	C22H28N2O4	384.2049	-
16-Methoxytabersonine	C22H26N2O3	366.1943	$[M+H]^+$
19-Hydroxytabersonine	C21H24N2O3	352.1787	$[M+H]^+$
19-*S*-vindolinine	C25H32N2O6	456.2260	$[M+H]^+$
3',4'-Anhydrovinblastine	C46H56N4O8	792.4098	$[M+2H]^{++}$
4,21-Dehydrogeissoschizine	C21H23N2O3	351.1709	$[M+H]^+$
7-Deoxyloganate	C16H24O9	360.1420	-
7-Deoxyloganetate	C10H14O4	198.0892	-
7-Deoxyloganetic alcohol	C10H16O3	184.1099	-
7-Deoxyloganetin	C11H16O4	212.1049	-
7-Deoxyloganin	C17H26O9	374.1577	-
8-Hydroxygeraniol	C10H18O2	170.1307	-
8-Oxogeranial	C10H14O2	166.0994	-
Ajmalicine	C21H24N2O3	352.1787	$[M+H]^+$
Ajmaline	C20H26N2O2	326.1994	$[M+H]^+$
Alstonine	C21H20N2O3	348.1474	$[M+H]^+$
Asperuloside	C18H22O11	414.1162	$[M+H]^+$
Catharanthamine	C46H56N4O9	808.4047	-
Catharanthine	C21H24N2O2	336.1838	$[M+H]^+$
Cathenamine	C21H22N2O3	350.1630	-
cis-trans-Nepetalactol	C10H16O2	168.1150	-

Compound	Neutral formula	Neutral monoisotopic mass	Characteristic adduct in ESI-MS
Deacetylvindoline	C23H30N2O5	414.2155	$[M+H]^+$
Desacetoxyvindoline	C23H30N2O4	398.2206	-
Echitovenine	C23H28N2O4	396.2049	$[M+H]^+$
Geissoschizine	C21H24N2O3	352.1787	$[M+H]^+$
Geniposidic acid	C16H22O10	374.1213	$[M-H]^-$
Gentiopicrin	C16H20O9	356.1107	$[M+Na]^+$
Geraniol	C10H18O	154.1358	$[M+H]^+$
Horhammericine	C21H24N2O4	368.1736	$[M+H]^+$
Iridotrial	C10H14O3	182.0943	-
Lochnericine	C21H24N2O3	352.1787	$[M+H]^+$
Lochnerinine	C22H26N2O4	382.1893	-
Loganic acid	C16H24O10	376.1370	$[M+H]^+$, $[M-H]^-$
Loganin	C17H26O10	390.1526	$[M+H]^+$, $[M-H]^-$
Minovincinine	C21H26N2O3	354.1943	$[M+H]^+$
Norajmaline	C19H24N2O2	312.1838	-
Norseredamine	C20H24N2O2	324.1838	$[M+H]^+$
Raucaffricine	C27H32N2O8	512.2159	$[M+H]^+$
Reserpine	C33H40N2O9	608.2734	$[M+H]^+$
Sarpagine	C19H22N2O2	310.1681	-
Secologanate	C16H22O10	374.1213	$[M-H]^-$
Secologanin	C17H24O10	388.1370	$[M+Na]^+$
Serpentine	C21H20N2O3	348.1474	$[M+H]^+$
Stemmadenine	C21H26N2O3	354.1943	-
Strictosidine	C27H34N2O9	530.2264	$[M+H]^+$
Strictosidine aglycone	C21H24N2O4	368.1736	-
Tabersonine	C21H24N2O2	336.1838	$[M+H]^+$
Tetrahydroalstonine	C21H24N2O3	352.1787	$[M+H]^+$
Vellosimine	C19H20N2O	292.1576	$[M+H]^+$
Vinblastine	C46H58N4O9	810.4204	$[M+H]^+$
Vincadifformine	C21H26N2O2	338.1994	$[M+H]^+$
Vincristine	C46H56N4O10	824.3996	$[M+H]^+$
Vindoline	C25H32N2O6	456.2260	$[M+H]^+$
Vindolinine	C21H24N2O2	336.1838	$[M+H]^+$
Vindorosine	C24H31N2O5	427.2233	$[M+H]^+$

Compound	Neutral formula	Neutral monoisotopic mass	Characteristic adduct in ESI-MS
Vinorine	C21H22N2O2	334.1681	-
Vomilenine	C21H22N2O3	350.1630	$[M+H]^+$
Yohimbine	C21H26N2O3	354.1943	$[M+H]^+$

App. Table 2. List of compounds previously identified in different parts of the dandelion plant

Hydrocarbons and derivatives			
Compound	**Formula**	**Plant part**	**Source**
2,5,5-Trimethylheptane	C10H22	essential oil (flower)	Bylka et al., 2010
6-Ethyl-2-methyloctane	C11H24	essential oil (flower)	Bylka et al., 2010
Pentadecane	C15H32	essential oil (flower)	Bylka et al., 2010
Hexadecane	C16H34	essential oil (flower)	Bylka et al., 2010
Nonadecane	C19H40	essential oil (flower)	Bylka et al., 2010
Eicosane	C20H42	essential oil (flower), plant (not specified)	Bylka et al., 2010; Jung et al., 2011
Heneicosane	C21H44	essential oil (flower)	Bylka et al., 2010
Tricosane	C23H48	essential oil (flower)	Bylka et al., 2010
Heptacosane	C27H56	not specified	Jung et al., 2011
1-Tridecyne	C13H24	essential oil (flower)	Bylka et al., 2010
1,2-Dimethylbenzene	C8H10	essential oil (flower)	Bylka et al., 2010
1,3-Dimethylbenzene	C8H10	essential oil (flower)	Bylka et al., 2010
1-Ethyl-3-methylbenzene	C9H12	essential oil (flower)	Bylka et al., 2010

Alcohols and derivatives			
Compound	**Formula**	**Plant part**	**Source**
1,9-Nonanediol	C9H20O2	essential oil (flower)	Bylka et al., 2010
1-Tridecanol	C13H28O	essential oil (flower)	Bylka et al., 2010
1-Nonadecanol	C19H40O	essential oil (flower)	Kamal et al., 2022

Compound	Formula	Plant part	Source
2-Nonen-1-ol	C9H18O	essential oil (flower)	Bylka et al., 2010
Dihydroconiferin	C16H24O8	root	Kisiel&Barszcz, 2000
Syringin	C17H24O9	root	Kisiel&Barszcz, 2000; Choi et al., 2017
Dihydrosyringin	C17H26O9	root	Kisiel&Barszcz, 2000
1-Hydroxymethyl-4-methylbenzene	C8H10O	essential oil (flower)	Bylka et al., 2010
4-Methylcatechol	C7H8O2	fermented plant	Liu et al., 2020
Aldehydes, ketones and derivatives			
Compound	**Formula**	**Plant part**	**Source**
Octanal	C8H16O	essential oil (flower)	Bylka et al., 2010
Nonanal	C9H18O	essential oil (flower)	Bylka et al., 2010
10-Undecenal	C11H20O	essential oil (flower)	Bylka et al., 2010
Pentadecanal	C15H30O	essential oil (flower)	Bylka et al., 2010
5-Methyl-2-hexanone	C7H14O	essential oil (flower)	Bylka et al., 2010
2-Methylbenzaldehyde	C8H8O	essential oil (flower)	Bylka et al., 2010
Phenylacetaldehyde	C8H8O	essential oil (flower)	Bylka et al., 2010
Vanillin	C8H8O3	root	Kenny et al., 2015(2)
Coniferyl aldehyde	C10H10O3	root	Kenny et al., 2015(2)
Juglone	C10H6O3	whole plant	Zou et al., 2023
Heptadecanolide	C17H32O2	essential oil (flower)	Kamal et al., 2022

Organic acids			
Compound	**Formula**	**Plant part**	**Source**
Formic acid	CH2O2	leaf	Grauso et al., 2019
Acetic acid	C2H4O2	leaf	Grauso et al., 2019
Malonic acid	C3H4O4	leaf	Grauso et al., 2019
Succinic acid	C4H6O4	leaf	Grauso et al., 2019
Malic acid	C4H6O5	leaf	Grauso et al., 2019
Tartaric acid	C4H6O6	leaf	Grauso et al., 2019
Citric acid	C6H8O7	leaf	Grauso et al., 2019
Quinic acid	C7H12O6	leaf	Grauso et al., 2019
Tetradecanoic acid	C14H28O2	essential oil (flower)	Kamal et al., 2022
Pentadecanoic acid	C15H30O2	essential oil (flower)	Kamal et al., 2022
Hexadecanoic acid	C16H32O2	essential oil (flower), plant (not specified), leaf	Bylka et al., 2010; Jung et al., 2011; Kamal et al., 2022; Grauso et al., 2019
Heptadecanoic acid	C17H34O2	essential oil (flower)	Jung et al., 2011; Kamal et al., 2022
Linolenic acid	C18H30O2	not specified	Jung et al., 2011
9-hydroxyoctadecatrienoic acid	C18H30O3	root	Kenny et al., 2015(2)
9,12-octadecadienoic acid	C18H32O2	essential oil (flower)	Jung et al., 2011; Kamal et al., 2022
Linoelaidic acid	C18H32O2	essential oil (flower)	Kamal et al., 2022
9-hydroxyoctadecadienoic acid	C18H32O3	root	Kenny et al., 2015(2)
Oleic acid	C18H34O2	leaf	Grauso et al., 2019
Octadecanoic acid	C18H36O2	essential oil (flower), leaf	Jung et al., 2011; Kamal et al., 2022; Grauso et al., 2019
Arachidic acid	C20H40O2	leaf	Grauso et al., 2019
Docosanoic acid	C22H44O2	leaf	Jung et al., 2011; Grauso et al., 2019

Compound	Formula	Plant part	Source
Tricosanoic acid	C23H46O2	not specified	Jung et al., 2011
Tetracosanoic acid	C24H48O2	leaf	Jung et al., 2011; Grauso et al., 2019
Hexacosanoic acid	C26H52O2	leaf	Jung et al., 2011; Grauso et al., 2019
Octacosanoic acid	C28H56O2	leaf	Grauso et al., 2019
p-methoxyphenylglyoxylic acid	C9H9O4	root	Kenny et al., 2015(2)

Organic esters			
Compound	**Formula**	**Plant part**	**Source**
Benzyl benzoate	C14H12O2	essential oil (flower)	Bylka et al., 2010
Taraxiroside D	C27H30O13	not specified	Choi et al., 2017
Taraxiroside E	C27H32O12	not specified	Choi et al., 2017
Taraxiroside F	C19H26O11	not specified	Choi et al., 2017

Terpenoids			
Compound	**Formula**	**Plant part**	**Source**
Lup-18-ene-3,21-dione	C30H45O2	root	Saeki et al., 2013
(17S)-17,18-seco-lup-19(21)-ene-3,18,22-trione	C30H45O3	root	Saeki et al., 2013
18α,19α-epoxy-21β-hydroxylupan-3-one	C30H47O3	root	Saeki et al., 2013
3β-hydroxylup-18(19)-ene-21-one	C30H48O2	root	Kisiel&Barszcz, 2000
Taraxasterol isomers	C30H50O	leaf, root	Bisset, 1994

Compound	Formula	Plant part	Source
Taraxerol	C30H50O	leaf, root	WHO, 1999
α-Amyrin	C30H50O	root	Schütz et al., 2006
β-Amyrin	C30H50O	leaf, root, flower	Bisset, 1994; Bylka et al., 2010; Jung et al., 2011
Arnidiol	C30H50O2	leaf, root, flower	Bisset, 1994; Bylka et al., 2010
Faradiol	C30H50O2	leaf, root, flower	Bisset, 1994; Bylka et al., 2010
Lupa-18,21-dien-3β-yl acetate	C32H49O2	root	Saeki et al., 2013
3β-acetoxyeupha-7,24-dien-6-one	C32H49O3	root	Kikuchi et al., 2016
3β-acetoxy-18α,19α-epoxylupan-21β-ol	C32H51O4	root	Saeki et al., 2013
Taraxasterolacetate isomers	C32H52O2	leaf, root	Bisset, 1994; Hänsel et al., 1980
18β,19β-epoxy-21β-methoxylupan-3β-yl acetate	C33H53O4	root	Kikuchi et al., 2016
Thunbergol	C20H34O	essential oil (flower)	Kamal et al., 2022
Phytol	C20H40O	leaf	Jung et al., 2011
6S,9R-Roseoside	C19H30O8	not specified	Choi et al., 2017
6S,9S-Roseoside	C19H30O8	not specified	Choi et al., 2017
11β, 13-Dihydrolactucin	C15H18O5	root	Kisiel&Barszcz, 2000
4,11,13,15-Tetrahydroridentin B	C15H24O4	root	Kisiel&Barszcz, 2000; WHO, 1999
Ainslioside	C21H28O9	root	Kisiel&Barszcz, 2000
Taraxinic acid β-D-glucopyranoside	C21H28O9	root	Kisiel&Barszcz, 2000; WHO, 1999
11β, 13-dihydrotaraxinic acid β-glucopyranoside	C21H30O9	root	Kisiel&Barszcz, 2000; WHO, 1999; Choi et al., 2017
Ixerin D	C21H30O9	root	Kisiel&Barszcz, 2000

Compound	Formula	Plant part	Source
Sonchuside	C21H32O8	root	Schütz et al., 2006
Taraxacolide 1-O-b-D-glucopyranoside	C21H32O9	root	Kisiel&Barszcz, 2000; WHO, 1999
Taraxinic acid-1´-O-glucoside	C22H30O11	fruit	Lis et al., 2020
Coumarins and derivatives			
Compound	**Formula**	**Plant part**	**Source**
Scopoletin	C10H8O4	root	Schütz et al., 2006
Cichoriin	C15H16O9	leaf	Williams et al., 1996; Buzdianowski, 1997
Esculetin	C9H6O4	root	Schütz et al., 2006
Esculin	C15H16O9	leaf	Williams et al., 1996; Buzdianowski, 1997
Umbelliferone	C9H6O3	root	Schütz et al., 2006

Phenolic acids and derivatives			
Compound	**Formula**	**Plant part**	**Source**
p-Hydroxybenzoic acid	C7H6O3	root	Schütz et al., 2006
Protocatechuic acid	C7H6O4	root	Schütz et al., 2006
Gallic acid	C7H6O5	flower	López-García et al., 2013
Ellagic acid	C14H6O8	fermented plant	Liu et al., 2020
Syringic acid	C9H10O5	root	Schütz et al., 2006
p-Hydroxyphenylacetic acid	C8H8O3	root	Schütz et al., 2006
Vanillic acid	C8H8O4	root, flower	Schütz et al., 2006; López-García et al., 2013
p-Coumaric acid	C9H8O3	root	Schütz et al., 2006

Compound	Formula	Plant part	Source
trans-Coutaric acid	C13H12O8	root and herb	Schütz et al., 2005
Coumaroylquinic acid	C16H18O8	root	Jedrejek et al., 2019
Ferulic acid	C10H10O4	root	Schütz et al., 2006; Zou et al., 2023
Feruloyltartaric acid	C14H14O9	root	Jedrejek et al., 2019
Feruloylquinic acid	C17H20O9	root	Jedrejek et al., 2019
Caffeic acid	C9H8O4	leaf, root, flower, fruit	Bisset, 1994; Hu&Kitts, 2004; Schütz et al., 2005; Lis et al., 2020; Zou et al., 2023
Methyl caffeate	C10H10O4	not specified	Choi et al., 2017
Caffeoylmalic acid	C13H12O8	leaf	Miłek et al., 2019
Caftaric acid isomers	C13H12O9	leaf, root, herb, flower, involucral bract, fruit	Williams et al., 1996; Buzdianowski, 1997; Schütz et al., 2005; Grauso et al., 2019; Lis et al., 2020; Zou et al., 2023
Chicoric acid isomers	C22H18O12	leaf, root, fruit	Williams et al., 1996; Gatto et al., 2011; Grauso et al., 2019; Lis et al., 2020; Zou et al., 2023
Caffeic acid 3-glucoside	C15H18O9	whole plant	Zou et al., 2023
Caffeoyl hexoside	C15H18O9	root and herb	Schütz et al., 2005
Chlorogenic acid	C16H18O9	leaf, flower, fruit	Kristó et al., 2002; Hu&Kitts, 2004; Grauso et al., 2019; Lis et al., 2020; Zou et al., 2023
Cryptochlorogenic acid	C16H18O9	root	Schütz et al., 2006; Schütz et al., 2005
Neochlorogenic acid	C16H18O9	leaf, root, flower, involucral bract	Williams et al., 1996; Grauso et al., 2019
1,3-Dicaffeoylquinic acid	C25H24O12	root	Kenny et al., 2015
1,5-Dicaffeoylquinic acid	C25H24O12	root	Kenny et al., 2015

Compound	Formula	Plant part	Source
3,4-Dicaffeoylquinic acid	C25H24O12	root and herb	Schütz et al., 2005
3,5-Dicaffeoylquinic acid	C25H24O12	root, herb, fruit	Schütz et al., 2005; Lis et al., 2020
4,5-Dicaffeoylquinic acid	C25H24O12	root and herb	Schütz et al., 2005
Caffeoyl-feruloylquinic acid	C26H26O12	flower	Jedrejek&Pawelec, 2024
Caffeoyl glycerol	C12H14O6	whole plant	Zou et al., 2023
Caffeoyl-dihydroxyphenyllactoyltartaric acid	C22H20O13	root and herb	Schütz et al., 2005
Sinapic acid	C11H12O5	flower, whole plant	López-García et al., 2013; Zou et al., 2023
Dihydrosinapic acid	C11H14O5	whole plant	Zou et al., 2023
4´-O-Demethylbroussonin A	C15H16O3	whole plant	Zou et al., 2023

Carotenoids and degraded derivatives			
Compound	**Formula**	**Plant part**	**Source**
Taraxanthin geometrical isomers	C40H56O3	flower	Meléndez-Martínez et al., 2006
Epiloliolide	C11H16O3	not specified	Choi et al., 2017
Loliolide	C11H16O3	not specified	Choi et al., 2017

Flavonoids and derivatives			
Compound	**Formula**	**Plant part**	**Source**
3-Hydroxyflavone	C15H10O3	whole plant	Liu et al., 2020
4´,7-Dihydroxyflavone	C15H10O4	fermented plant	Liu et al., 2020
Myricitrin	C21H20O12	fermented plant	Liu et al., 2020

Compound	Formula	Plant part	Source
Quercetin pentoside	C20H18O11	root and herb	Schütz et al., 2005
Quercetin 7-O-glucoside	C21H20O12	leaf, flower	Schütz et al., 2005
Quercetin 7-rutinoside	C27H30O16	leaf	Grauso et al., 2019
Rutin	C27H30O16	flower, whole plant	López-García et al., 2013; Liu et al., 2020
Quercetin diglycoside	C27H30O17	root and herb	Schütz et al., 2005
3,7-di-O-Methylquercetin	C17H14O7	whole plant	Zou et al., 2023
Quercetin triglycoside	C33H40O22	root and herb	Schütz et al., 2005
Daidzein	C15H10O4	whole plant	Liu et al., 2020
2´-Hydroxydaidzein	C15H10O5	fermented plant	Liu et al., 2020
Formononetin	C16H12O4	herb, root	Tsagkaris et al., 2022
Methylophiopogonone A	C19H16O6	whole plant	Zou et al., 2023
Apigenin	C15H10O5	fruit, herb	Lis et al., 2020; Tsagkaris et al., 2022
Apigenin 7-O-glucoside	C21H20O10	leaf, root	Bisset, 1994; Kristó et al., 2002; Grauso et al., 2019
Amentoflavone	C30H18O10	whole plant	Liu et al., 2020
Baicalein	C15H10O5	fermented plant	Liu et al., 2020
Luteolin	C15H10O6	flower, fruit	Williams et al., 1996; Hu&Kitts, 2004; Lis et al., 2020
Luteolin 4´-O-glucoside	C21H20O11	root, herb, fruit	Schütz et al., 2005; Lis et al., 2020
Luteolin 7-O-glucoside	C21H20O11	leaf, flower, involucral bract, fruit	Williams et al., 1996; Kristó et al., 2002; Hu&Kitts, 2004; Gatto et al., 2011; Grauso et al., 2019; Lis et al., 2020
Luteolin 3´-O-glucoside	C21H20O11	fruit	Lis et al., 2020
Luteolin 7-O-rutinoside	C27H30O15	leaf	Schütz et al., 2005; Grauso et al., 2019
Luteolin 7-diglucoside isomers	C27H30O16	leaf, flower, involucral bract	Williams et al., 1996

Compound	Formula	Plant part	Source
Luteolin diglycoside	C27H30O16	root and herb	Schütz et al., 2005
Luteolin triglycoside	C33H40O21	root and herb	Schütz et al., 2005
Dicranolomin	C30H18O12	flower	Jedrejek&Pawelec, 2024
Philonotisflavone	C30H18O12	fruit, flower	Lis et al., 2020; Jedrejek&Pawelec, 2024
Taraxabiluteolin A	C30H18O12	flower	Jedrejek&Pawelec, 2024
Taraxabiluteolin B	C30H18O12	flower	Jedrejek&Pawelec, 2024
Chrysoeriol	C16H12O6	flower, fruit	Williams et al., 1996; Miłek et al., 2019; Lis et al., 2020
Chrysoeriol-O-hexoside	C22H22O11	flower	Jedrejek&Pawelec, 2024
Chrysoeriol diglycoside	C28H32O16	root and herb	Schütz et al., 2005
Methyltricetin	C16H12O7	fruit	Lis et al., 2020
Tricin	C17H14O7	fruit, flower	Lis et al., 2020; Jedrejek&Pawelec, 2024
Pedalitin	C16H12O7	fermented plant	Liu et al., 2020
Apometzgerin	C17H14O7	fruit, flower	Lis et al., 2020; Jedrejek&Pawelec, 2024
Eupatilin	C18H16O7	whole plant	Zou et al., 2023
Cyanidin	C15H11O6+	fermented plant	Liu et al., 2020
Myrtillin	C21H21O12+	whole plant	Liu et al., 2020
Garbanzol	C15H12O5	whole plant	Liu et al., 2020
Dihydromyricetin	C15H12O8	fermented plant	Liu et al., 2020
Epigallocatechin	C15H14O7	whole plant	Liu et al., 2020
Isorhamnetin 3-O-glucoside	C22H22O12	leaf	Schütz et al., 2005
Farrerol	C17H16O5	fermented plant	Liu et al., 2020
Prunin	C21H22O10	whole plant	Liu et al., 2020

Compound	Formula	Plant part	Source
Calquiquelignan D	C26H24O10	flower	Choi et al., 2017; Jedrejek&Pawelec, 2024
Calquiquelignan E	C26H24O10	flower	Choi et al., 2017; Jedrejek&Pawelec, 2024
7´´-methoxycalquiquelignan D	C27H26O10	flower	Jedrejek&Pawelec, 2024
7´´-methoxycalquiquelignan E	C27H26O10	flower	Jedrejek&Pawelec, 2024
Salcolin A	C27H26O11	flower	Jedrejek&Pawelec, 2024
Salcolin B	C27H26O11	flower	Jedrejek&Pawelec, 2024
Methoxysalcolin A	C28H28O11	flower	Jedrejek&Pawelec, 2024
Methoxysalcolin B	C28H28O11	flower	Jedrejek&Pawelec, 2024

Chalcones			
Compound	**Formula**	**Plant part**	**Source**
Isoliquiritigenin	C15H12O4	fermented plant	Liu et al., 2020
Liquiritigenin	C15H12O4	fermented plant	Liu et al., 2020
Butein	C15H12O5	fermented plant	Liu et al., 2020
Xanthohumol	C21H22O5	fermented plant	Liu et al., 2020
Liquiritin	C21H22O9	fermented plant	Liu et al., 2020

Stilbene derivatives			
Compound	**Formula**	**Plant part**	**Source**
Resveratrol	C14H12O3	flower	López-García et al., 2013
Thunalbene	C15H14O3	whole plant	Zou et al., 2023

Butyrolactones and derivatives			
Compound	**Formula**	**Plant part**	**Source**
Taraxacoside	C18H22O10	leaf, root	WHO, 1999; Schütz et al., 2006
Taraxiroside A	C26H28O12	not specified	Choi et al., 2017
Taraxiroside B	C26H28O11	not specified	Choi et al., 2017
Taraxiroside C	C18H22O10	not specified	Choi et al., 2017

Curcuminoides			
Compound	**Formula**	**Plant part**	**Source**
Demethoxycurcumin	C20H18O5	fermented plant	Liu et al., 2020
Curcumin	C21H20O6	fermented plant	Liu et al., 2020

Phytosterols			
Compound	**Formula**	**Plant part**	**Source**
Stigmasterol	C29H48O	leaf, root, plant (not specified)	Bisset, 1994; Jung et al., 2011
β-Sitosterol	C29H50O	not specified	Hänsel et al., 1980; Bisset, 1994; Jung et al., 2011
Lanosterol	C30H50O	not specified	Jung et al., 2011
β-Sitosterol β-D-glucopyranoside	C35H60O6	not specified	Hänsel et al., 1980

Other			
Compound	**Formula**	**Plant part**	**Source**
3-glycerindole	C10H9NO2	not specified	Choi et al., 2017
Annuionone D	C13H20O3	not specified	Choi et al., 2017
α-Tocopherol	C29H50O2	not specified	Jung et al., 2011
Benzyl O-β-glucopyranoside	C13H18O6	root	Kisiel&Barszcz, 2000

A3: Chromatographic, MS and ion mobility data of the identified compounds in dandelion samples

No.	Compound name	Elemental composition (neutral)	Theoretical *m/z* $[M-H]^-$	Experimental *m/z* $[M-H]^-$	Difference, ppm	CCS in ESI '-' mode, $(Å)^2$	Theoretical *m/z* $[M+H]^+$	Experimental *m/z* $[M+H]^+$	Difference, ppm	CCS in ESI '+' mode, $(Å)^2$	Retention time, min	VIP	Identification level[#]	Identified by
1	Caffeic acid glucoside_1	C15H18O9	341.0878	341.0882	1.14	182.13					1.31		D2	MoNA (ID: PM003718)
2	Caffeic acid derivative_1	C9H8O7S	258.9918	258.9914	-1.54	149.72					1.59	10.0 (F/L)**	D2	Piazzon et al., 2012
3	Caffeic acid glucoside_2	C15H18O9	341.0878	341.0875	-0.91	182.29					1.86		D2	MoNA (ID: PM003718)
4	Protocatechuoylglucose_1 *	C13H16O9	315.0722	315.0712	-3.05	170.98					1.94		D2	MoNA (ID: PR309056)
5	Caffeic acid sulfate_1*	C9H8O7S	258.9918	258.9913	-1.93	143.28					2.10		D2	Piazzon et al., 2012
6	Protocatechuoylglucose_2 *	C13H16O9	315.0722	315.0714	-2.41	166.23					2.63		D2	MassBank (ID: MSBNK-RIKEN-PR309056)
7	Esculetin sulfate*	C9H6O7S	256.9762	256.9756	-2.14	141.07					2.71		D2	Zuo et al., 2020
8	Caftaric acid	C13H12O9	311.0409	311.0406	-0.96	225.97					2.74	10.0 (D/F)**, 9.9 (F/L)**	C	authentic standard
9	Neochlorogenic acid (3CQA)	C16H18O9	353.0878	353.0873	-1.44	171.90					2.96		C	authentic standard
10	Caffeic acid sulfate_2*	C9H8O7S	258.9918	258.9913	-1.93	144.97					3.23		D2	Piazzon et al., 2012
11	Esculin	C15H16O9	339.0722	339.0717	-1.47	174.60	341.0867	341.0869	0.59	178.18	3.64		C	authentic standard
12	Caffeoylsucrose*	C21H28O14	503.1406	503.1395	-2.25	208.51					4.55		D2	Commisso et al., 2019

No.	Compound name	Elemental composition (neutral)	Theoretical *m/z* $[M-H]^-$	Experimental *m/z* $[M-H]^-$	Difference, ppm	CCS in ESI '-' mode, $(Å)^2$	Theoretical *m/z* $[M+H]^+$	Experimental *m/z* $[M+H]^+$	Difference, ppm	CCS in ESI '+' mode, $(Å)^2$	Retention time, min	VIP	Identification level#	Identified by
13	Chlorogenic acid (5CQA)	C16H18O9	353.0878	353.0873	-1.42	254.93	355.1024	355.1022	-0.56	184.32	4.92		C	authentic standard
14	Esculetin	C9H6O4	177.0193	177.0191	-1.13	126.94	179.0339	179.0341	1.12	130.21	5.00	8.2 (F/L)**	C	authentic standard
15	Caffeic acid	C9H8O4	179.0350	179.0349	-0.56	132.84					5.19		C	authentic standard
16	1-caffeyllaminaribiose*	C21H28O14	503.1406	503.1400	-1.25	206.17					5.42		D2	Yang et al., 2017
17	Cryptochlorogenic acid (4CQA)	C16H18O9	353.0878	353.0873	-1.44	183.83					5.67		C	authentic standard
18	Daphnetin*	C9H6O4	177.0193	177.0191	-1.13	127.97	179.0339	179.0341	1.12	130.94	6.41		C	authentic standard
19	12-Hydroxyjasmonate sulfate_1*	C12H18O7S	305.0701	305.0692	-2.79	159.29					6.58	12.7 (D/F)**	D2	Gidda et al., 2003
20	Taraxinositol A/B*	C22H24O10	447.1297	447.1288	-1.95	193.81	449.1442	449.1448	1.29	211.90	6.63	8.8 (F/L)**	E	
21	Fraxin*	C16H18O10	369.0827	369.0824	-0.81	178.09					6.69		C	authentic standard
22	12-Hydroxyjasmonate sulfate_2*	C12H18O7S	305.0701	305.0691	-3.28	160.98					6.77		D2	Gidda et al., 2003
23	Caffeoylglycerol	C12H14O6	253.0718	253.0713	-1.82	159.47					6.81		D2	Wu et al., 2016
24	Quercetin dihexoside_1	C27H30O17	625.1410	625.1402	-1.31	243.71	627.1556	627.1556	0.03	254.49	6.87		E	MassBank (ID: MSBNK-RIKEN-PR100914)
25	Pyroglutamylisoleucine	C11H18N2O4	241.1194	241.1191	-1.16	161.60	243.1339	243.1340	0.29	168.35	7.67	6.3 (F/L)**	D2	MoNA (ID: PR309064)

No.	Compound name	Elemental composition (neutral)	Theoretical *m/z* $[M-H]^-$	Experimental *m/z* $[M-H]^-$	Difference, ppm	CCS in ESI '-' mode, $(Å)^2$	Theoretical *m/z* $[M+H]^+$	Experimental *m/z* $[M+H]^+$	Difference, ppm	CCS in ESI '+' mode, $(Å)^2$	Retention time, min	VIP	Identification level[#]	Identified by
26	Quercetin derivative_1 (pentose+hexose moiety)	C26H28O16	595.1304	595.1288	-2.69	236.12	597.1450	597.1457	1.16	241.74	7.70	12.7 (D/F)**	E	MassBank (ID: MSBNK-RIKEN_RePSpect-PT204313)
27	Chicoric acid derivative	C28H28O17	635.1254	635.1240	-2.16	235.69					7.88	6.9 (D/F)**	E	
28	Quercetin dihexoside_2	C27H30O17	625.1410	625.1404	-0.99	242.49	627.1556	627.1558	0.35	254.46	7.89		E	MassBank (ID: MSBNK-RIKEN-PR100914)
29	Unknown_1	C21H32O11	459.1872	459.1866	-1.28	197.11					7.94		F	
30	Unknown_2	C24H32O5S	431.1898	431.1897	-0.16	203.44					8.30		F	
31	Umbelliferone	C9H6O3	161.0244	161.0242	-1.24	125.51	163.0390	163.0392	1.23	127.24	8.59		C	authentic standard
32	Quercetin dihexoside_3	C27H30O17	625.1410	625.1402	-1.28	235.32					9.12		E	MassBank (ID: MSBNK-RIKEN-PR100914)
33	Quercetin derivative_2 (pentose+hexose moiety)	C26H28O16	595.1305	595.1294	-1.78	240.33	597.1450	597.1458	1.32	247.70	9.36	9.7 (D/F)**	E	MassBank (ID: MSBNK-RIKEN_RePSpect-PT204313)
34	Ferulic acid	C10H10O4	193.0506	193.0504	-1.04	139.98					10.12		C	authentic standard
35	Quercetin 3,4´-diglucoside	C27H30O17	625.1410	625.1402	-1.28	243.95	627.1556	627.1564	1.28	242.35	10.27		C	authentic standard

No.	Compound name	Elemental composition (neutral)	Theoretical *m/z* $[M-H]^-$	Experimental *m/z* $[M-H]^-$	Difference, ppm	CCS in ESI '-' mode, $(Å)^2$	Theoretical *m/z* $[M+H]^+$	Experimental *m/z* $[M+H]^+$	Difference, ppm	CCS in ESI '+' mode, $(Å)^2$	Retention time, min	VIP	Identification level#	Identified by
36	Schaftoside isomer_1	C26H28O14	563.1406	563.1399	-1.30	232.36	565.1552	565.1557	0.92	234.38	10.39		E	MassBank (ID: MSBNK-Fiocruz-FIO00726)
37	Quercetin hexosyl derivative	C27H30O15	593.1512	593.1510	-0.32	241.86	595.1658	595.1661	0.59	245.26	10.43		E	
38	Luteolin/kaempferol dihexoside_1	C27H30O16	609.1461	609.1456	-0.84	256.67	611.1607	611.1612	0.88	263.56	10.45	6.4 (F/L)**	E	MassBank (ID: MSBNK-BS-BS003234)
39	Quercetin derivative_3 (pentose+hexose moiety)	C26H28O16	595.1304	595.1293	-1.85	244.36	597.1450	597.1452	0.32	244.77	10.53		E	MassBank (ID: MSBNK-RIKEN_ReSpect-PT204313)
40	Taraxinositol A/B*	C22H24O10	447.1297	447.1288	-1.95	192.54					10.68		E	
41	Quercetin rutinoside	C27H30O16	609.1461	609.1452	-1.48	235.45	611.1607	611.1609	0.39	248.42	11.06		E	MoNA (ID: RIKENPlaSMA006420)
42	Chicoric acid	C22H18O12	473.0726	473.0721	-1.06	202.67	475.0871	475.0869	-0.42	207.40	11.08	10.9 (D/F)**	C	authentic standard
43	Schaftoside isomer_2	C26H28O14	563.1406	563.1402	-0.76	232.09	565.1552	565.1553	0.21	235.48	11.40	7.1 (D/F)**	E	MassBank (ID: MSBNK-Fiocruz-FIO00726)

No.	Compound name	Elemental composition (neutral)	Theoretical *m/z* $[M-H]^-$	Experimental *m/z* $[M-H]^-$	Difference, ppm	CCS in ESI '-' mode, $(Å)^2$	Theoretical *m/z* $[M+H]^+$	Experimental *m/z* $[M+H]^+$	Difference, ppm	CCS in ESI '+' mode, $(Å)^2$	Retention time, min	VIP	Identification level#	Identified by
44	Luteolin/kaempferol dihexoside_2	C27H30O16	609.1461	609.1442	-3.14	231.60	611.1607	611.1609	0.39	249.51	11.89		E	MassBank (ID: MSBNK-BS-BS003234)
45	Luteolin/kaempferol dihexoside_3	C27H30O16	609.1461	609.1455	-1.00	240.95	611.1607	611.1609	0.39	242.72	12.61		E	MassBank (ID: MSBNK-BS-BS003234)
46	Robinin*	C33H40O19	739.2091	739.2080	-1.49	279.93	741.2237	741.2240	0.40	277.63	12.68		C	authentic standard
47	Quercetin pentoside_1	C20H18O11	433.0776	433.0771	-1.22	196.03	435.0922	435.0923	0.25	200.39	12.75	8.5 (D/F)**	E	MassBank (ID: MSBNK-RIKEN-PR306789)
48	Rutin	C27H30O16	609.1461	609.1454	-1.15	234.34	611.1607	611.1617	1.64	240.80	13.20		C	authentic standard
49	Quercetin glucoside	C21H20O12	463.0882	463.0878	-0.86	200.95	465.1028	465.1030	0.54	206.52	13.40		E	MassBank (ID: MSBNK-Fiocruz-FIO00168)
50	Isorhamnetin disaccharide_1	C27H30O16	609.1461	609.1447	-2.31	232.97	611.1607	611.1619	2.03	244.86	13.54	9.4 (D/F)**	E	
51	Luteolin 7-O-glucoside	C21H20O11	447.0933	447.0925	-1.79	211.23	449.1078	449.1079	0.22	210.52	14.09	14.8 (D/F)**, 29.1 (F/L)**	C	authentic standard

No.	Compound name	Elemental composition (neutral)	Theoretical *m/z* $[M-H]^-$	Experimental *m/z* $[M-H]^-$	Difference, ppm	CCS in ESI '-' mode, $(Å)^2$	Theoretical *m/z* $[M+H]^+$	Experimental *m/z* $[M+H]^+$	Difference, ppm	CCS in ESI '+' mode, $(Å)^2$	Retention time, min	VIP	Identification level[#]	Identified by
52	Luteolin/kaempferol rutinoside	C27H30O15	593.1512	593.1495	-2.85	229.92	595.1658	595.1662	0.76	244.29	14.22	16.5 (D/F)**	E	MassBank (ID: MSBNK-BS-BS003279)
53	Isorhamnetin disaccharide_2	C27H30O16	609.1461	609.1451	-1.66	235.95					14.49		E	
54	Quercetin pentoside_2	C20H18O11	433.0776	433.0776	-0.07	267.79	435.0922	435.0925	0.71	202.82	14.92		E	MassBank (ID: MSBNK-RIKEN-PR306789)
55	Quercetin derivative_4	C23H22O13	505.0988	505.0983	-0.91	213.56					14.99		E	MassBank (ID: MSBNK-RIKEN-PR040189)
56	Kaempferol 3-O-rutinoside*	C27H30O15	593.1512	593.1502	-1.69	232.47	595.1658	595.1660	0.34	238.26	15.63		C	authentic standard
57	Apigenin derivative	C20H34O11	449.2028	449.2016	-2.76	197.17					15.72	7.9 (D/F)**	E	Marinaccio et al., 2025
58	Quercitrin*	C21H20O11	447.0933	447.0925	-1.79	197.57	449.1078	449.1082	0.89	208.73	16.01		C	authentic standard
59	Dicaffeoylquinic acid_1	C25H24O12	515.1195	515.1183	-2.33	211.50					16.02	16.2 (D/F)**	D2	MoNA (ID: VF-NPL-QTOF003239)
60	Isorhamnetin 3-rutinoside*	C28H32O16	623.1618	623.1608	-1.60	237.08	625.1763	625.1762	-0.16	245.35	16.24		C	authentic standard
61	Isorhamnetin 3-glucoside	C22H22O12	477.1039	477.1029	-1.99	209.08					16.40	6.4 (D/F)**, 7.0 (F/L)**	D2	MassBank (ID: MSBNK-RIKEN-PR040093)

No.	Compound name	Elemental composition (neutral)	Theoretical *m/z* $[M-H]^-$	Experimental *m/z* $[M-H]^-$	Difference, ppm	CCS in ESI '-' mode, $(Å)^2$	Theoretical *m/z* $[M+H]^+$	Experimental *m/z* $[M+H]^+$	Difference, ppm	CCS in ESI '+' mode, $(Å)^2$	Retention time, min	VIP	Identification level#	Identified by
62	Caffeic acid derivative_2	C23H24O11	475.1246	475.1241	-1.03	206.54					16.52		E	
63	Rosmarinic acid*	C18H16O8	359.0772	359.0777	1.39	173.37					16.73		C	authentic standard
64	Chrysoeriol-rutinoside	C28H32O15	607.1668	607.1660	-1.32	239.49	609.1814	609.1817	0.49	250.56	16.75		D2	Plazonić et al., 2009
65	Hesperidin*	C28H34O15	609.1825	609.1816	-1.48	238.38	611.1971	611.1957	-2.29	249.75	16.79		C	authentic standard
66	Dicaffeoylquinic acid_2	C25H24O12	515.1195	515.1185	-1.94	213.45					16.80		D2	MoNA (ID: VF-NPL-QTOF003239)
67	Luteolin/kaempferol glycoside	C21H20O11	447.0933	447.0928	-1.10	205.72	449.1078	449.1080	0.36	206.58	16.91		E	MassBank (ID: MSBNK-BS-BS003262)
68	Phlorizin*	C21H24O10	435.1297	435.1299	0.46	197.80	437.1442	437.1450	1.83	196.56	16.92		C	authentic standard
69	Abscisic acid glucose ester (formate adduct)	C22H32O11	471.1872	471.1868	-0.83	209.63					16.95		D2	Fan et al., 2020
70	Daidzein	C15H10O4	253.0506	253.0506	0.00	156.63	255.0652	255.0649	-1.18	154.13	17.20		C	authentic standard
71	Eriodictyol	C15H12O6	287.0561	287.0556	-1.74	165.66	289.0707	289.0708	0.35	166.55	17.36		C	authentic standard
72	Sebacic acid*	C10H18O4	201.1132	201.1131	-0.50	144.98					17.61		C	authentic standard
73	Luteolin	C15H10O6	285.0405	285.0400	-1.75	159.14	287.0550	287.0553	1.05	162.27	17.63	19.4 (D/F)**, 21.4 (F/L)**	C	authentic standard
74	Ethyl caffeate*	C11H12O4	207.0663	207.0661	-0.97	147.55					17.76	9.9 (F/L)**	C	authentic standard

No.	Compound name	Elemental composition (neutral)	Theoretical *m/z* $[M-H]^-$	Experimental *m/z* $[M-H]^-$	Difference, ppm	CCS in ESI '-' mode, $(Å)^2$	Theoretical *m/z* $[M+H]^+$	Experimental *m/z* $[M+H]^+$	Difference, ppm	CCS in ESI '+' mode, $(Å)^2$	Retention time, min	VIP	Identification level[#]	Identified by
75	Naringenin*	C15H12O5	271.0612	271.0615	1.11	163.46	273.0758	273.0757	-0.37	163.12	18.14		C	authentic standard
76	Apigenin	C15H10O5	269.0456	269.0451	-1.67	158.90	271.0601	271.0603	0.74	157.69	18.16		C	authentic standard
77	Chrysoeriol	C16H12O6	299.0561	299.0562	0.33	169.10	301.0707	301.0711	1.46	167.24	18.43	7.4 (D/F)**, 9.2 (F/L)**	D2	MassBank (ID: MSBNK-BS-BS003343)
78	Unknown_3	C38H58O17	785.3601	785.3590	-1.43	269.68					18.43	17.0 (D/F)**, 11.2 (F/L)**	F	
79	9,12,13-trihydroxy-10E,15Z-octadecadienoic acid	C18H32O5	327.2177	327.2171	-1.83	185.48					18.55		D2	LIPID MAPS® (ID: LMFA02000022)
80	9,12,13-trihydroxy-10E-octadecenoic acid	C18H34O5	329.2334	329.2327	-1.97	187.59					18.89		D2	LIPID MAPS® (ID: LMFA02000014)
81	Chrysin*	C15H10O4	253.0506	253.0503	-1.19	157.01	255.0652	255.0653	0.39	153.45	19.32		C	authentic standard
82	9,10-dihydroxy-12Z-octadecenoic acid	C18H34O4	313.2384	313.2381	-1.05	184.95					19.75		D2	LIPID MAPS® (ID: LMFA02000229)
83	Hydroxyoctadecatrienoic acid derivative	C18H30O3	293.2122	293.2118	-1.43	181.56					19.96	6.4 (D/F)**	E	LIPID MAPS® (ID: LMFA02000029)

No.	Compound name	Elemental composition (neutral)	Theoretical *m/z* $[M-H]^-$	Experimental *m/z* $[M-H]^-$	Difference, ppm	CCS in ESI '-' mode, $(Å)^2$	Theoretical *m/z* $[M+H]^+$	Experimental *m/z* $[M+H]^+$	Difference, ppm	CCS in ESI '+' mode, $(Å)^2$	Retention time, min	VIP	Identification level#	Identified by
84	9-hydroxy-10E,12Z-octadecadienoic acid	C18H32O3	295.2279	295.2274	-1.59	184.92					20.14		D2	LIPID MAPS® (ID: LMFA02000151)

* first reported from *T. officinale*

** VIP values between sample groups: D/F – leaf-root drug and flowers, F/L - flowers and liqueur

#, according to Çiçek et al., 2024

A4: Chromatograms

App. Figure 1. Extracted ion chromatograms of the vinca alkaloid analytes. Different colors were used visualizing overlapping chromatographic peaks.

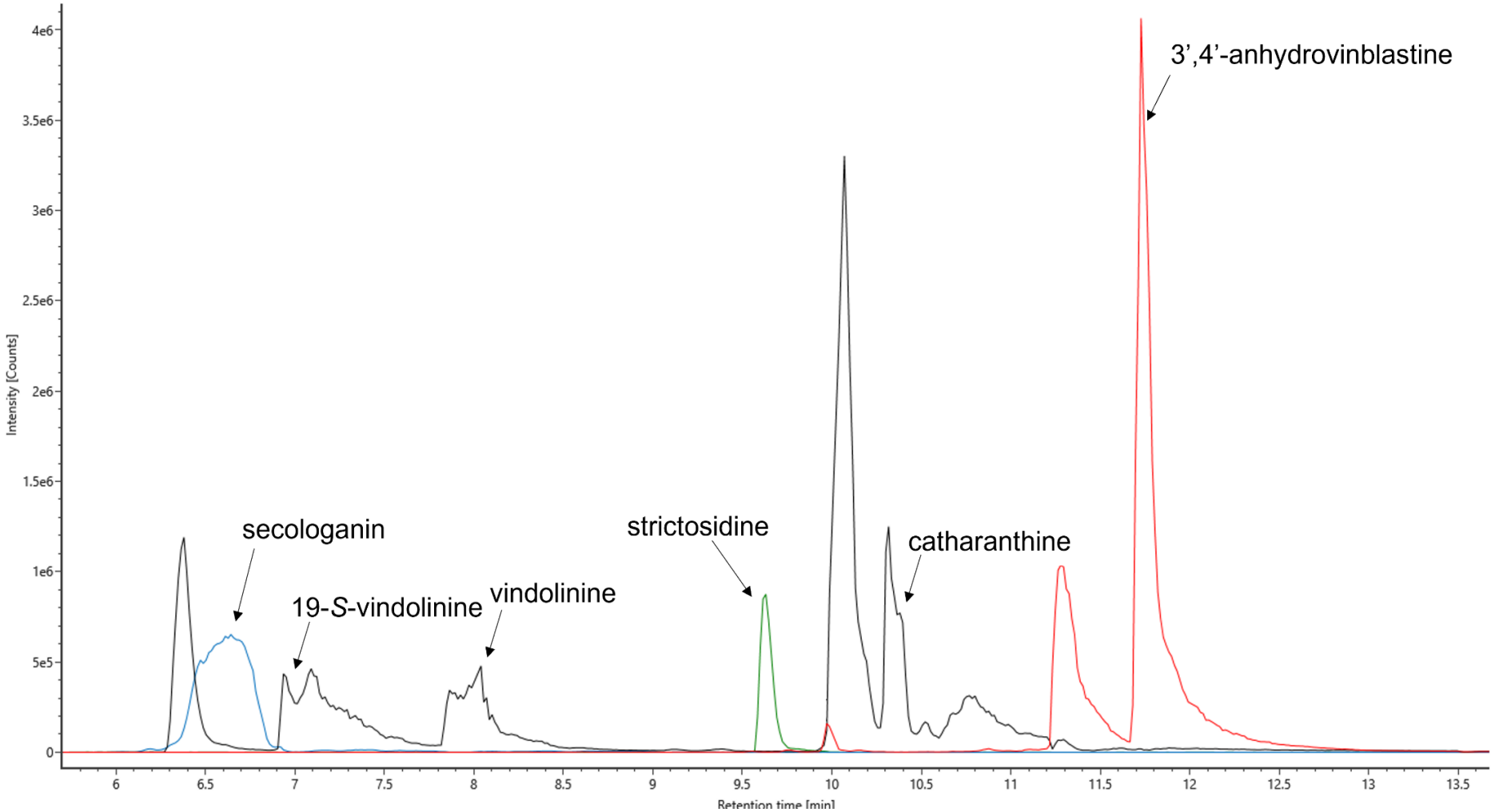

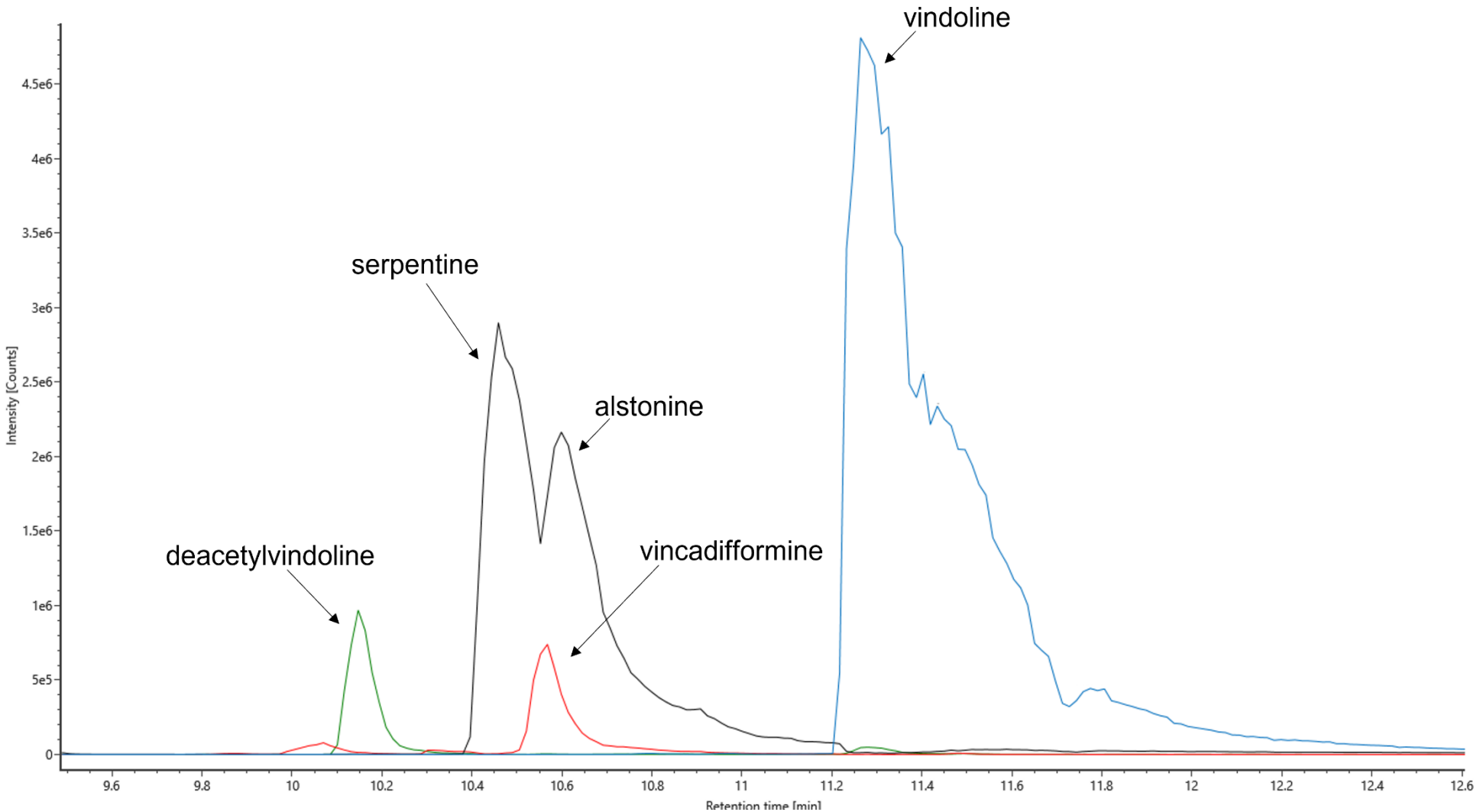
vindoline
serpentine
alstonine
vincadifformine
deacetylvindoline
Intensity [Counts]
4.5e6
4e6
3.5e6
3e6
2.5e6
2e6
1.5e6
1e6
5e5
0
9.6
9.8
10
10.2
10.4
10.6
10.8
11
11.2
11.4
11.6
11.8
12
12.2
12.4
12.6
Retention time [min]

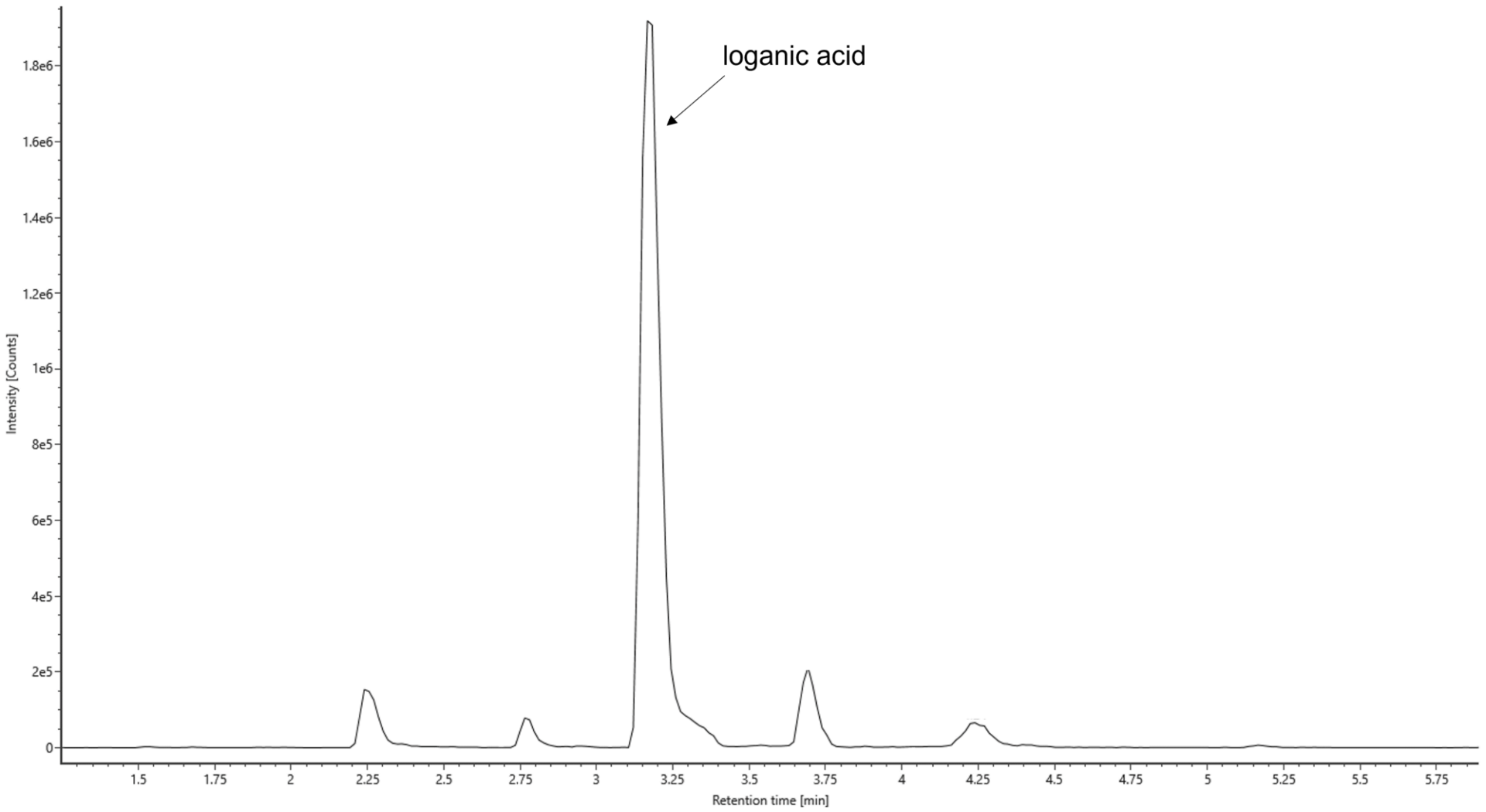
loganic acid
Intensity [Counts]
1.8e6
1.6e6
1.4e6
1.2e6
1e6
8e5
6e5
4e5
2e5
0
1.5
1.75
2
2.25
2.5
2.75
3
3.25
3.5
3.75
4
4.25
4.5
4.75
5
5.25
5.5
5.75
Retention time [min]

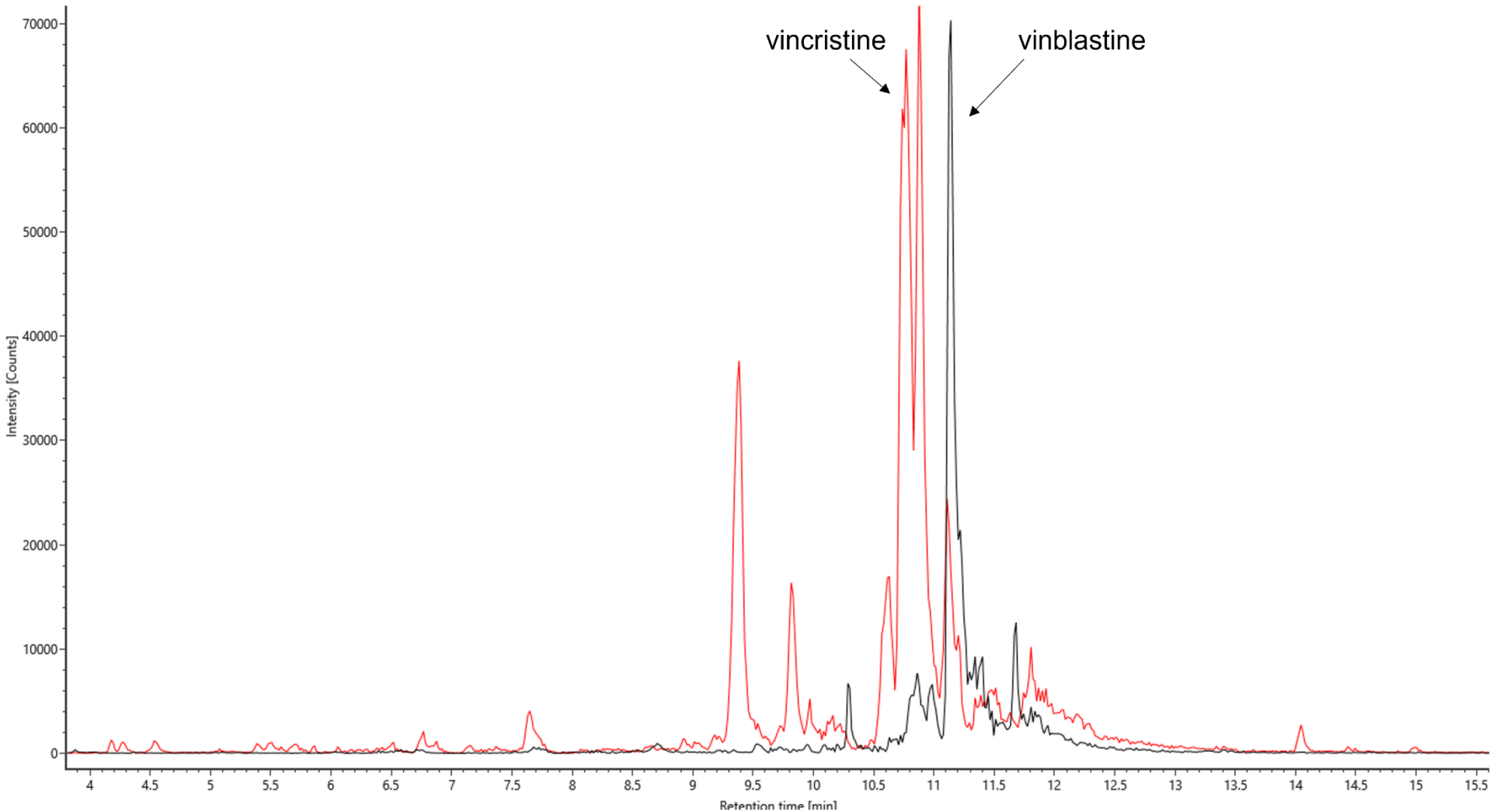
vincristine
vinblastine
Intensity [Counts]
70000
60000
50000
40000
30000
20000
10000
0
4
4.5
5
5.5
6
6.5
7
7.5
8
8.5
9
9.5
10
10.5
11
11.5
12
12.5
13
13.5
14
14.5
15
15.5
Retention time [min]

A5: Full scan spectra of the vinca alkaloid compounds

19-*S*-vindolinine

Elemental composition (neutral): C21H24N2O2

$[M+H]^+$: 337.1911

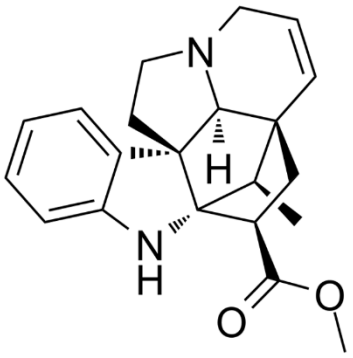

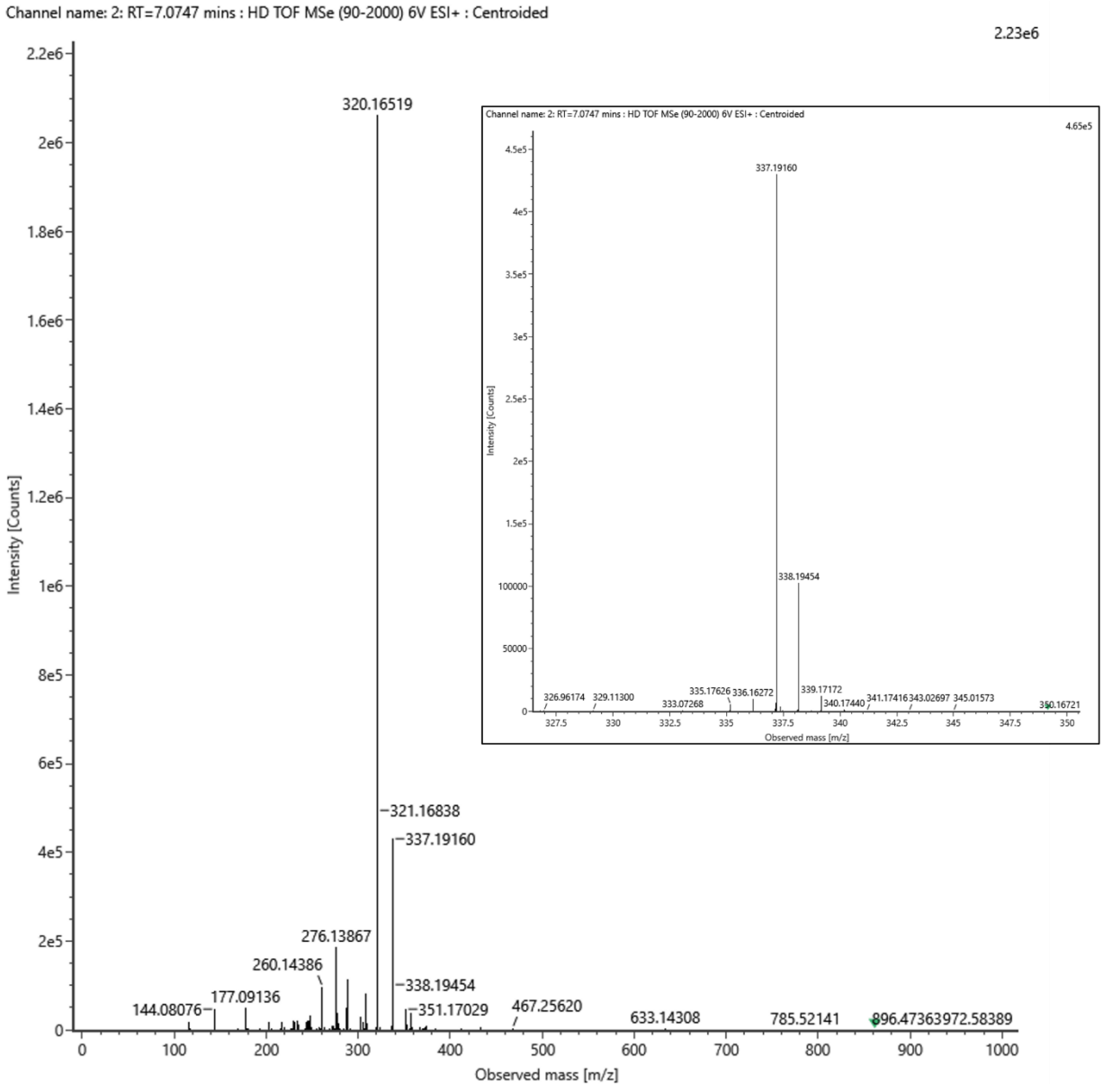

3’,4’-anhydrovinblastine
Elemental composition: C46H56N4O8
$[M+2H]^{++}$: 397.2122

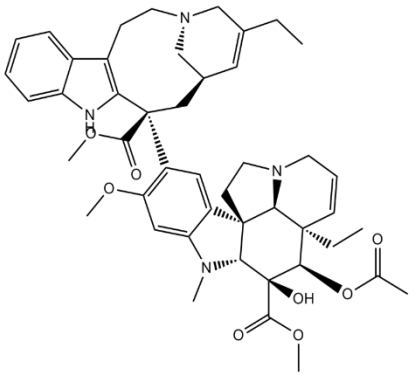

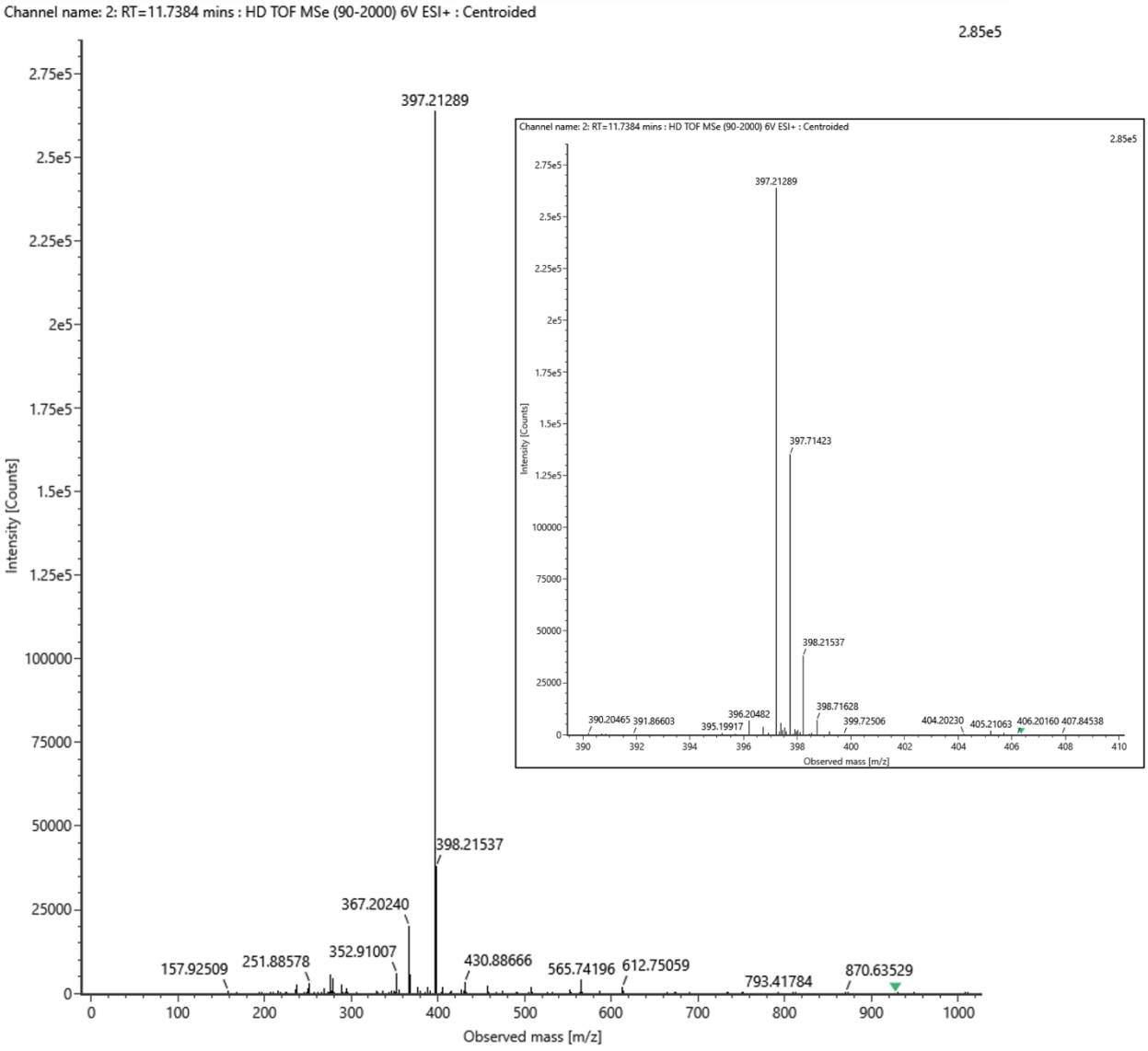

Alstonine
Elemental composition: C21H20N2O3
$[M+H]^+$: 349.1547

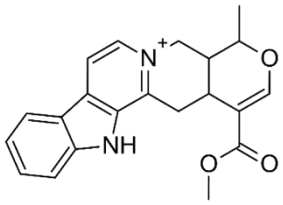

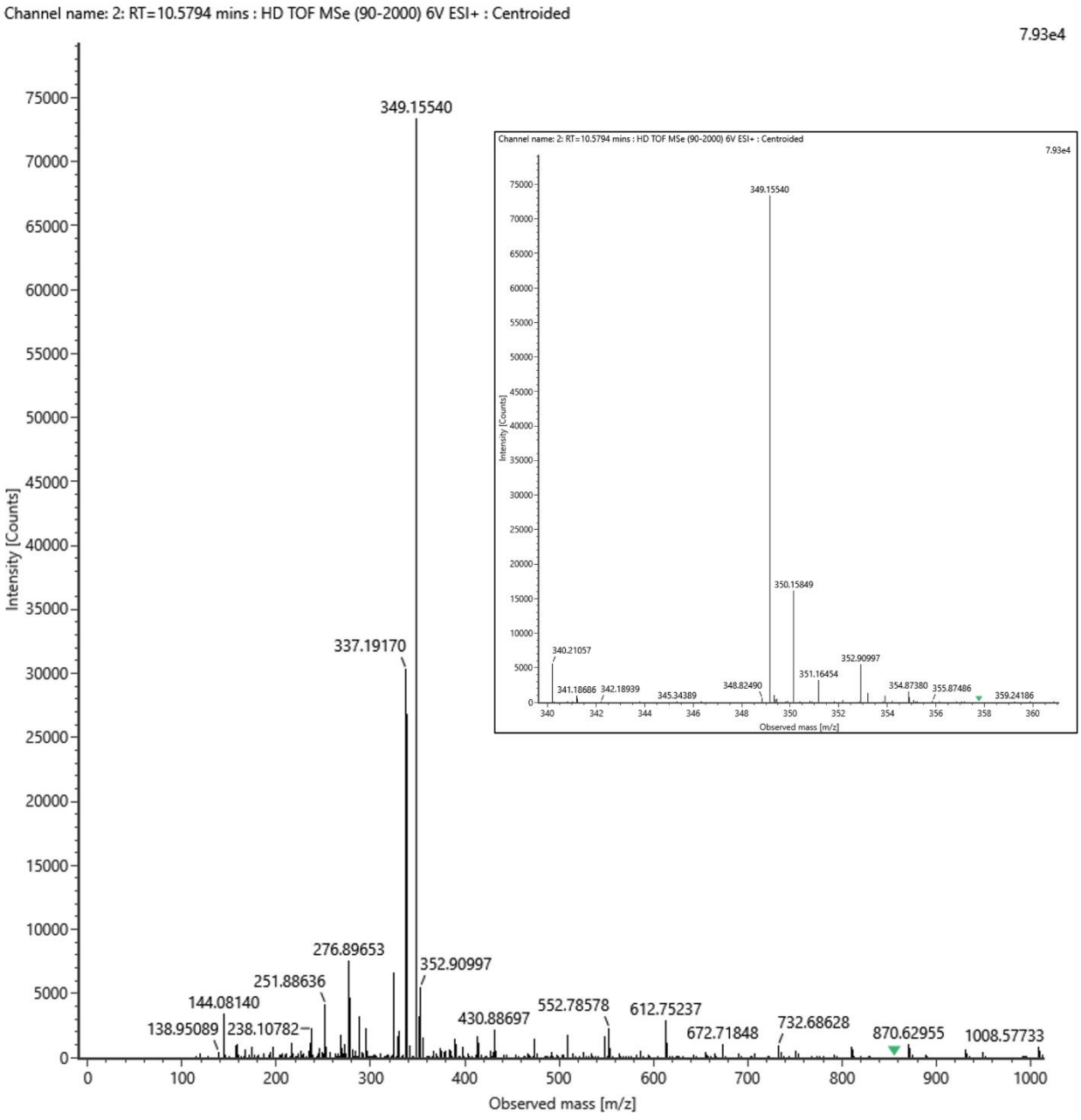

Catharanthine
Elemental composition: C21H24N2O2
$[M+H]^+$: 337.1911

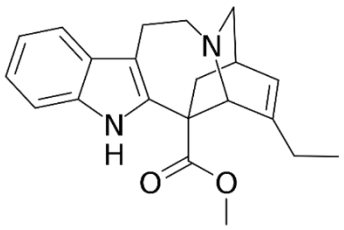

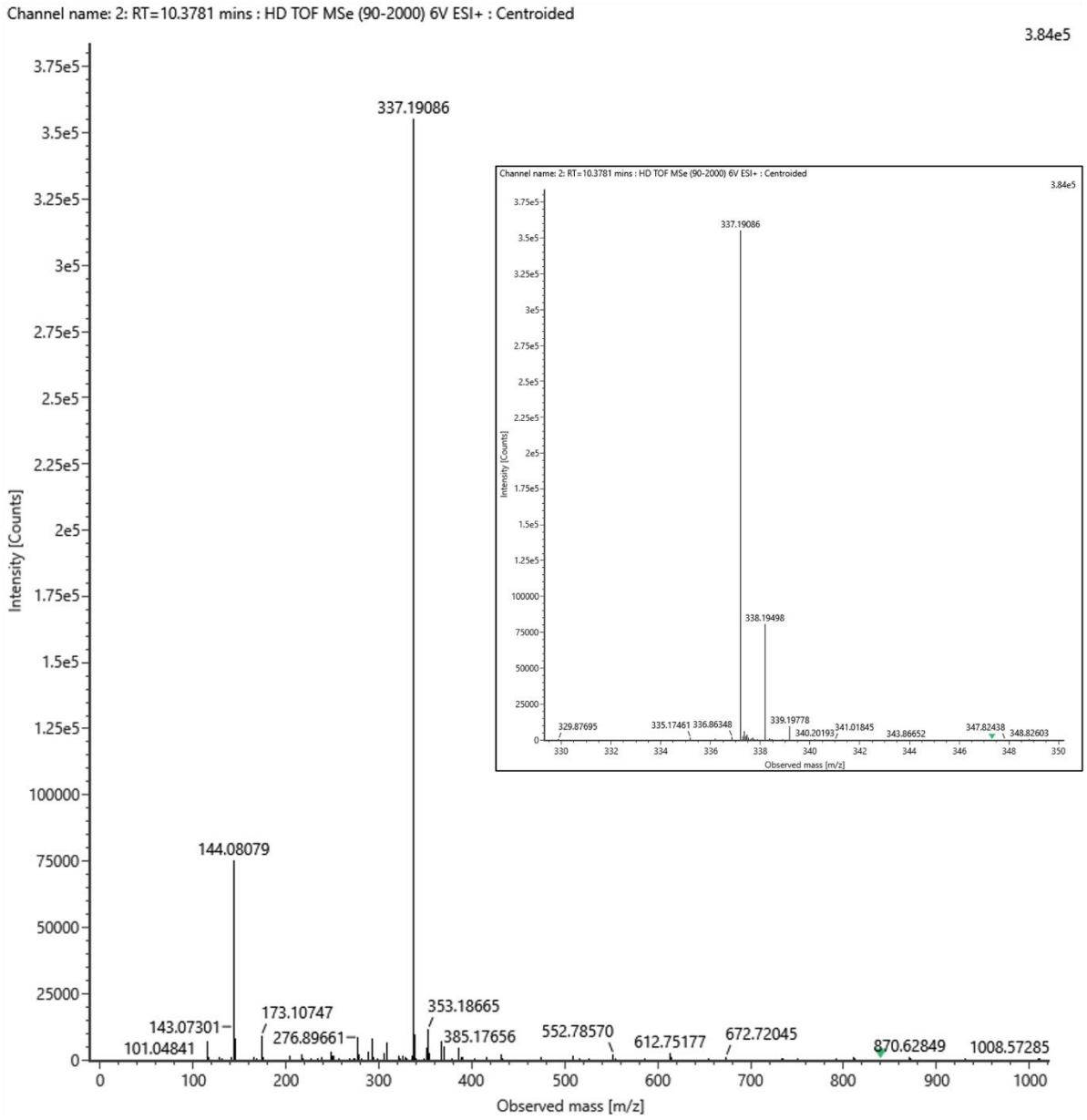

Deacetylvindoline
Elemental composition: C23H30N2O5
$[M+H]^+$: 415.2228

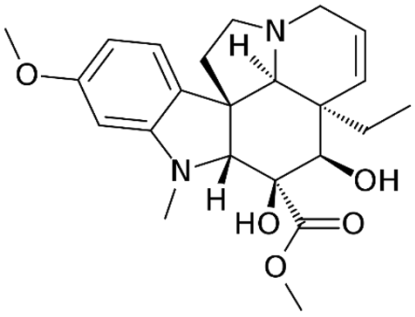

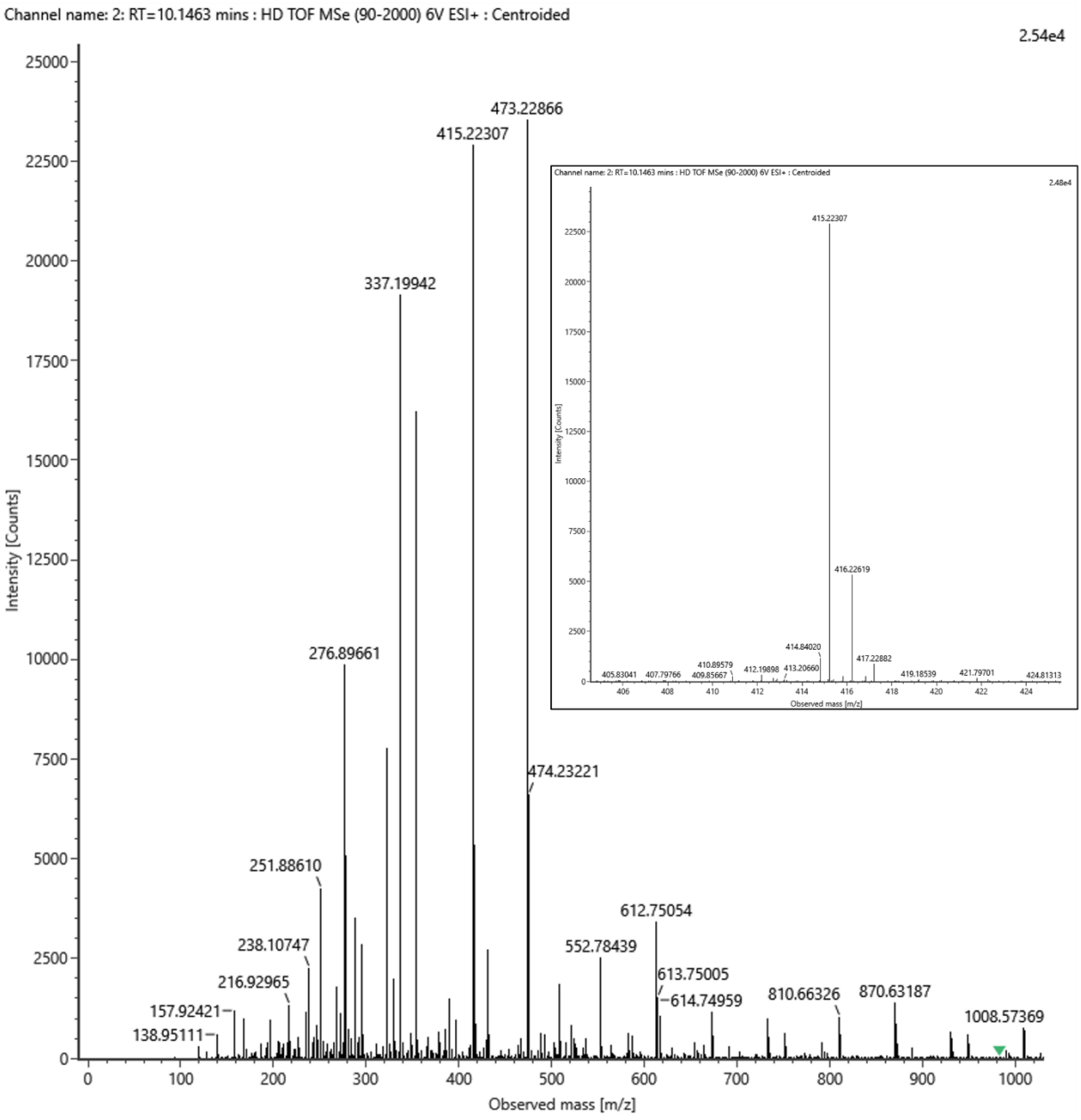

Loganic acid
Elemental composition: C16H24O10
$[M-H]^-$: 375.1297

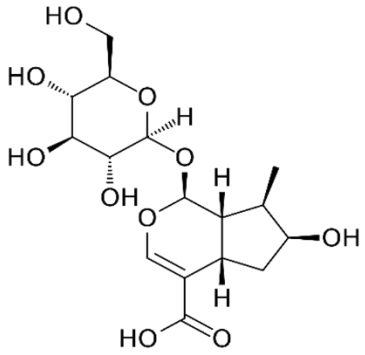

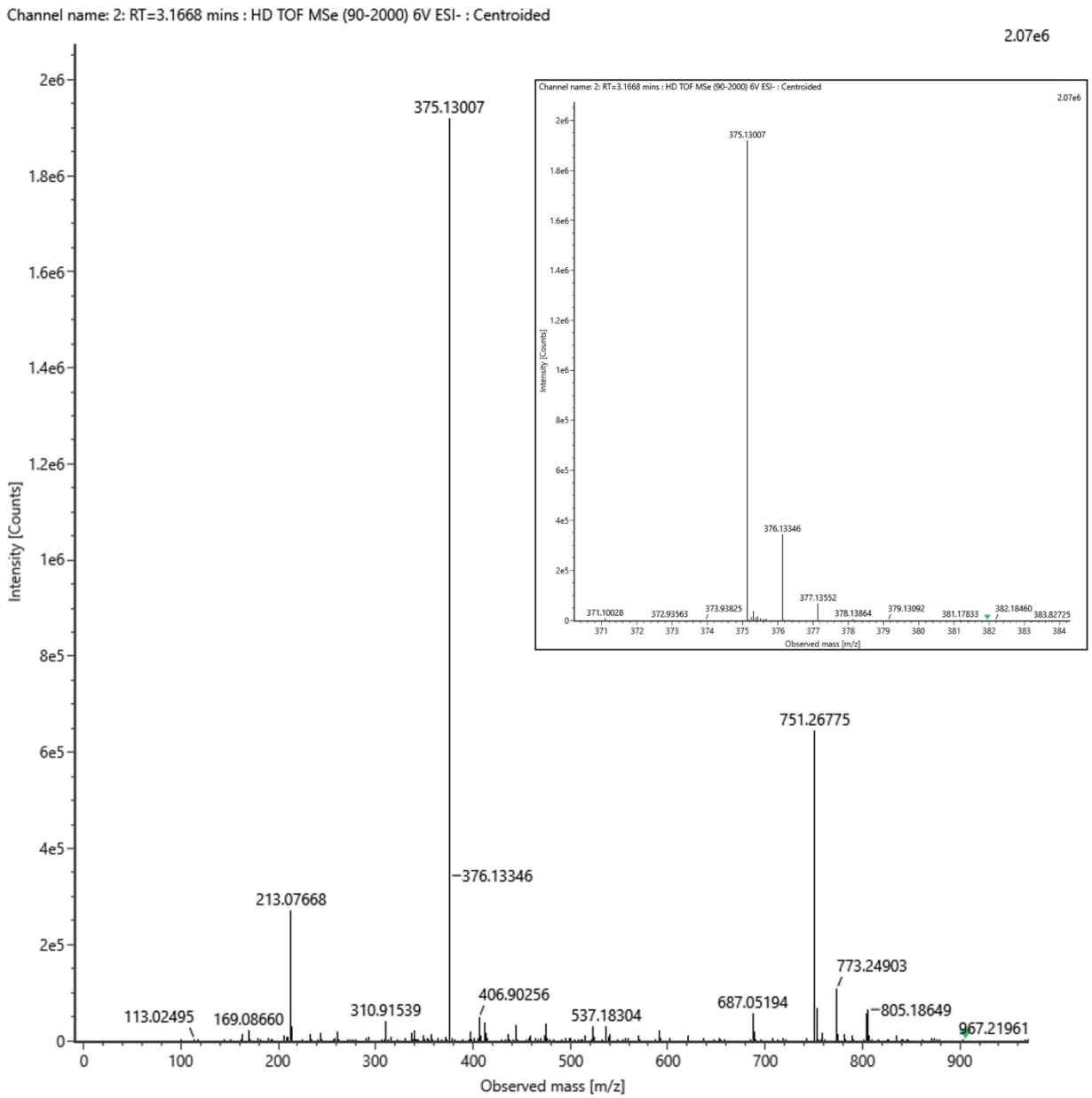

Secologanin
Elemental composition: $C_{17}H_{24}O_{10}$
$[M+Na]^+$: 411.1262

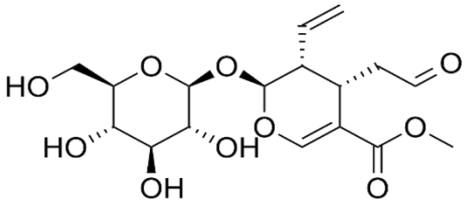

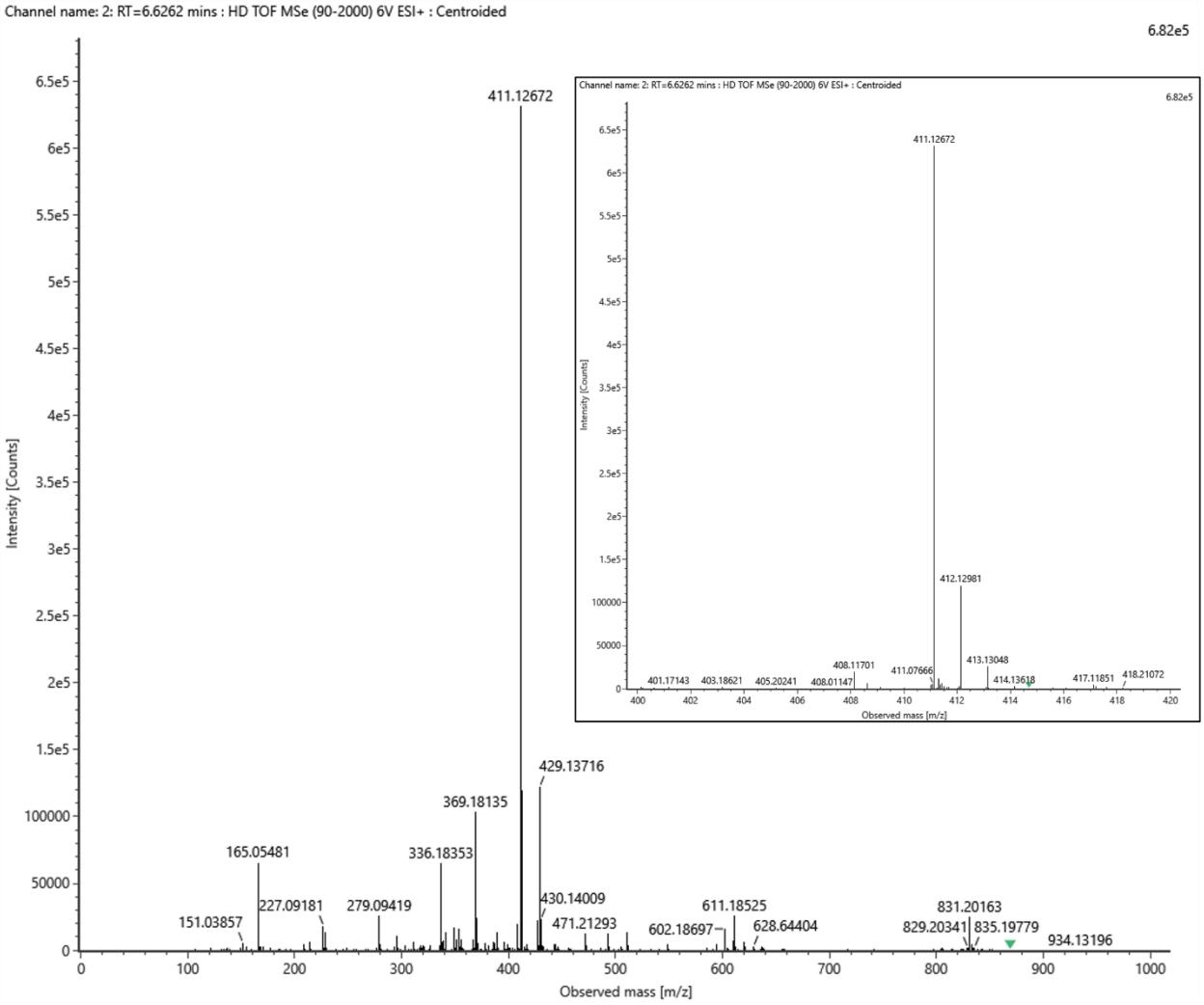

Serpentine
Elemental composition: C21H20N2O3
$[M+H]^+$: 349.1547

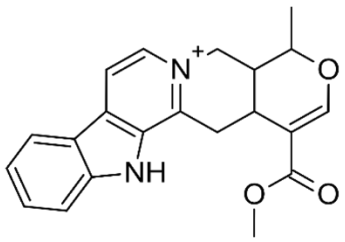

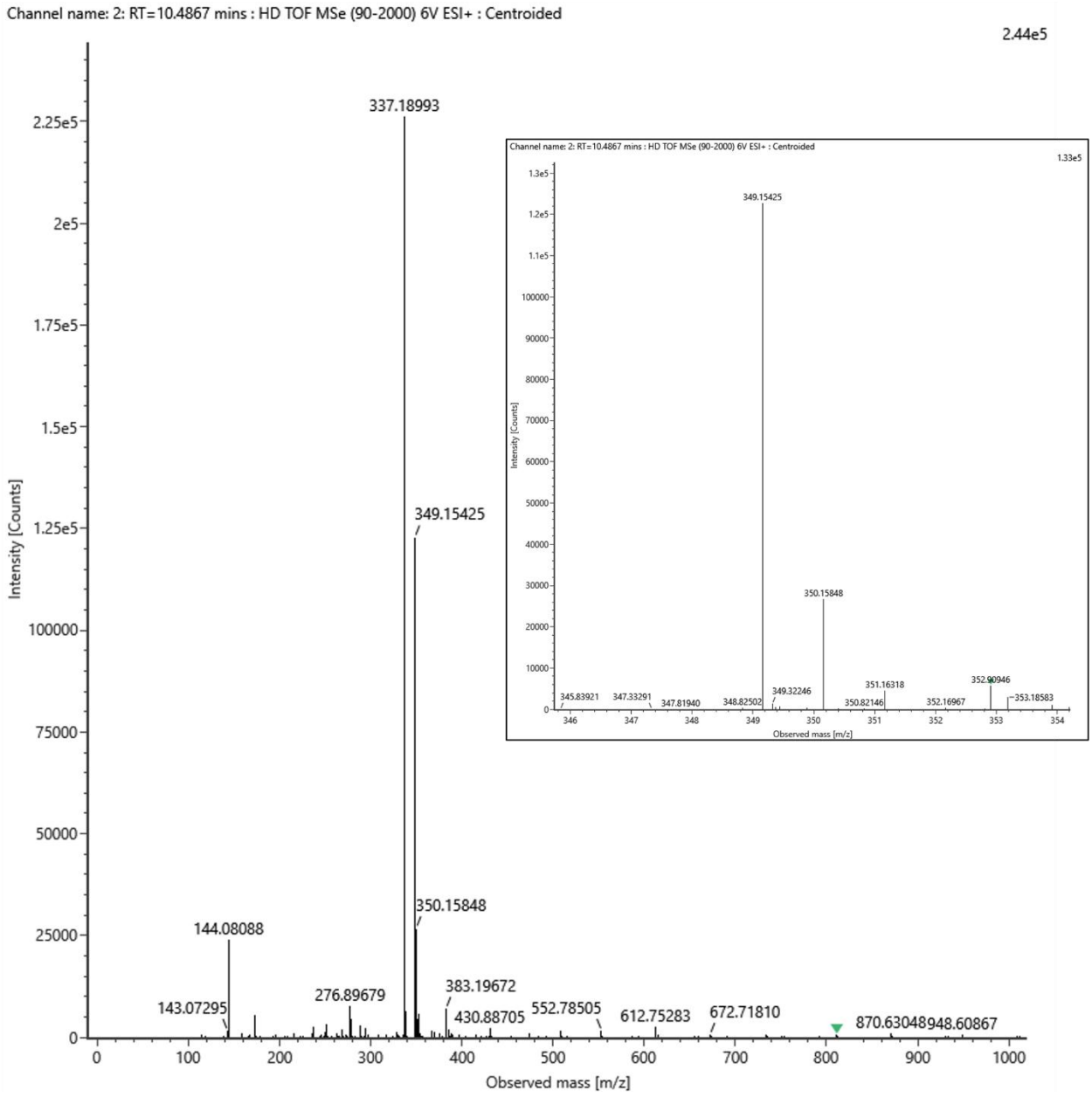

Strictosidine
Elemental composition: $C_{27}H_{34}N_2O_9$
$[M+H]^+$: 531.2337

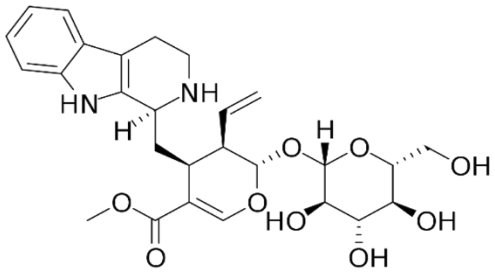

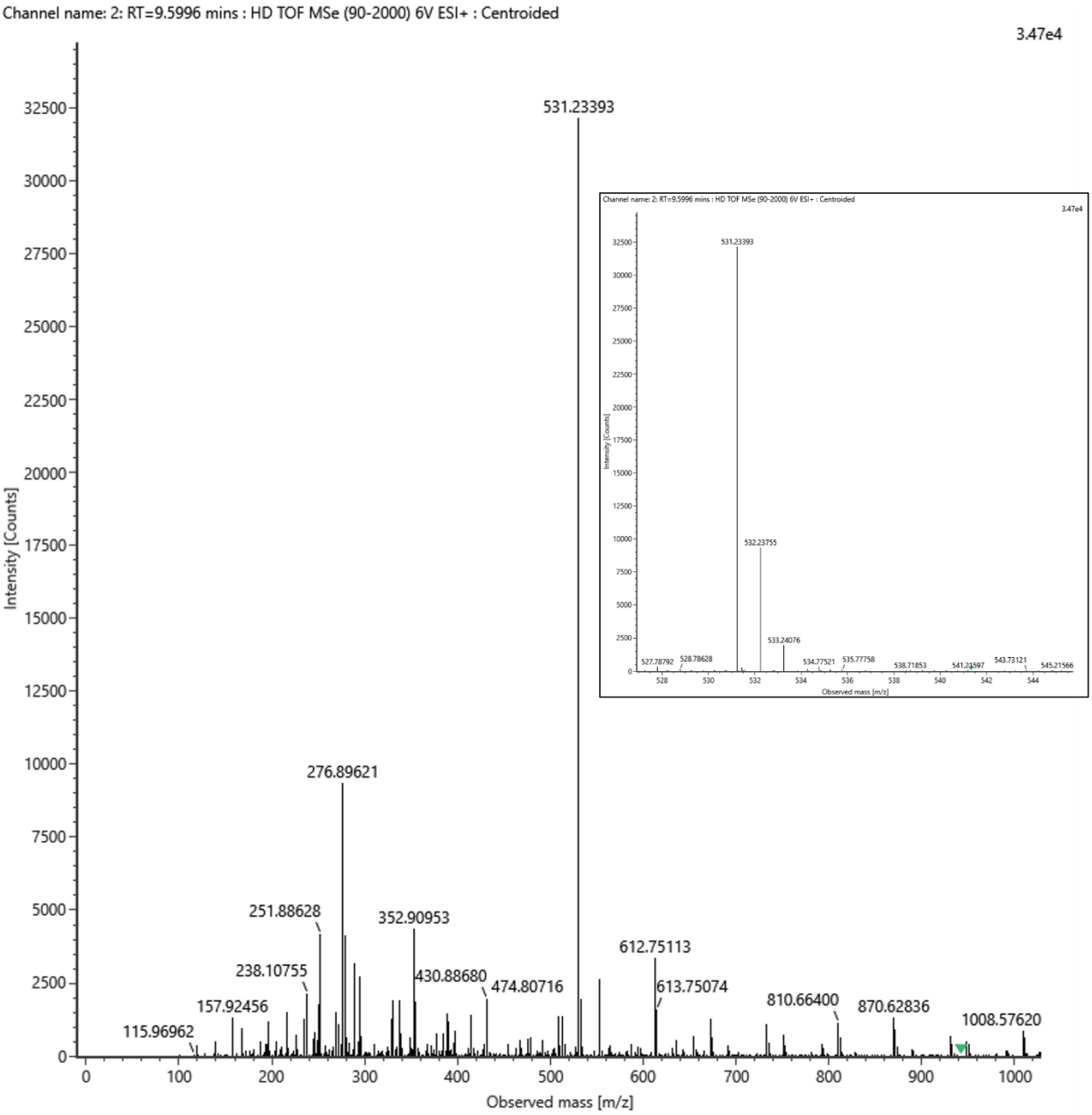

Vinblastine
Elemental composition: C46H58N4O9
$[M+2H]^{++}$: 406.2175

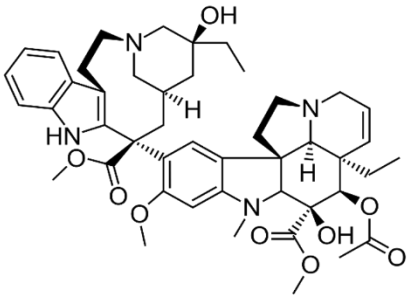

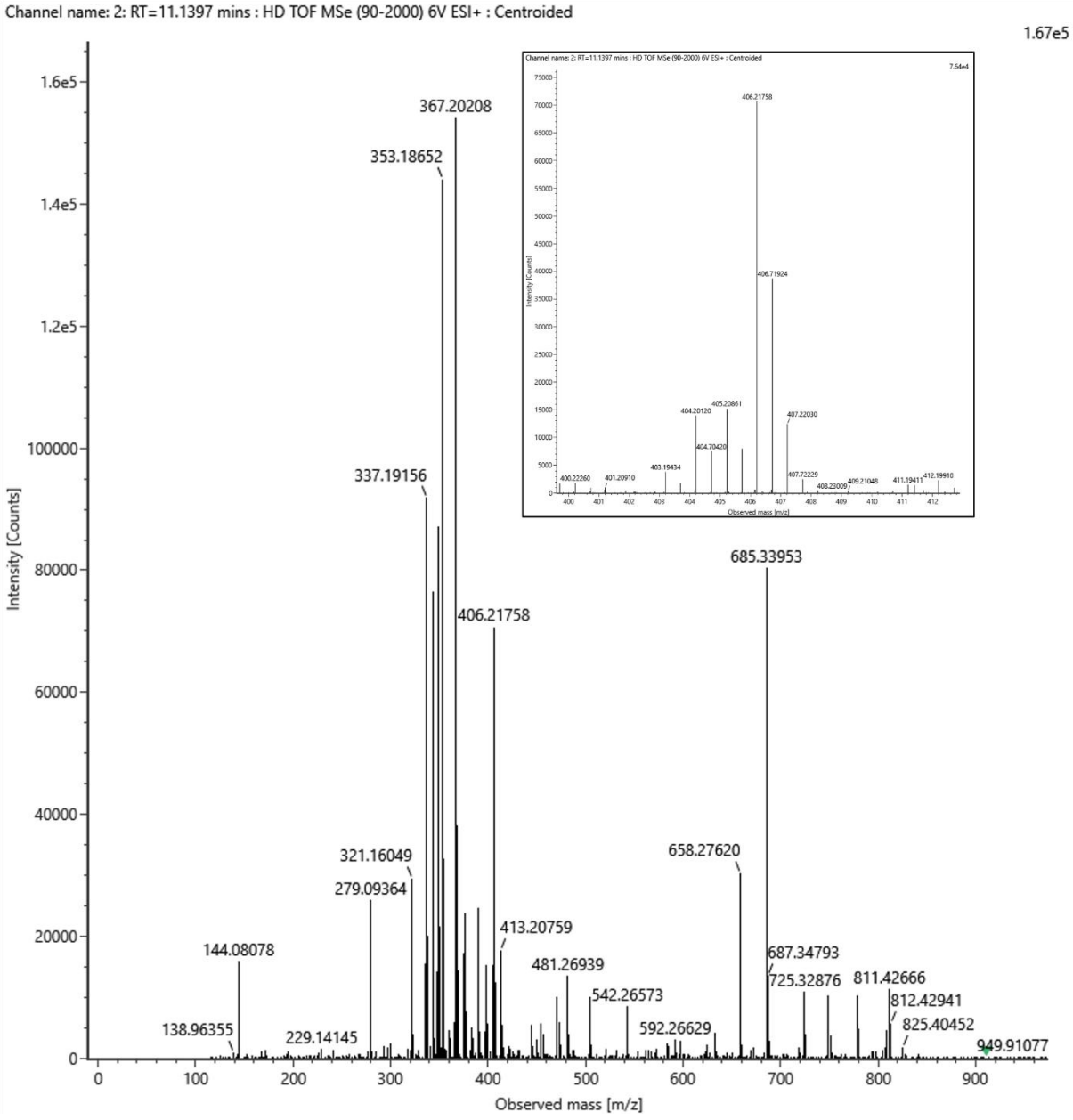

Vincadifformine
Elemental composition: C21H26N2O2
$[M+H]^+$: 339.2067

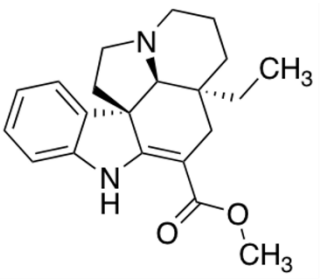

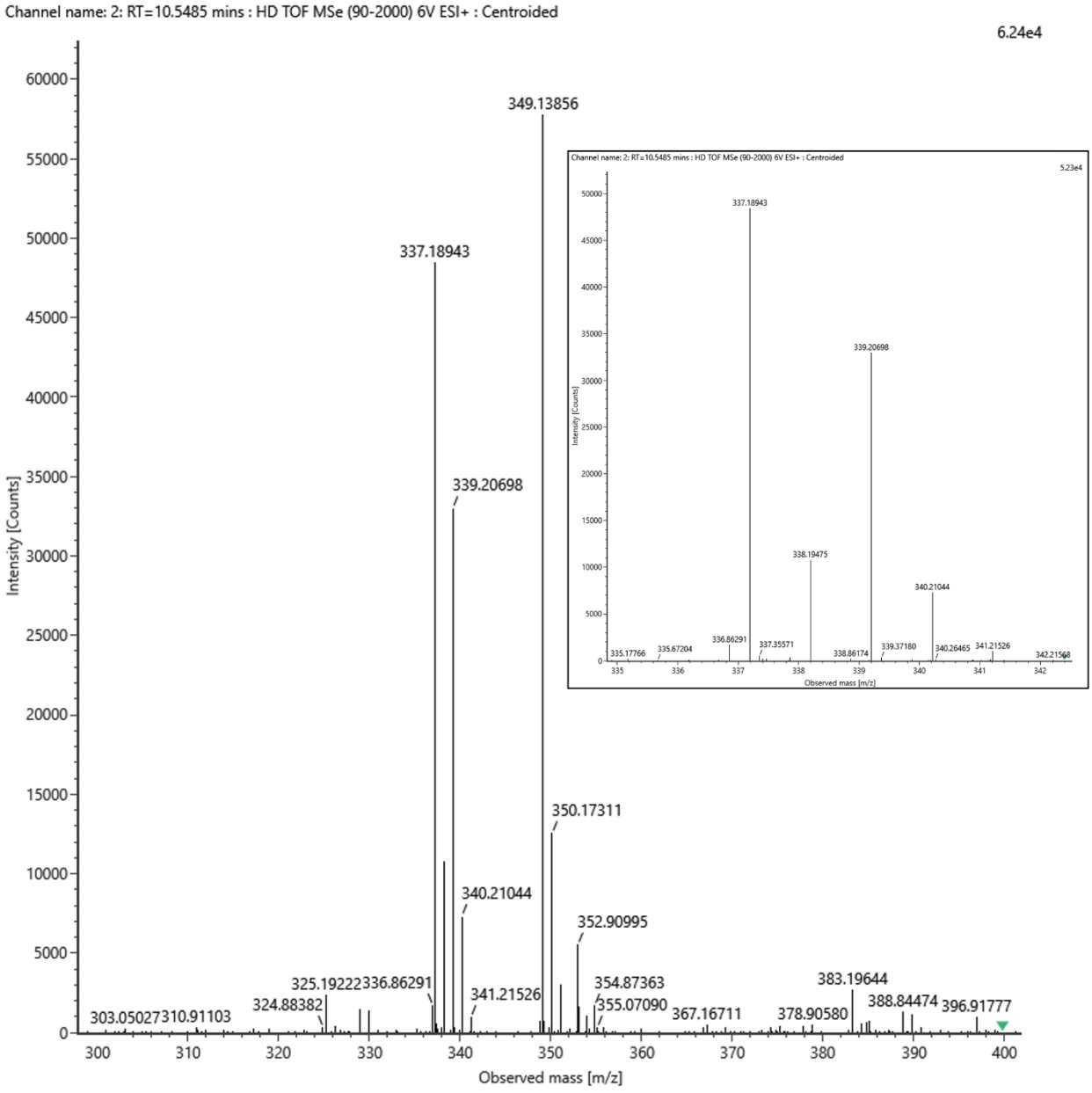

Vincristine
Elemental composition: C46H56N4O10
$[M+2H]^{++}$: 413.2071

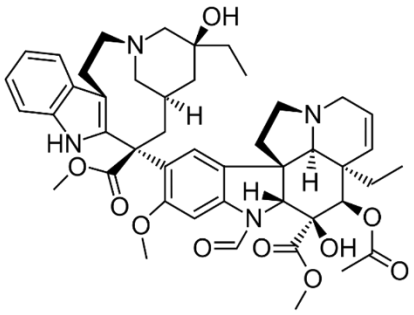

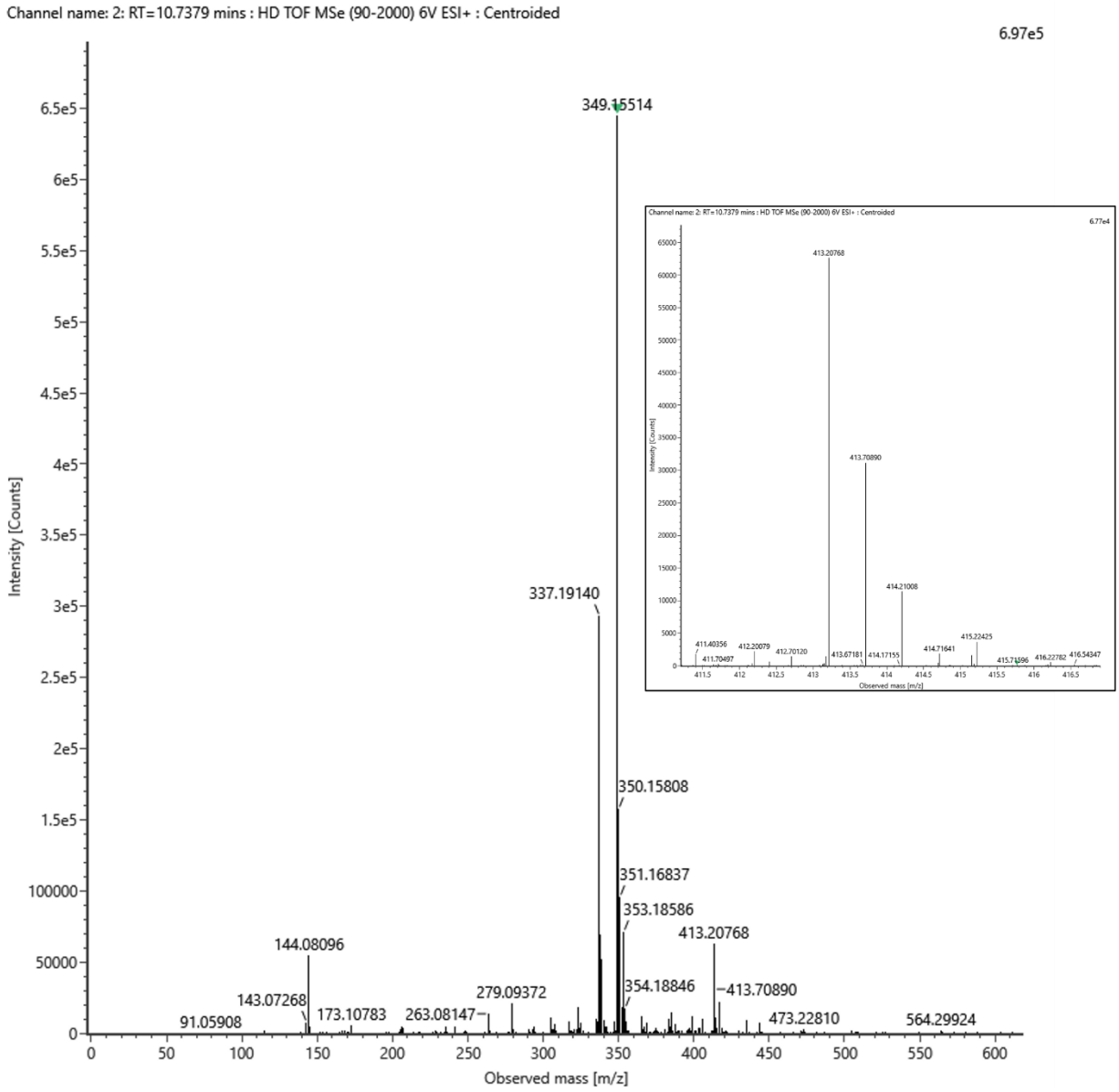

Vindoline
Elemental composition: C25H32N2O6
$[M+H]^+$: 457.2333

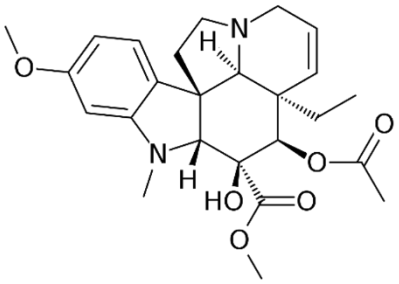

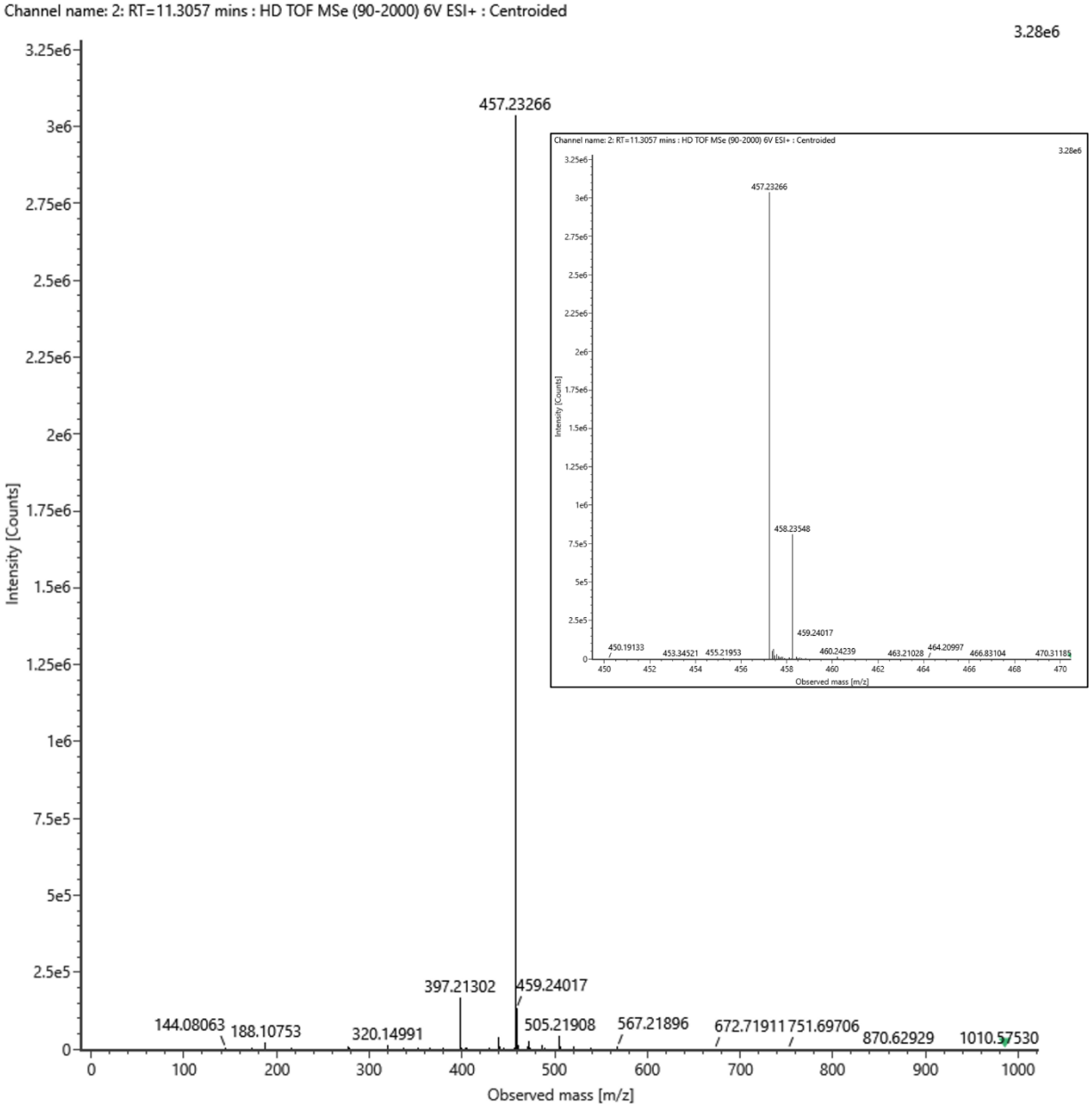

Vindolinine
Elemental composition: C21H24N2O2
$[M+H]^+$: 337.1911

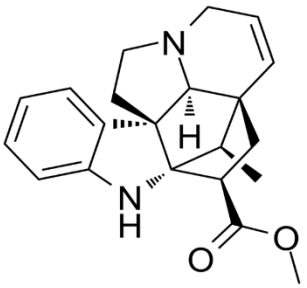

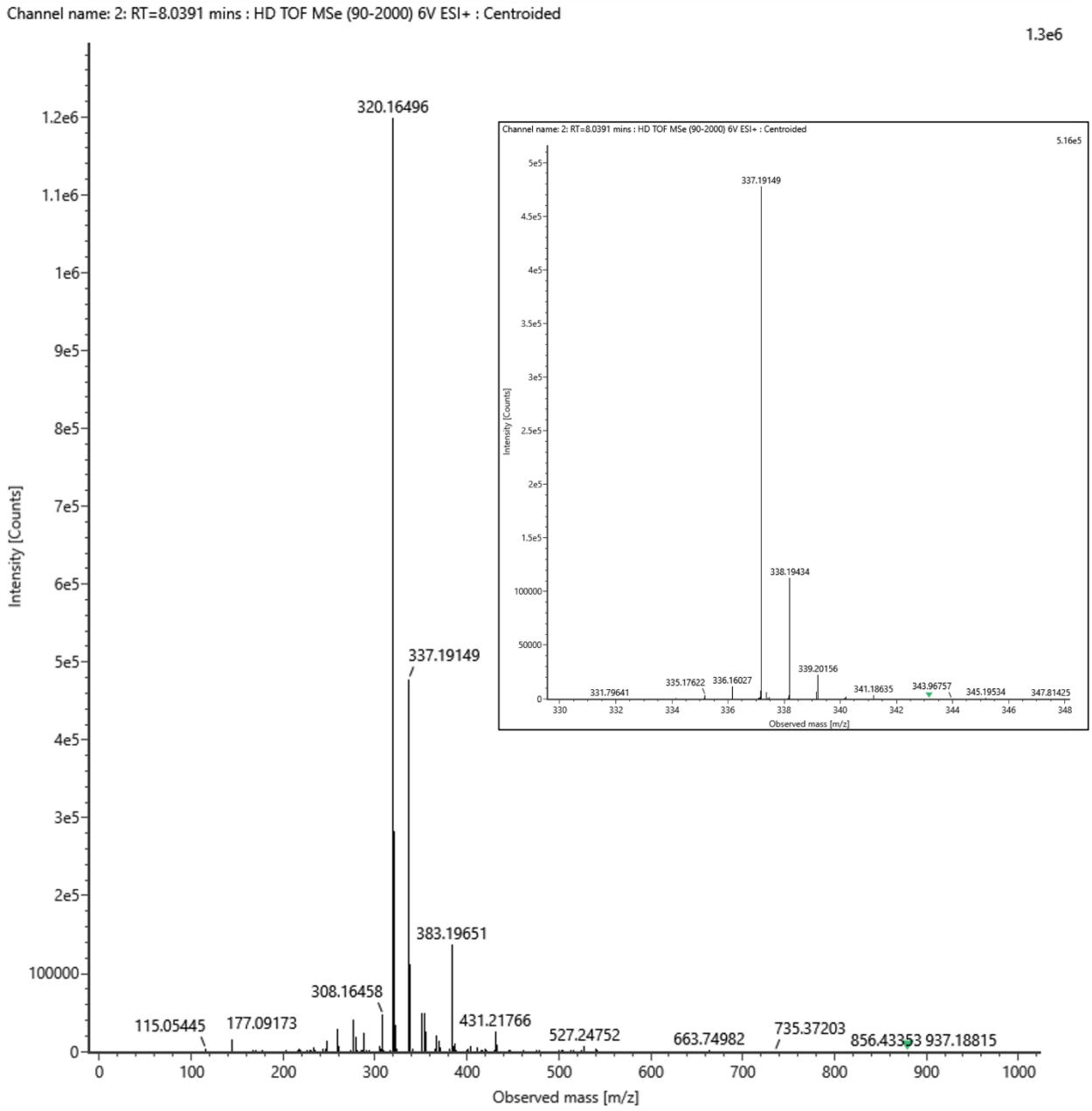

A6: MS/MS datasets

App. Figure 2. MS/MS spectra of the tentatively identified vinca alkaloid compounds with reference m/z data in the insets. [A – 19-*S*-Vindolinine, B – 3',4'-Anhydrovinblastine, C – Alstonine, D – Catharanthine, E – Deacetylvindoline, F – Loganic acid, G – Secologanin, H – Serpentine, I – Strictosidine, J – Vincadifformine, K – Vindoline, L – Vindolinine]. 'CE' refers to collision energy.

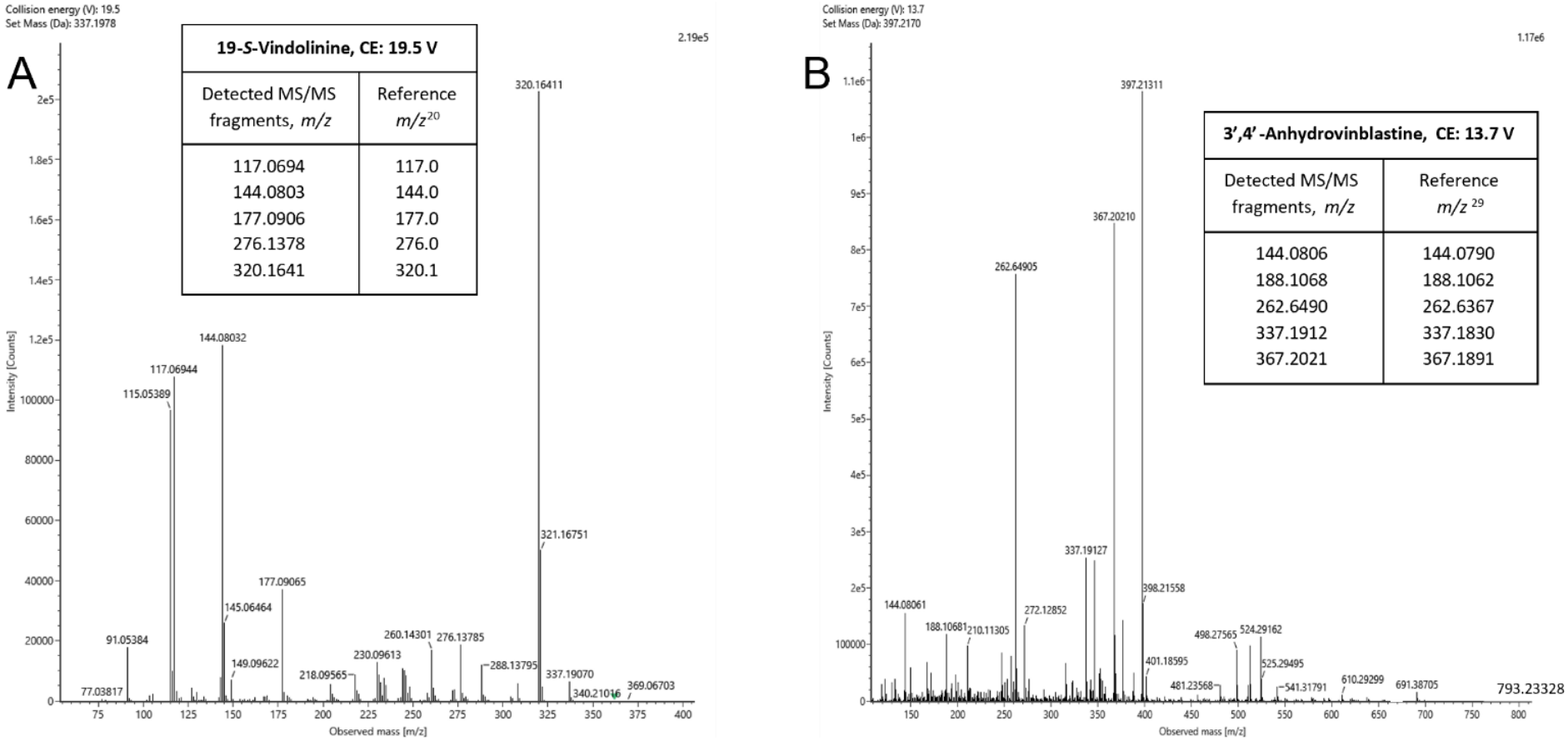

C

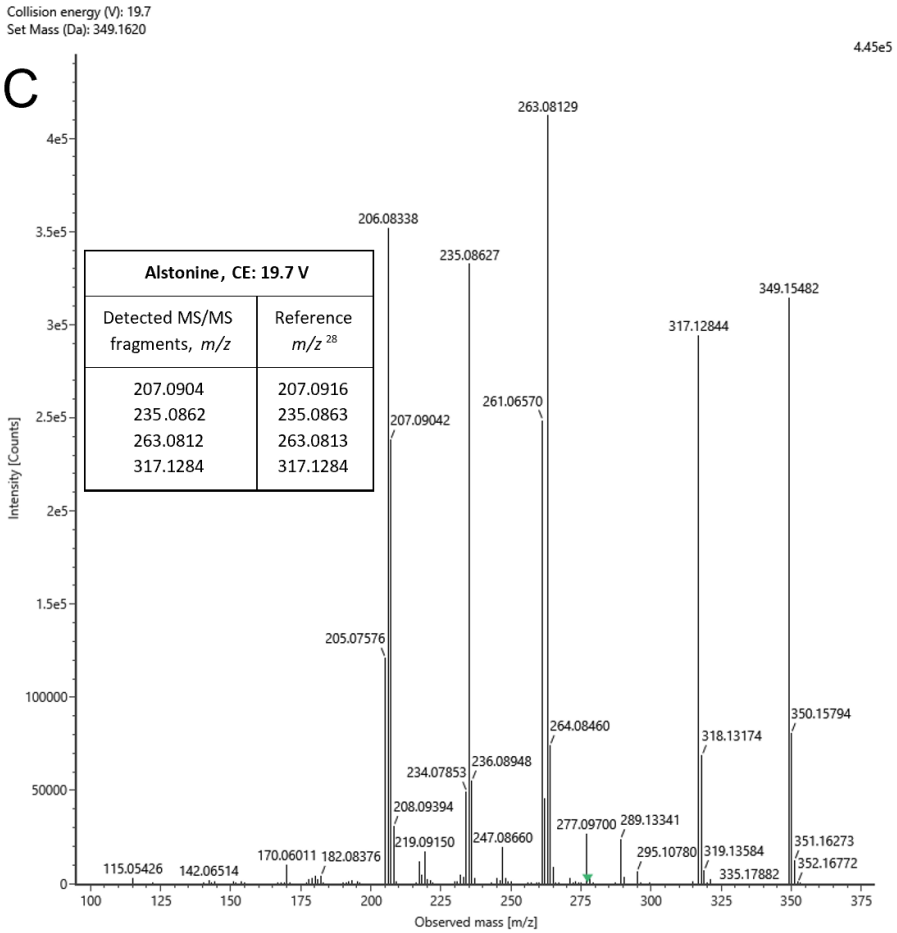

Alstonine, CE: 19.7 V	
Detected MS/MS fragments, *m/z*	Reference *m/z* [28]
207.0904	207.0916
235.0862	235.0863
263.0812	263.0813
317.1284	317.1284

D

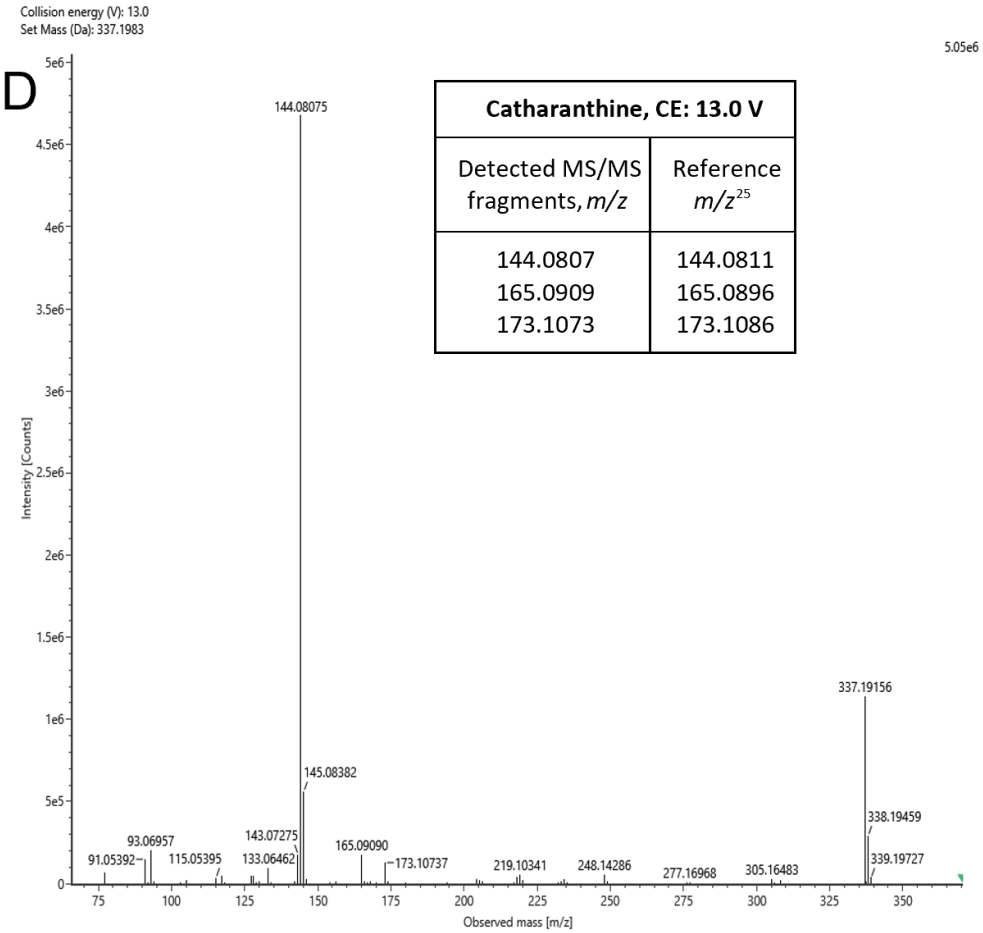

Catharanthine, CE: 13.0 V	
Detected MS/MS fragments, *m/z*	Reference *m/z* [25]
144.0807	144.0811
165.0909	165.0896
173.1073	173.1086

E

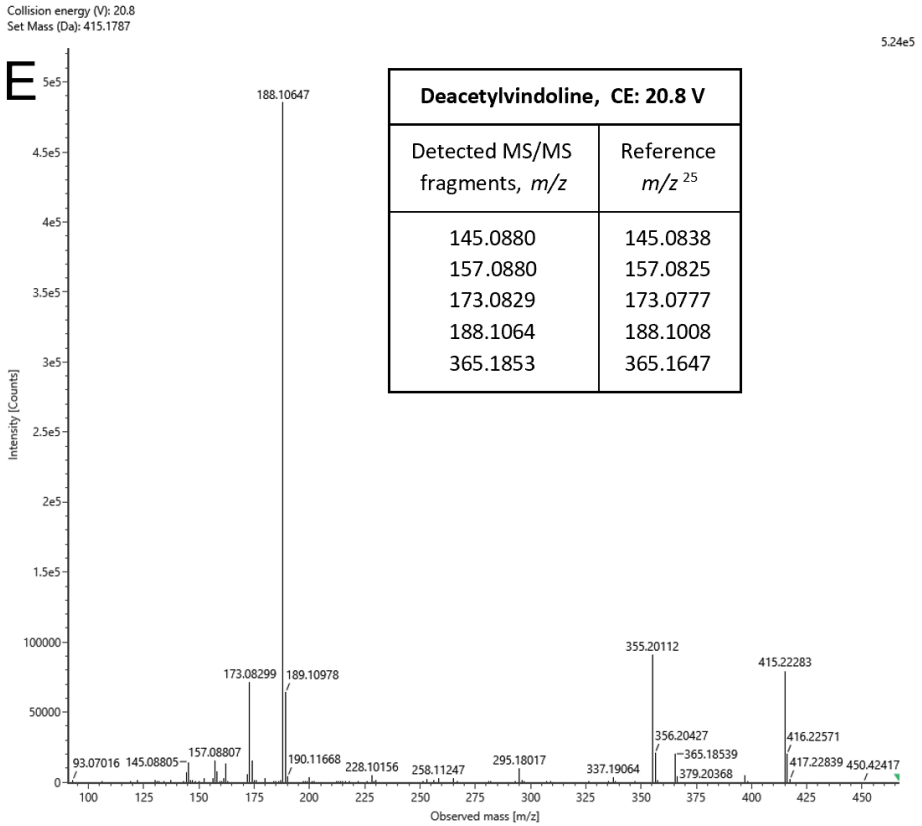

Deacetylvindoline, CE: 20.8 V	
Detected MS/MS fragments, *m/z*	Reference *m/z* [25]
145.0880	145.0838
157.0880	157.0825
173.0829	173.0777
188.1064	188.1008
365.1853	365.1647

F

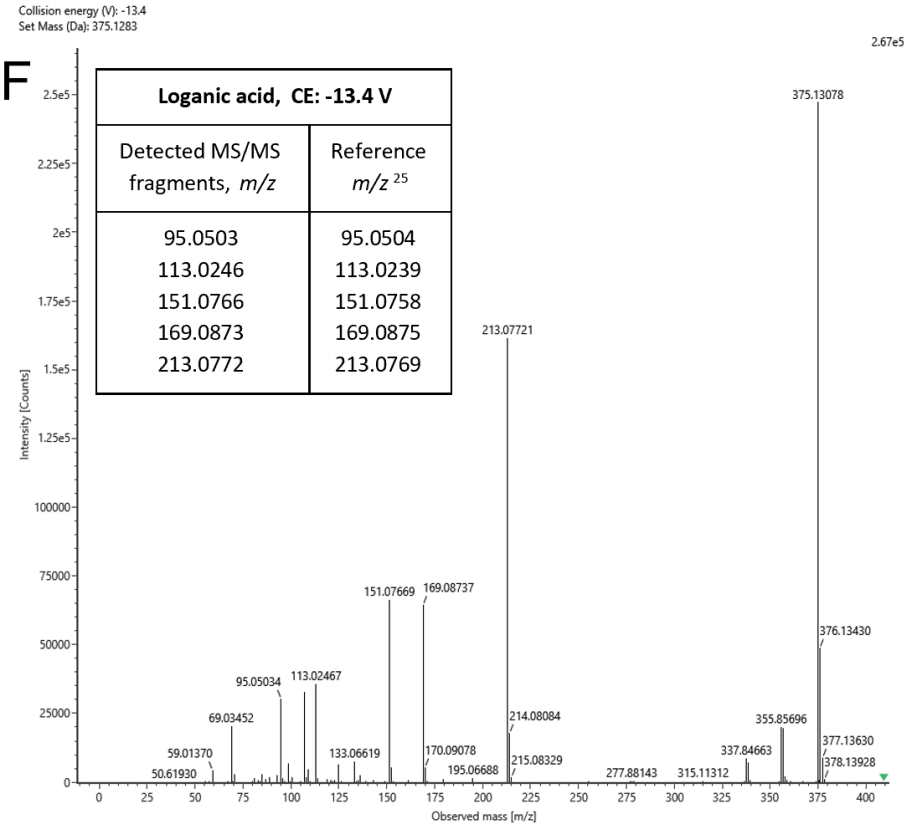

Loganic acid, CE: -13.4 V	
Detected MS/MS fragments, *m/z*	Reference *m/z* [25]
95.0503	95.0504
113.0246	113.0239
151.0766	151.0758
169.0873	169.0875
213.0772	213.0769

G

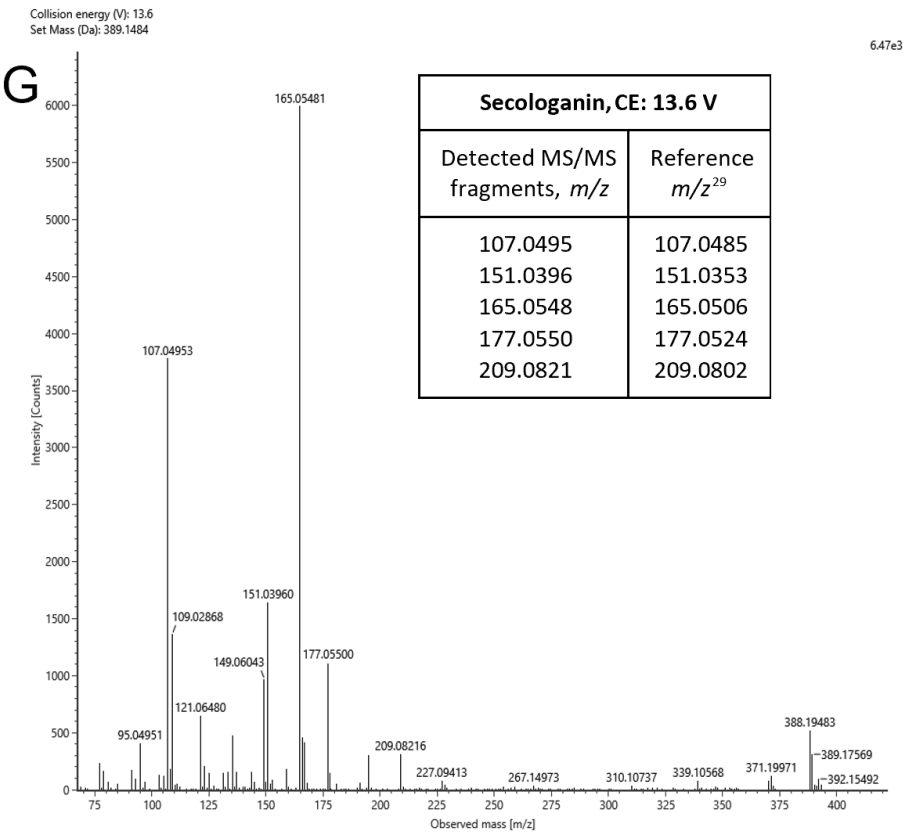

Secologanin, CE: 13.6 V	
Detected MS/MS fragments, *m/z*	Reference *m/z*[29]
107.0495	107.0485
151.0396	151.0353
165.0548	165.0506
177.0550	177.0524
209.0821	209.0802

H

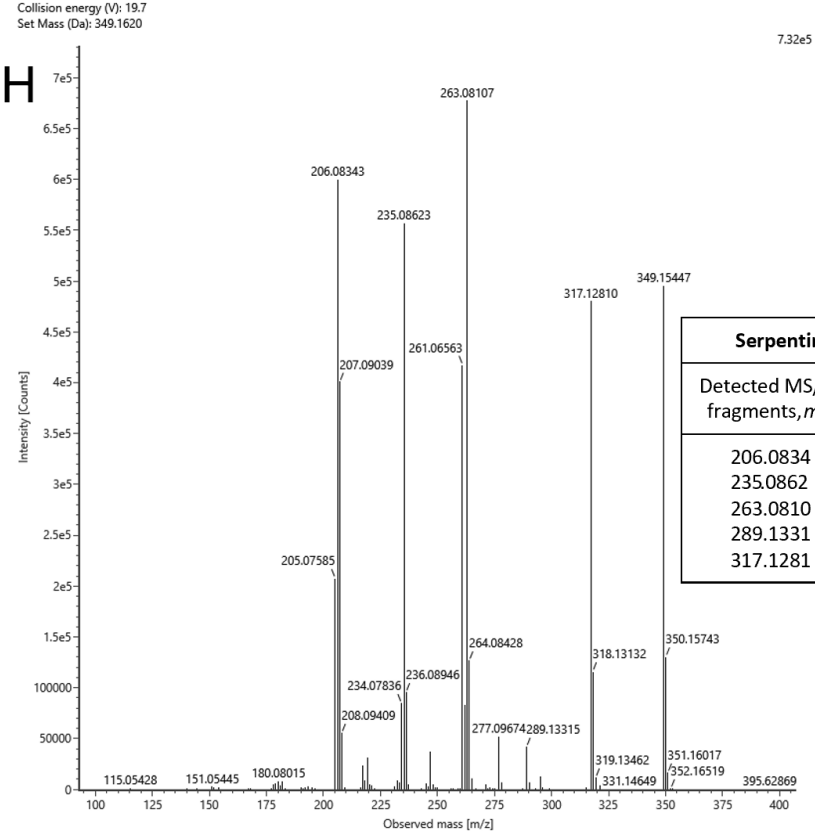

Serpentine, CE: 19.7 V	
Detected MS/MS fragments, *m/z*	Reference *m/z*[26]
206.0834	206.0821
235.0862	235.0841
263.0810	263.0789
289.1331	289.1290
317.1281	317.1252

I

Strictosidine, CE: 22.6 V	
Detected MS/MS fragments, *m/z*	Reference *m/z*[25]
144.0806	144.0804
222.0910	222.0906
334.1440	334.1386
352.1546	352.1445
514.2080	514.2153

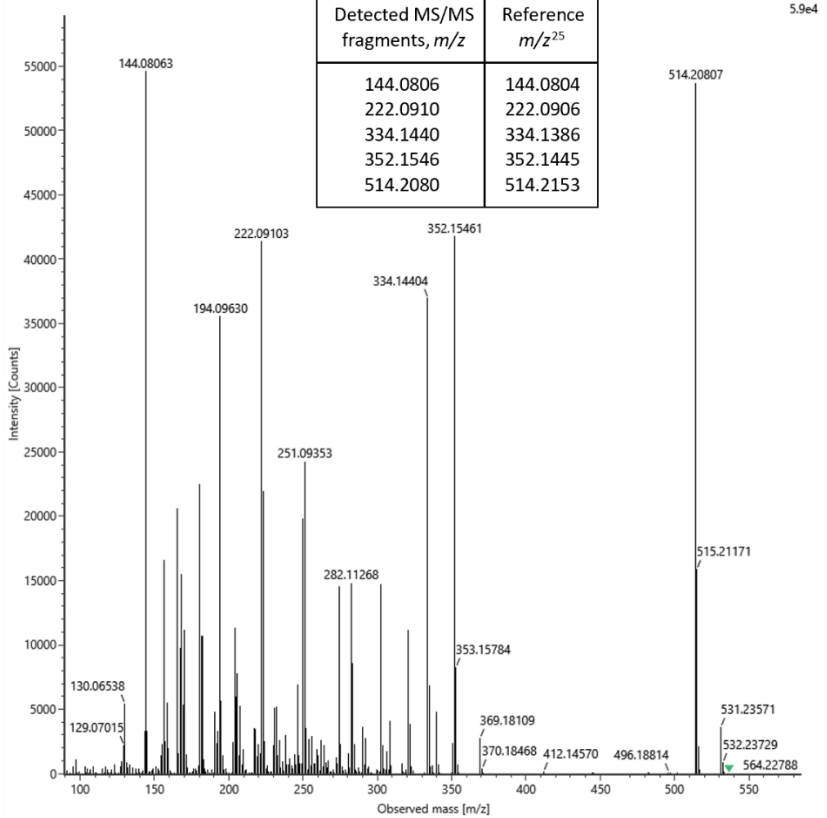

J

Vincadifformine, CE: 13.0 V	
Detected MS/MS fragments, *m/z*	Reference *m/z* [27]
168.0834	168.0808
194.1042	194.0966
307.1817	307.1811

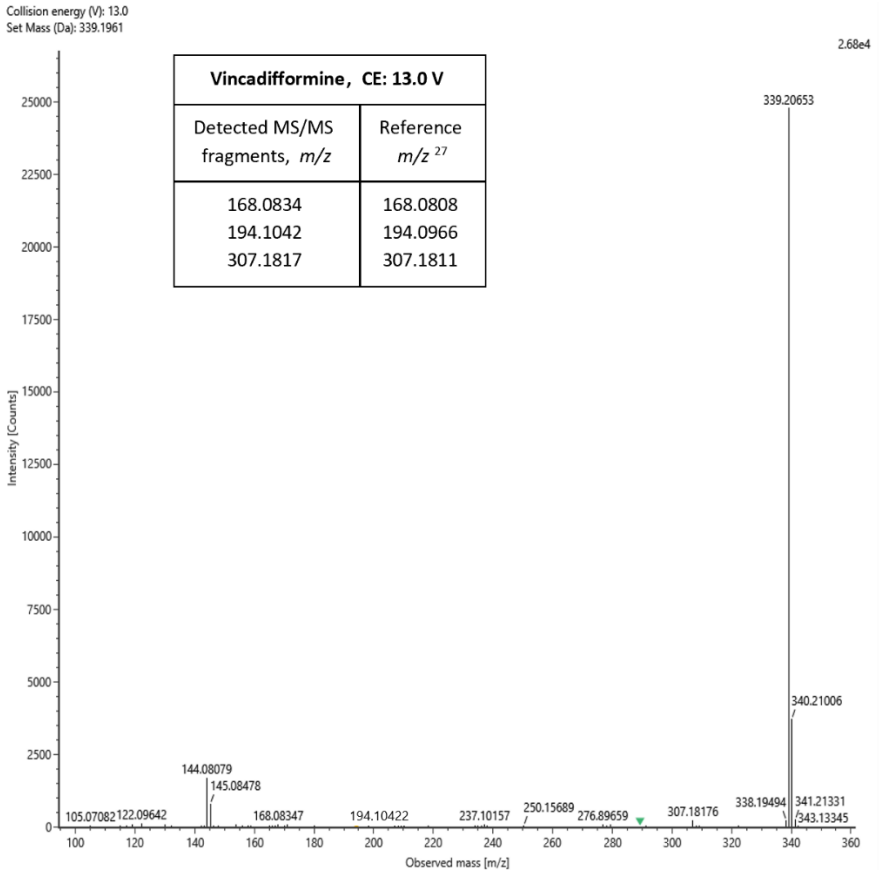

K

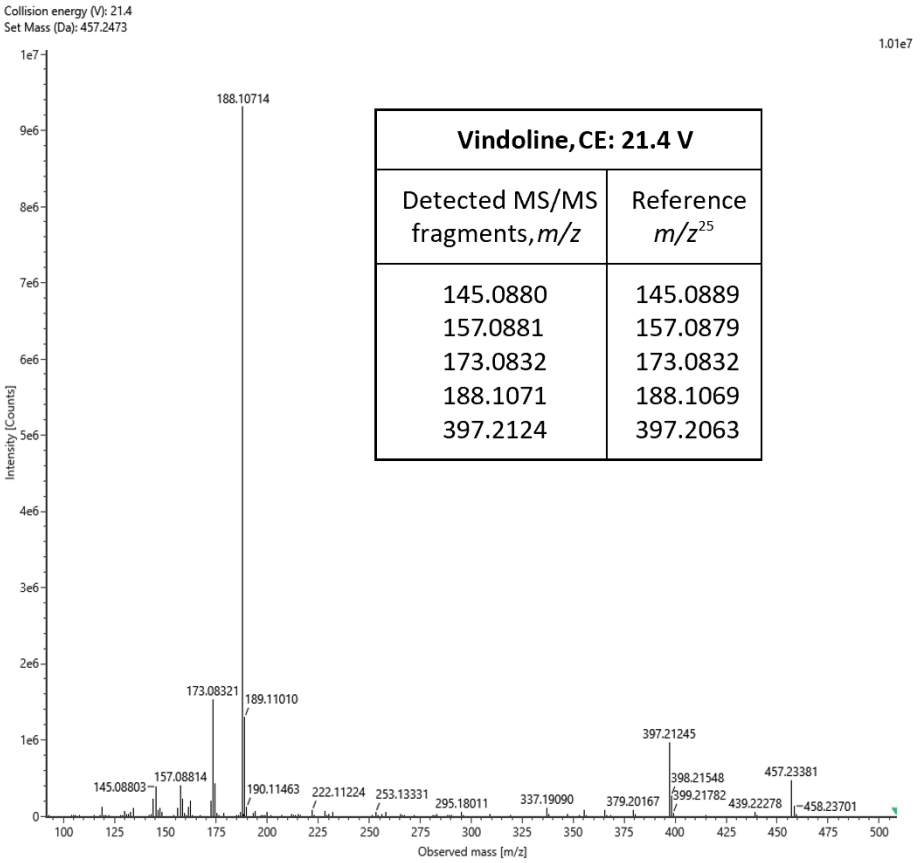

Vindoline, CE: 21.4 V	
Detected MS/MS fragments, *m/z*	Reference *m/z*[25]
145.0880	145.0889
157.0881	157.0879
173.0832	173.0832
188.1071	188.1069
397.2124	397.2063

L

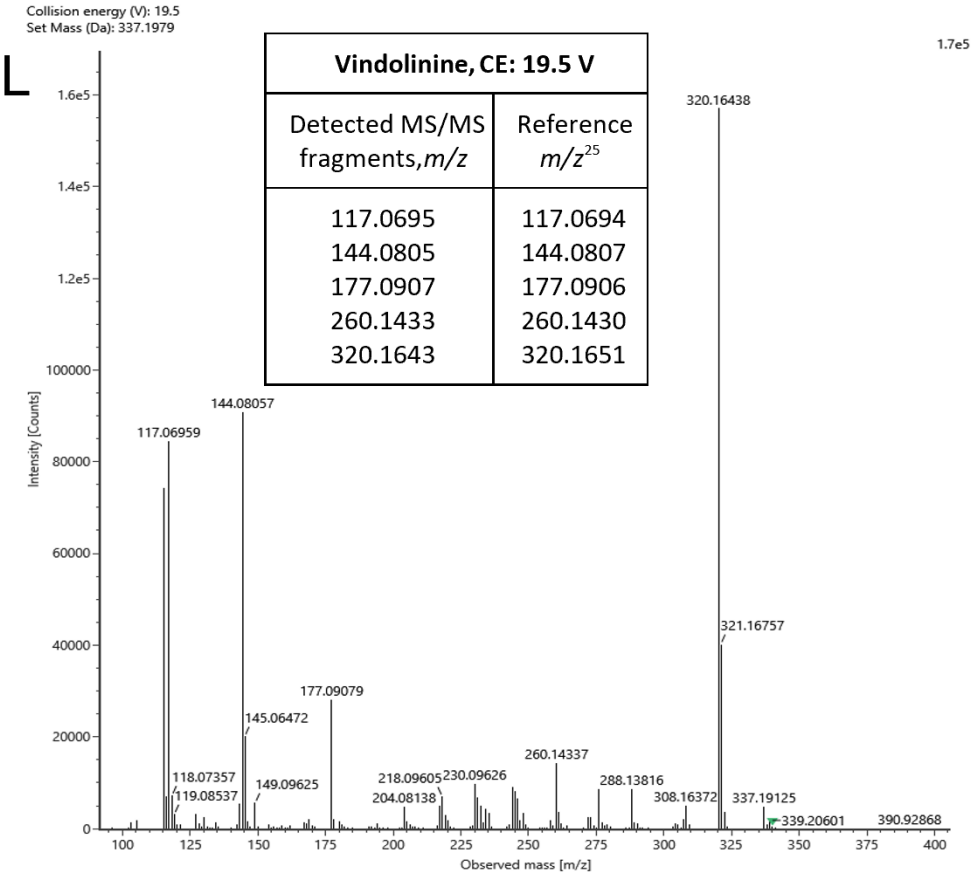

Vindolinine, CE: 19.5 V	
Detected MS/MS fragments, *m/z*	Reference *m/z*[25]
117.0695	117.0694
144.0805	144.0807
177.0907	177.0906
260.1433	260.1430
320.1643	320.1651

App. Figure 3. MS/MS spectra of the identified dandelion compounds.

No. 1 Caffeic acid glucoside_1 C15H18O9 (neutral) Rt = 1.31 min

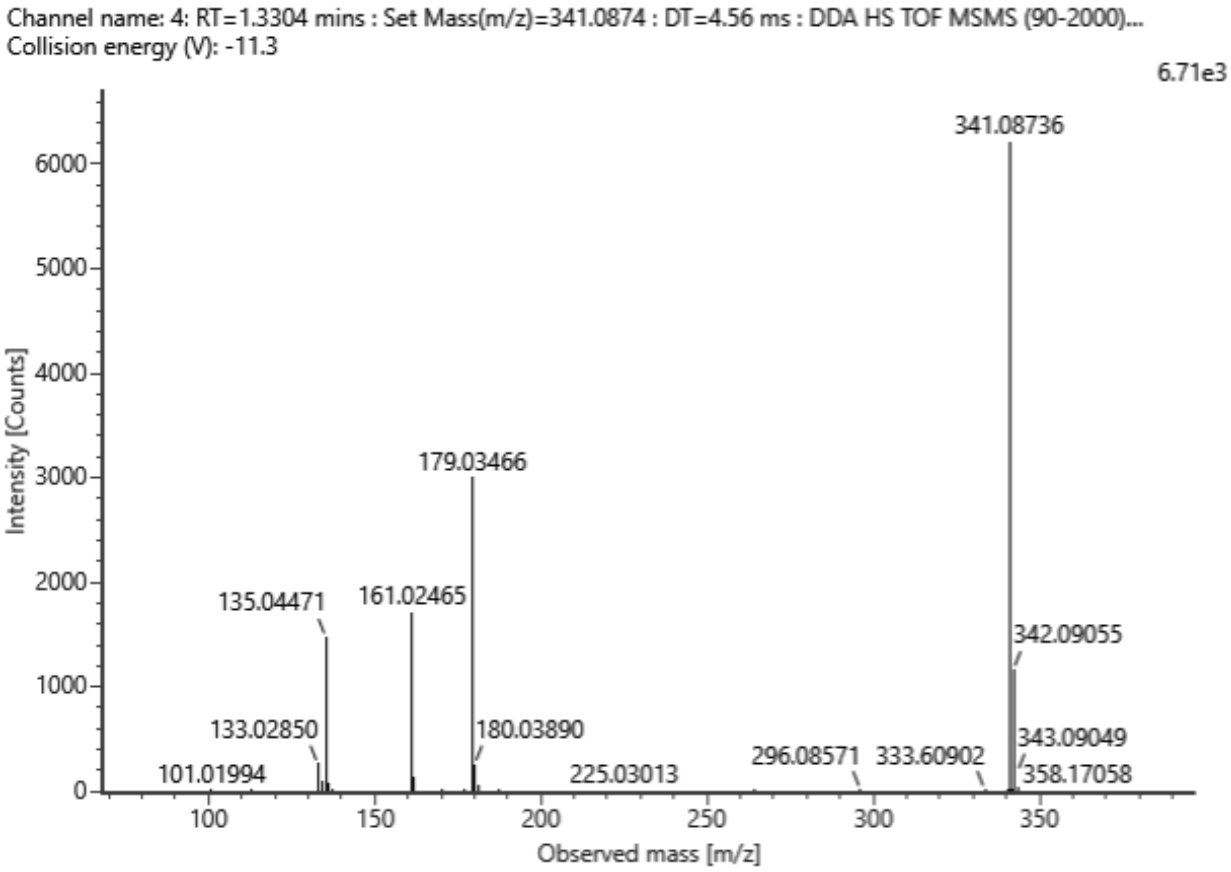

No. 2 Caffeic acid derivative_1 C9H8O7S (neutral) Rt = 1.59 min

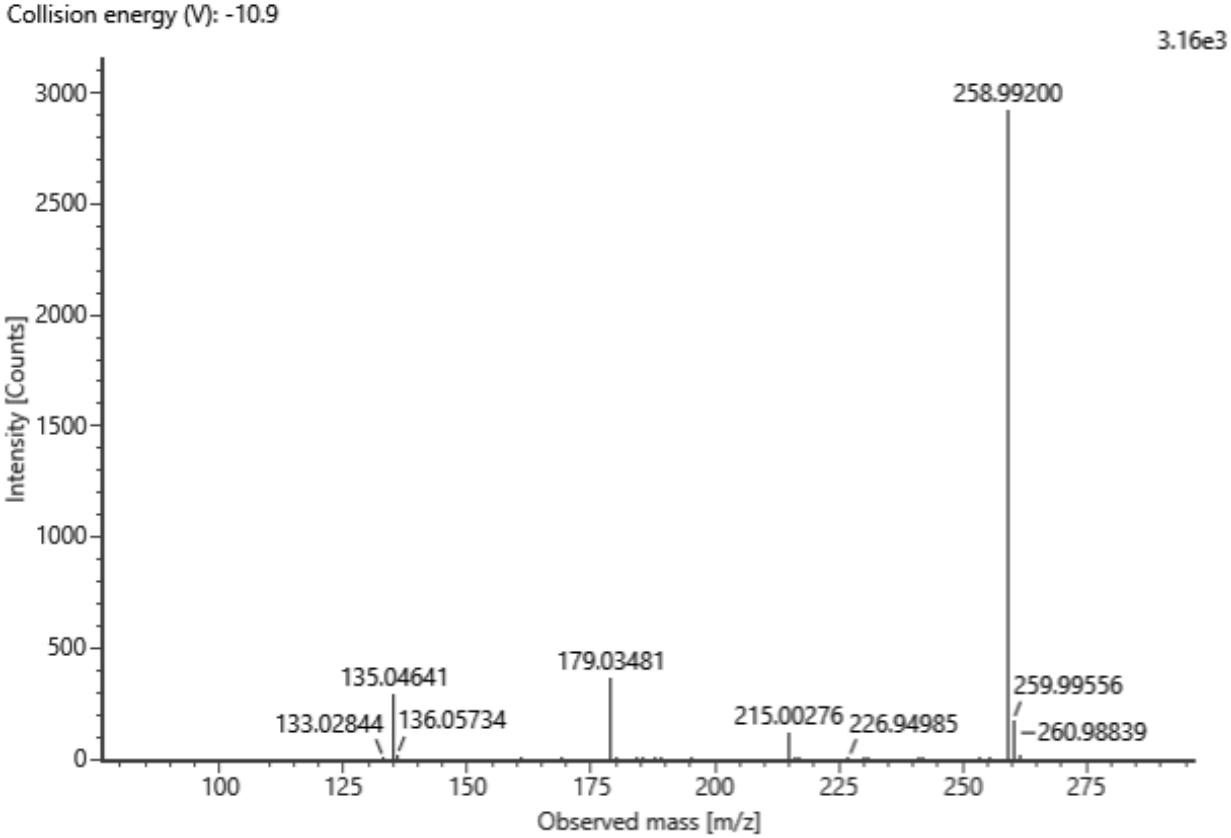

No. 3 Caffeic acid glucoside_2 C15H18O9 (neutral) Rt = 1.86 min

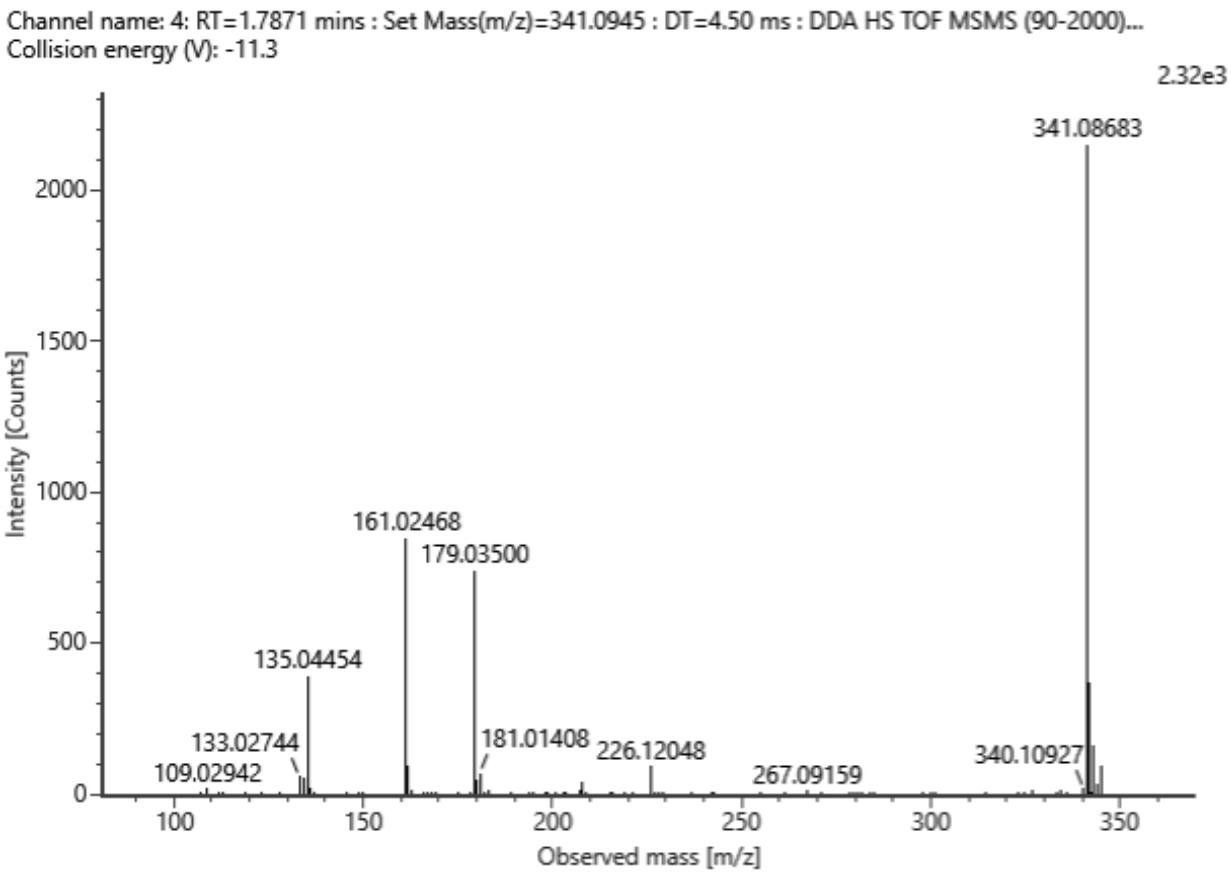

No. 4 Protocatechuoylglucose_1 C13H16O9 (neutral) Rt = 1.94 min

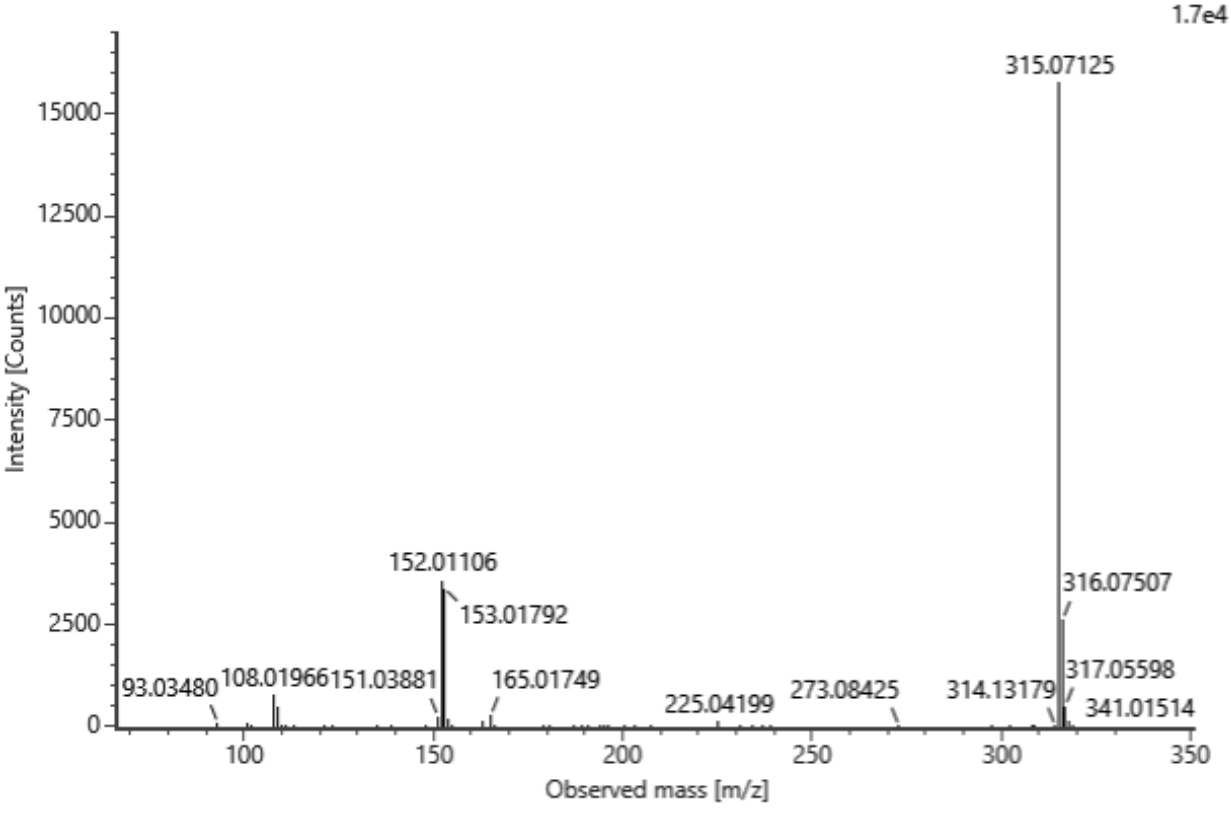

No. 5 Caffeic acid sulfate_1 C9H8O7S (neutral) Rt = 2.10 min

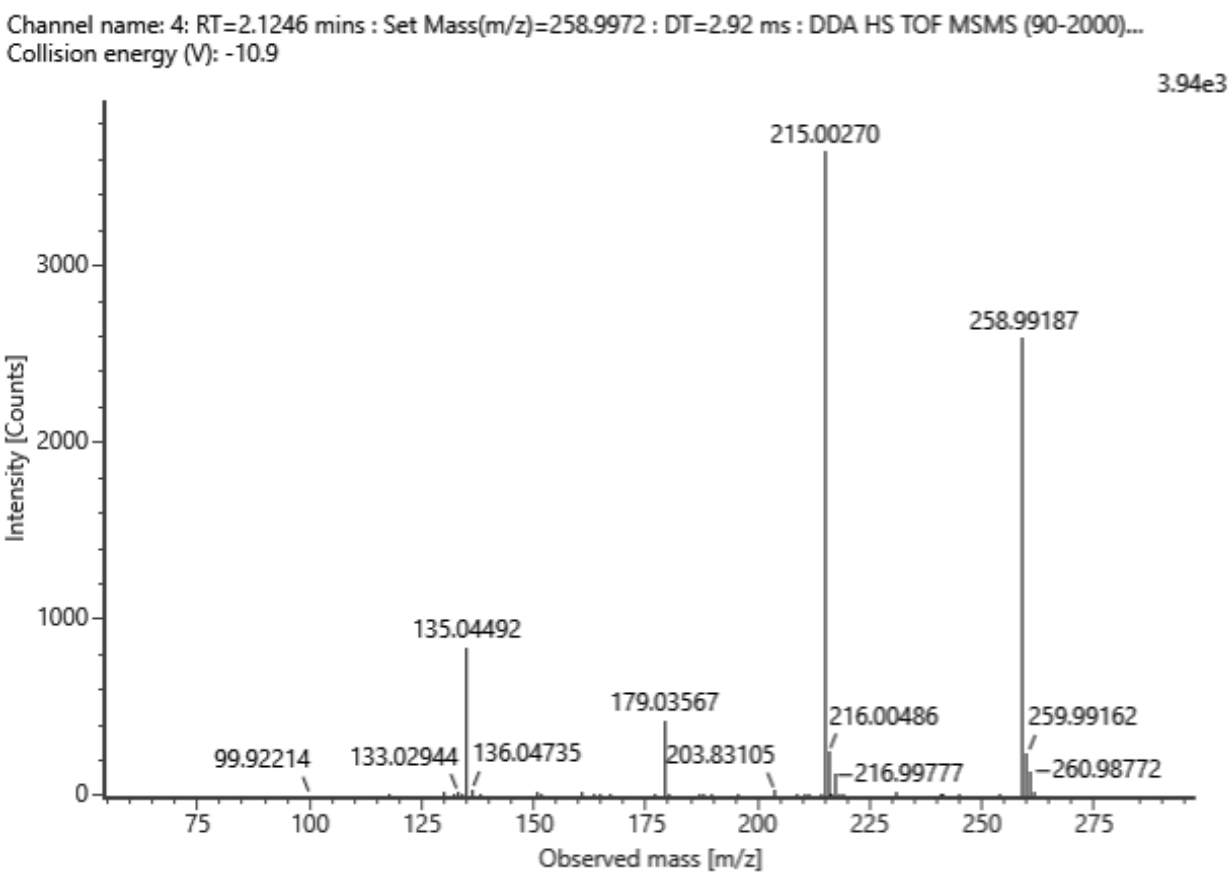

No. 6 Protocatechuoylglucose_2 C13H16O9 (neutral) Rt = 2.63 min

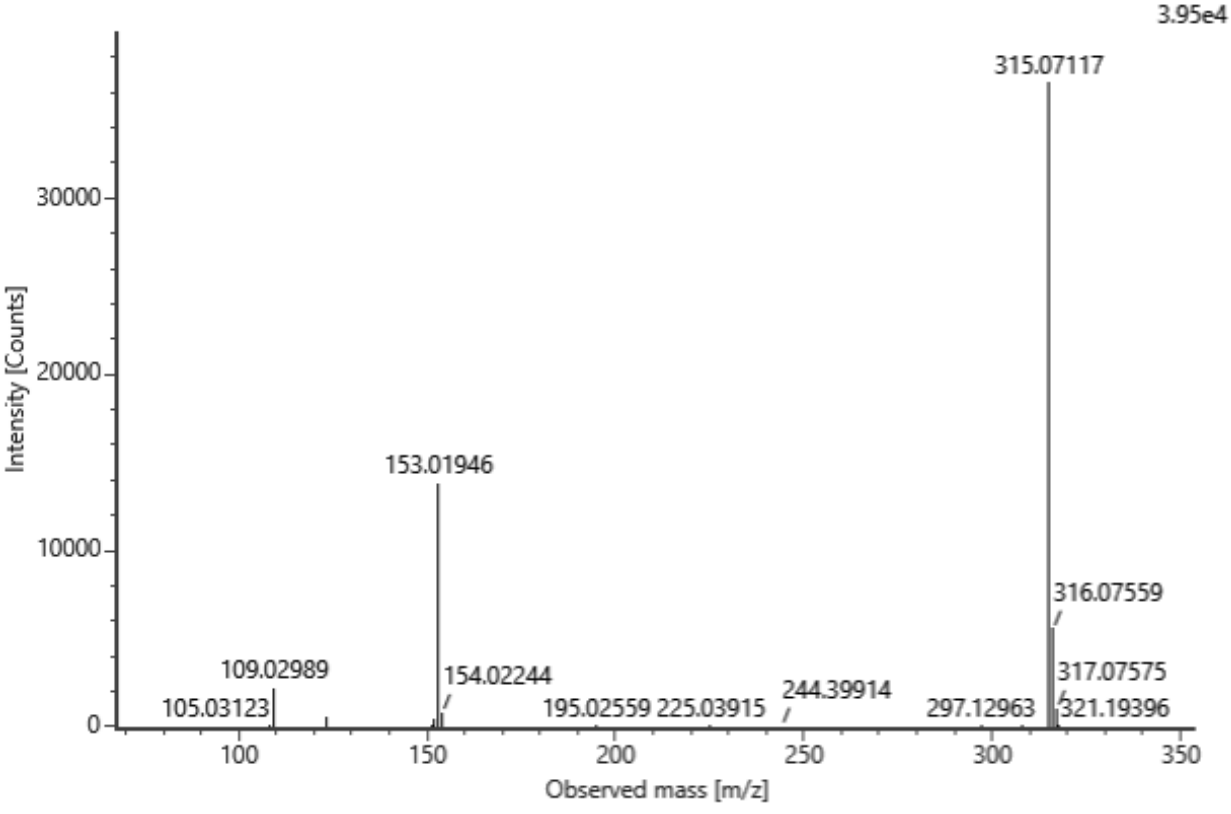

No. 7 Esculetin sulfate C9H6O7S (neutral) Rt = 2.71 min

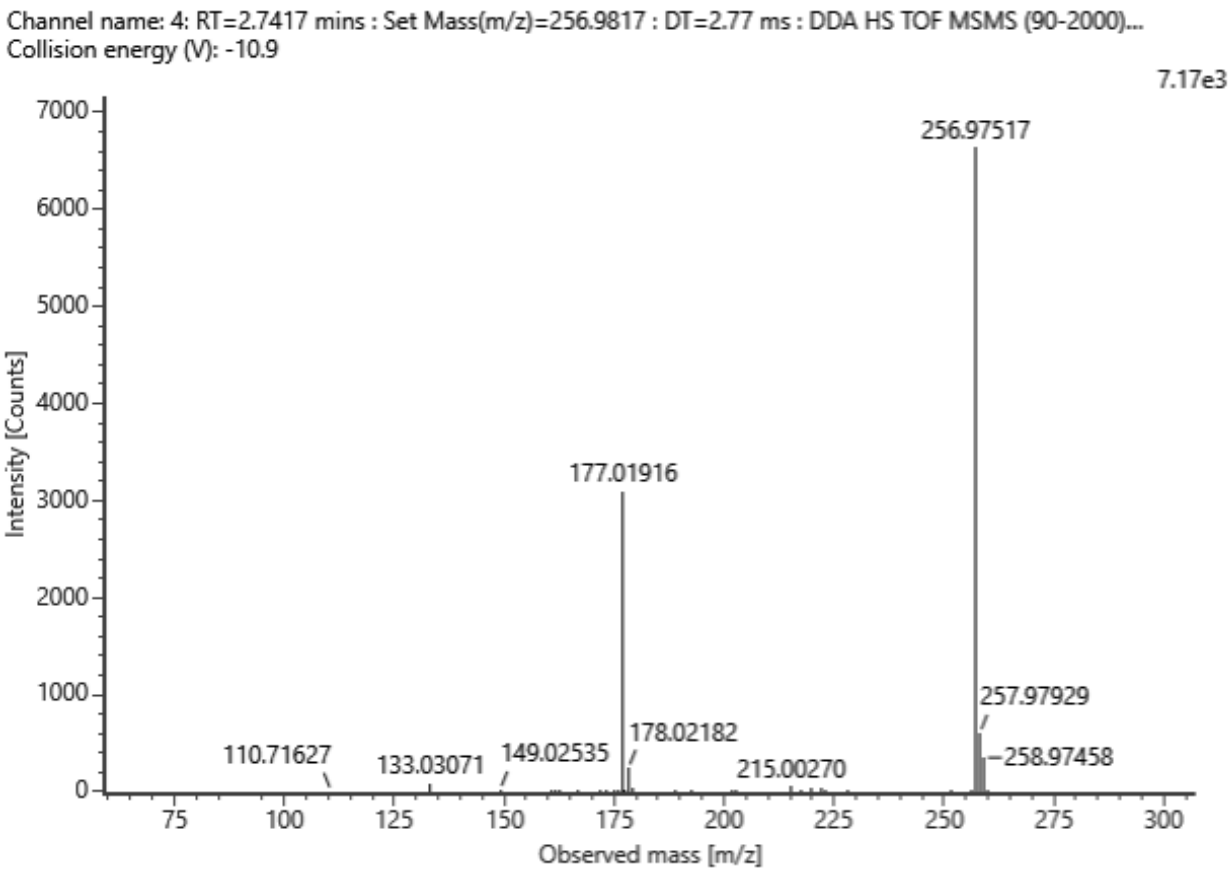

No. 8 Caftaric acid C13H12O9 (neutral) Rt = 2.74 min

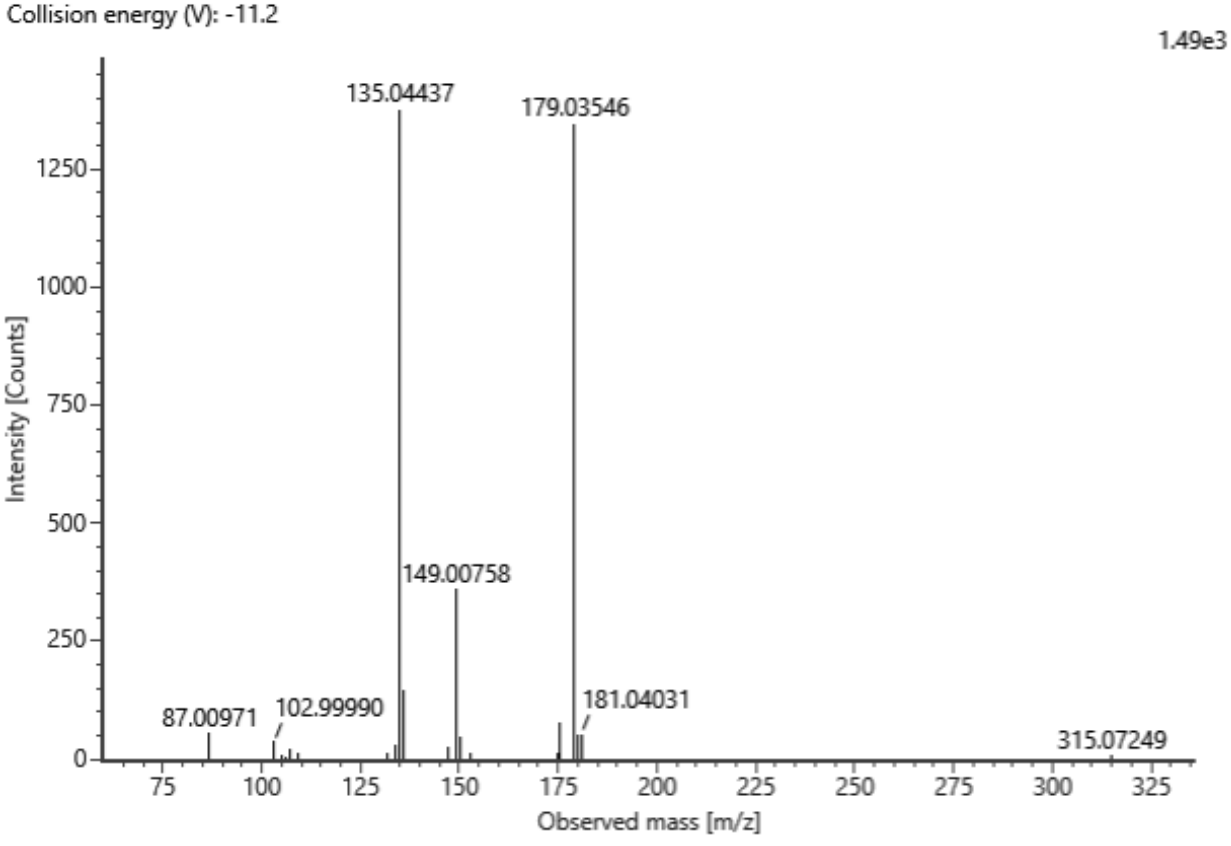

No. 9 Neochlorogenic acid C16H18O9 (neutral) Rt = 2.96 min

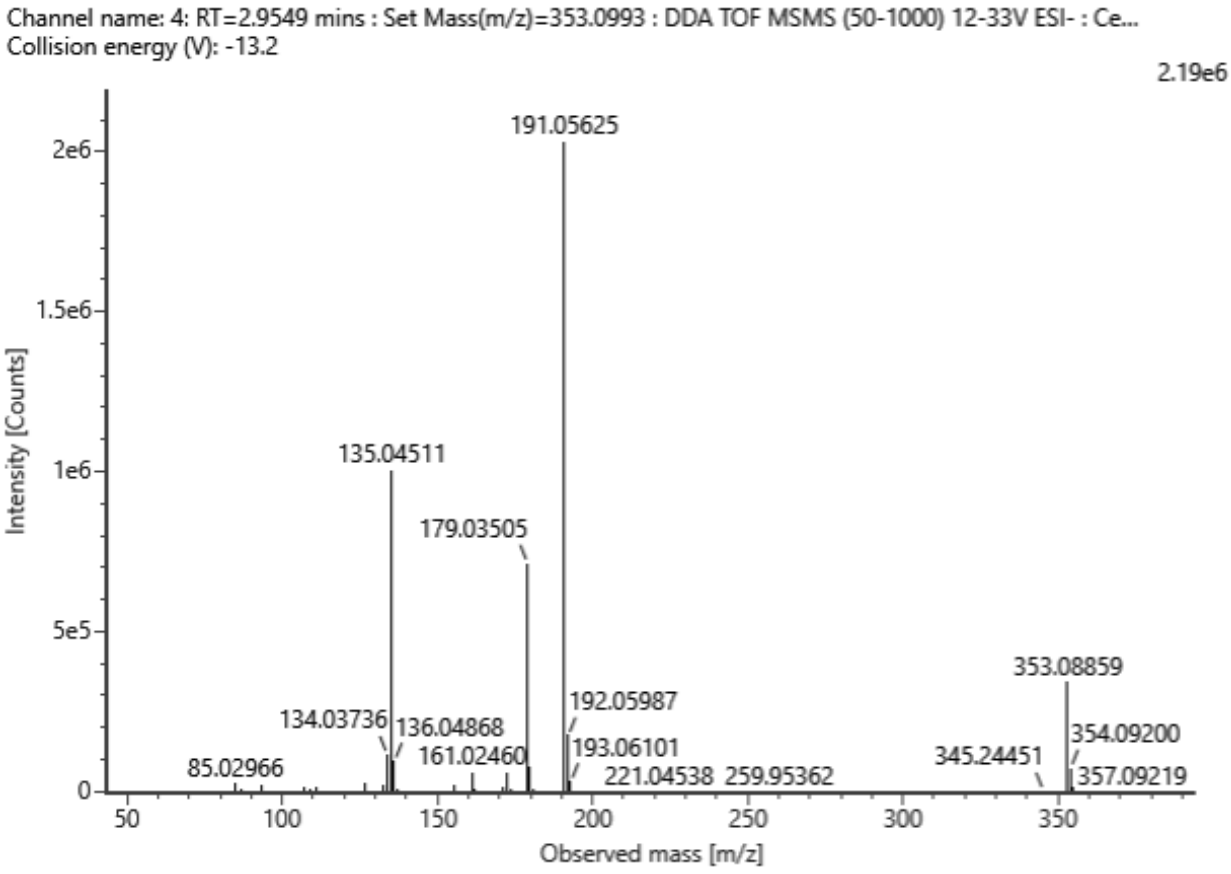

No. 10 Caffeic acid sulfate_2 C9H8O7S (neutral) Rt = 3.23 min

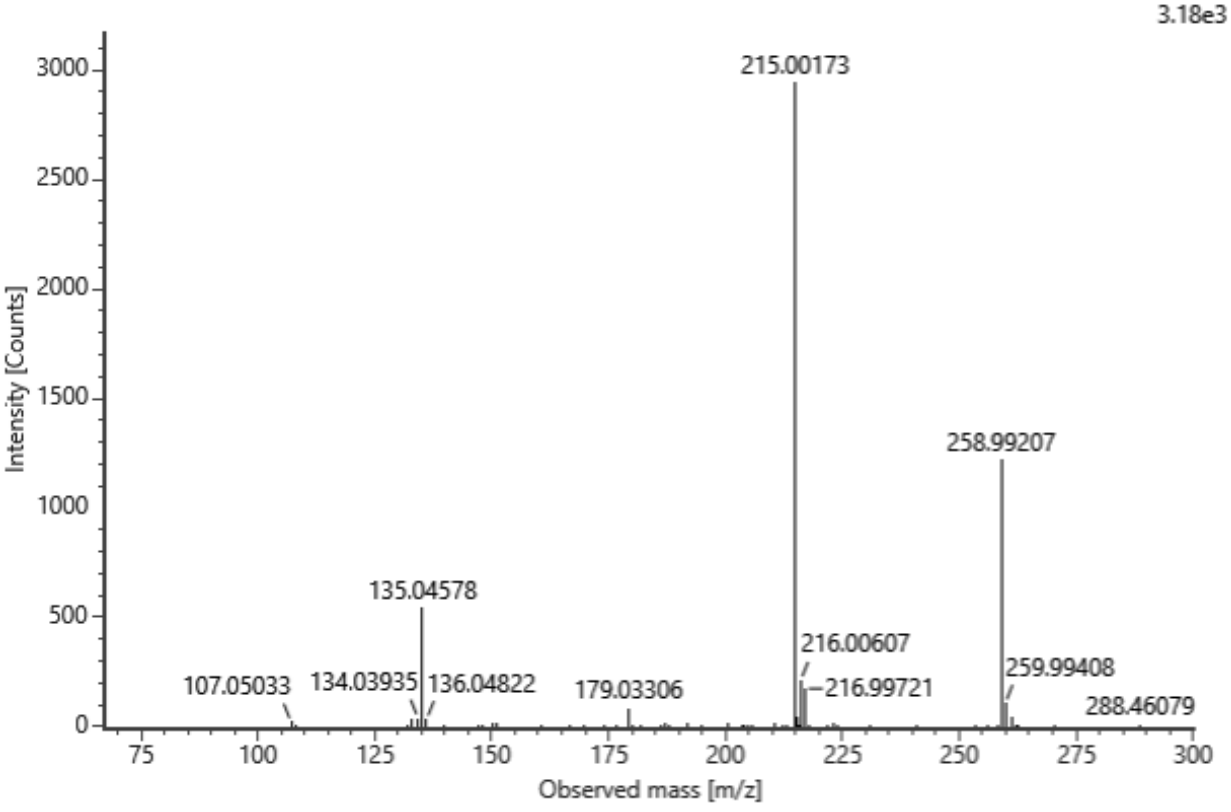

No. 11 Esculin C15H16O9 (neutral) Rt = 3.64 min

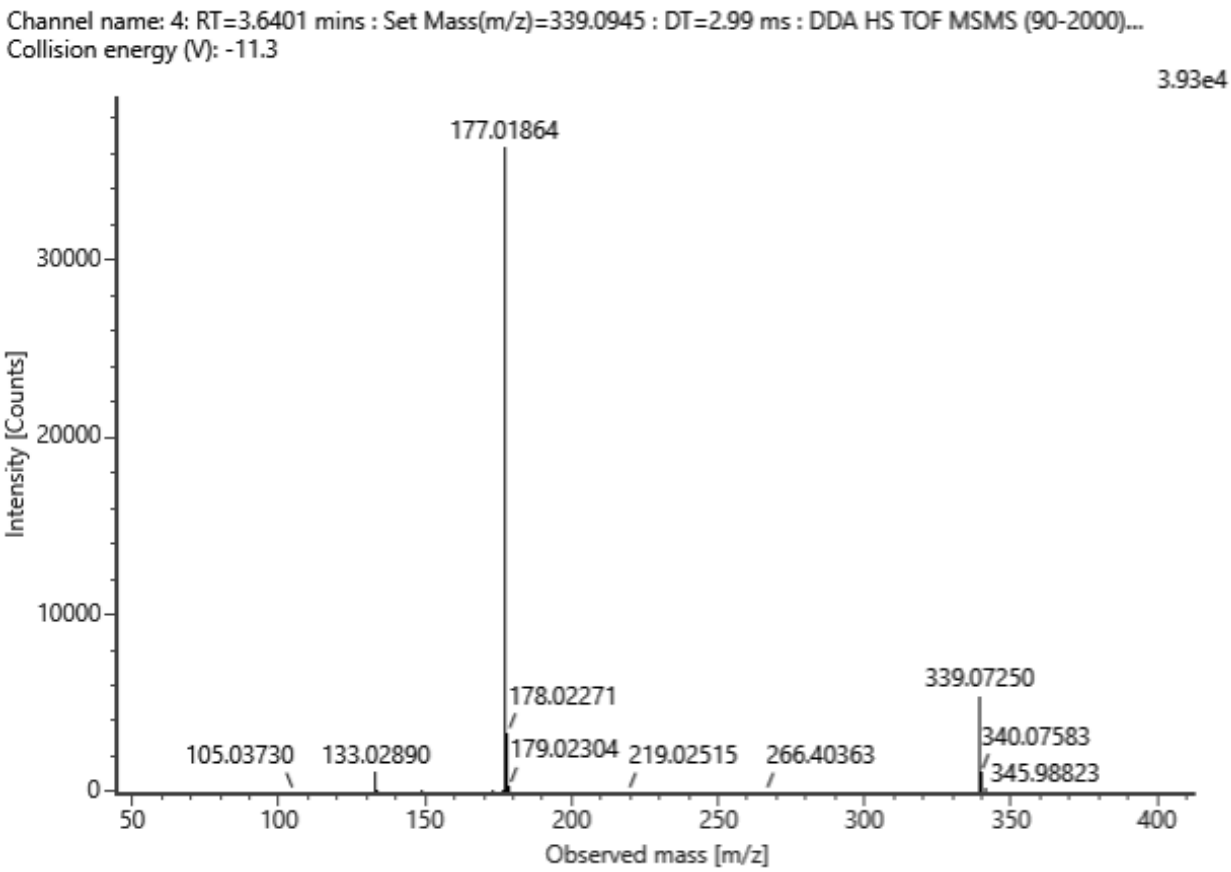

No. 12 Caffeoylsucrose C21H28O14 (neutral) Rt = 4.55 min

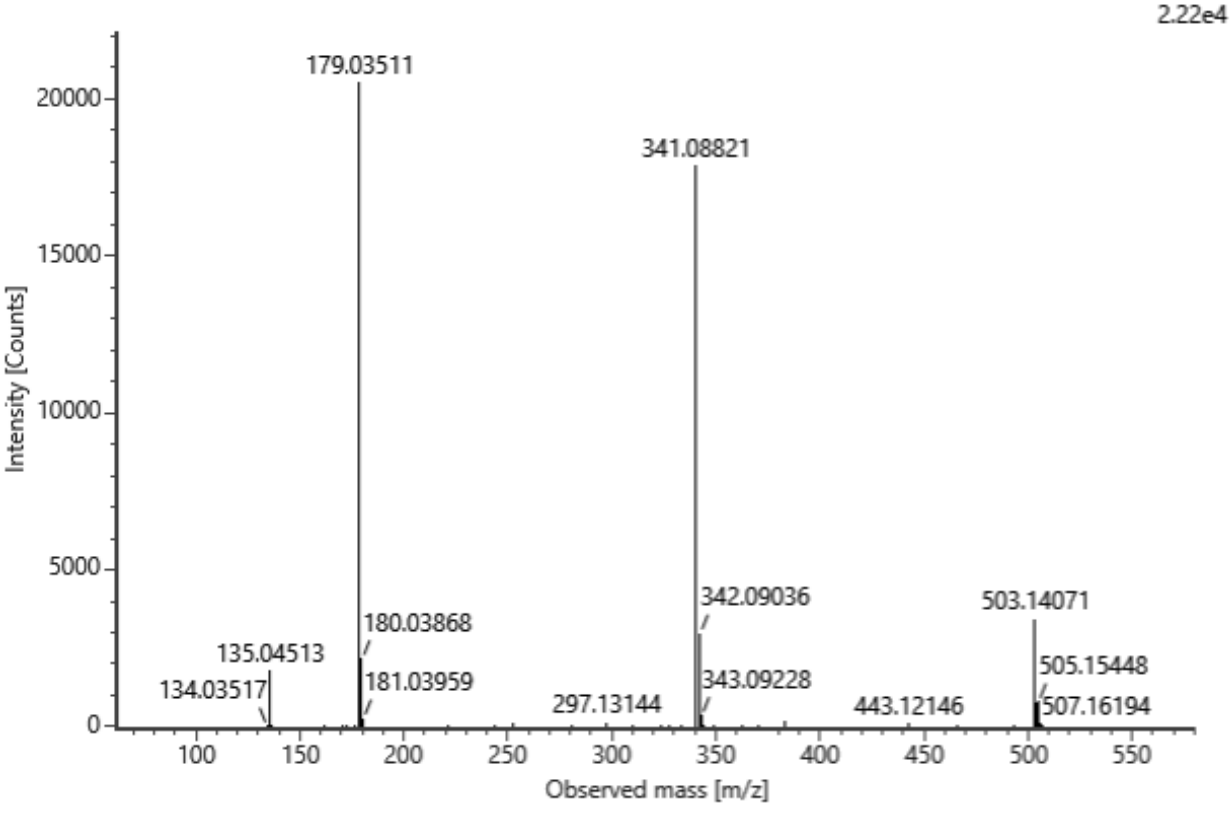

No. 13 Chlorogenic acid C16H18O9 (neutral) Rt = 4.92 min

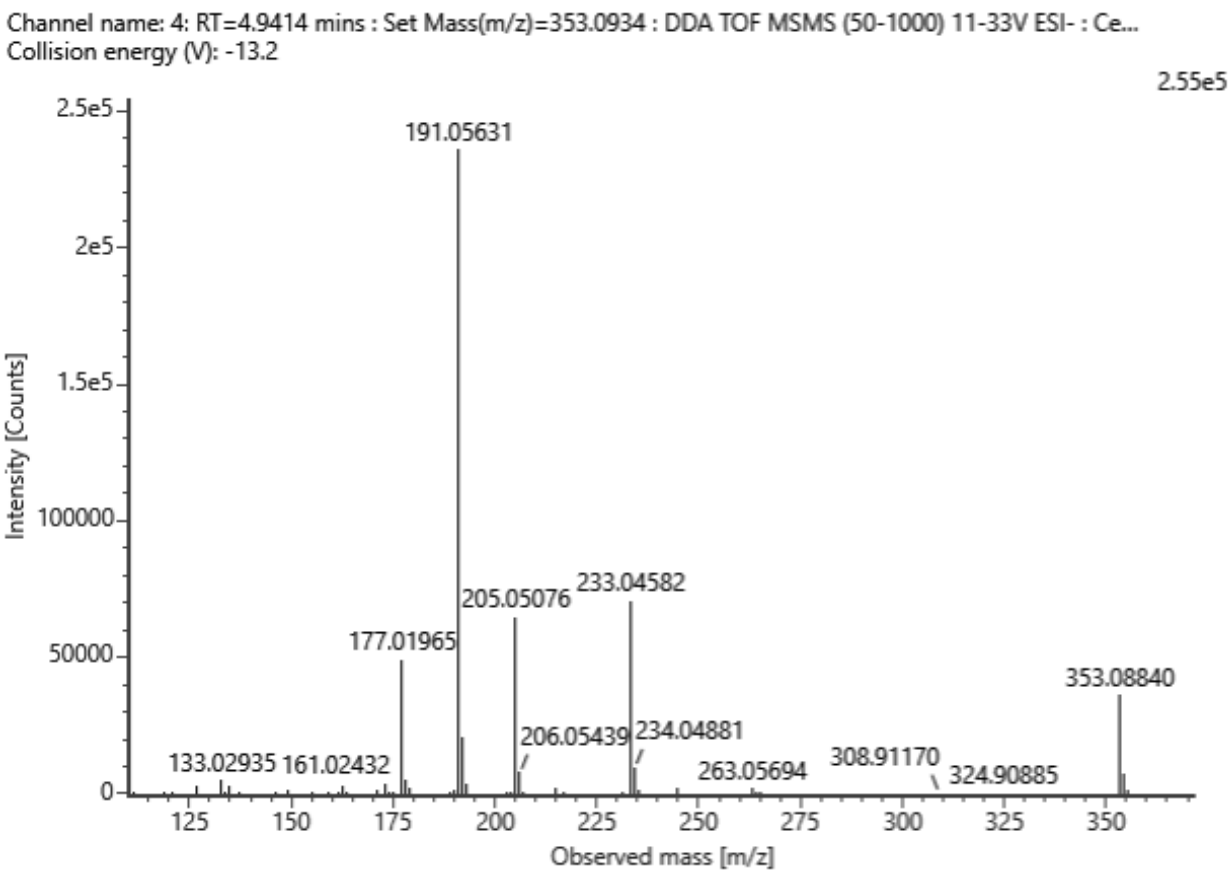

No. 14 Esculetin C9H6O4 (neutral) Rt = 5.00 min

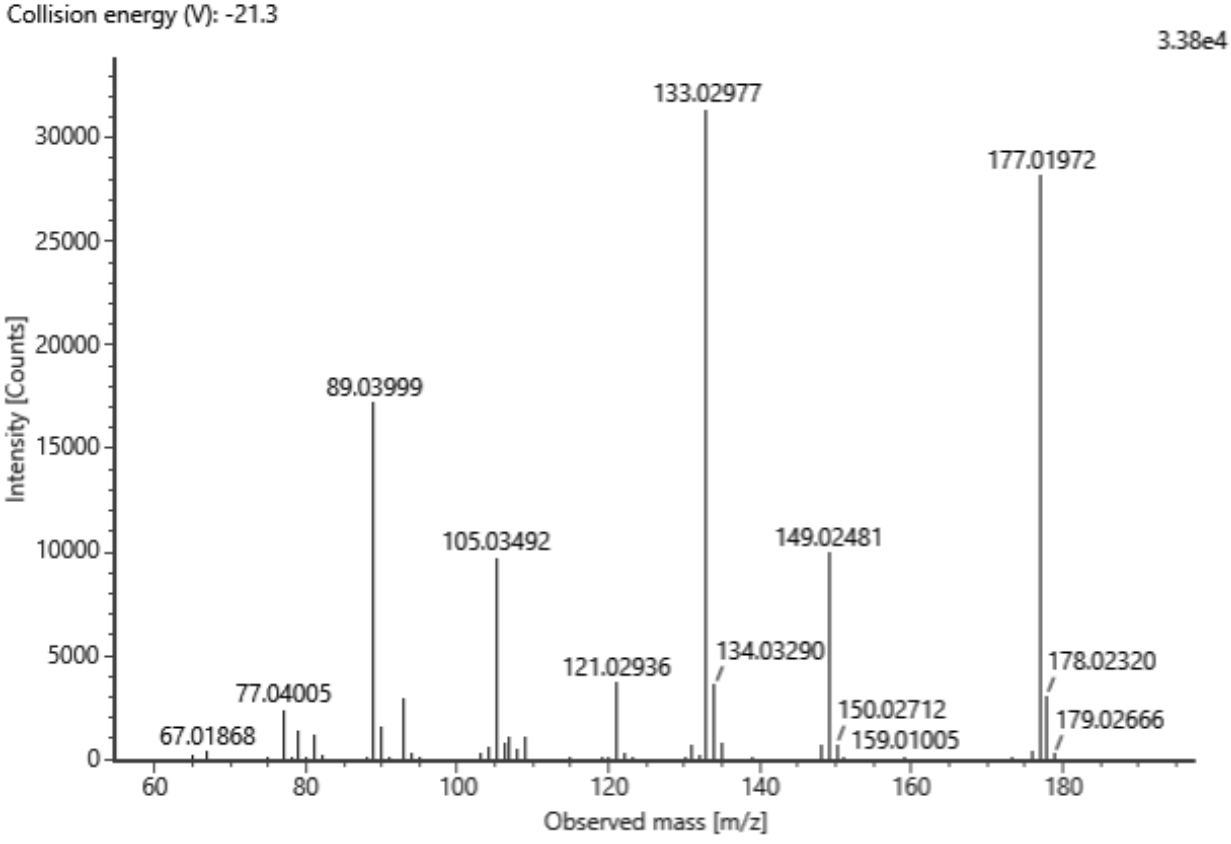

No. 15 Caffeic acid C9H8O4 (neutral) Rt = 5.19 min

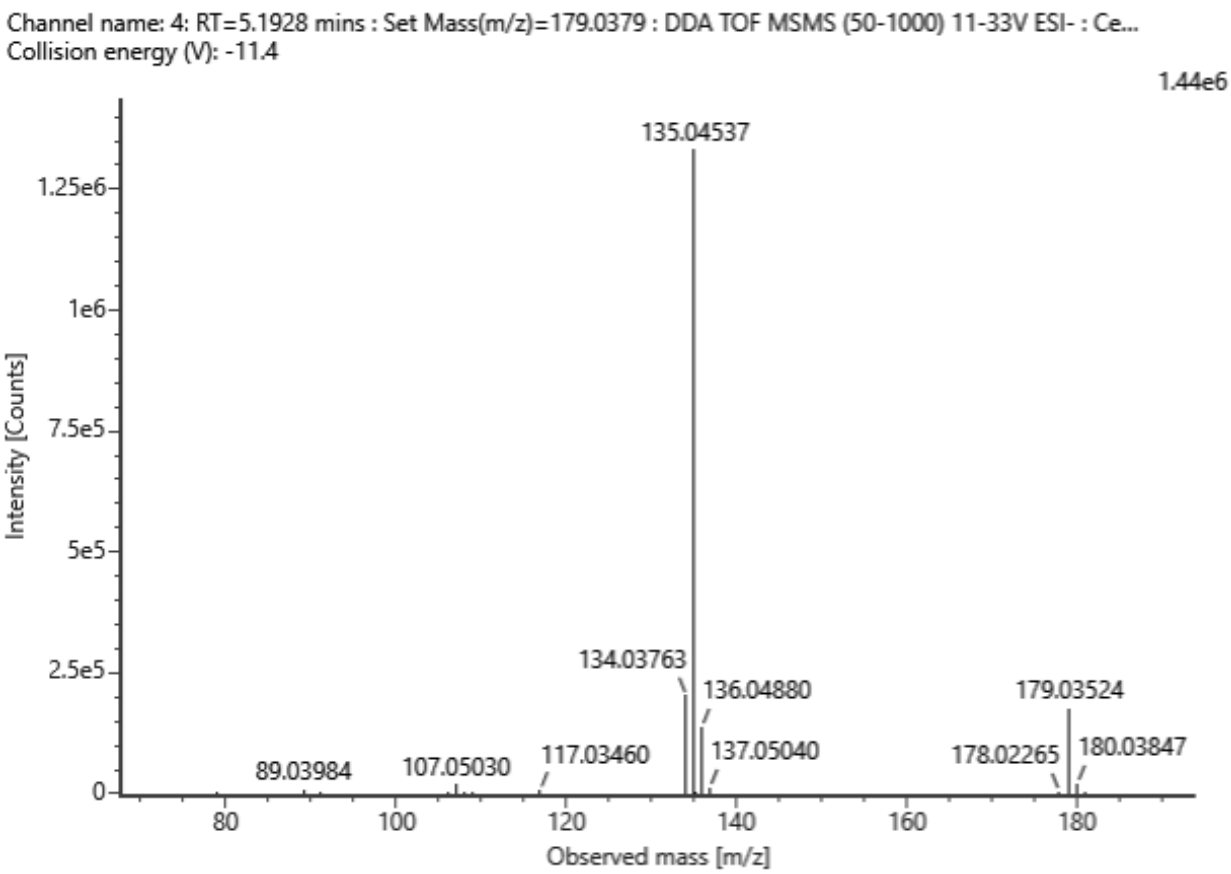

No. 16 1-caffeyllaminaribiose C21H28O14 (neutral) Rt = 5.42 min

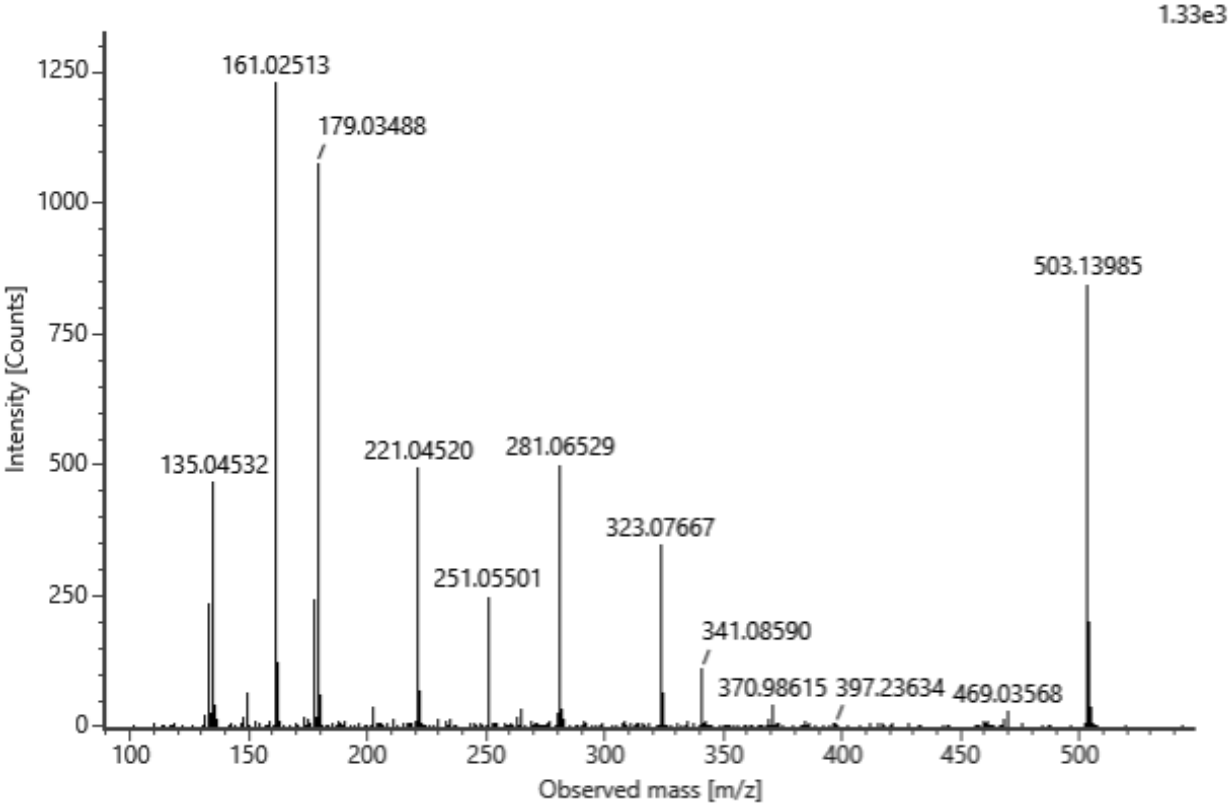

No. 17 Cryptochlorogenic acid C16H18O9 (neutral) Rt = 5.67 min

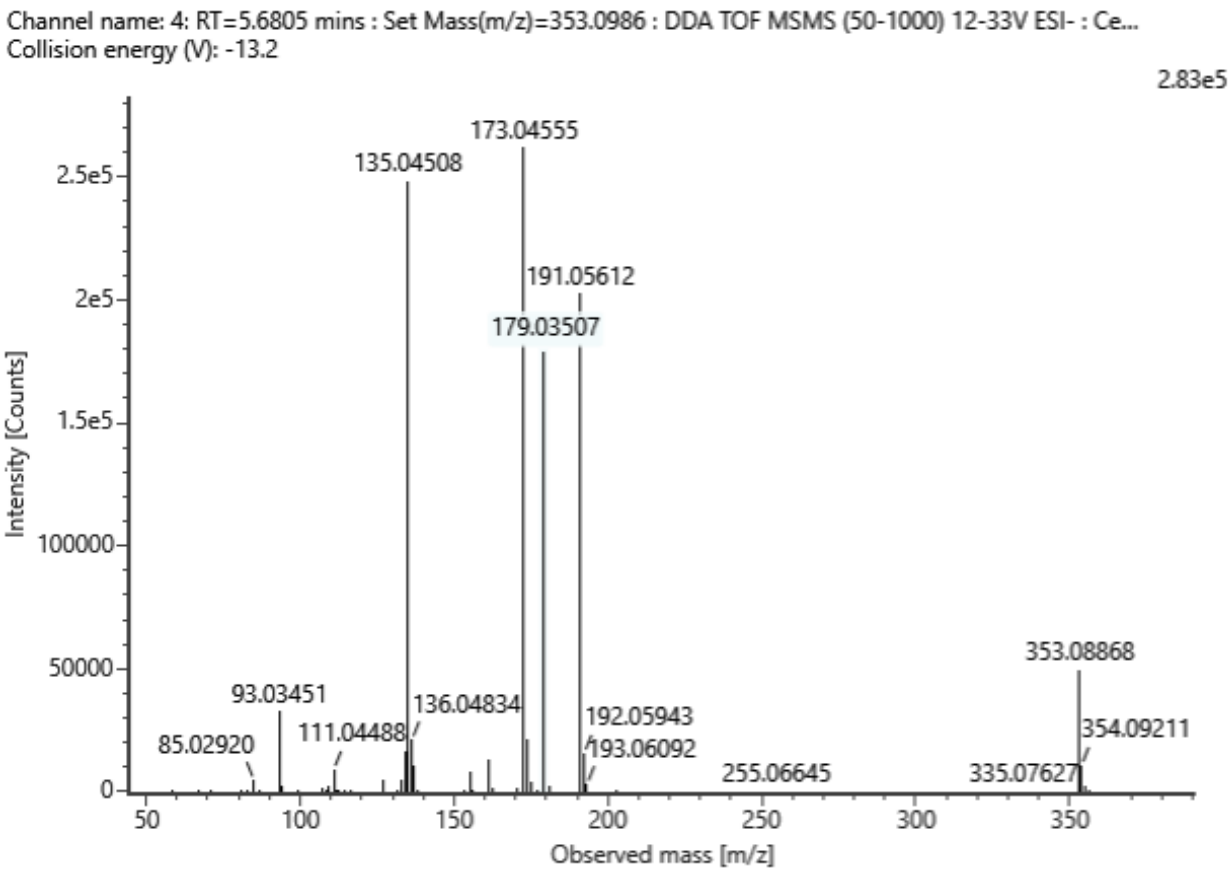

No. 19 12-Hydroxyjasmonate sulfate_1 C12H18O7S (neutral) Rt = 6.58 min

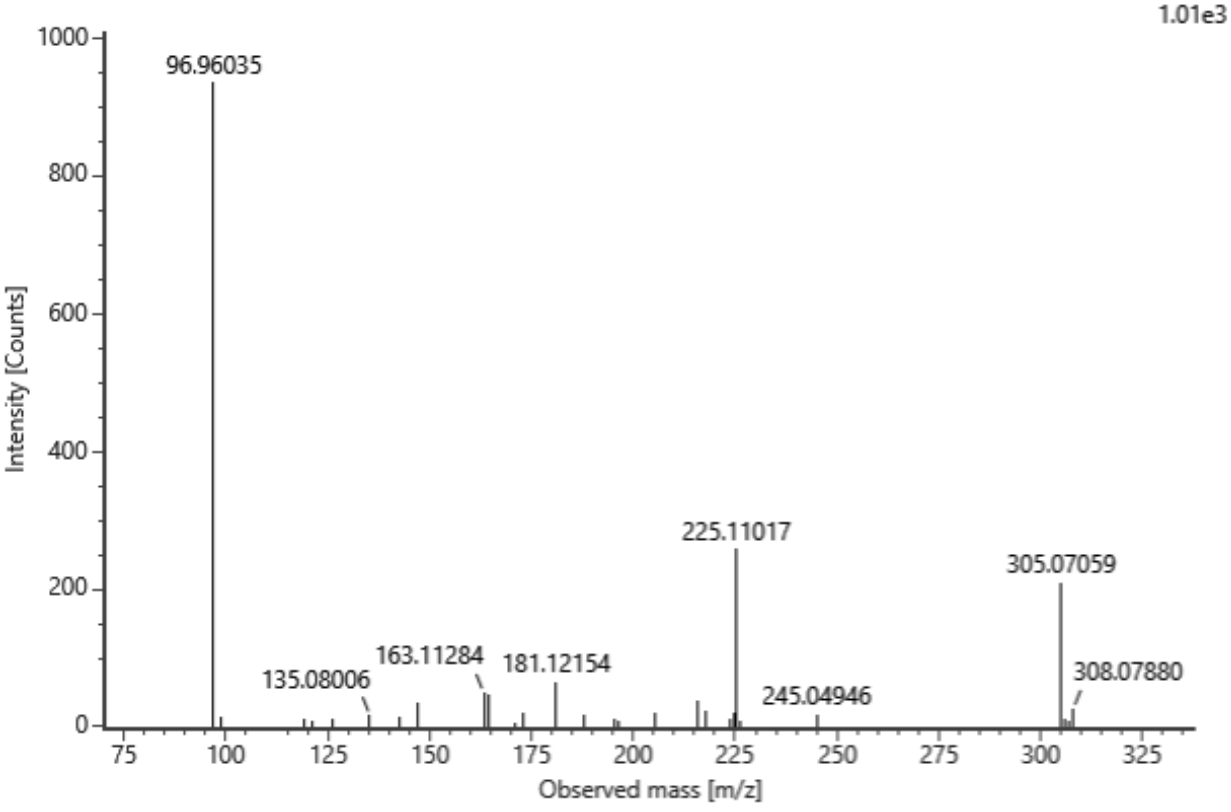

No. 20 Taraxinositol A/B C22H24O10 (neutral) Rt = 6.63 min

Channel name: 4: RT=6.6224 mins : Set Mass(m/z)=447.1292 : DT=5.13 ms : DDA HS TOF MSMS (90-2000)...
Collision energy (V): -11.9

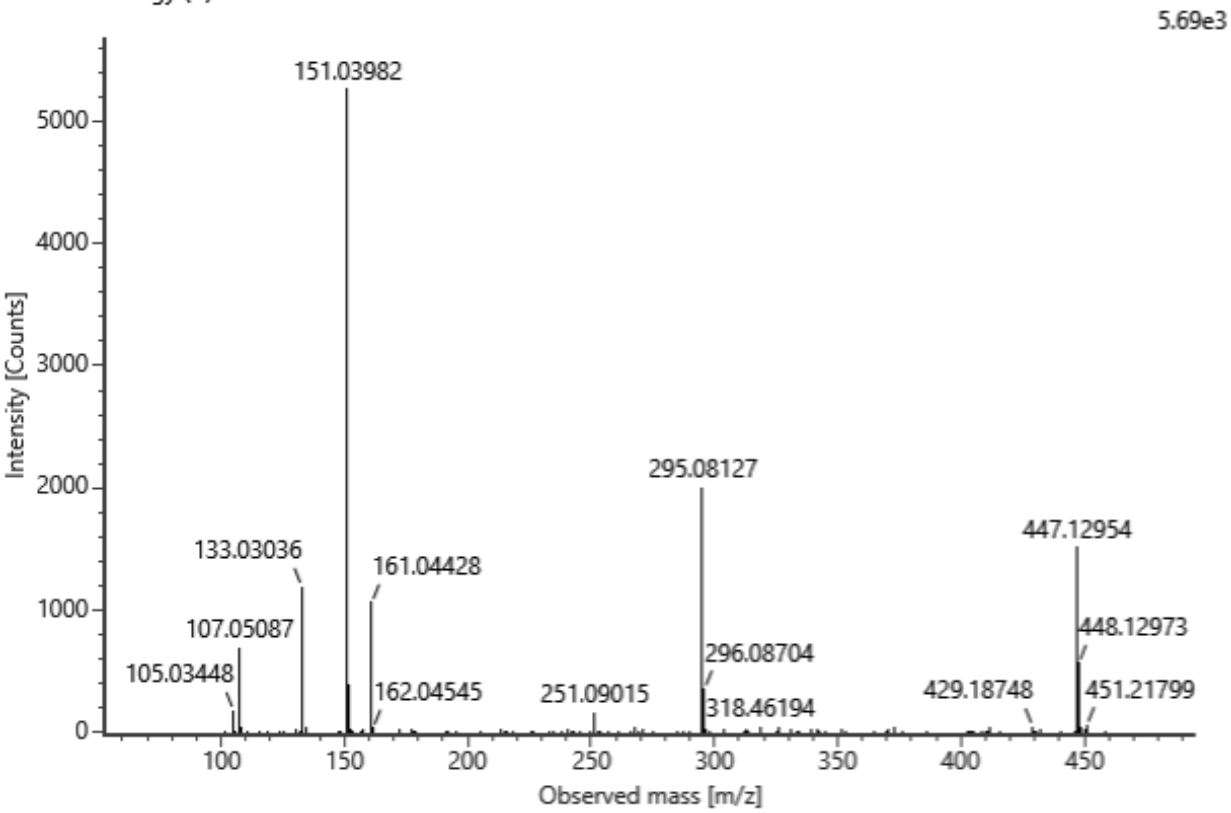

No. 21 Fraxin C16H18O10 (neutral) Rt = 6.69 min

Channel name: 4: RT=6.6868 mins : Set Mass(m/z)=369.0815 : DT=4.44 ms : DDA HS TOF MSMS (90-2000)...
Collision energy (V): -21.5

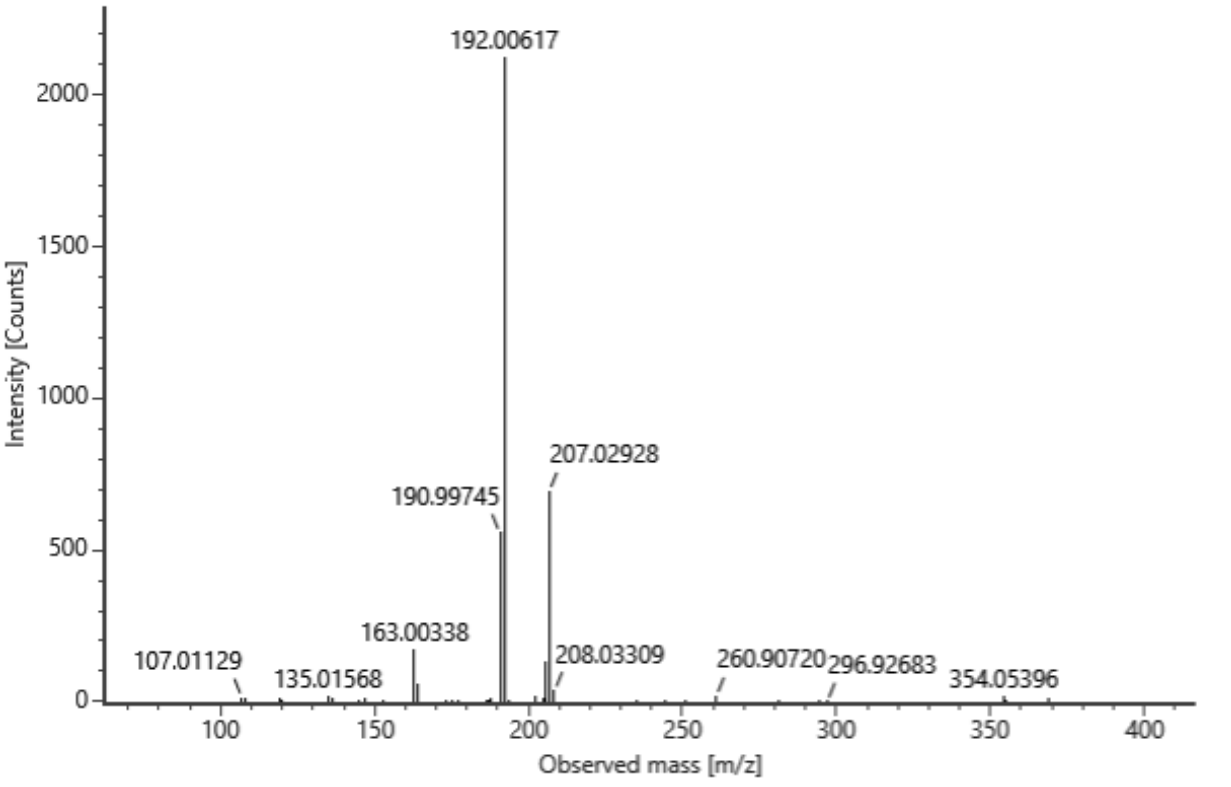

No. 22 12-Hydroxyjasmonate sulfate_2 C12H18O7S (neutral) Rt = 6.77 min

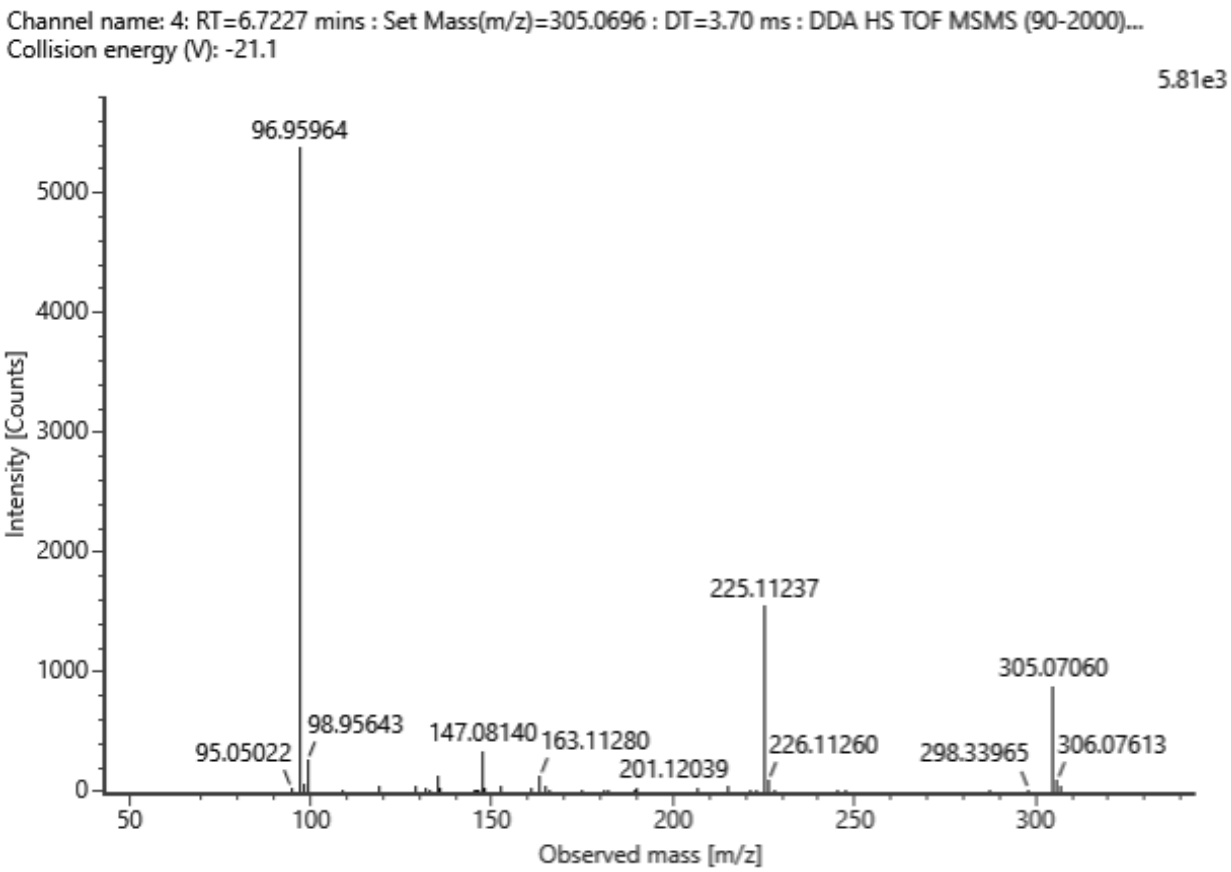

No. 23 Caffeoylglycerol C12H14O6 (neutral) Rt = 6.81 min

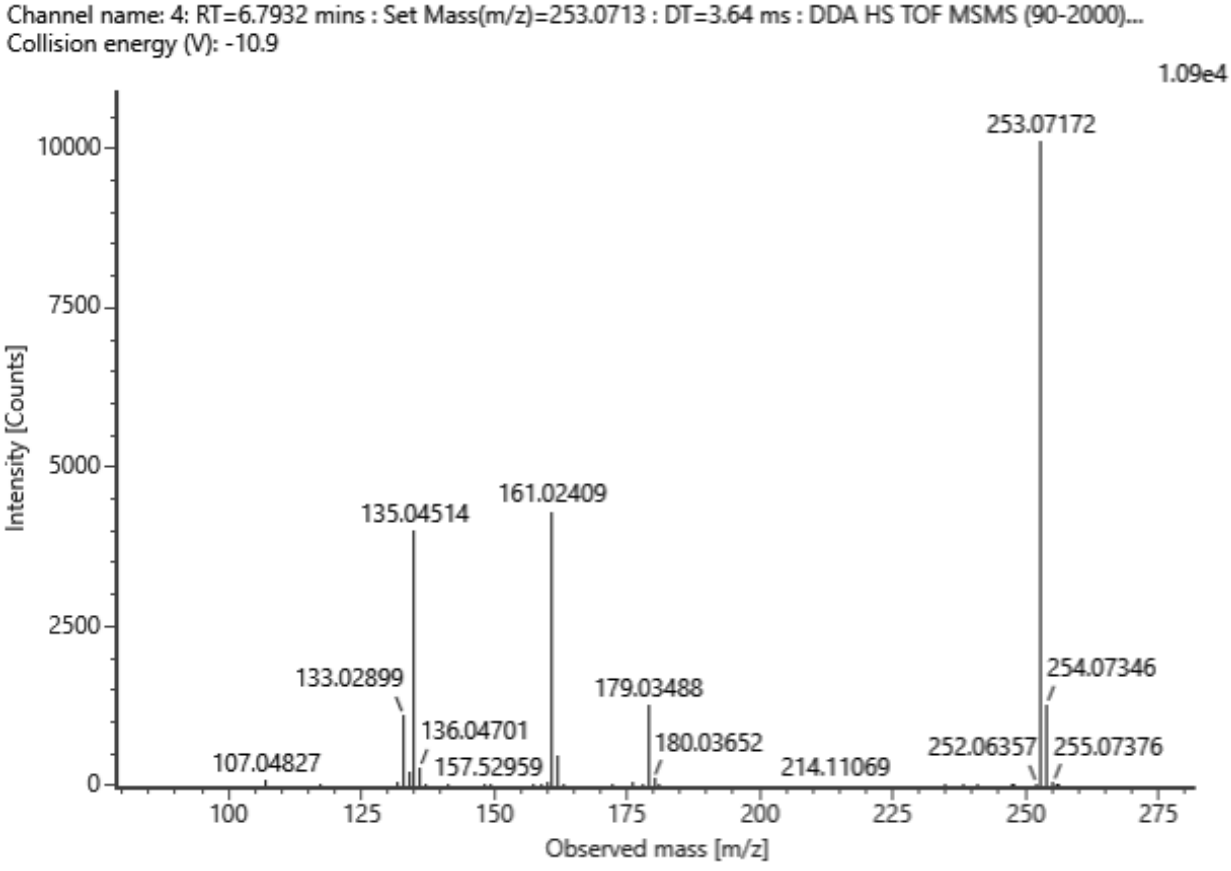

No. 24 Quercetin dihexoside_1 C27H30O17 (neutral) Rt = 6.87 min

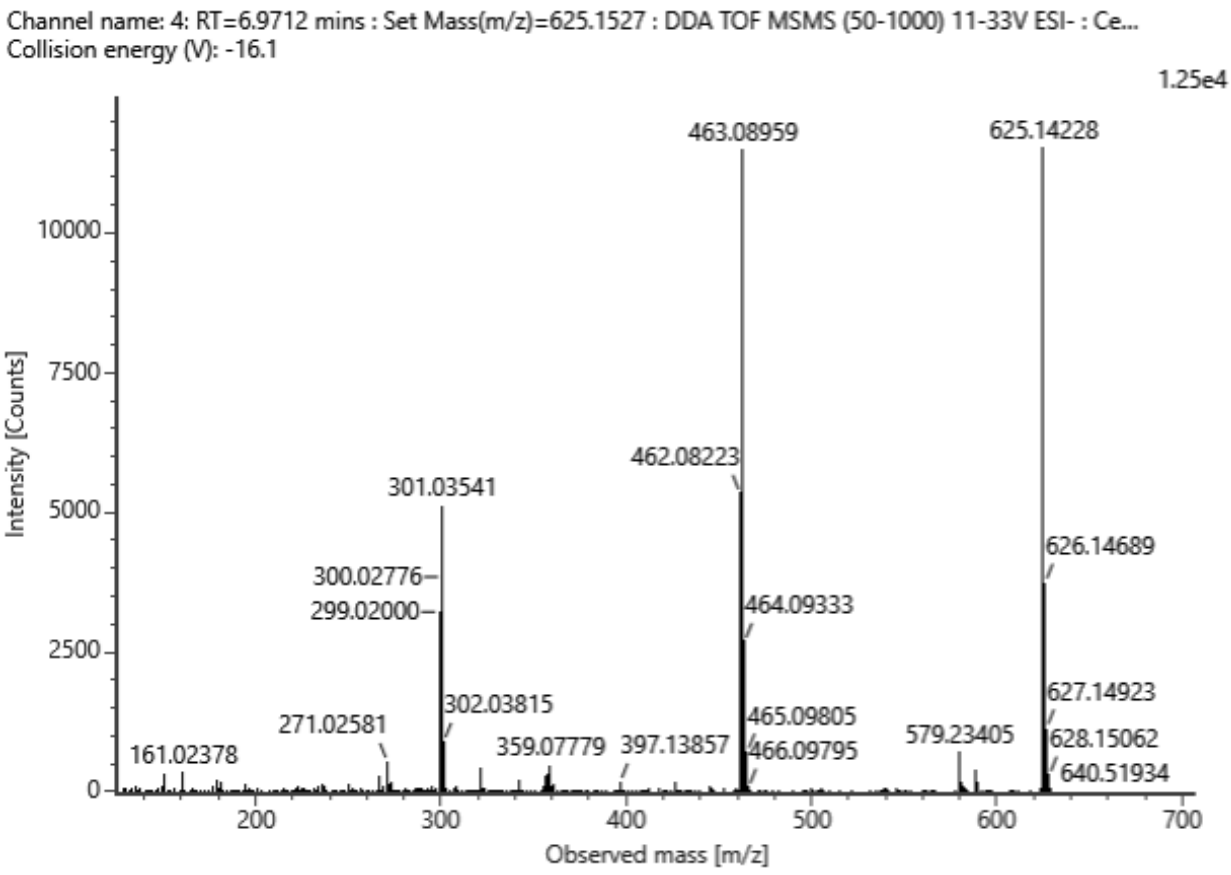

No. 25 Pyroglutamylisoleucine C11H18N2O4 (neutral) Rt = 7.67 min

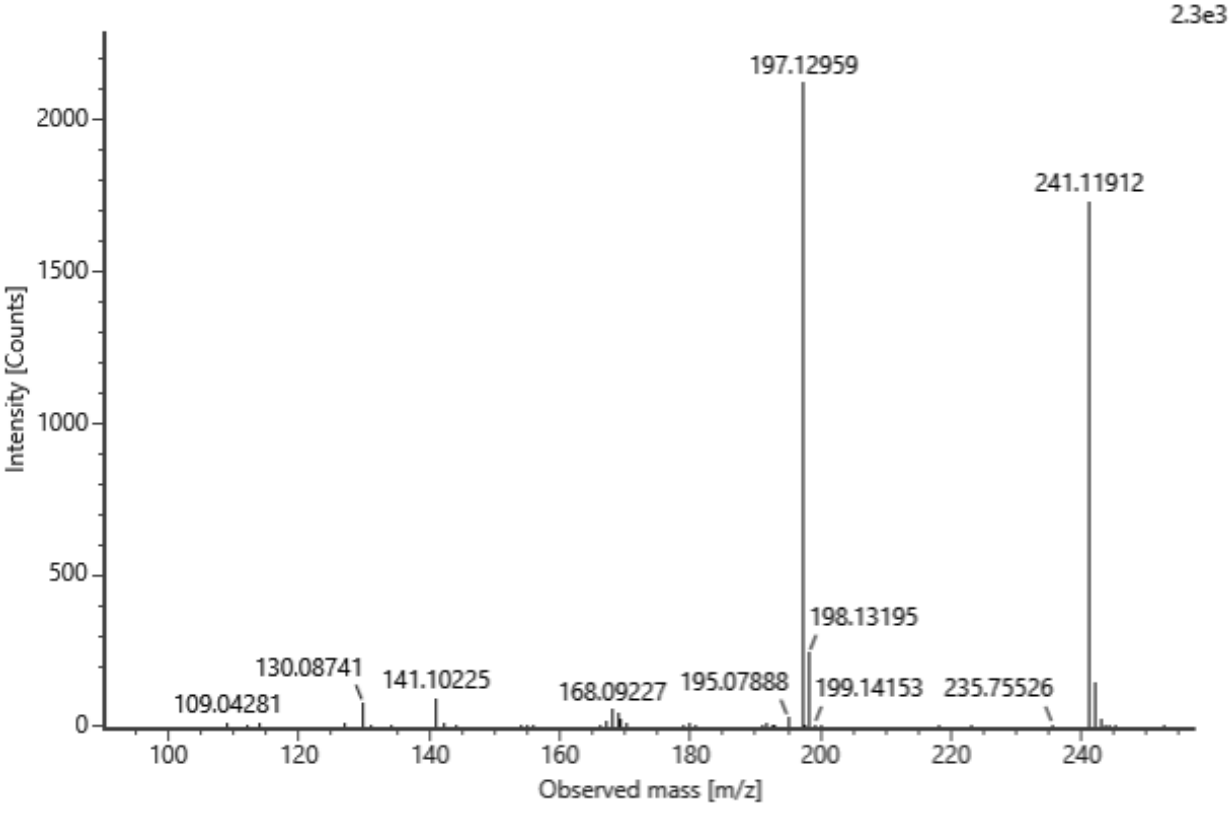

No. 26 Quercetin derivative_1 C26H28O16 (neutral) Rt = 7.70 min

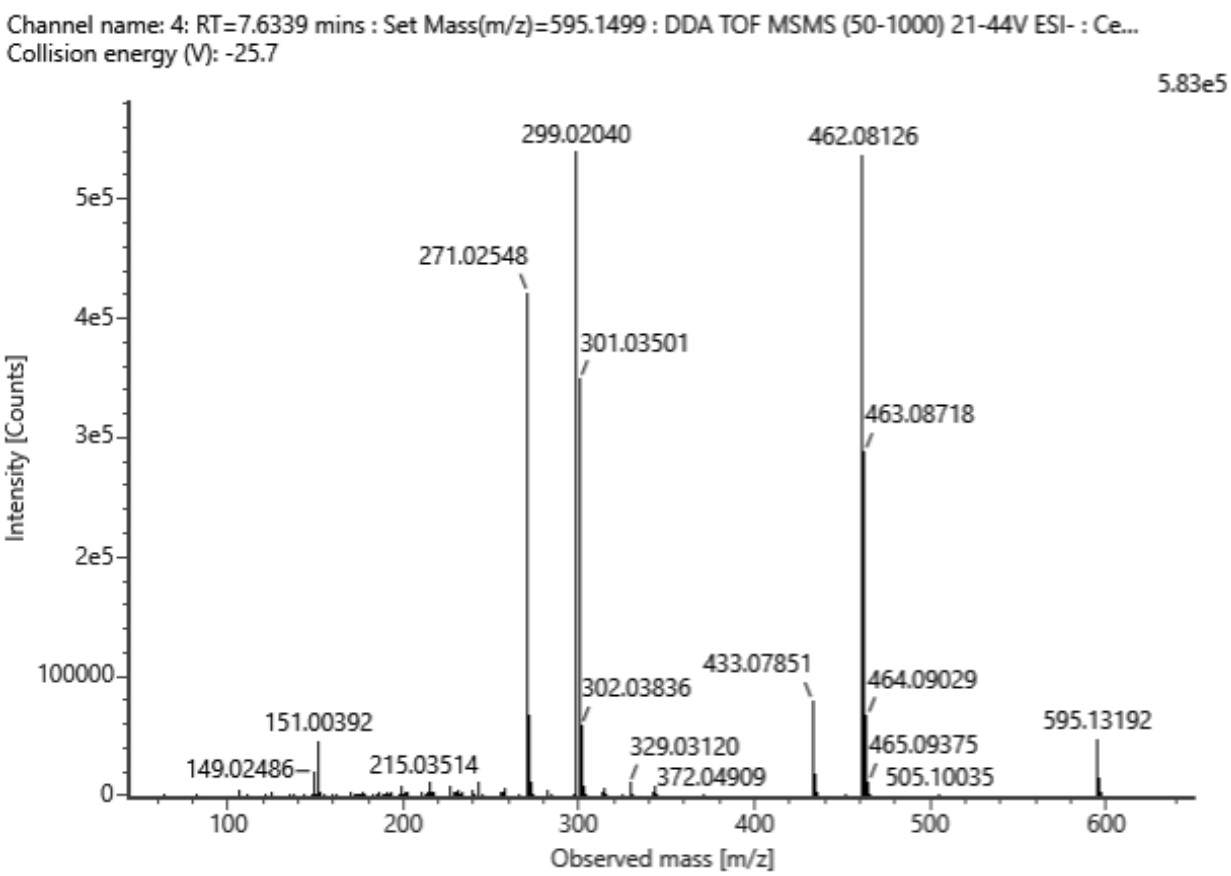

No. 27 Chicoric acid derivative C28H28O17 (neutral) Rt = 7.88 min

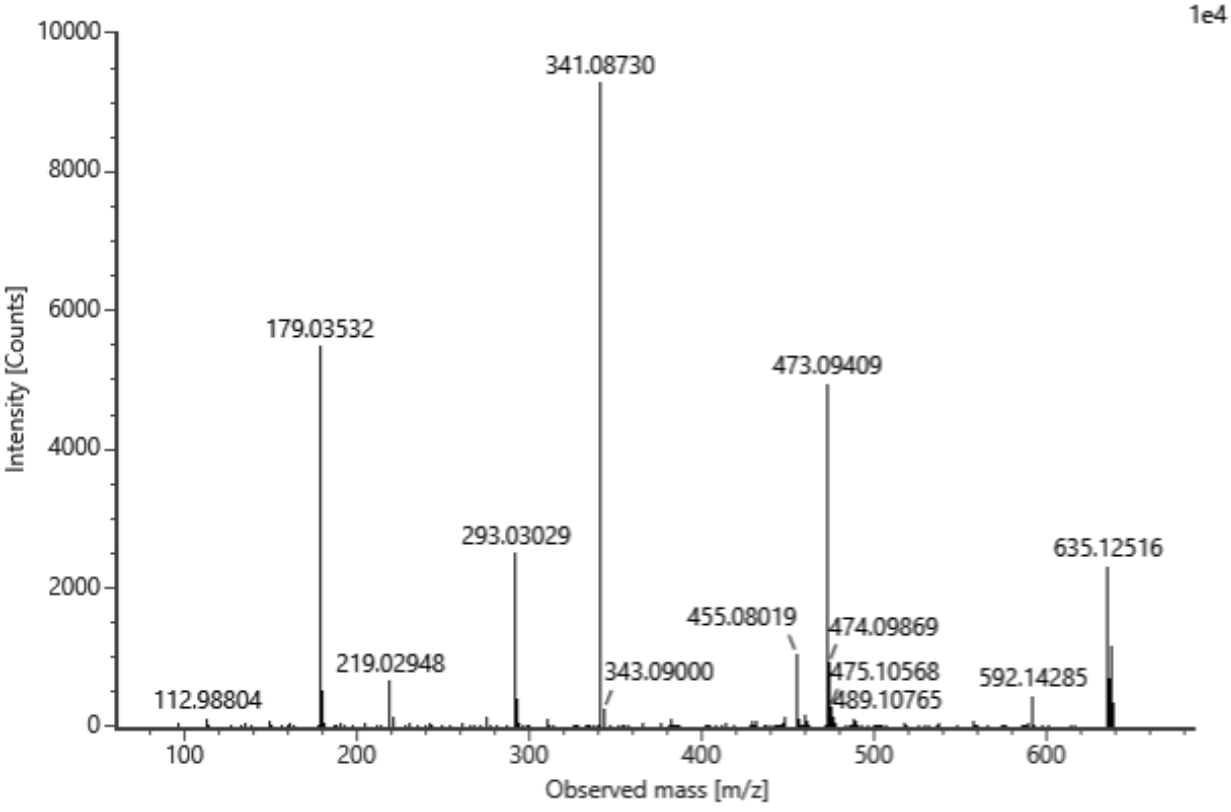

No. 28 Quercetin dihexoside_2 C27H30O17 (neutral) Rt = 7.89 min

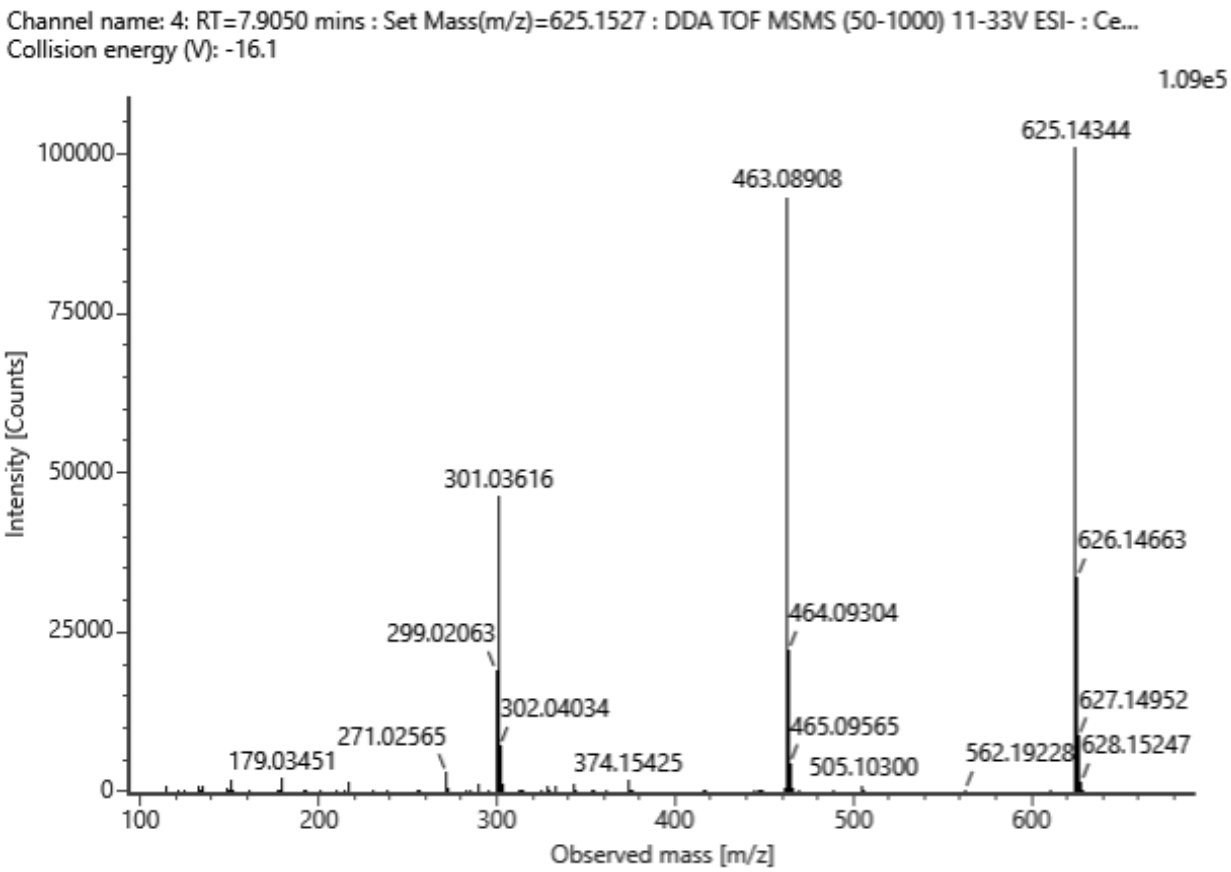

No. 29 Unknown_1 C21H32O11 (neutral) Rt = 7.94 min

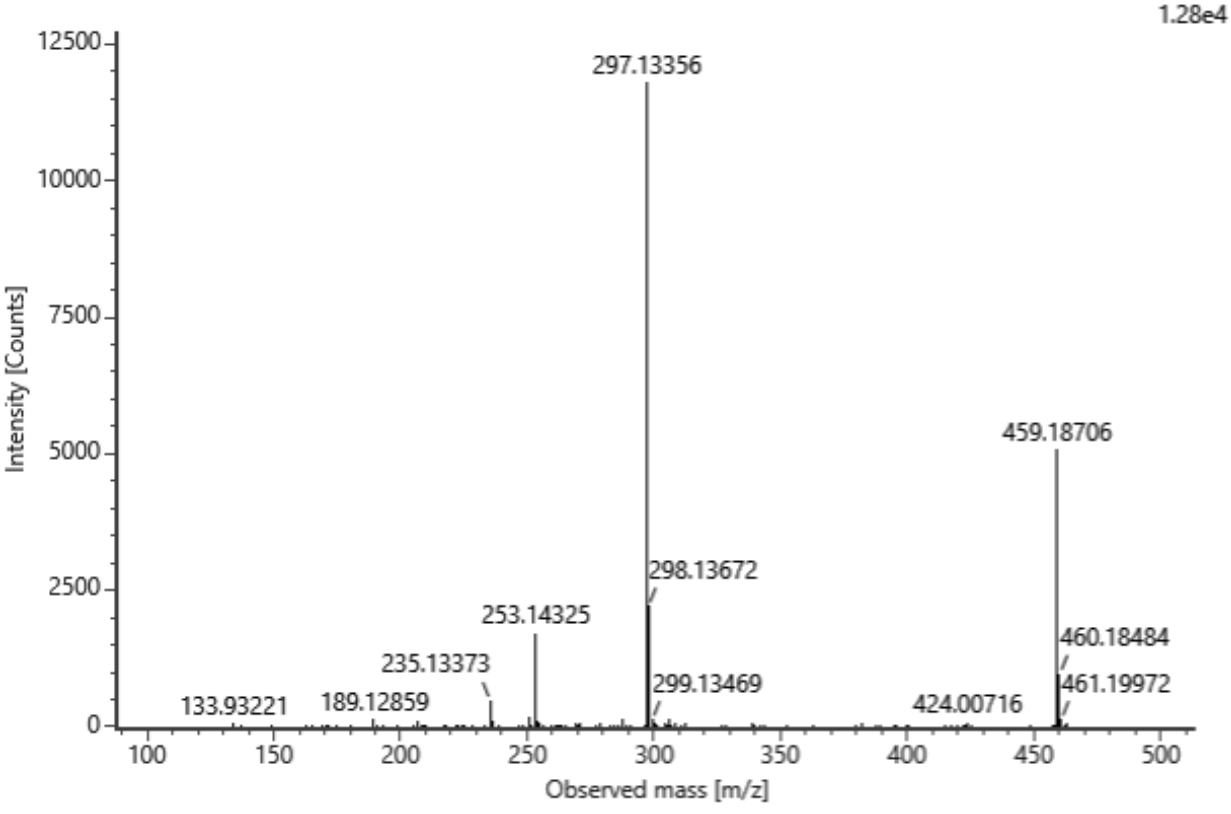

No. 30 Unknown_2 C24H32O5S (neutral) Rt = 8.30 min

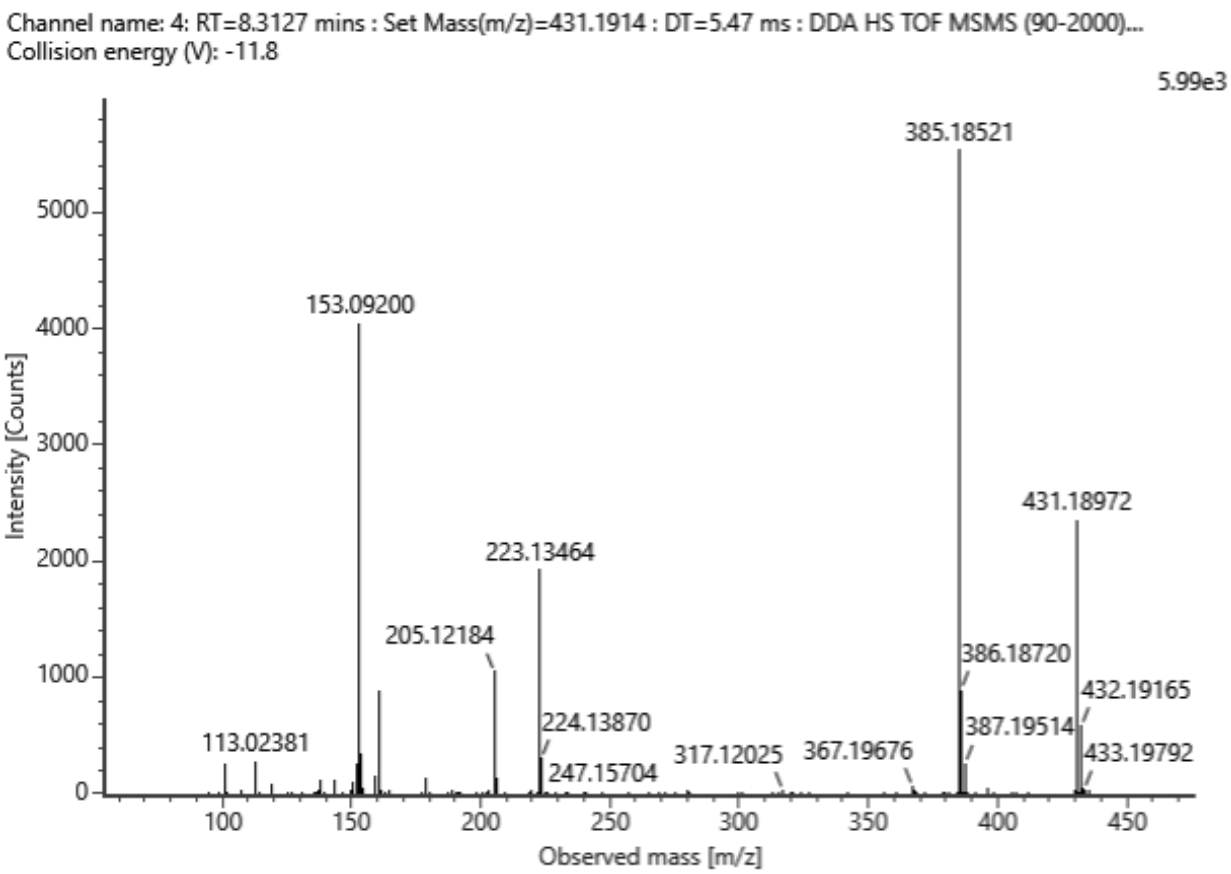

No. 31 Umbelliferone C9H6O3 (neutral) Rt = 8.59 min

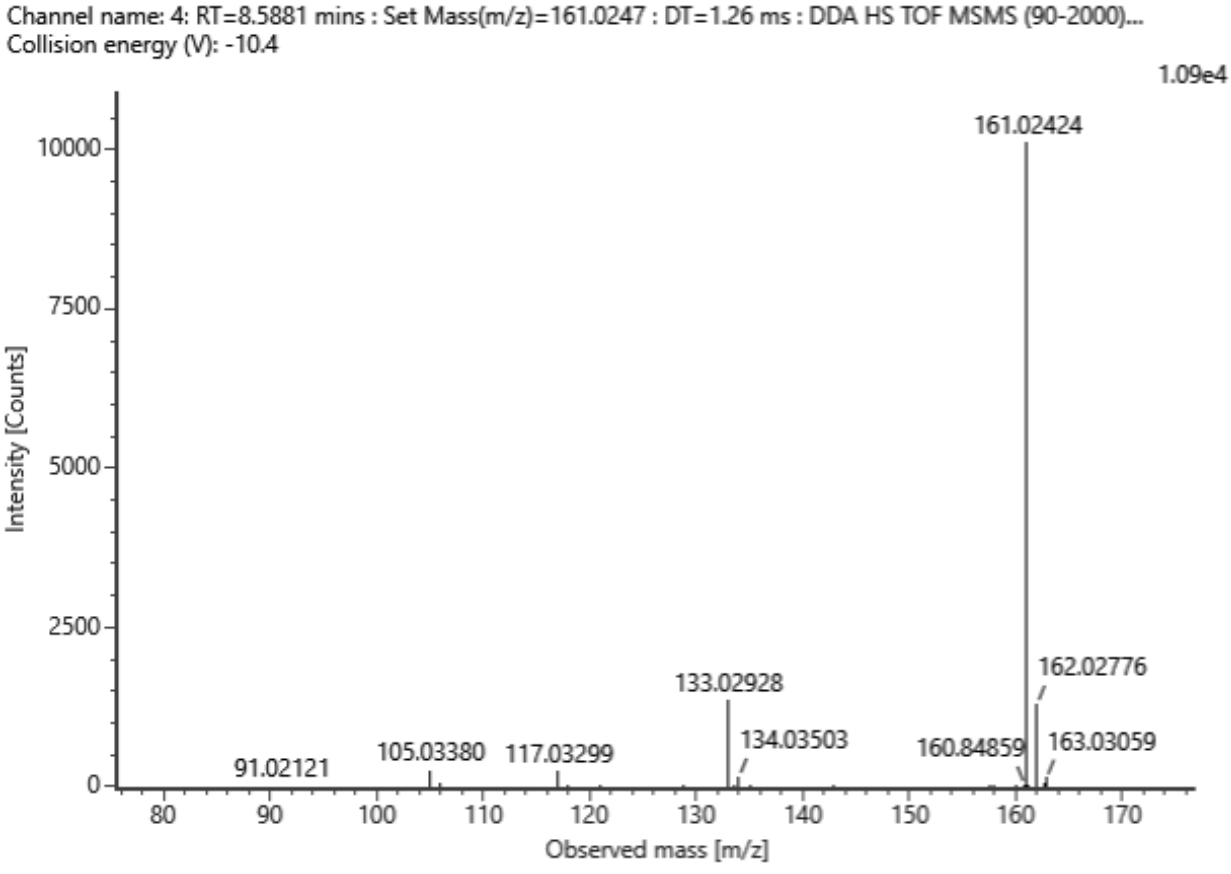

No. 32 Quercetin dihexoside_3 C27H30O17 (neutral) Rt = 9.12 min

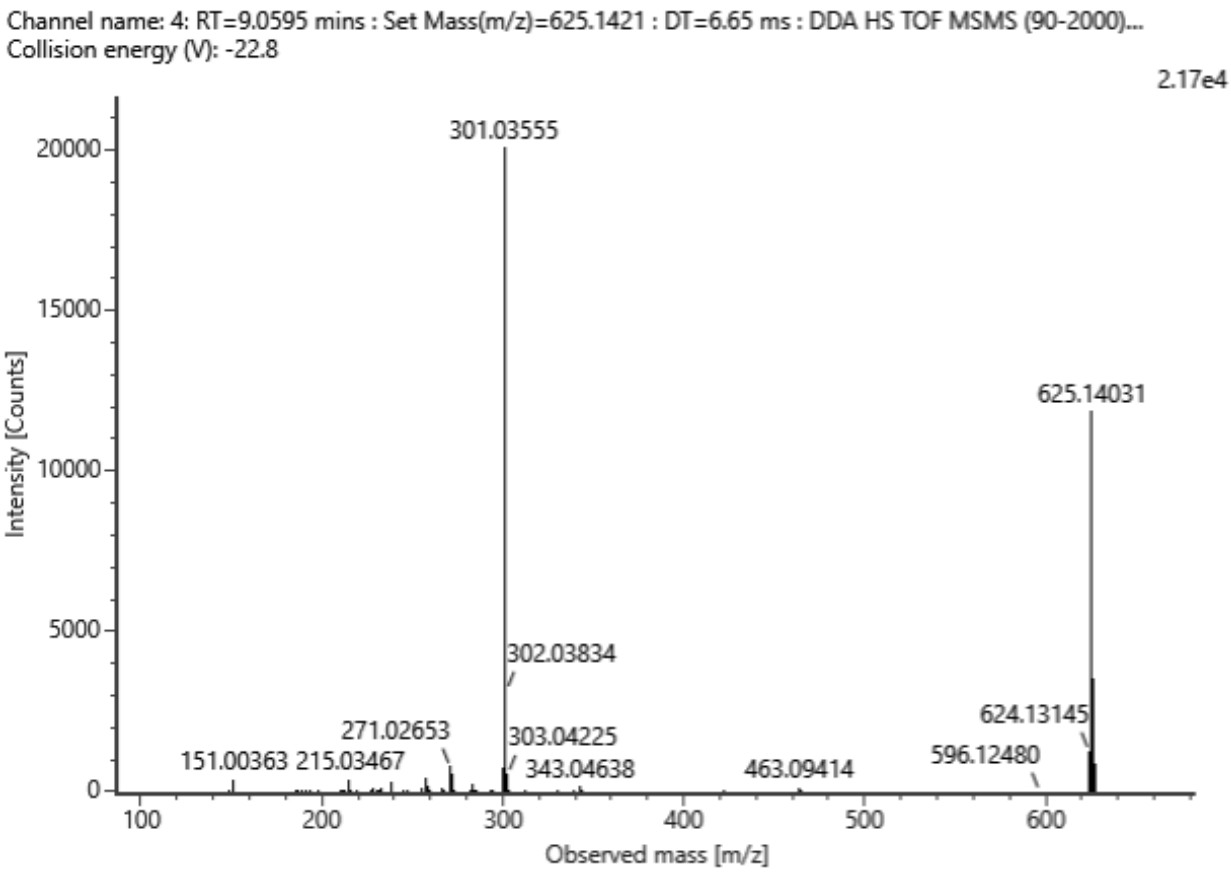

No. 33 Quercetin derivative_2 C26H28O16 (neutral) Rt = 9.36 min

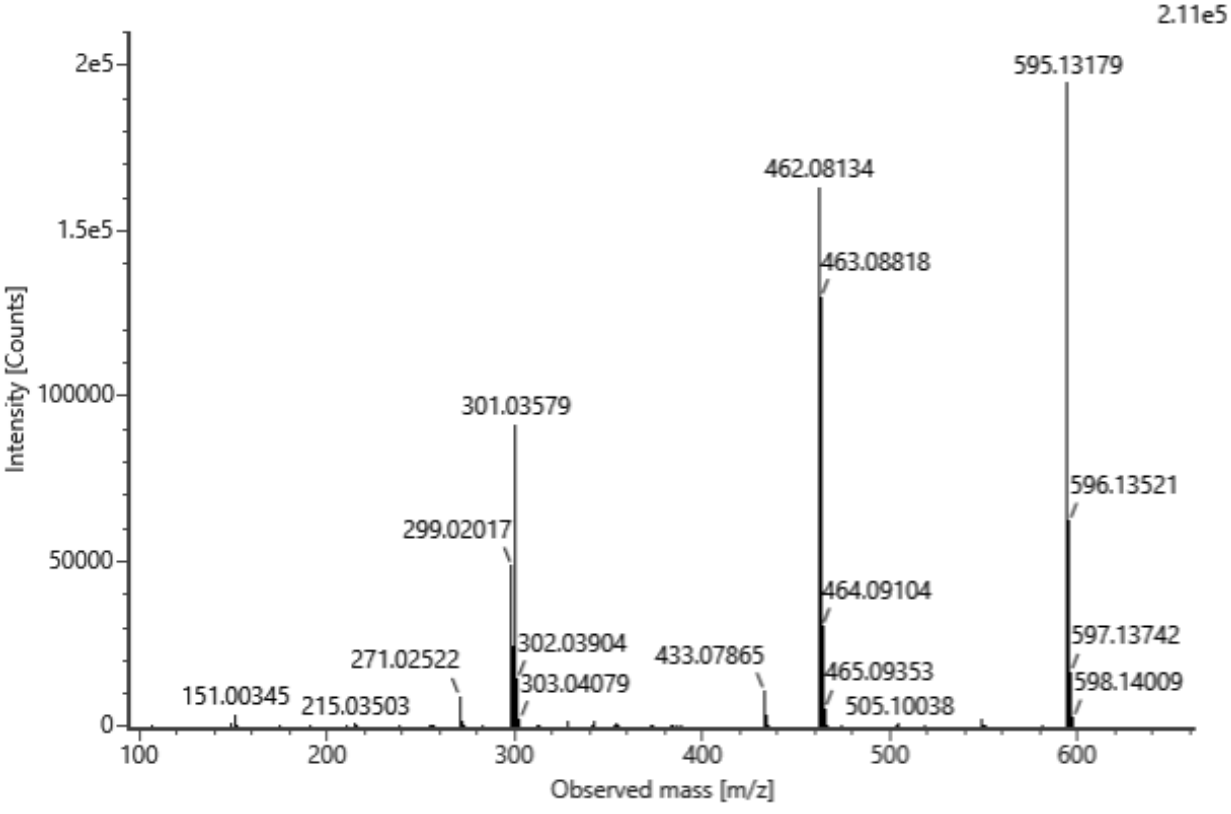

No. 35 Quercetin 3,4'-diglucoside C27H30O17 (neutral) Rt = 10.27 min

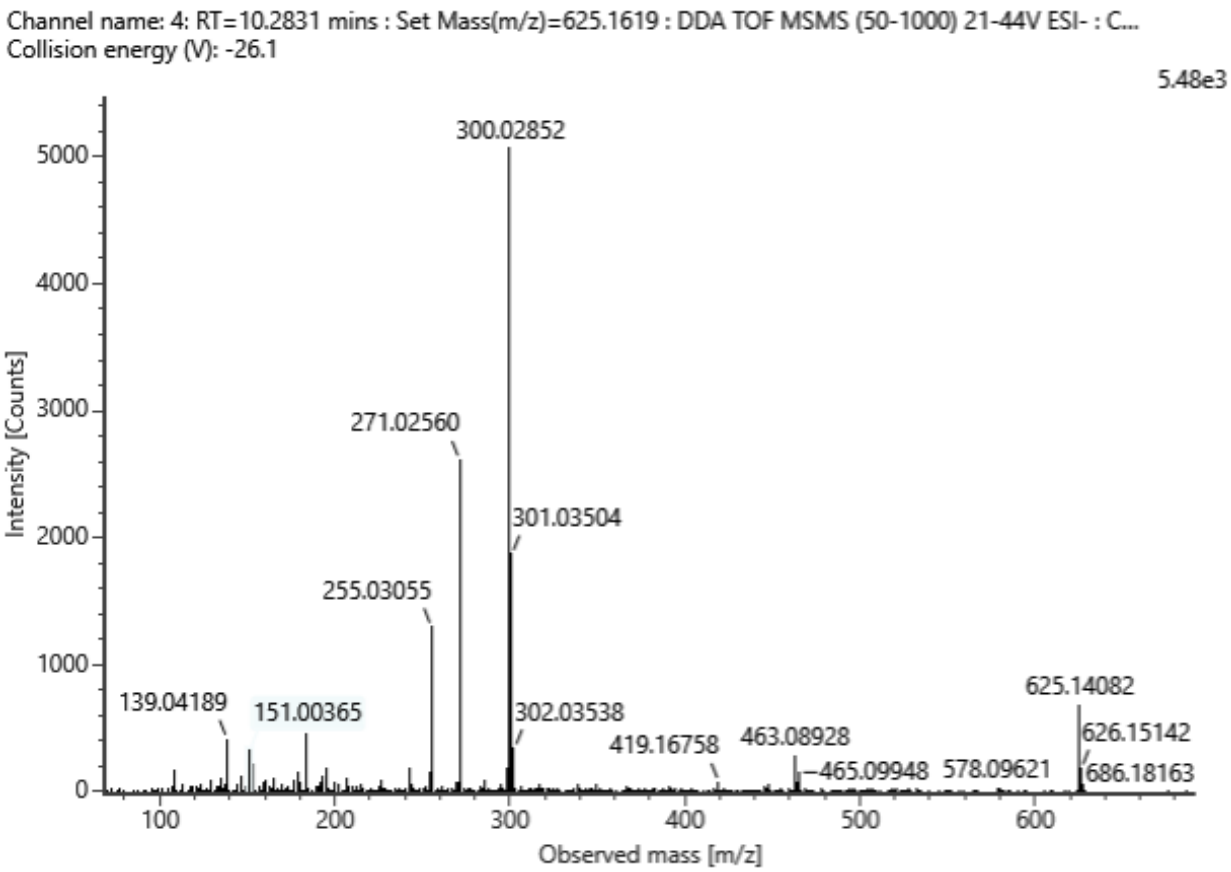

No. 36 Schaftoside isomer_1 C26H28O14 (neutral) Rt = 10.39 min

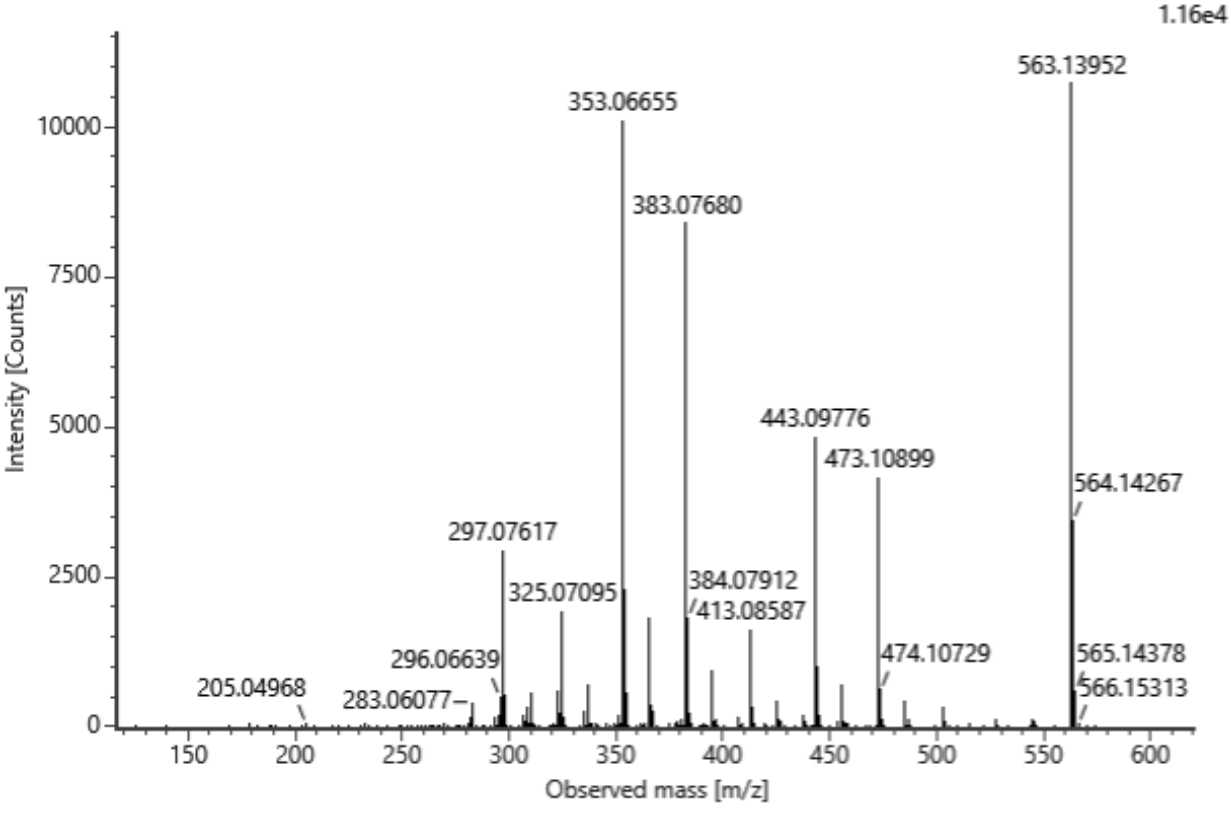

No. 37 Quercetin hexosyl derivative C27H30O15 (neutral) Rt = 10.43 min

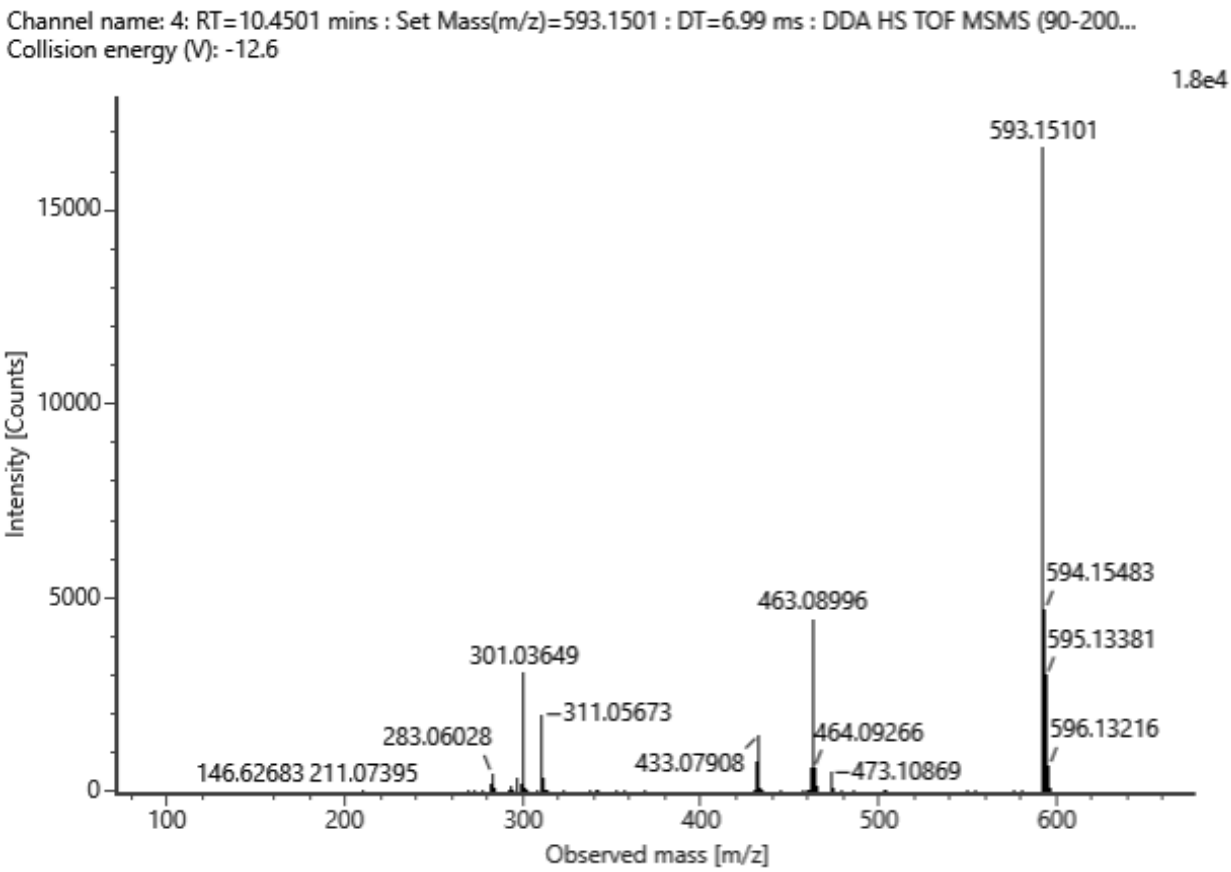

No. 38 Luteolin/kaempferol dihexoside_1 C27H30O16 (neutral) Rt = 10.45 min

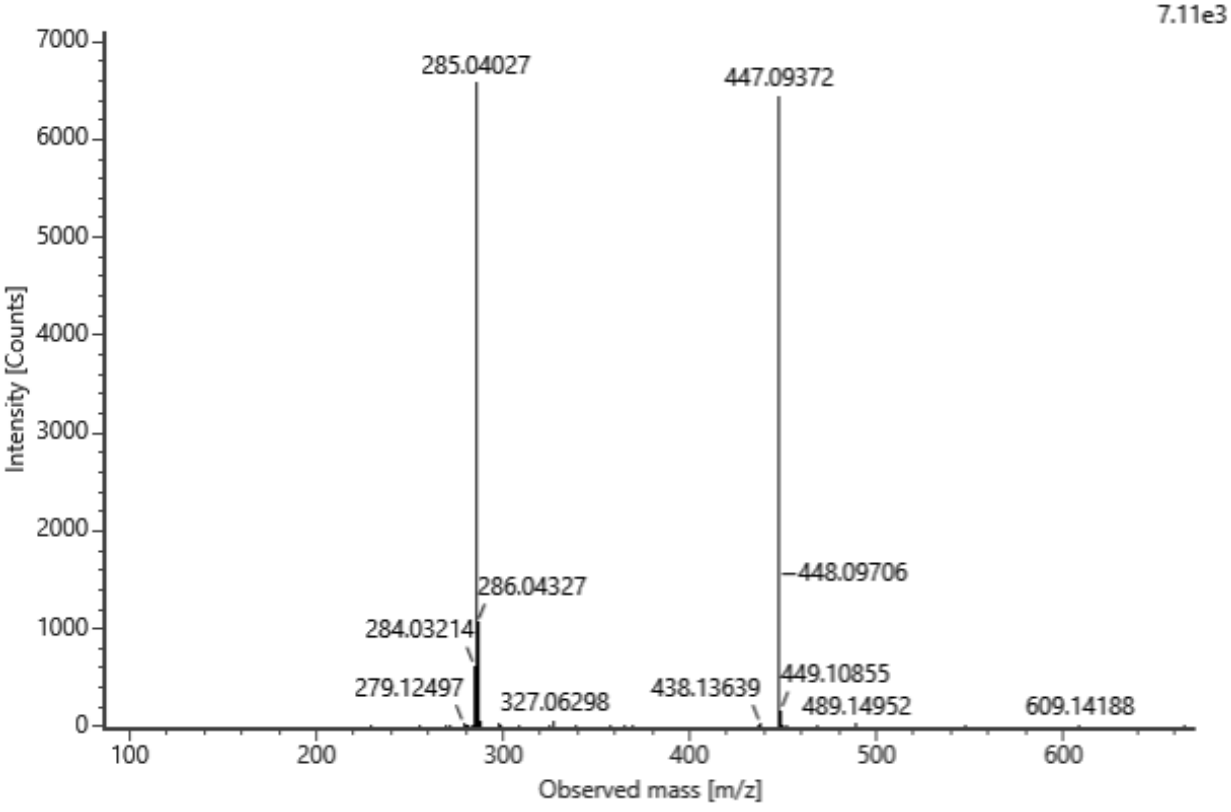

No. 39 Quercetin derivative_3 C26H28O16 (neutral) Rt = 10.53 min

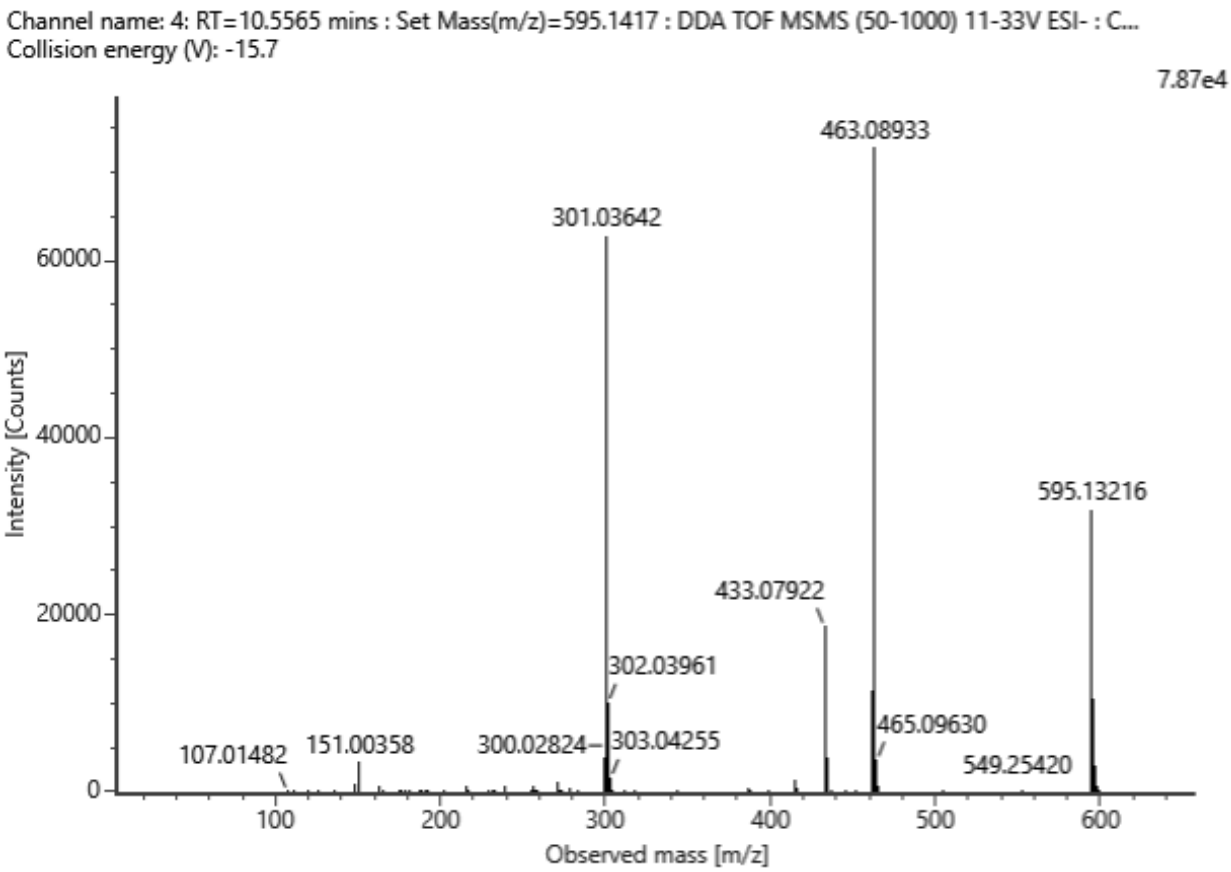

No. 40 Taraxinositol A/B C22H24O10 (neutral) Rt = 10.68 min

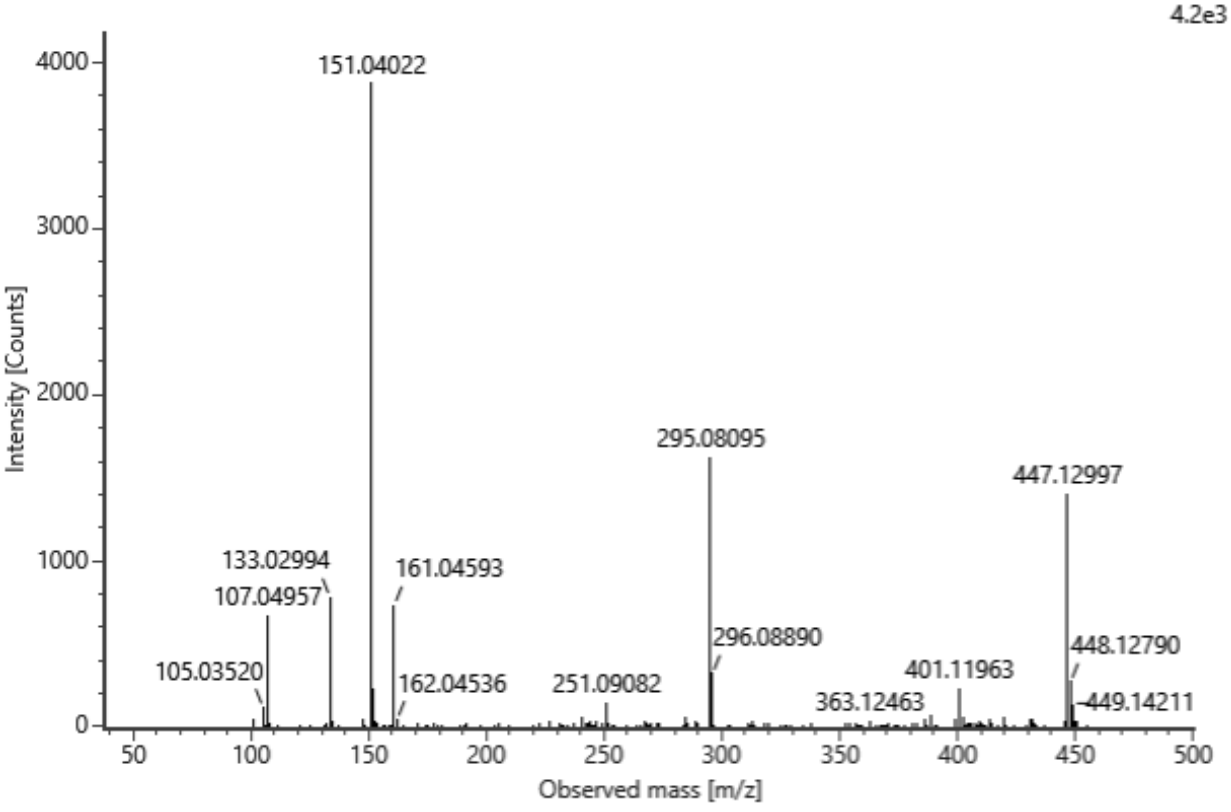

No. 41 Quercetin rutinoside C27H30O16 (neutral) Rt = 11.06 min

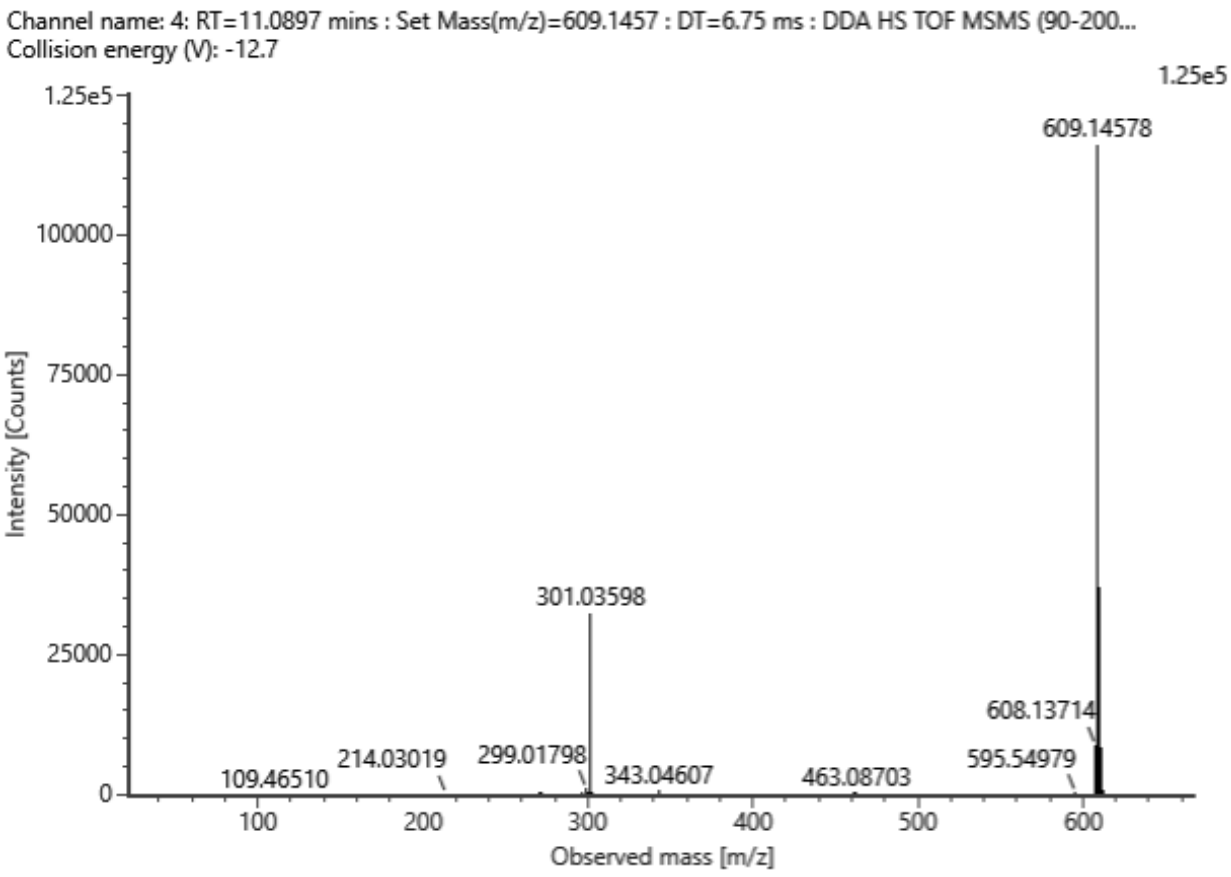

No. 42 Chicoric acid C22H18O12 (neutral) Rt = 11.08 min

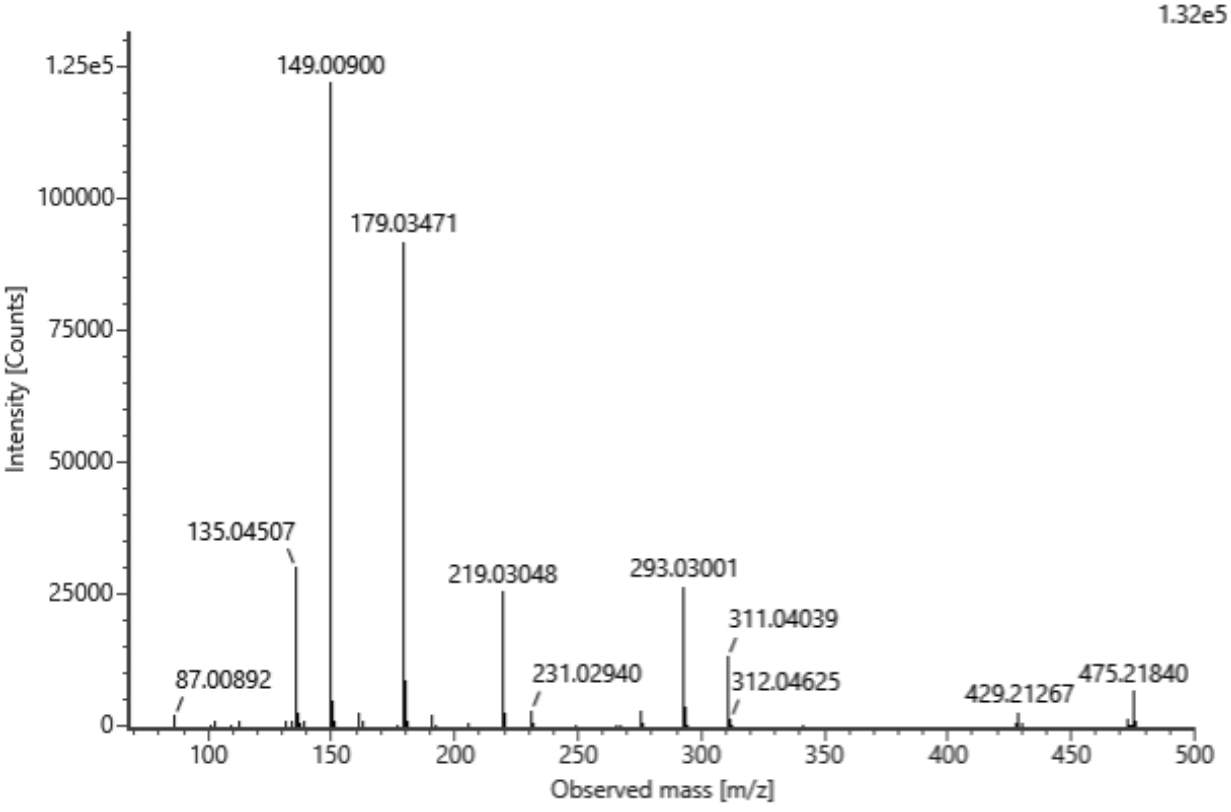

No. 43 Schaftoside isomer_2 C26H28O14 (neutral) Rt = 11.40 min

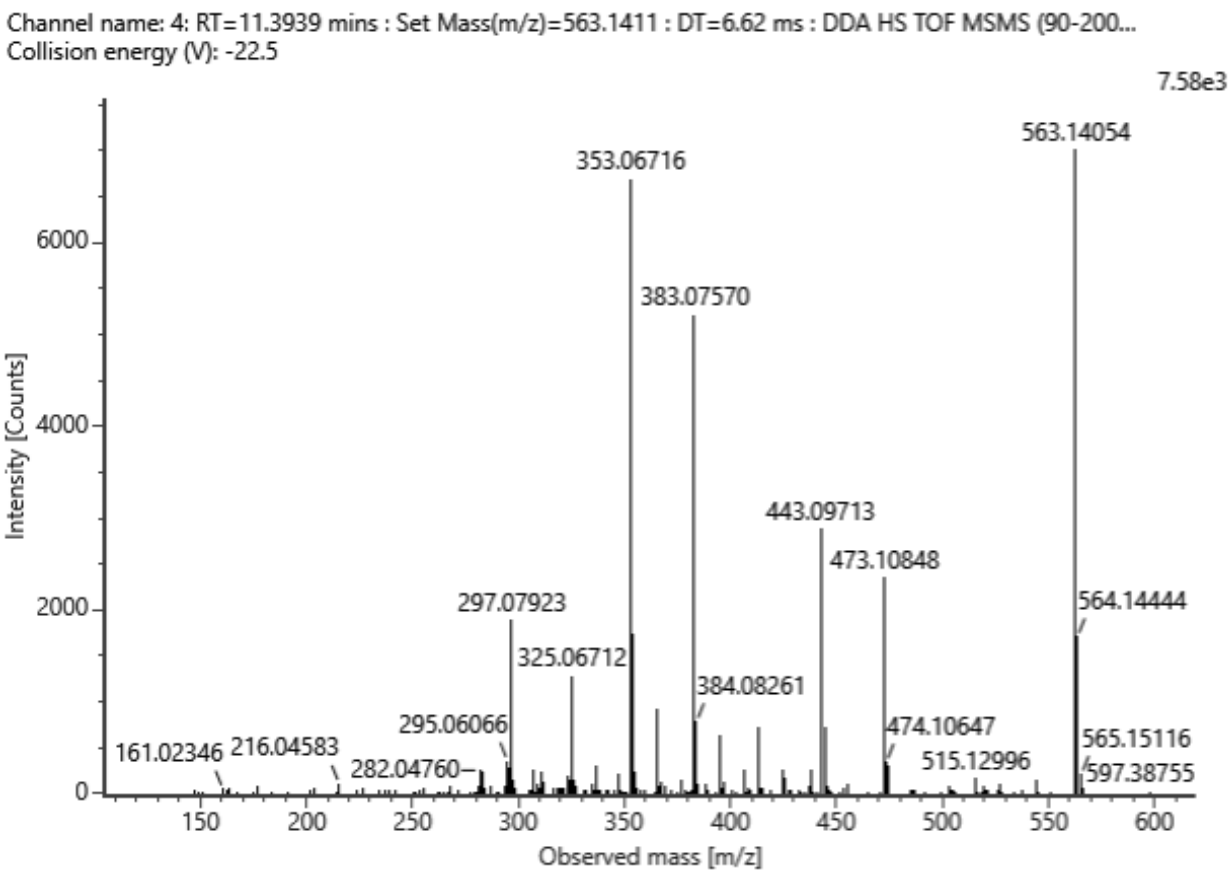

No. 44 Luteolin/kaempferol dihexoside_2 C27H30O16 (neutral) Rt = 11.89 min

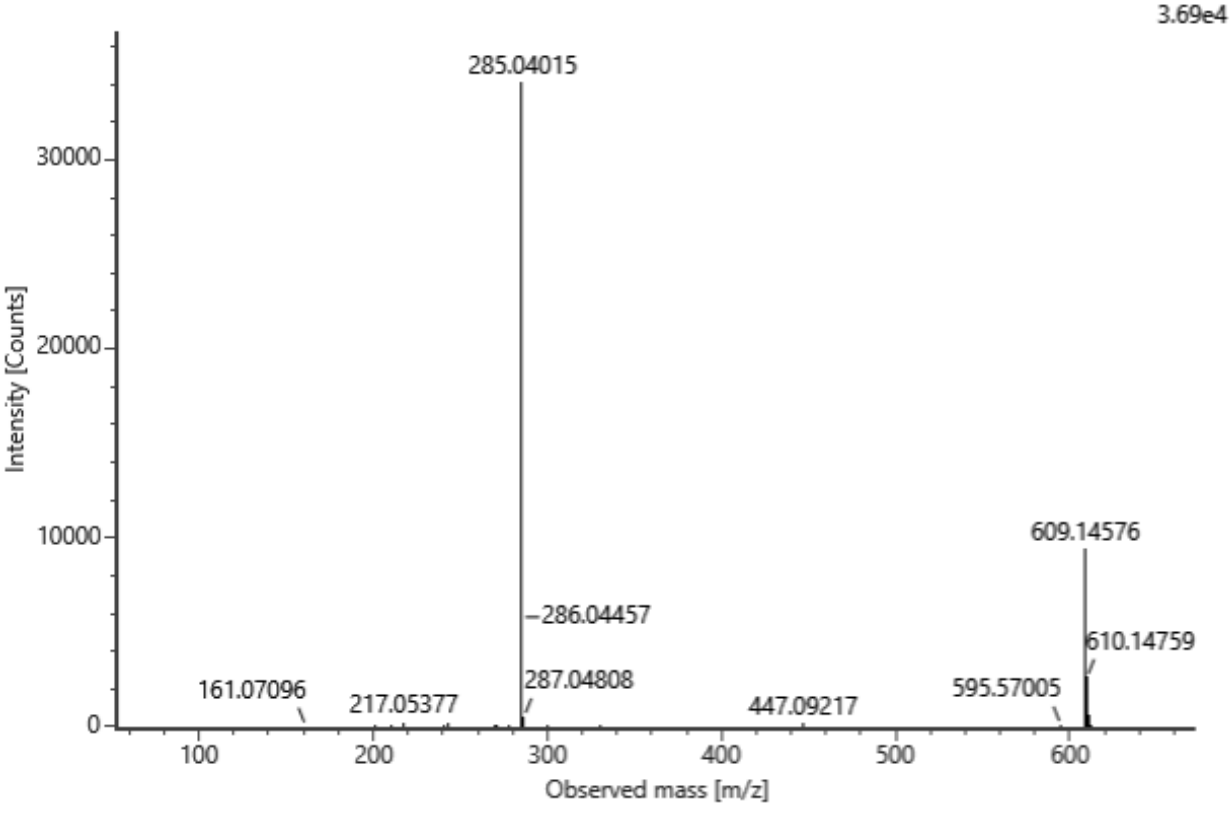

No. 45 Luteolin/kaempferol dihexoside_3 C27H30O16 (neutral) Rt = 12.61 min

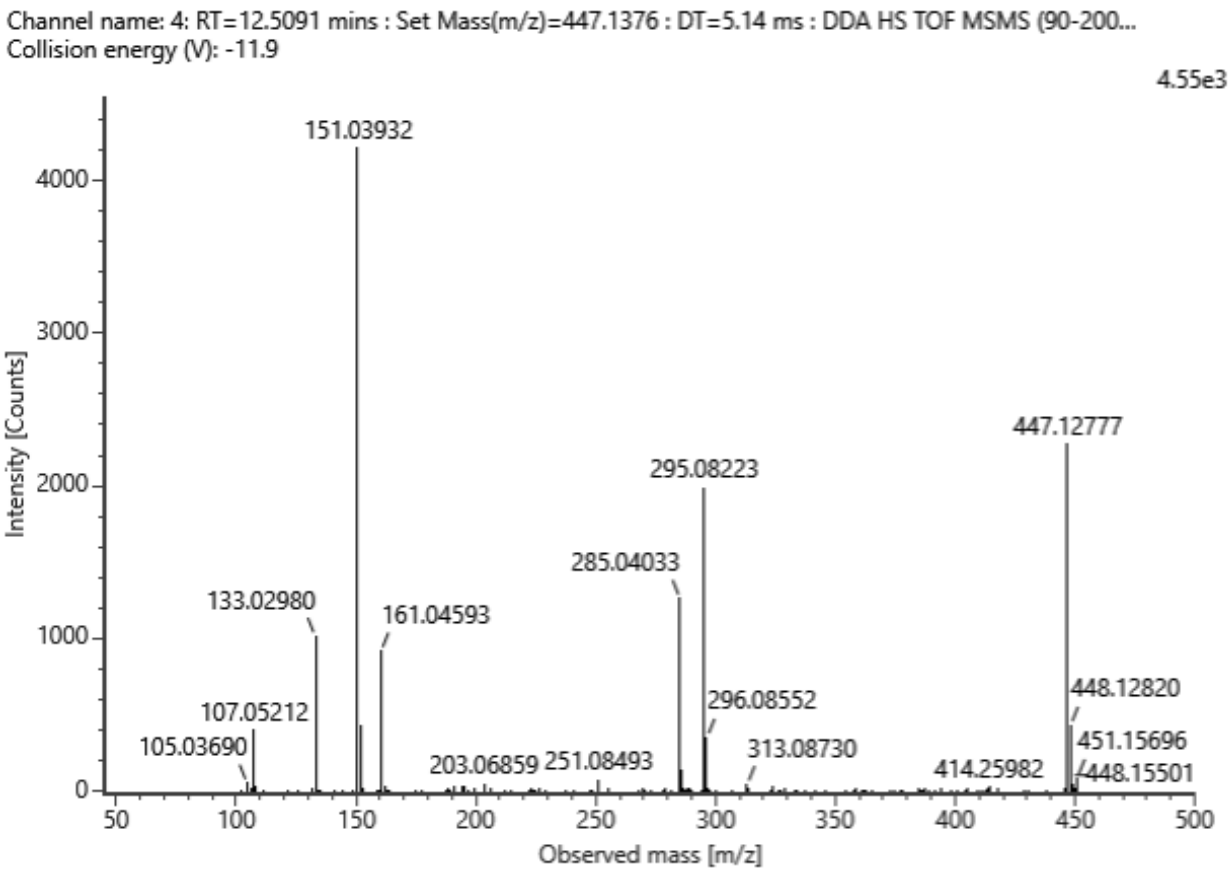

No. 46 Robinin C33H40O19 (neutral) Rt = 12.68 min

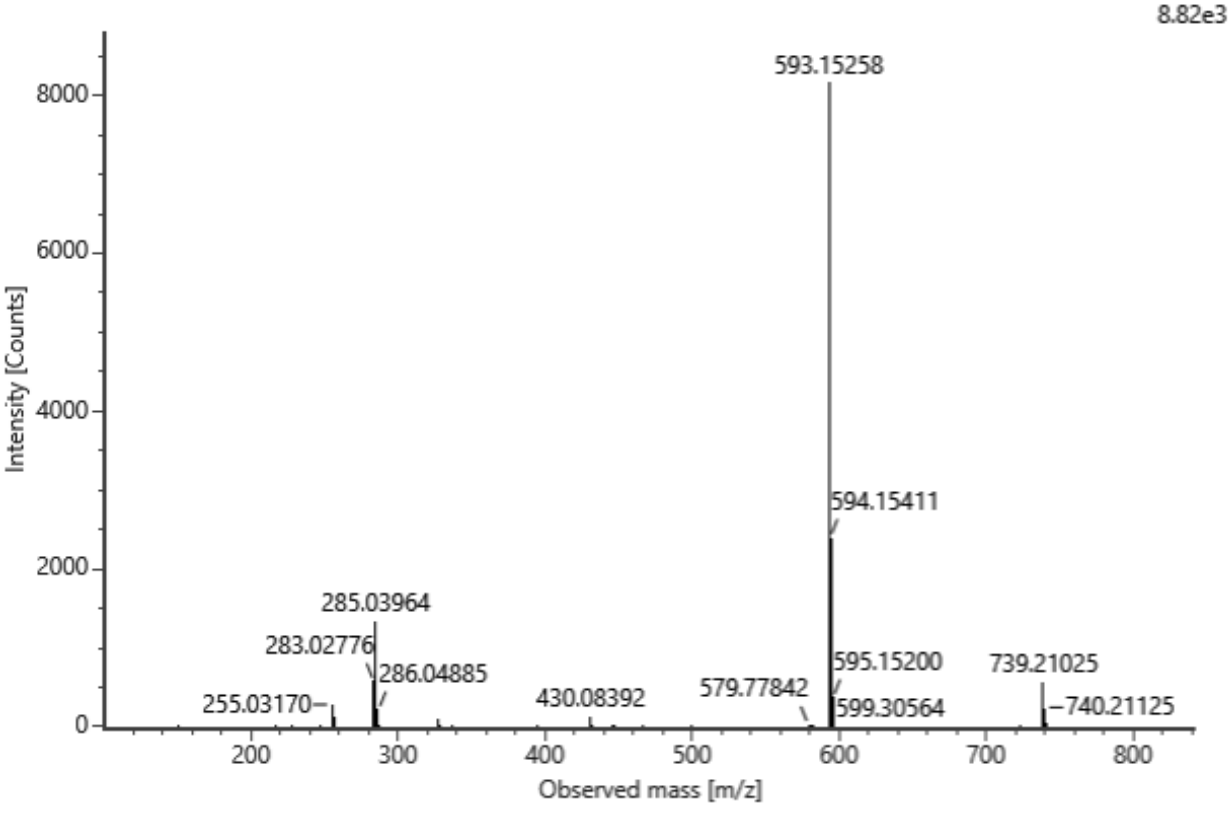

No. 47 Quercetin pentoside_1 C20H18O11 (neutral) Rt = 12.75 min

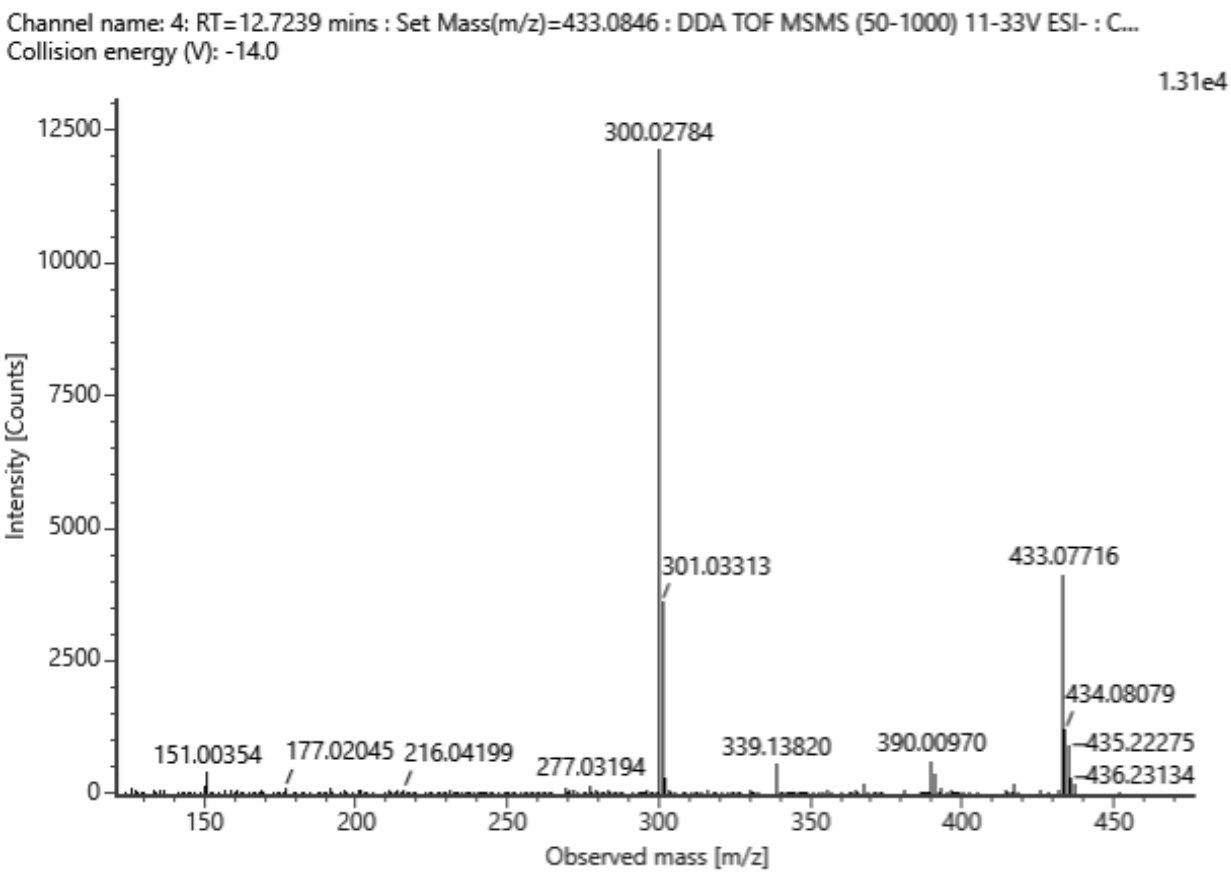

No. 48 Rutin C27H30O16 (neutral) Rt = 13.20 min

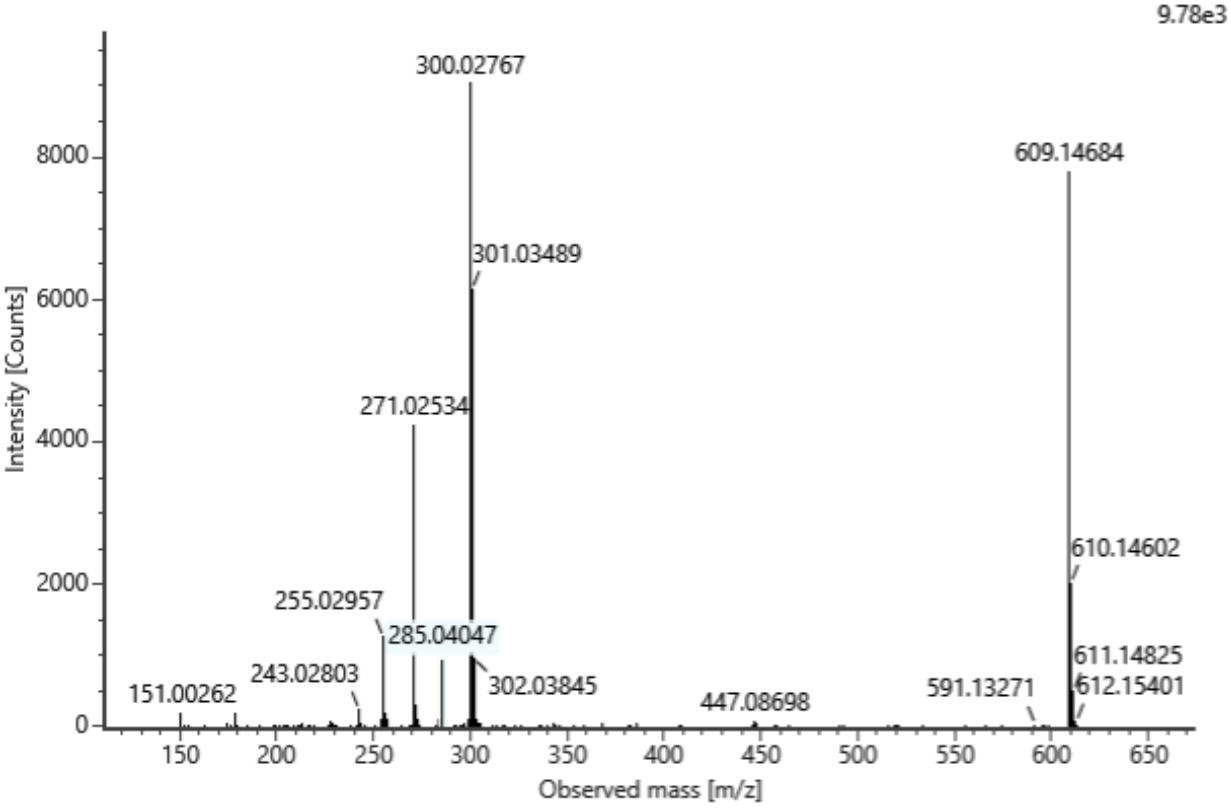

No. 49 Quercetin glucoside C21H20O12 (neutral) Rt = 13.40 min

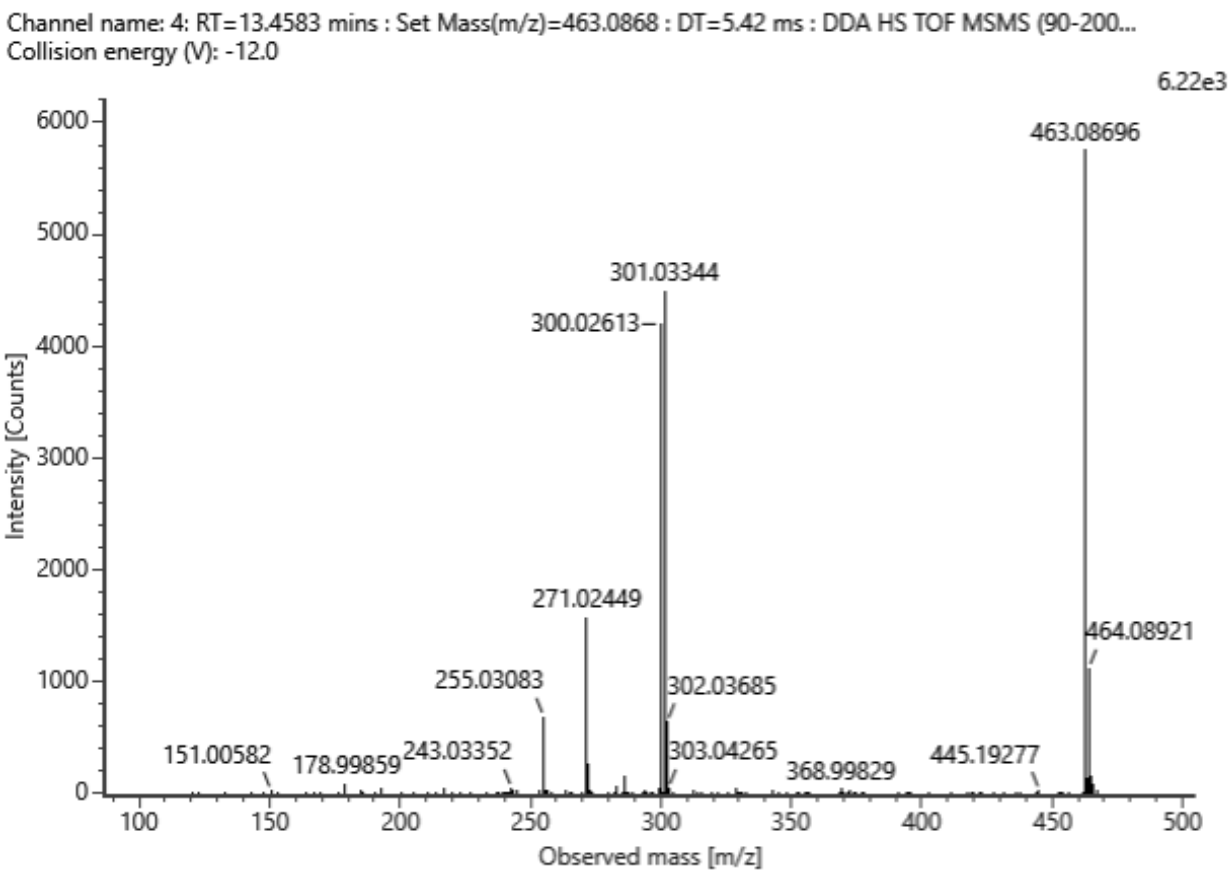

No. 50 Isorhamnetin disaccharide_1 C27H30O16 (neutral) Rt = 13.54 min

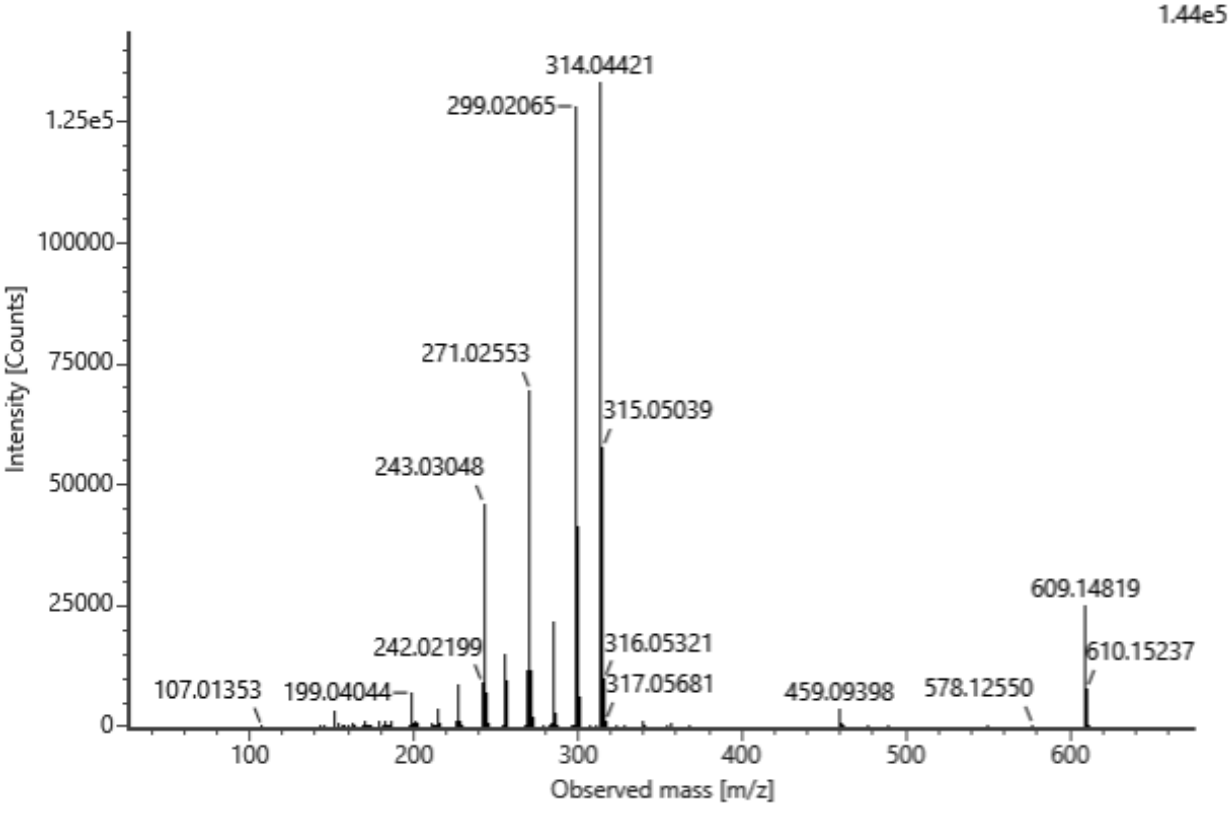

No. 51 Luteolin 7-O-glucoside C21H20O11 (neutral) Rt = 14.09 min

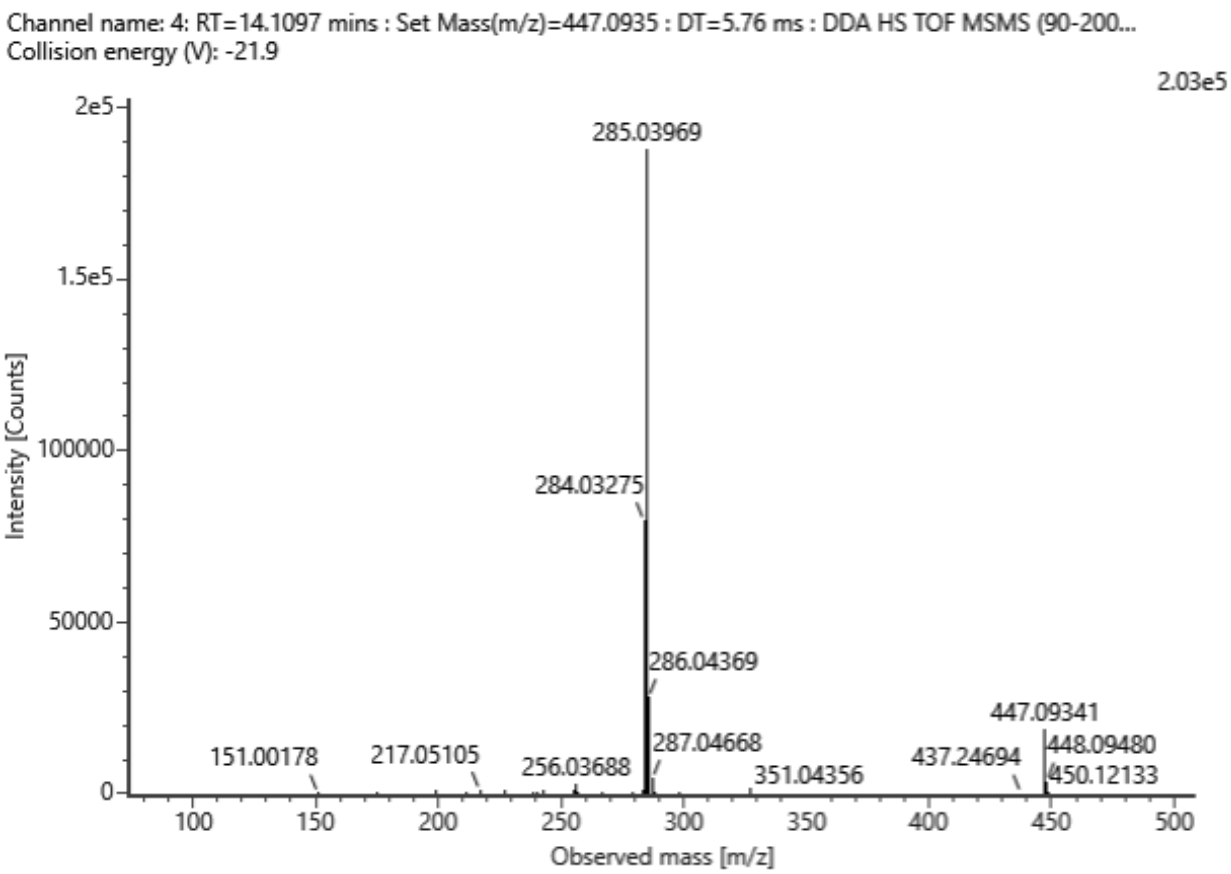

No. 52 Luteolin/kaempferol rutinoside C27H30O15 (neutral) Rt = 14.22 min

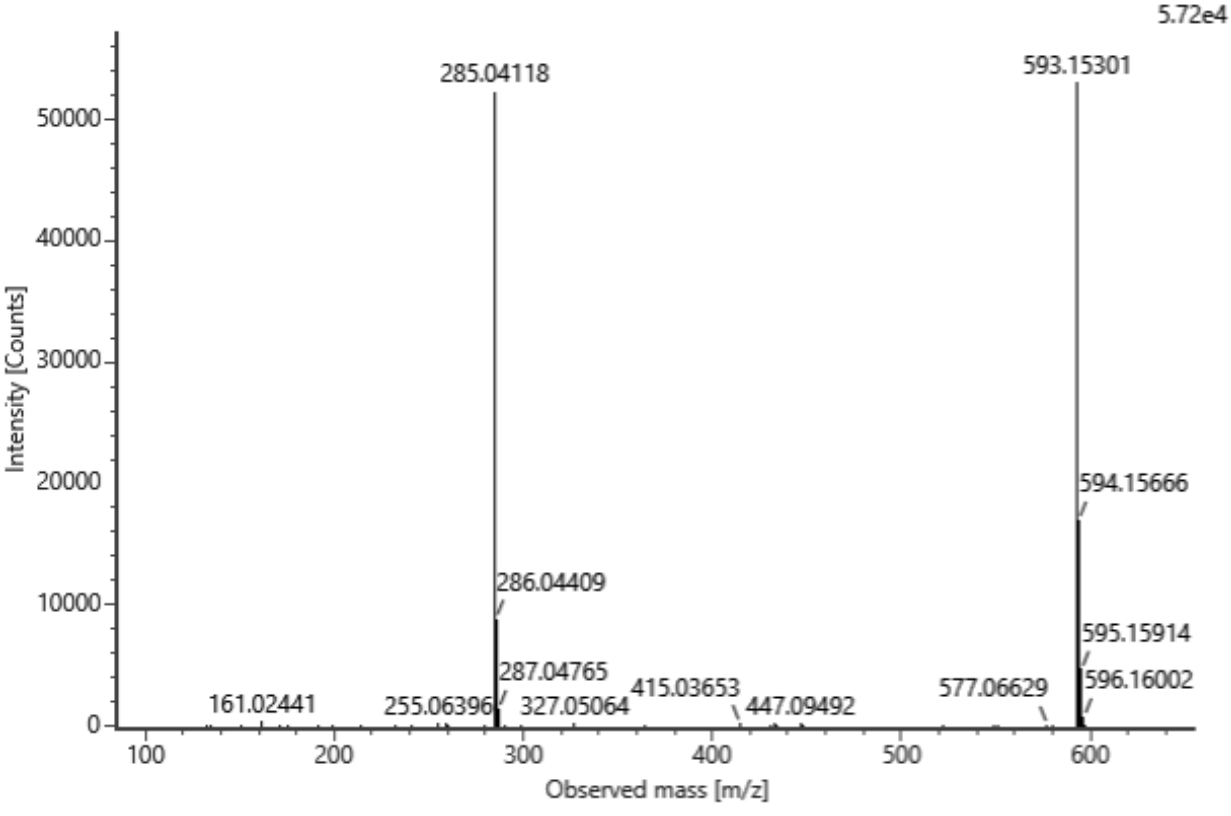

No. 53 Isorhamnetin disaccharide_2 C27H30O16 (neutral) Rt = 14.49 min

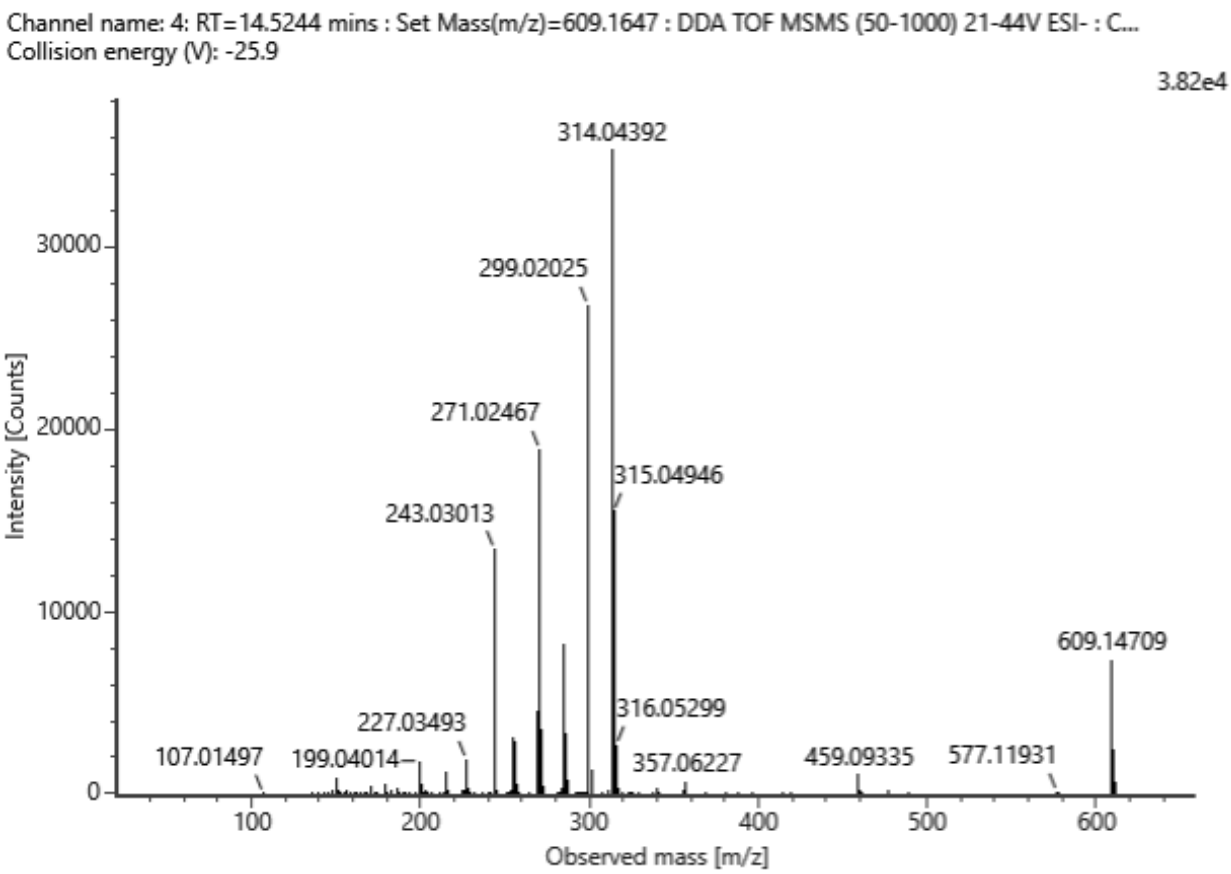

No. 54 Quercetin pentoside_2 C20H18O11 (neutral) Rt = 14.92 min

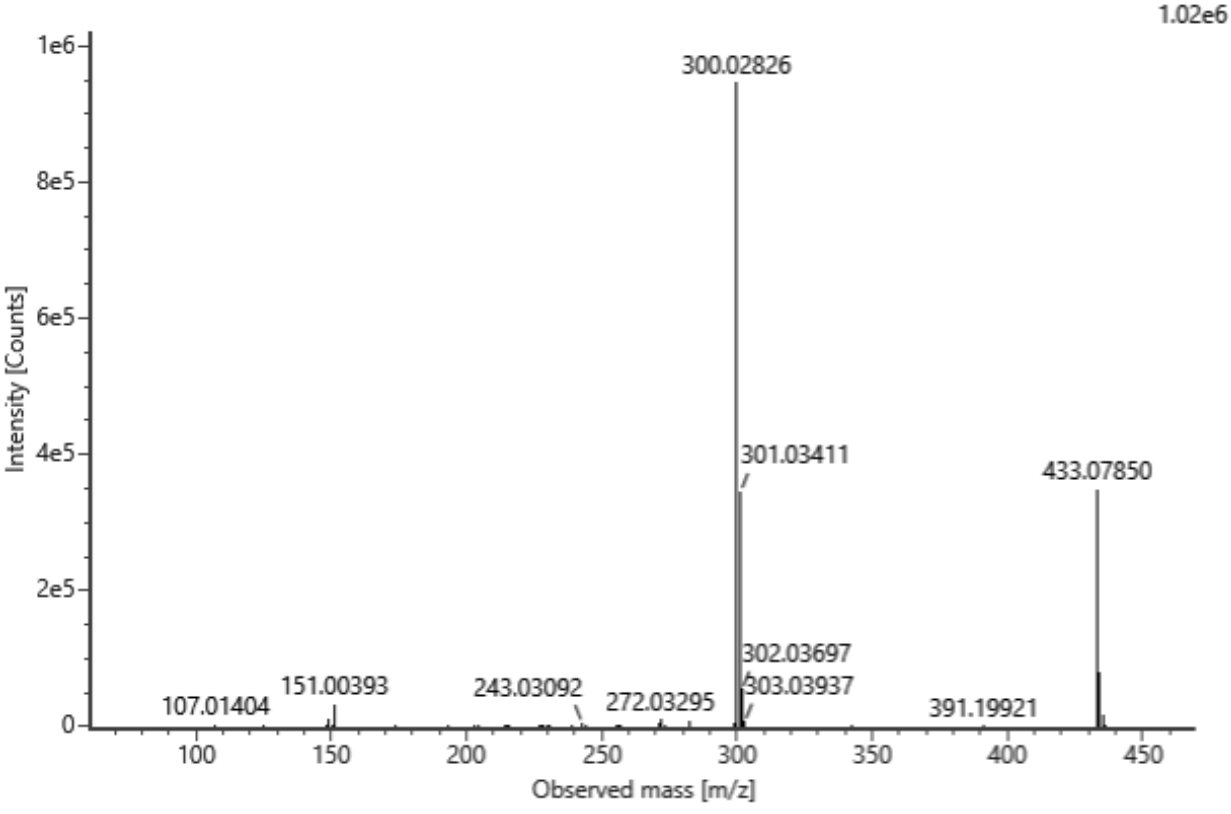

No. 55 Quercetin derivative_4 C23H22O13 (neutral) Rt = 14.99 min

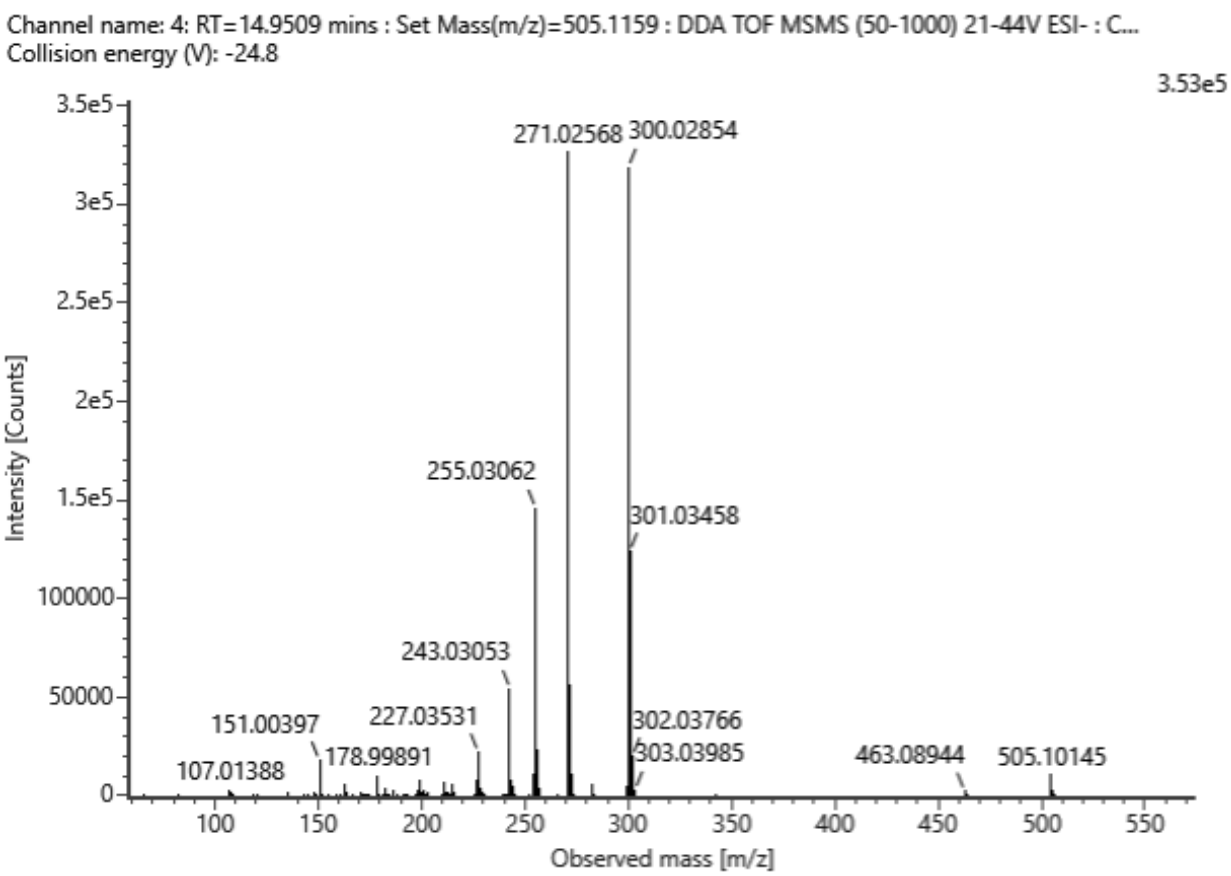

No. 56 Kaempferol 3-O-rutinoside C27H30O15 (neutral) Rt = 15.63 min

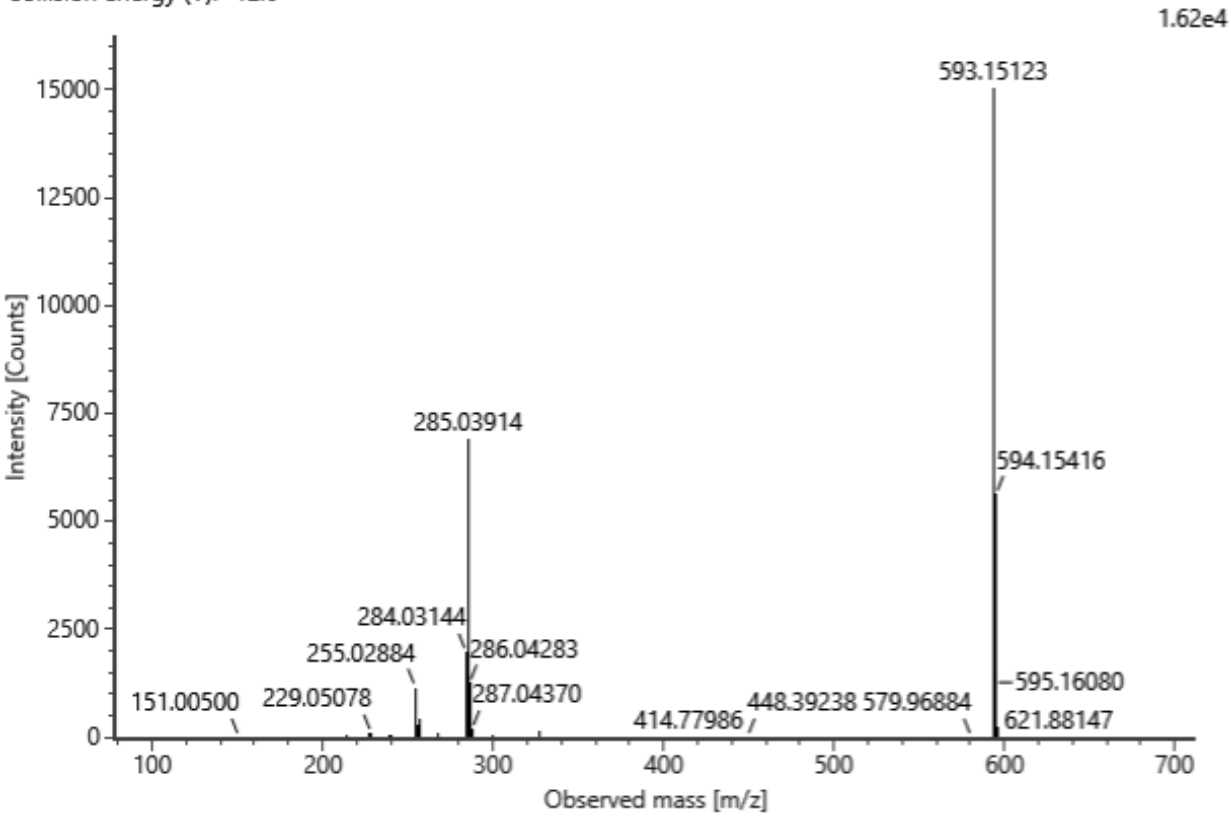

No. 57 Apigenin derivative C20H34O11 (neutral) Rt = 15.72 min

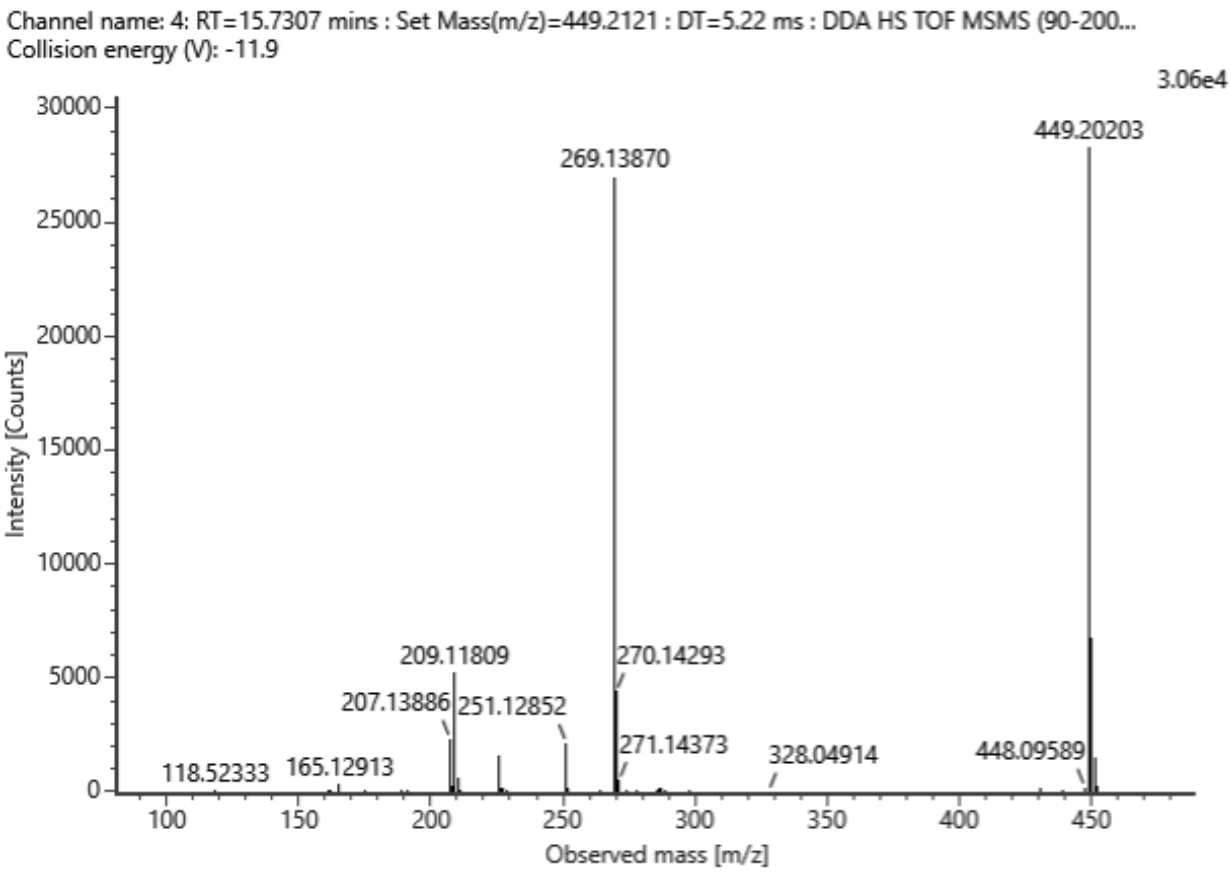

No. 58 Quercitrin C21H20O11 (neutral) Rt = 16.01 min

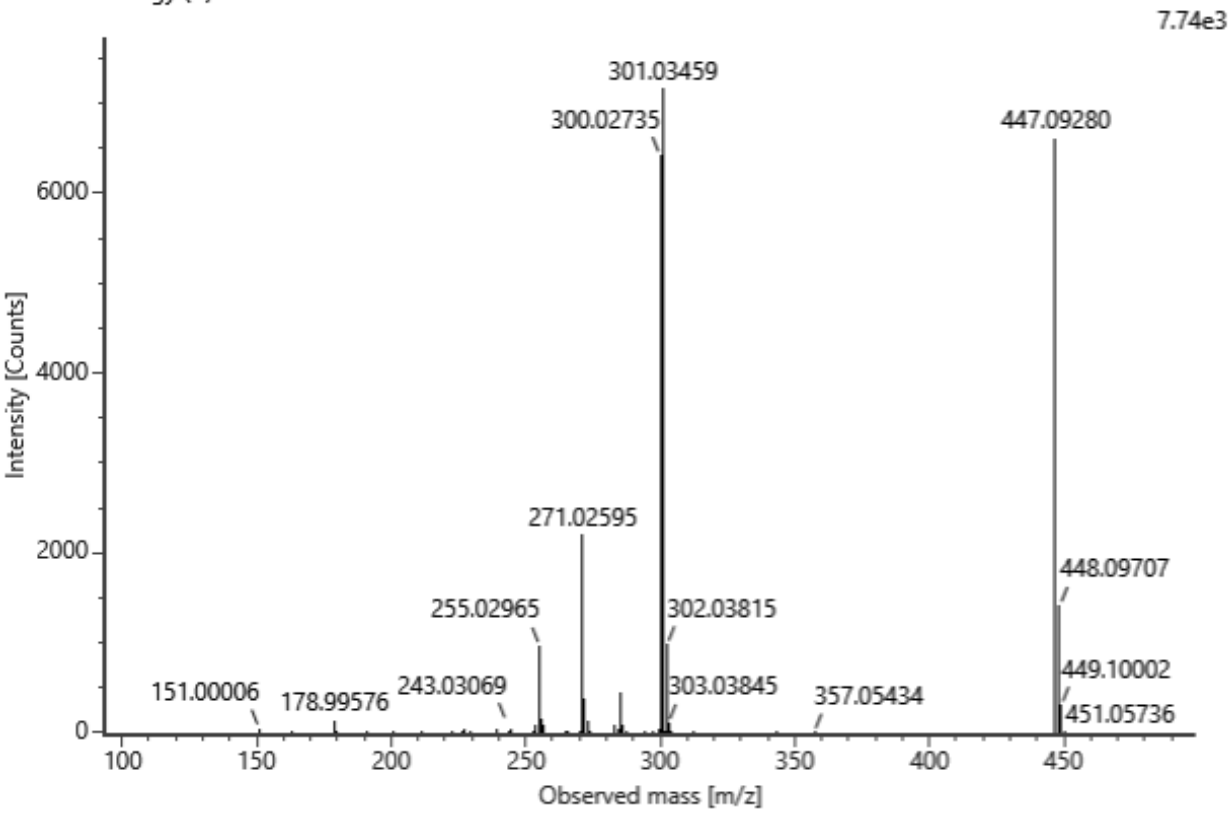

No. 59 Dicaffeoylquinic acid_1 C25H24O12 (neutral) Rt = 16.02 min

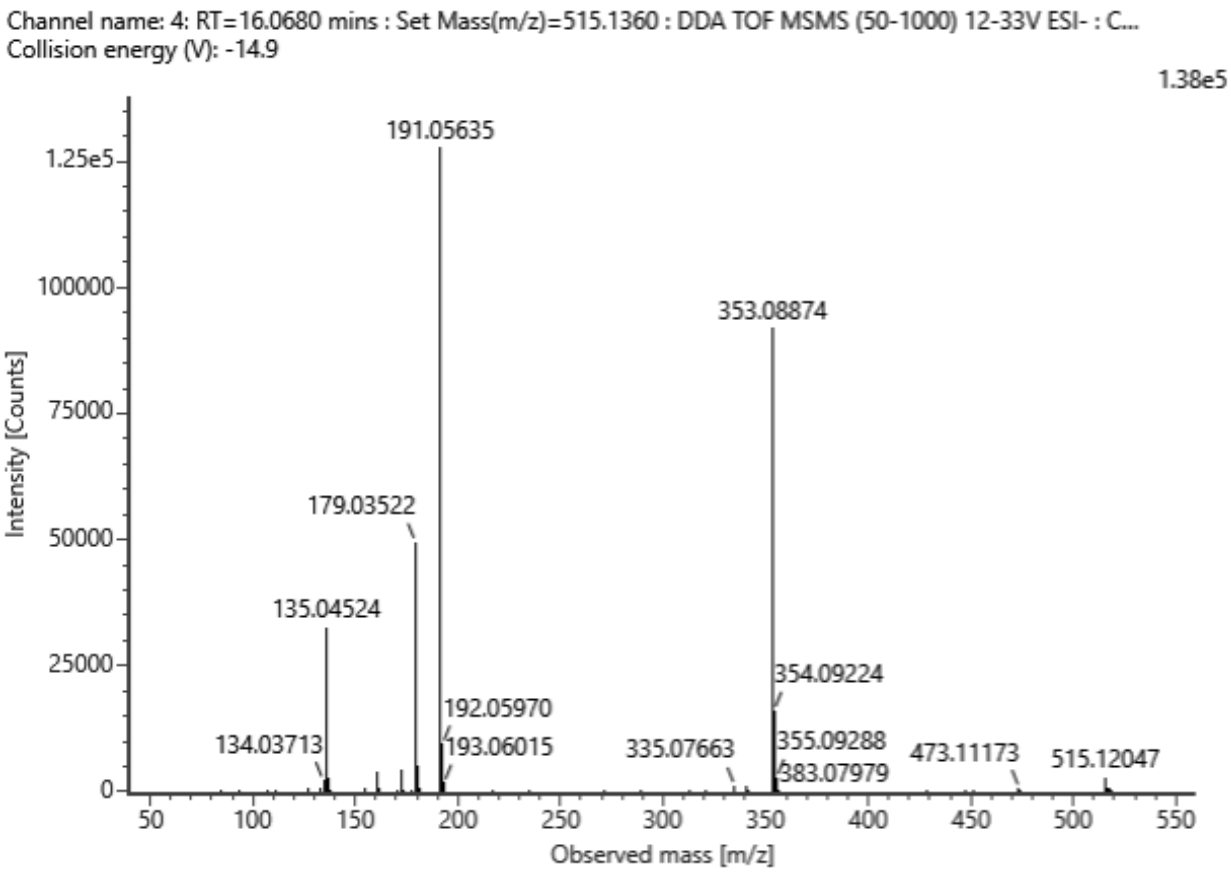

No. 60 Isorhamnetin 3-rutinoside C28H32O16 (neutral) Rt = 16.24 min

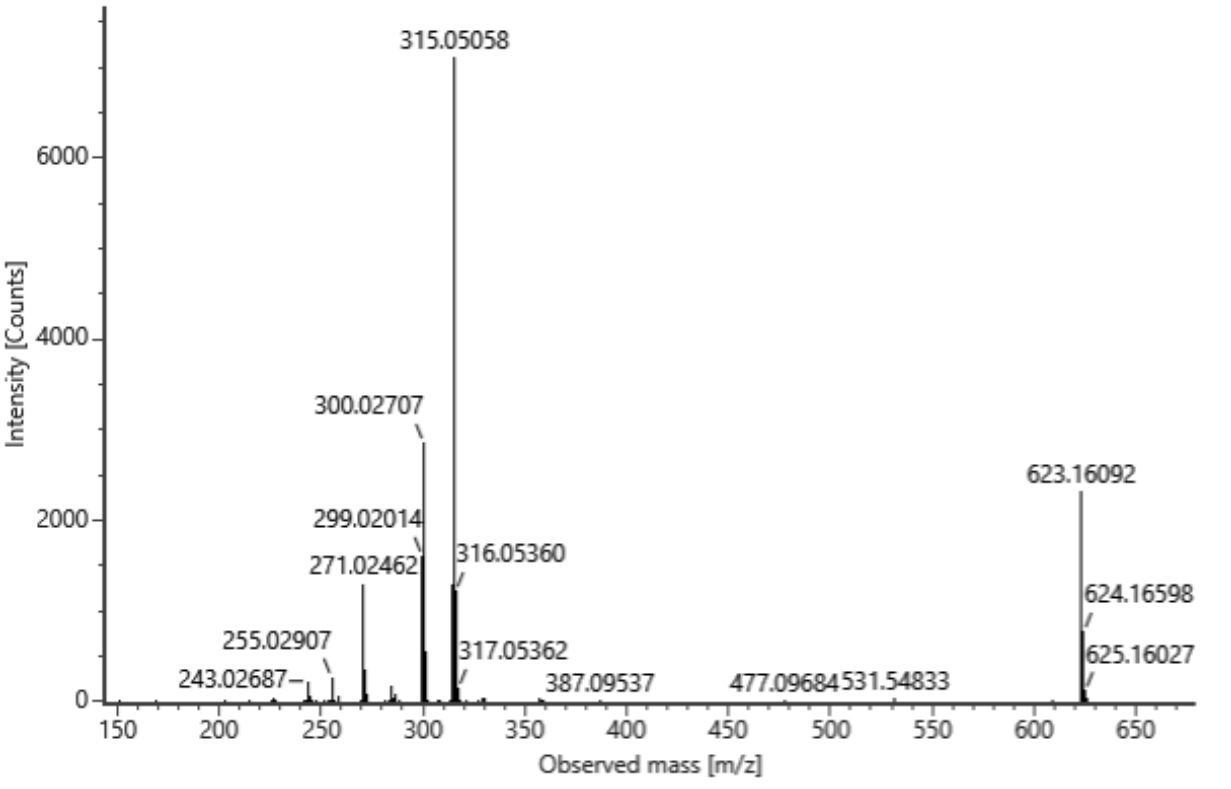

No. 61 Isorhamnetin 3-glucoside C22H22O12 (neutral) Rt = 16.40 min

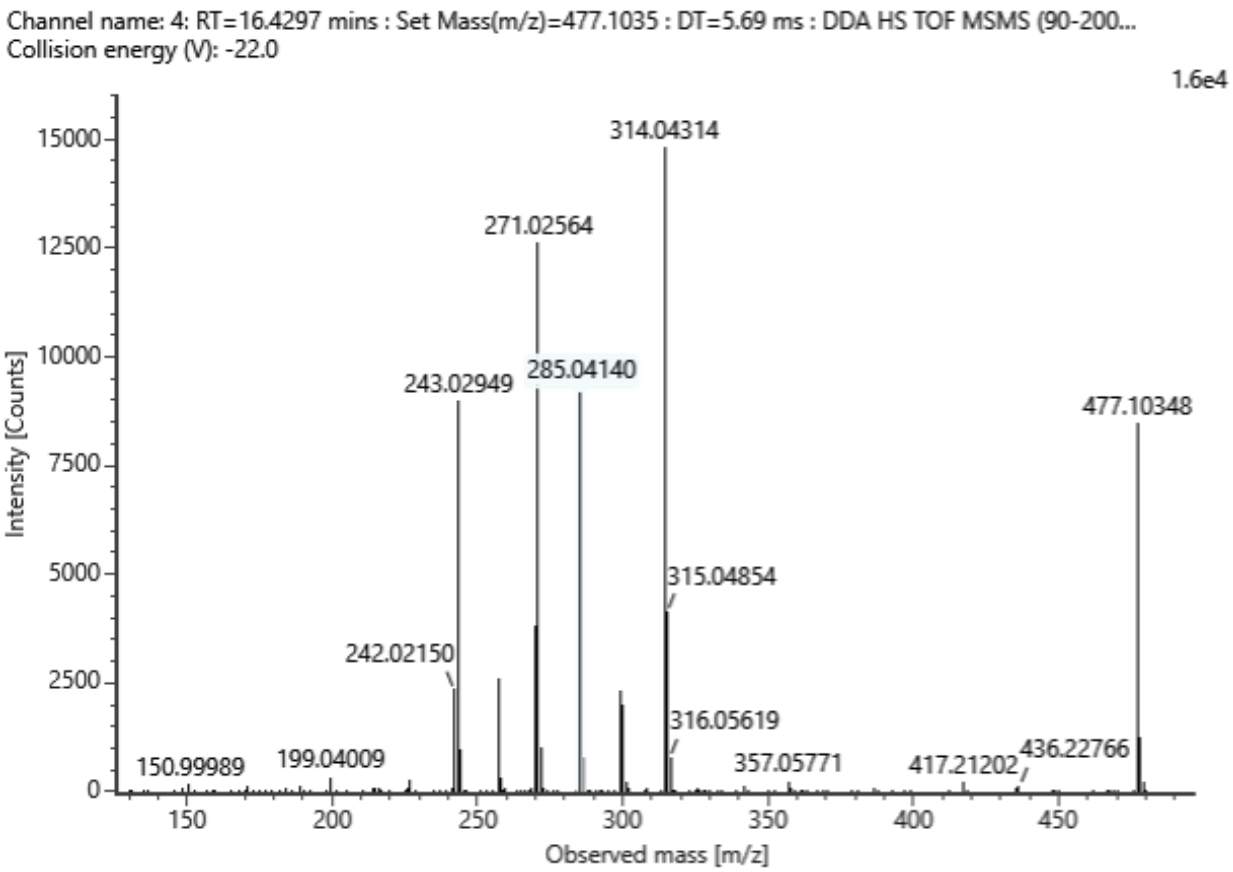

No. 62 Caffeic acid derivative_2 C23H24O11 (neutral) Rt = 16.52 min

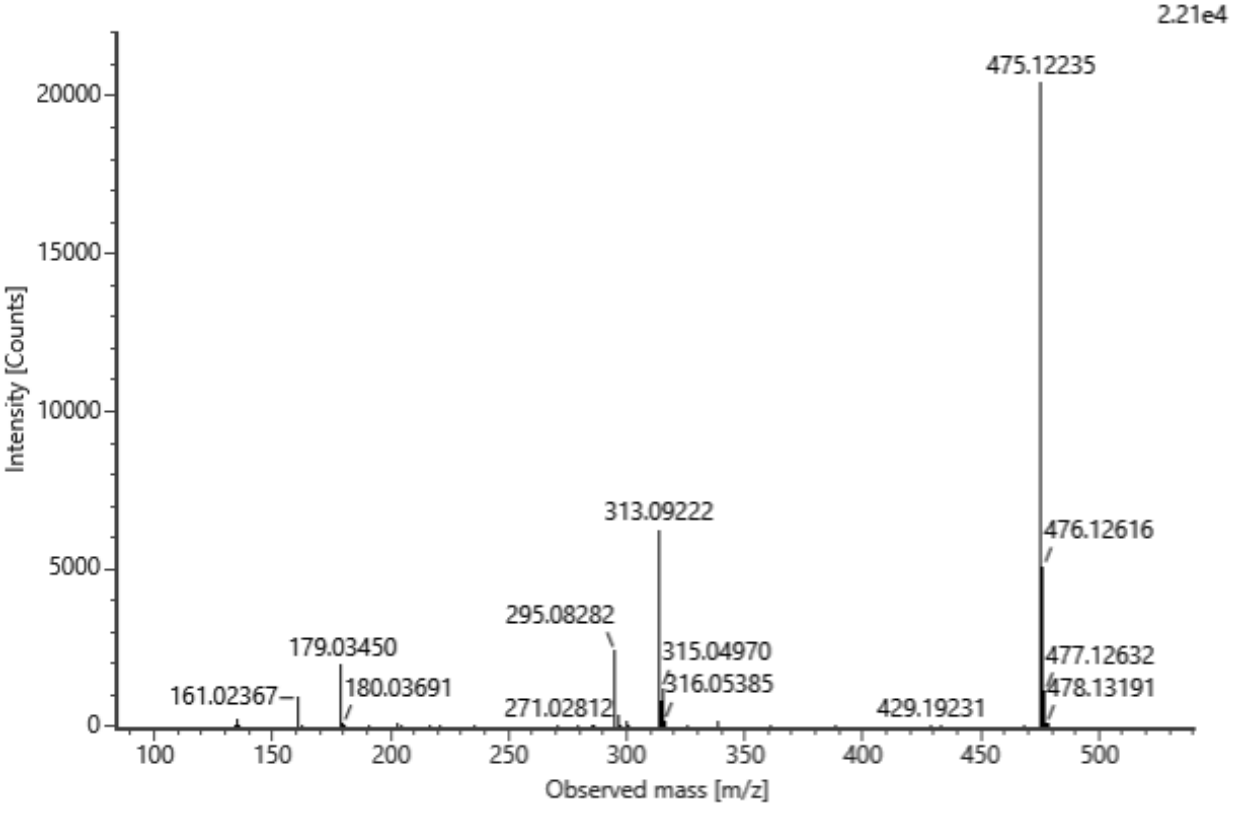

No. 63 Rosmarinic acid C18H16O8 (neutral) Rt = 16.73 min

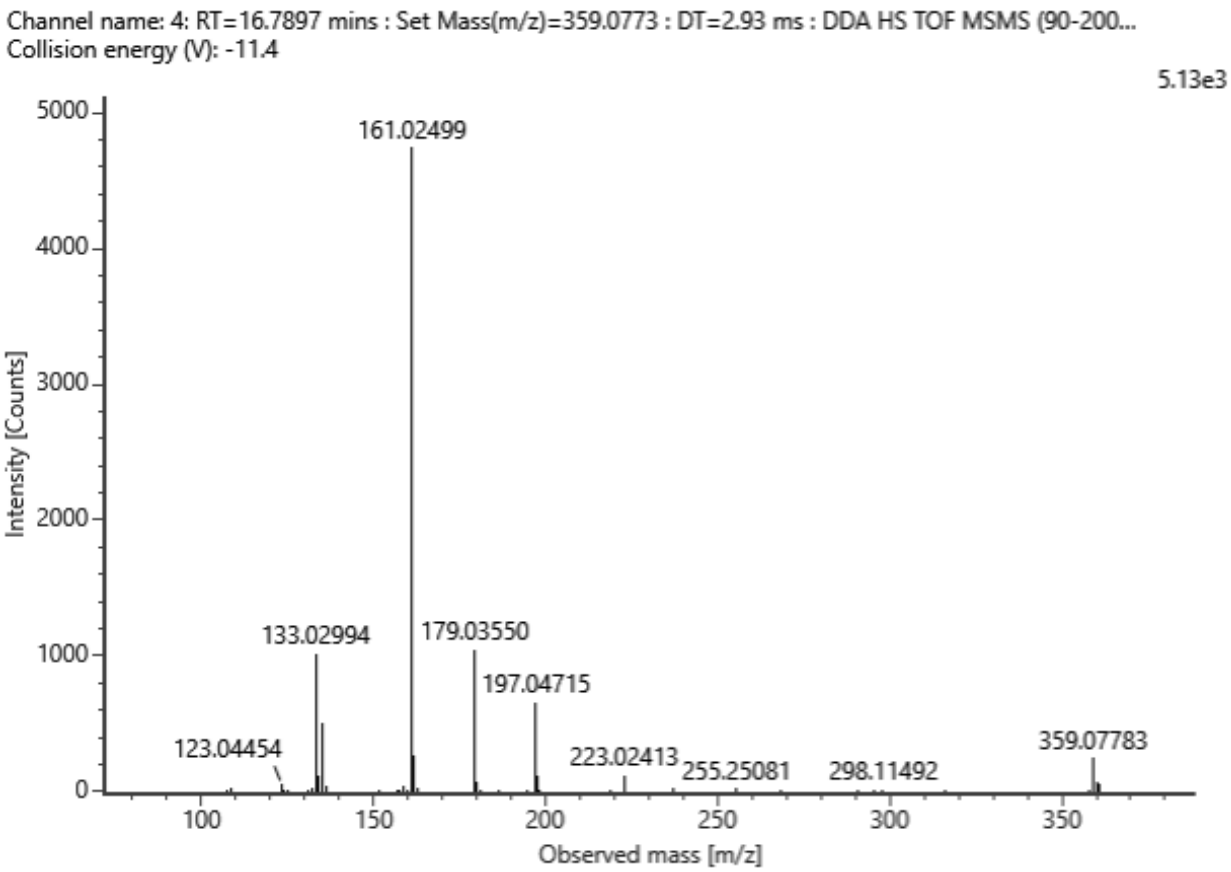

No. 64 Chrysoeriol-rutinoside C28H32O15 (neutral) Rt = 16.75 min

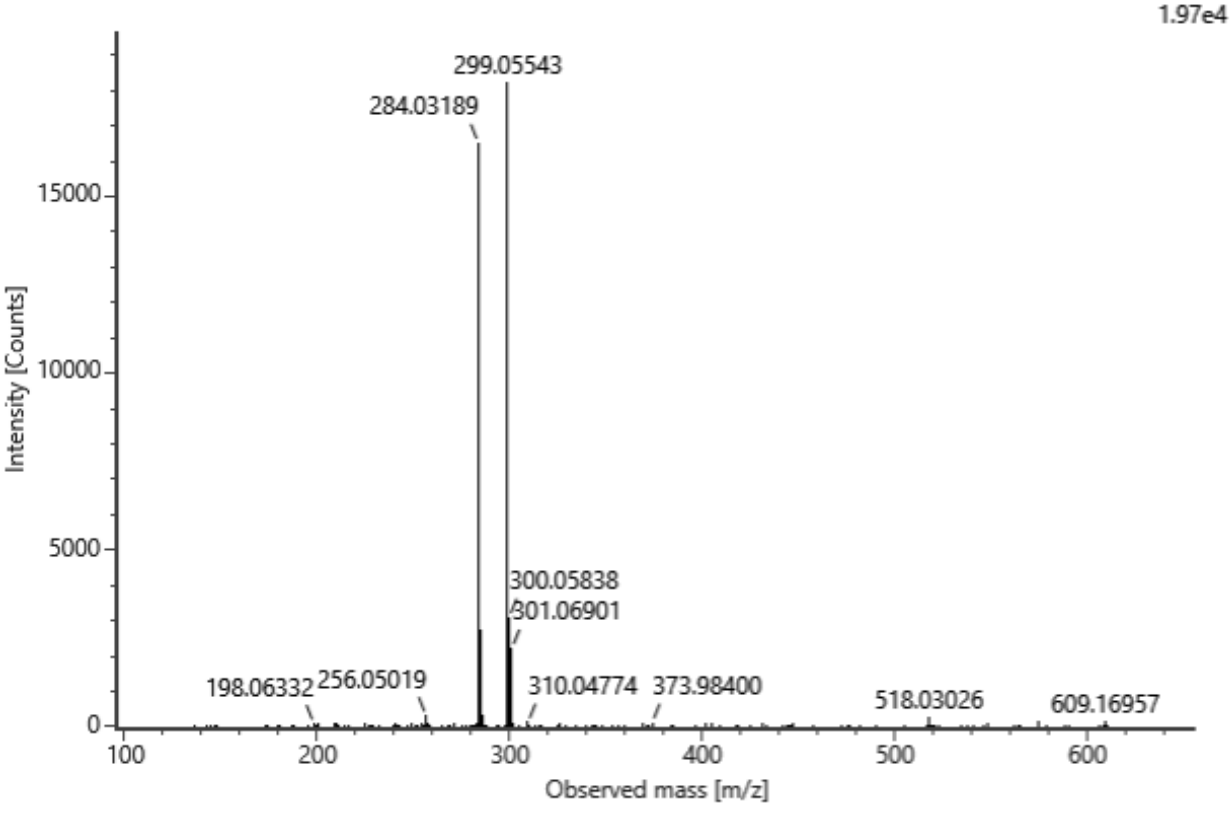

No. 65 Hesperidin C28H34O15 (neutral) Rt = 16.79 min

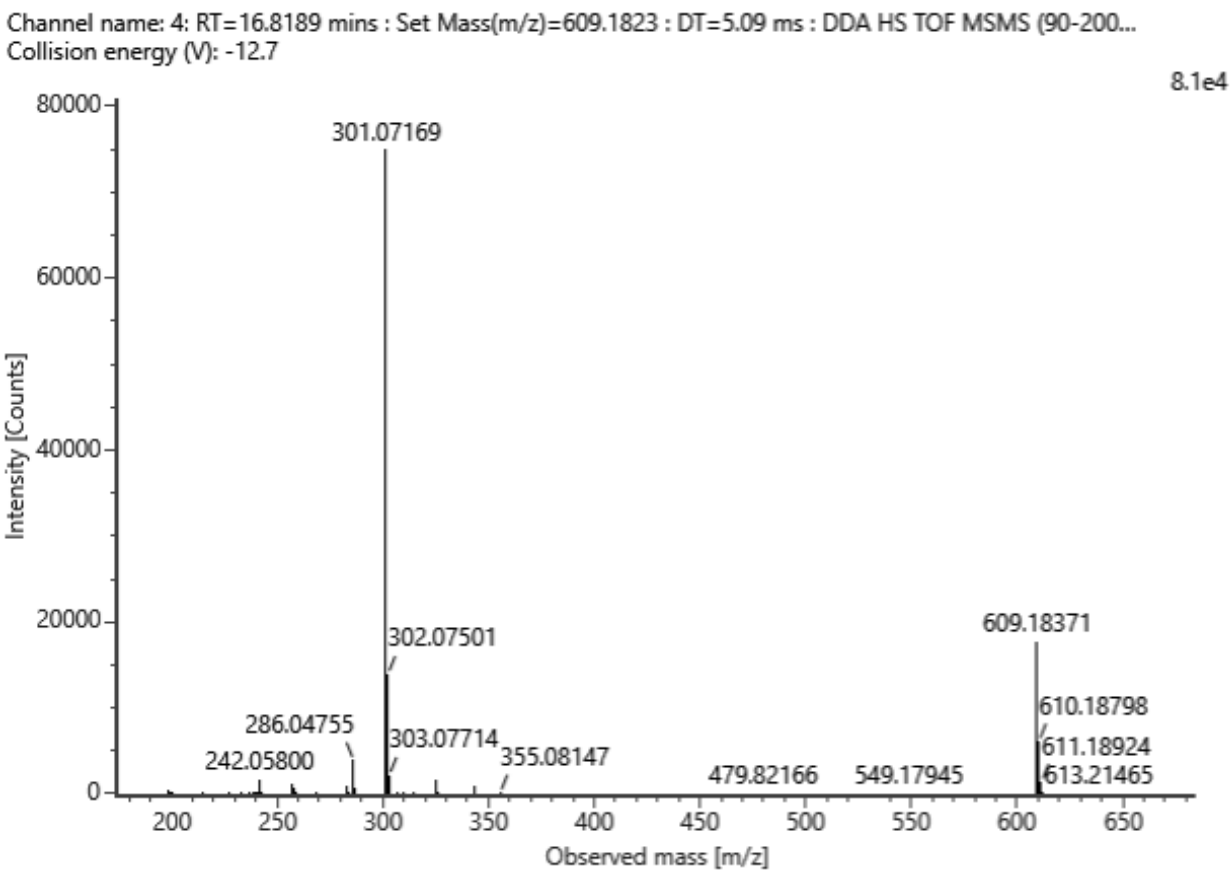

No. 66 Dicaffeoylquinic acid_2 C25H24O12 (neutral) Rt = 16.80 min

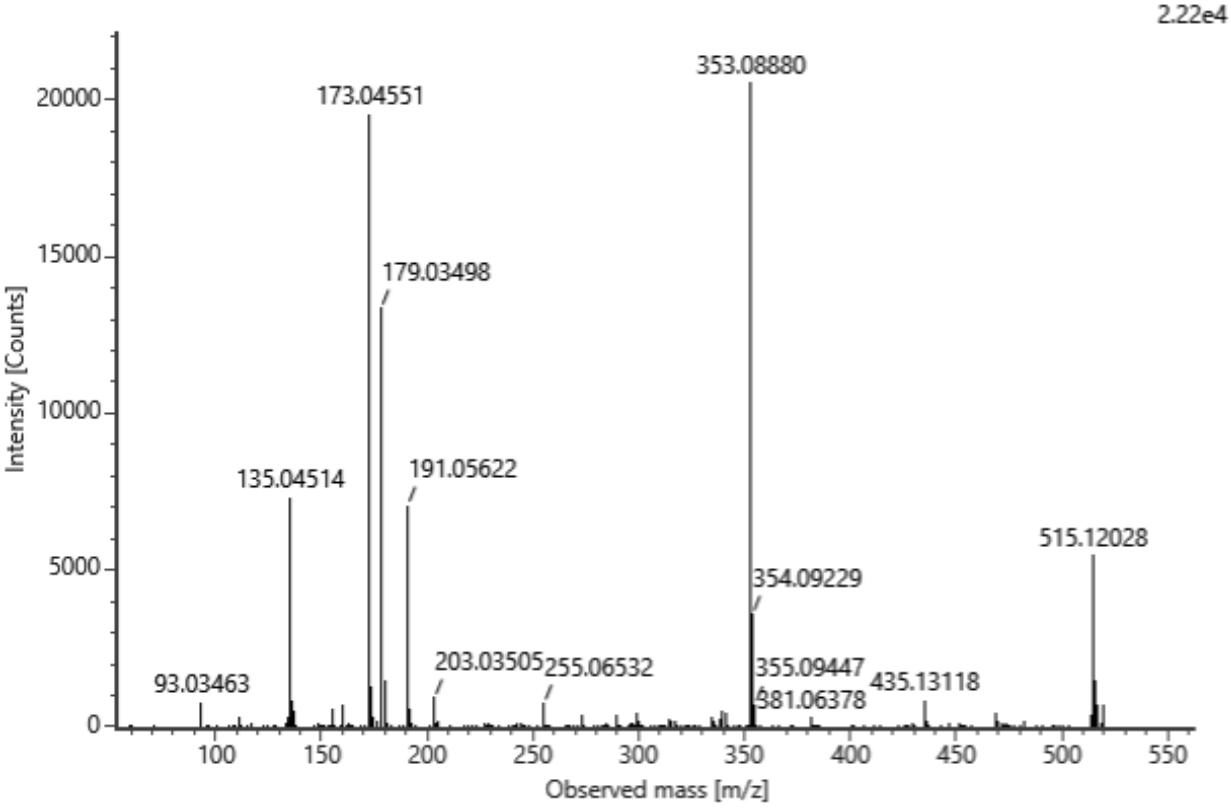

No. 67 Luteolin/kaempferol glycoside C21H20O11 (neutral) Rt = 16.91 min

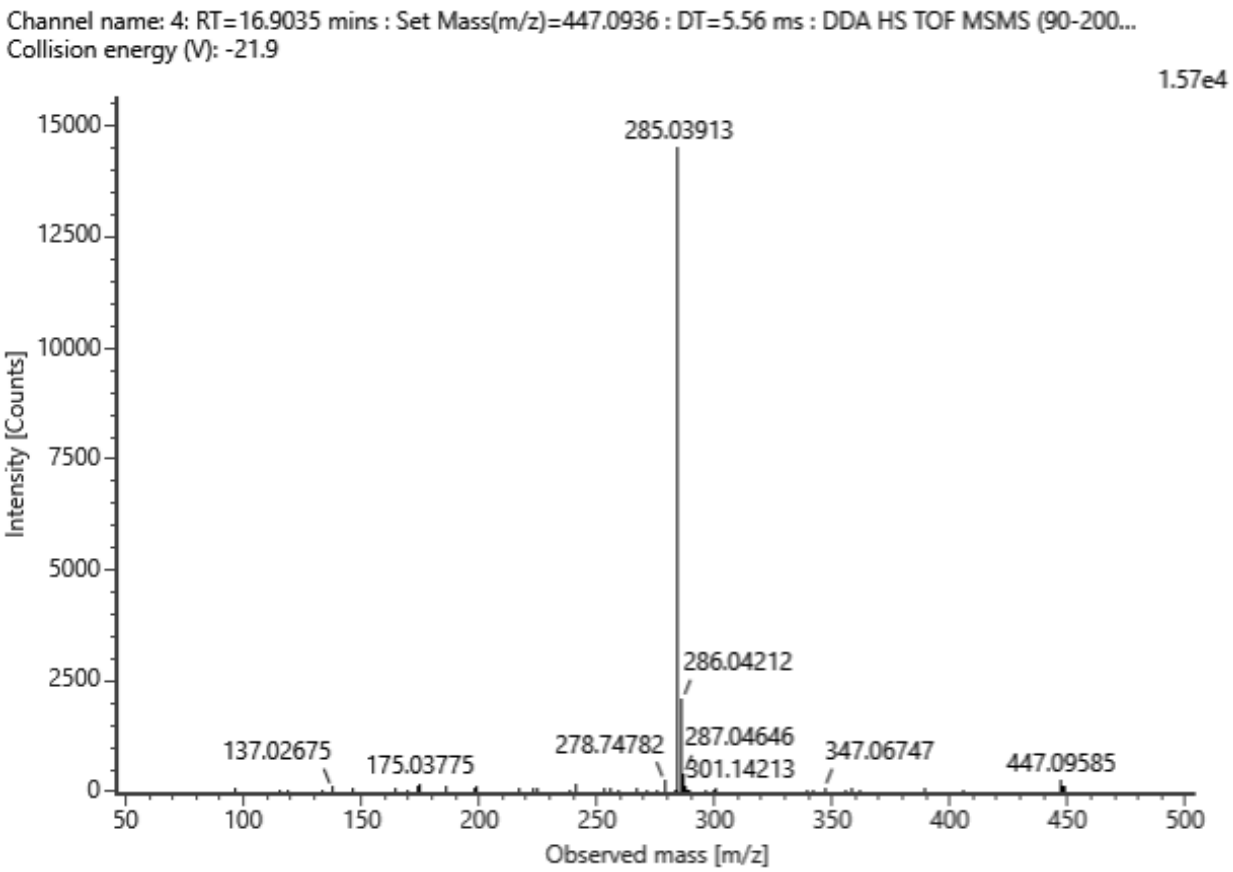

No. 68 Phlorizin C21H24O10 (neutral) Rt = 16.92 min

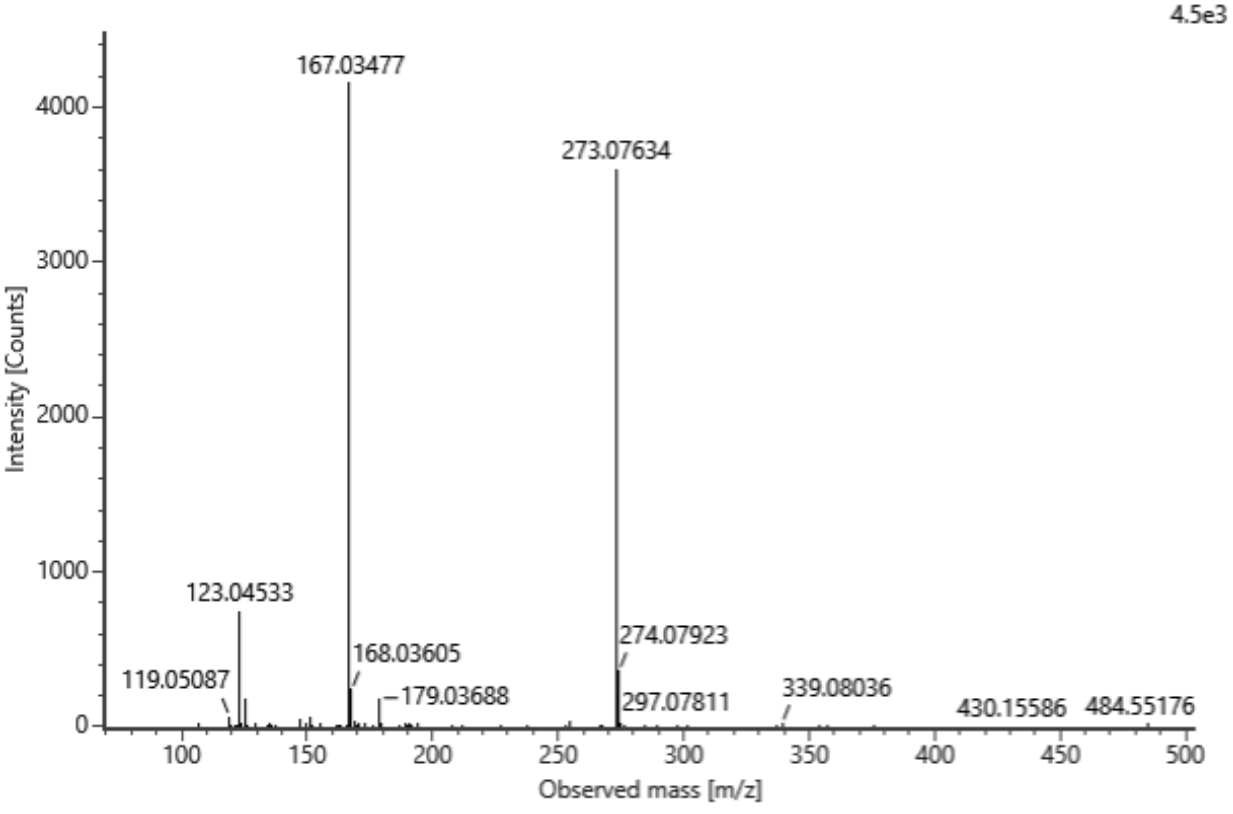

No. 69 Abscisic acid glucose ester C22H32O11 (neutral) Rt = 16.95 min

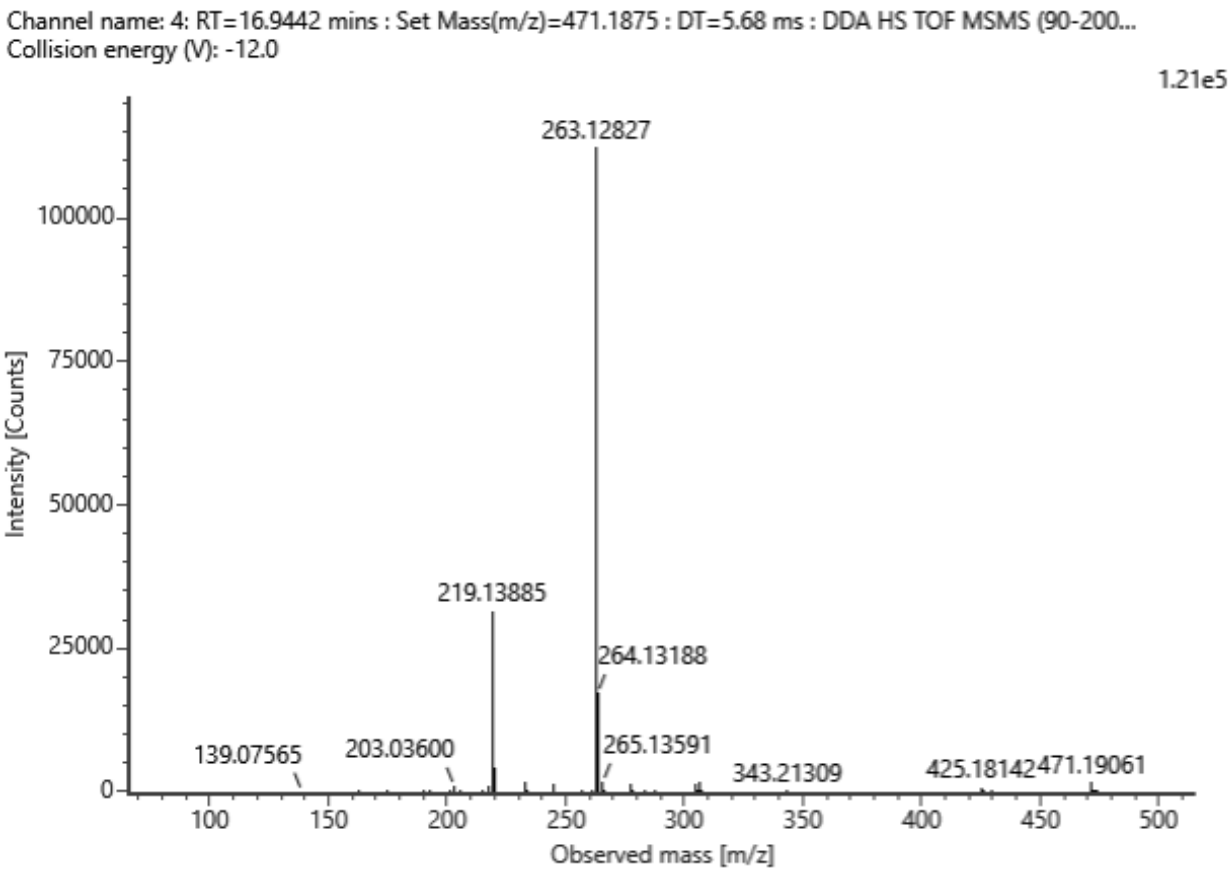

No. 70 Daidzein C15H10O4 (neutral) Rt = 17.20 min

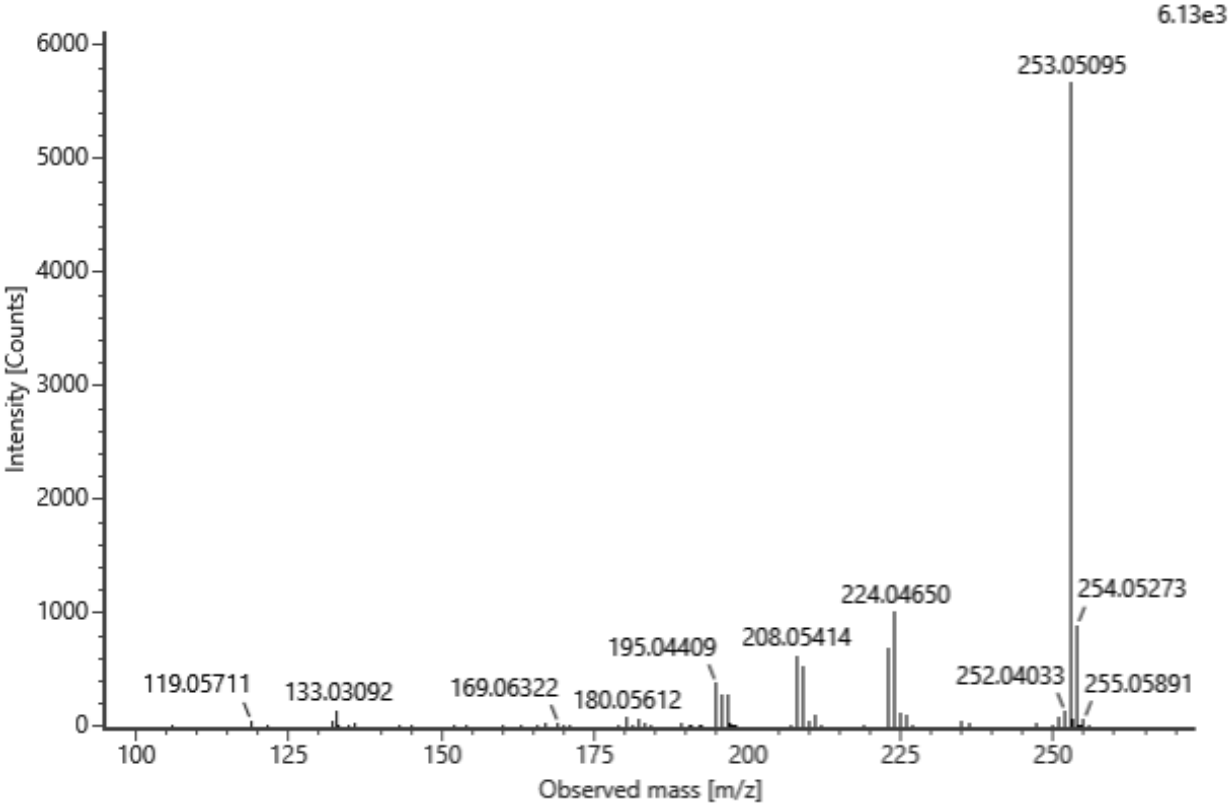

No. 71 Eriodictyol C15H12O6 (neutral) Rt = 17.36 min

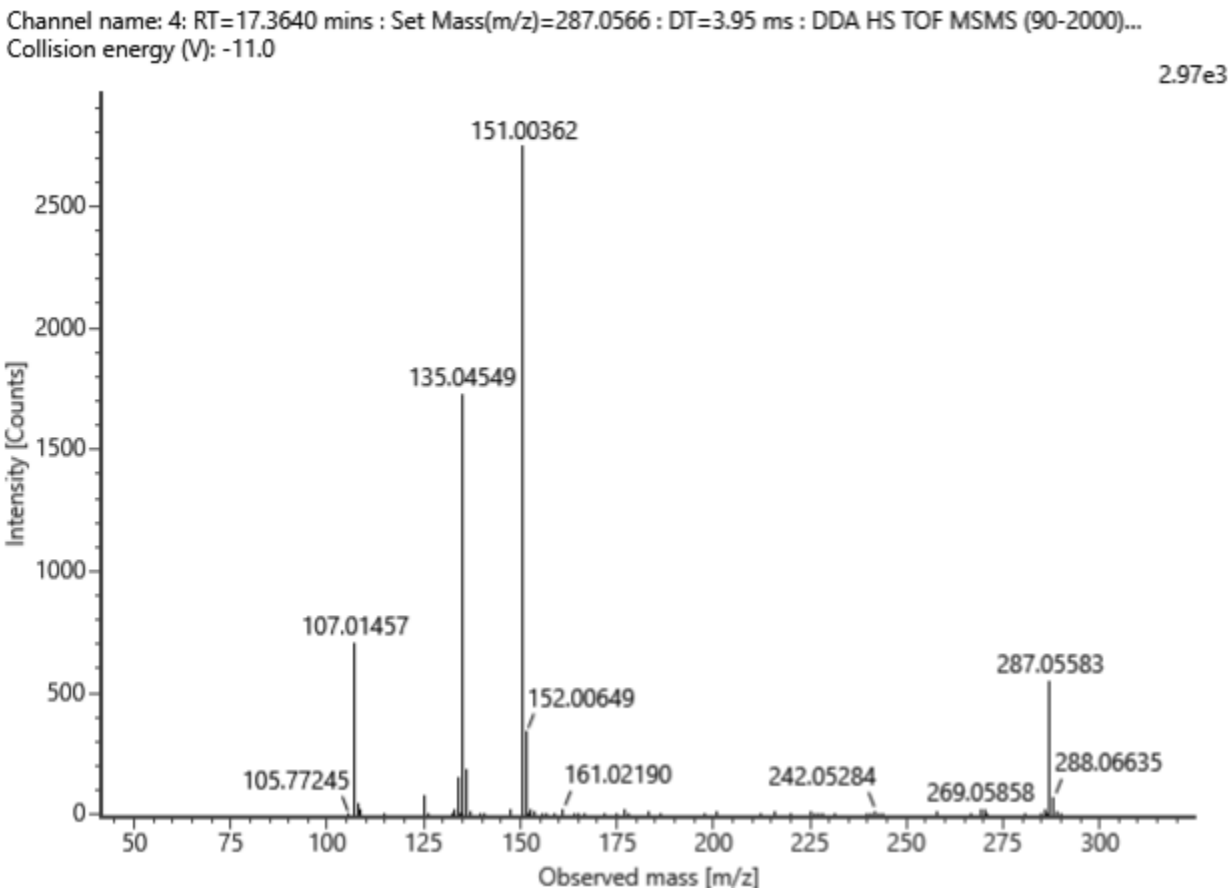

No. 72 Sebacic acid C10H18O4 (neutral) Rt = 17.61 min

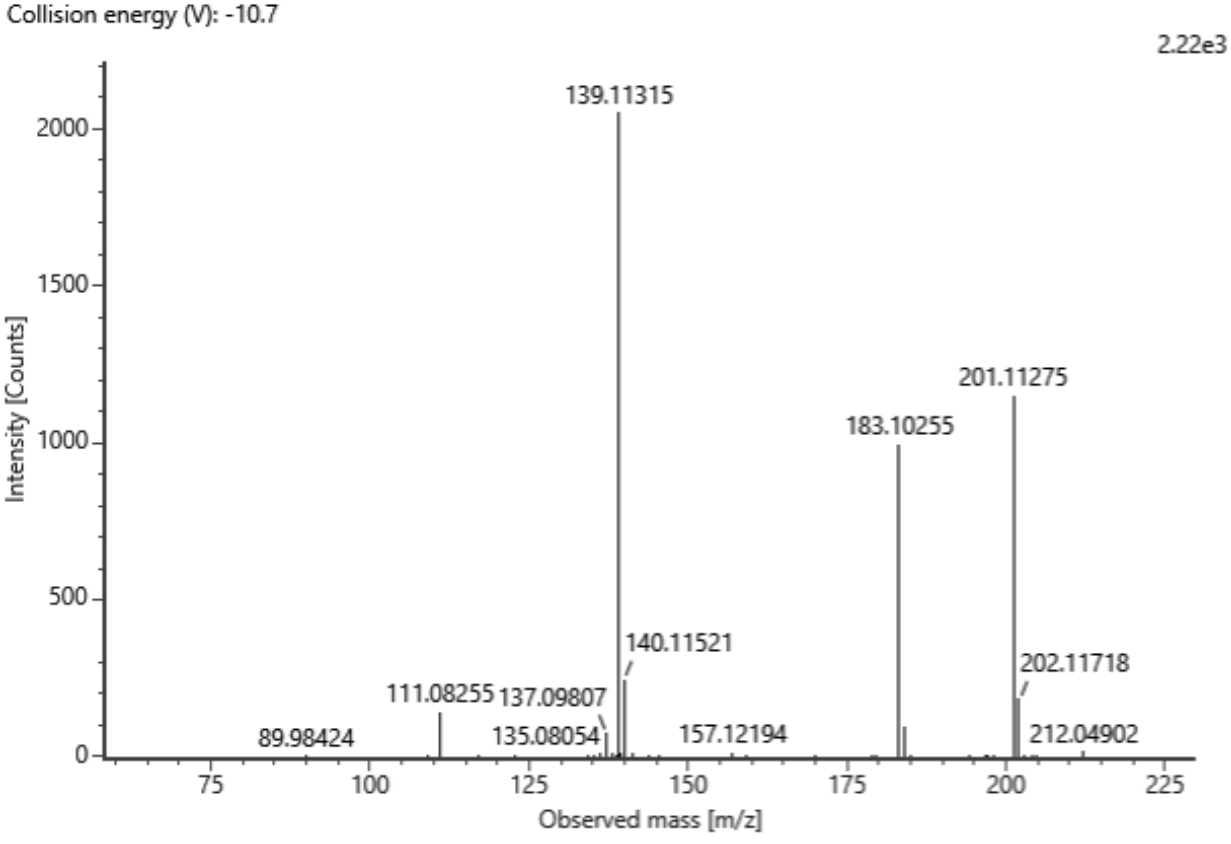

No. 73 Luteolin C15H10O6 (neutral) Rt = 17.63 min

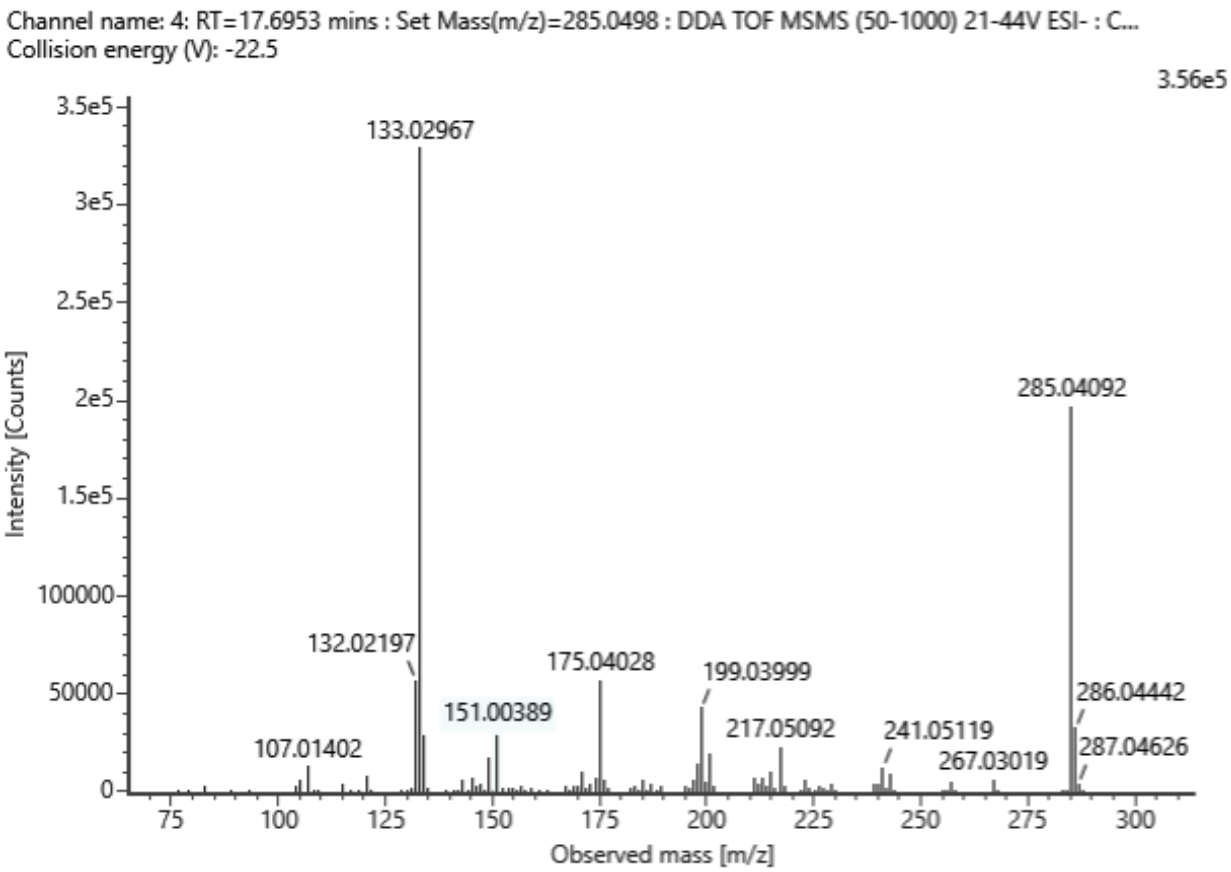

No. 74 Ethyl caffeate C11H12O4 (neutral) Rt = 17.76 min

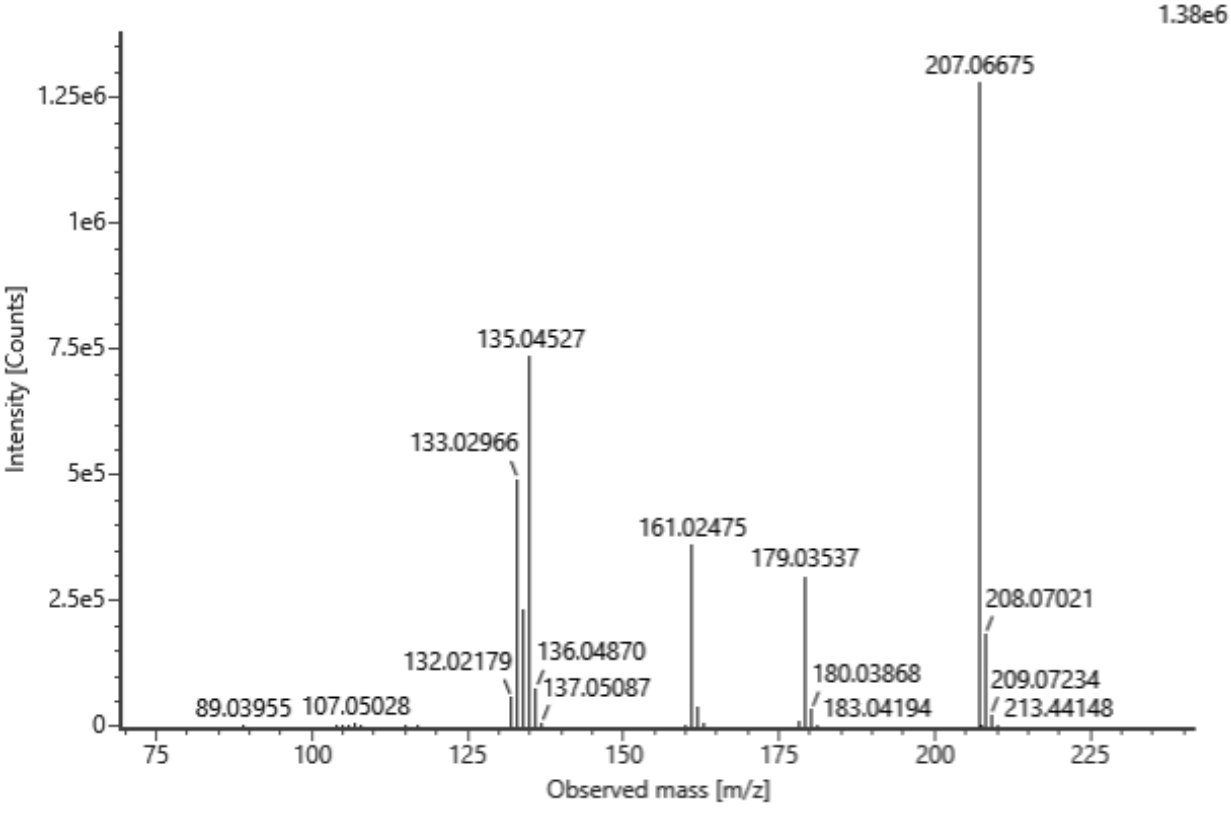

No. 75 Naringenin C15H12O5 (neutral) Rt = 18.14 min

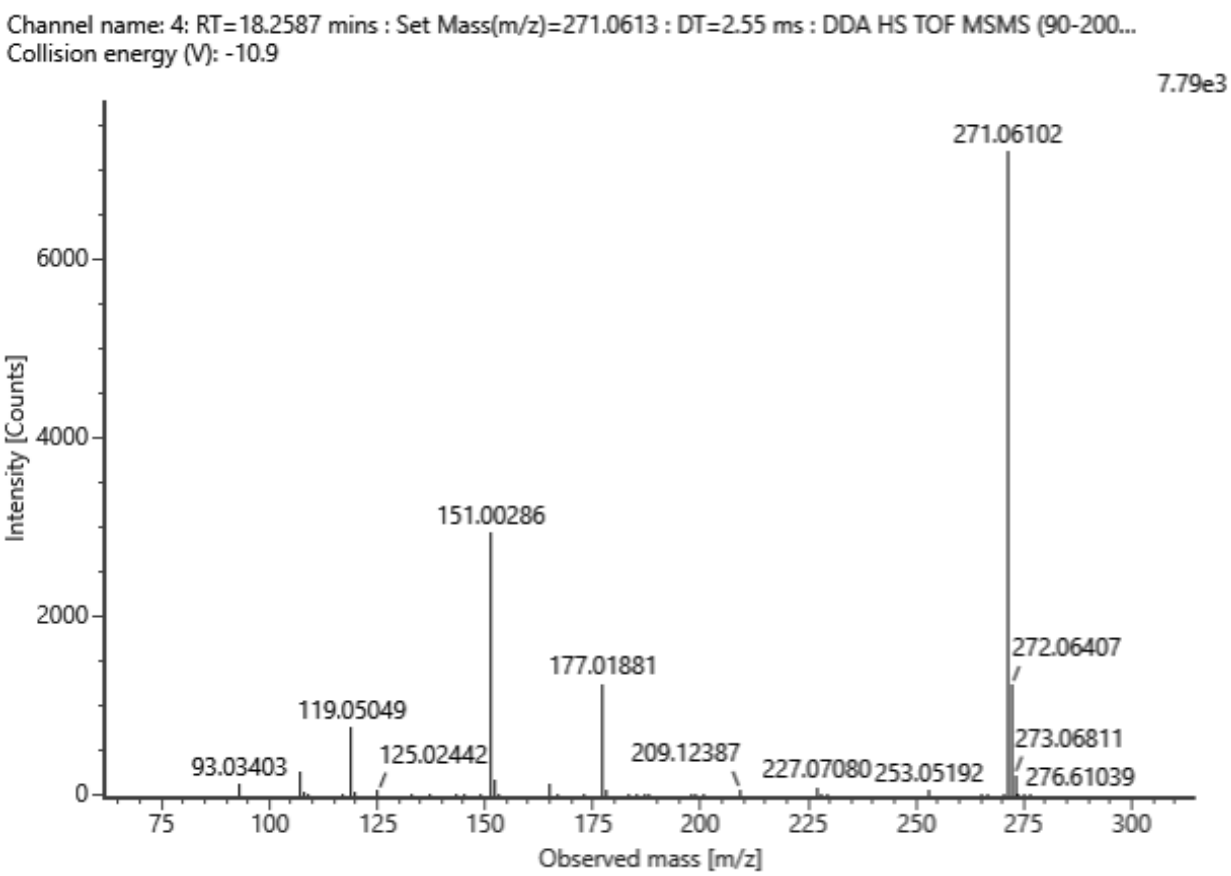

No. 76 Apigenin C15H10O5 (neutral) Rt = 18.16 min

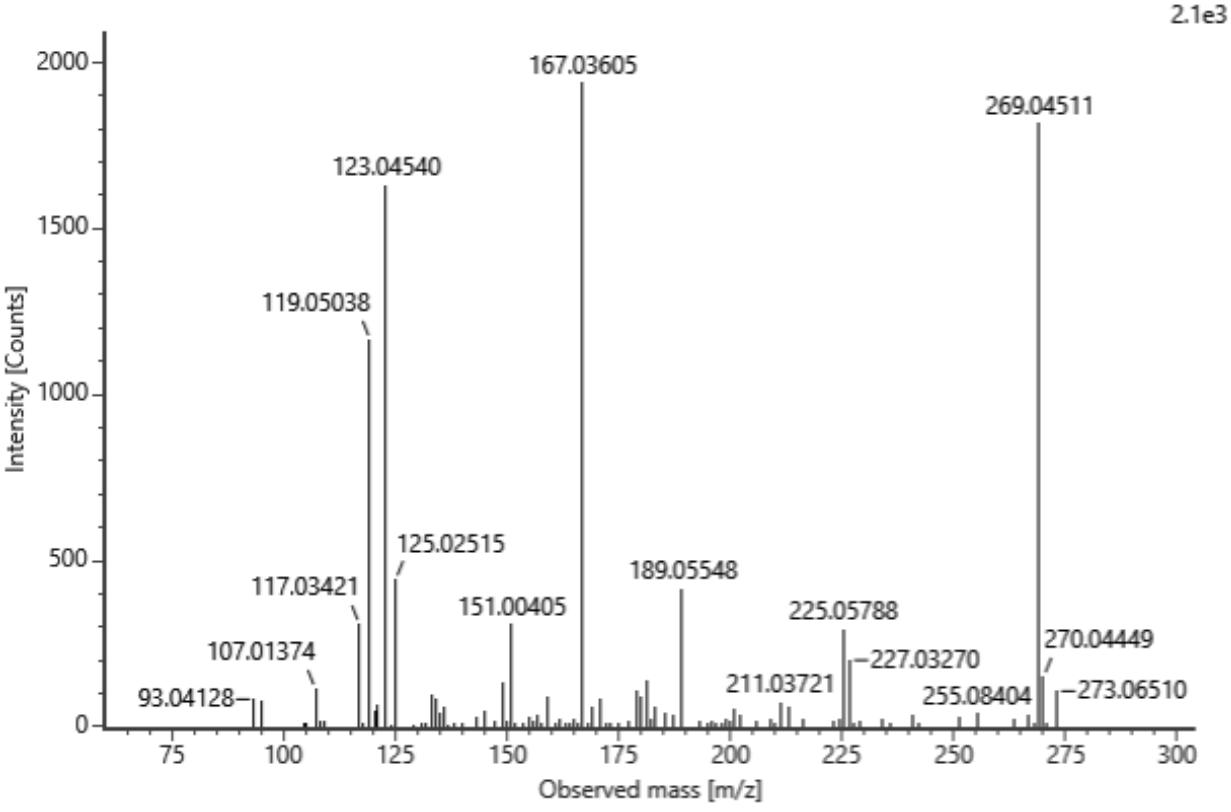

No. 77 Chrysoeriol C16H12O6 (neutral) Rt = 18.43 min

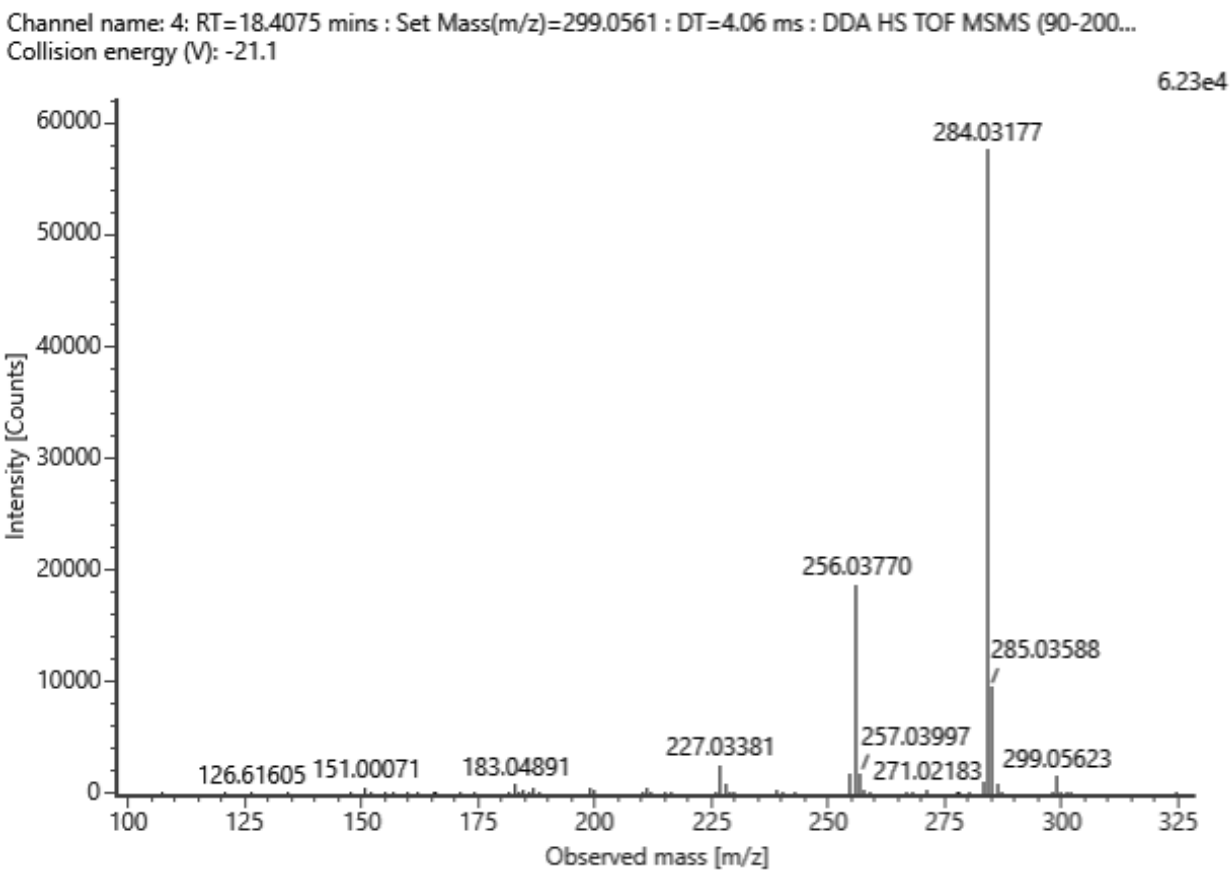

No. 78 Unknown_3 C38H58O17 (neutral) Rt = 18.43 min

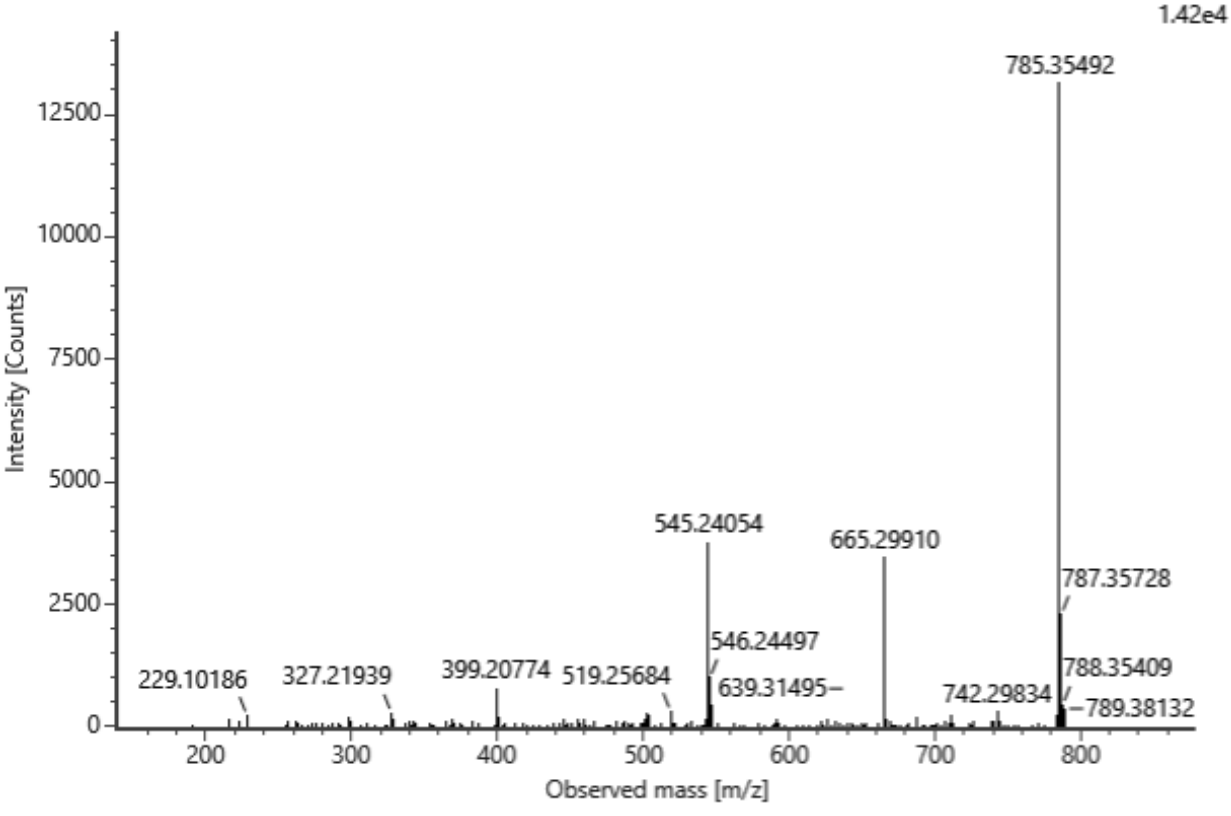

No. 79 9,12,13-trihydroxy-10E,15Z-octadecadienoic acid C18H32O5 (neutral) Rt = 18.55 min

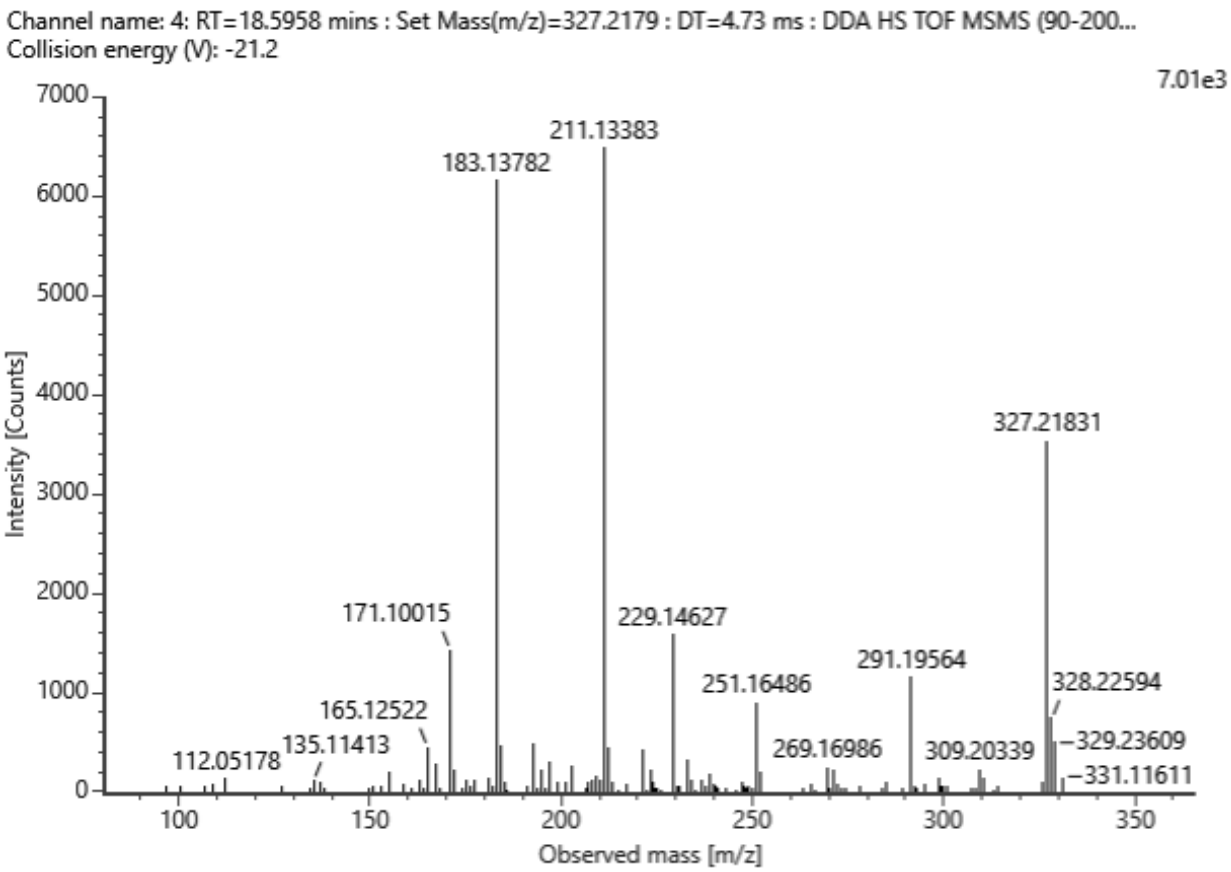

No. 80 9,12,13-trihydroxy-10E-octadecenoic acid C18H34O5 (neutral) Rt = 18.89 min

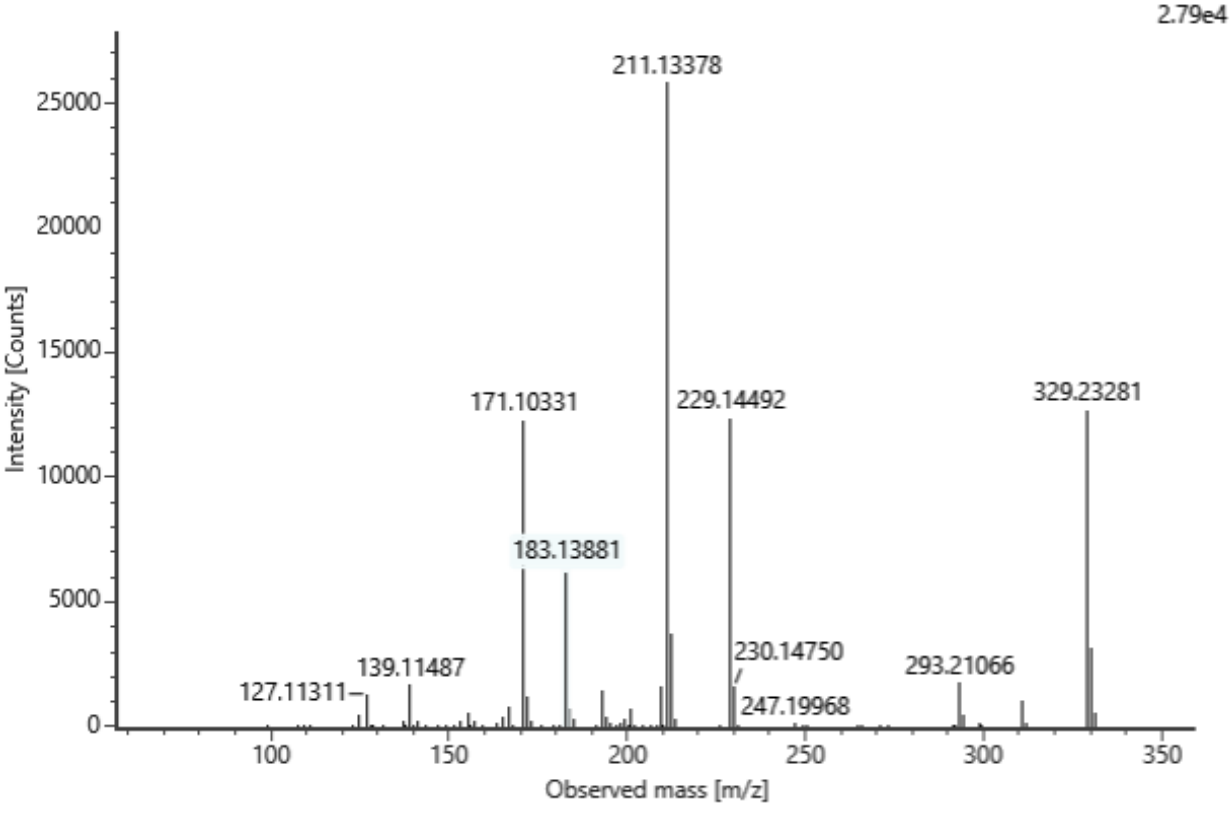

No. 81 Chrysin C15H10O4 (neutral) Rt = 19.32 min

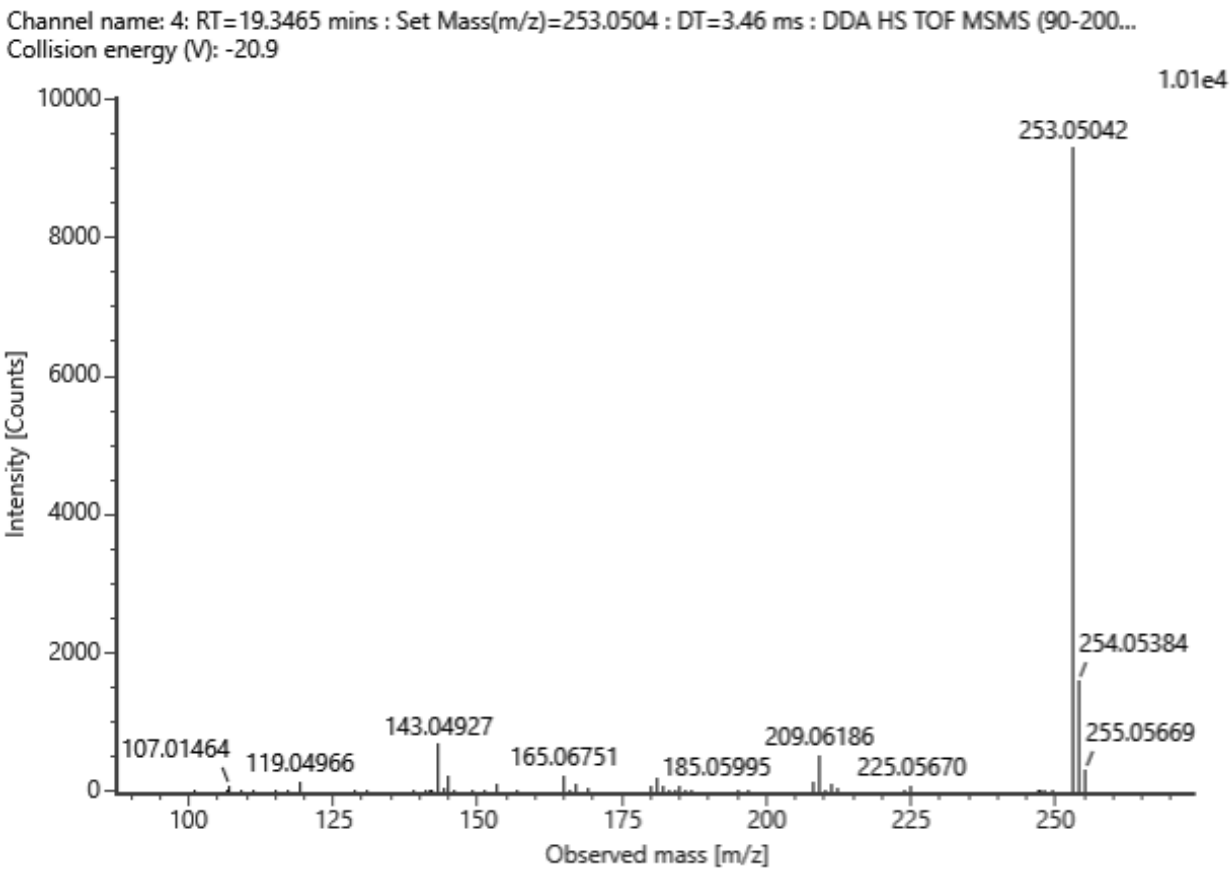

No. 82 9,10-dihydroxy-12Z-octadecenoic acid C18H34O4 (neutral) Rt = 19.75 min

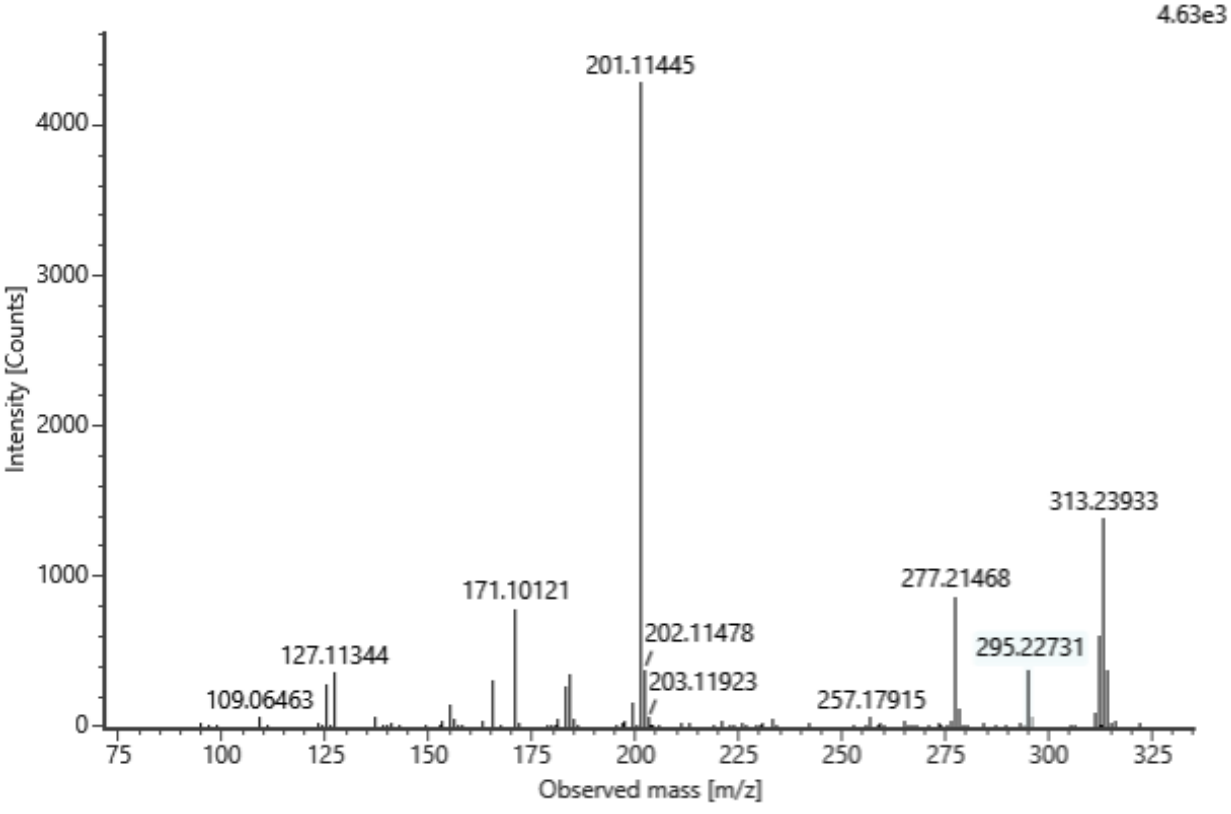

No. 83 Hydroxyoctadecatrienoic acid derivative C18H30O3 (neutral) Rt = 19.96 min

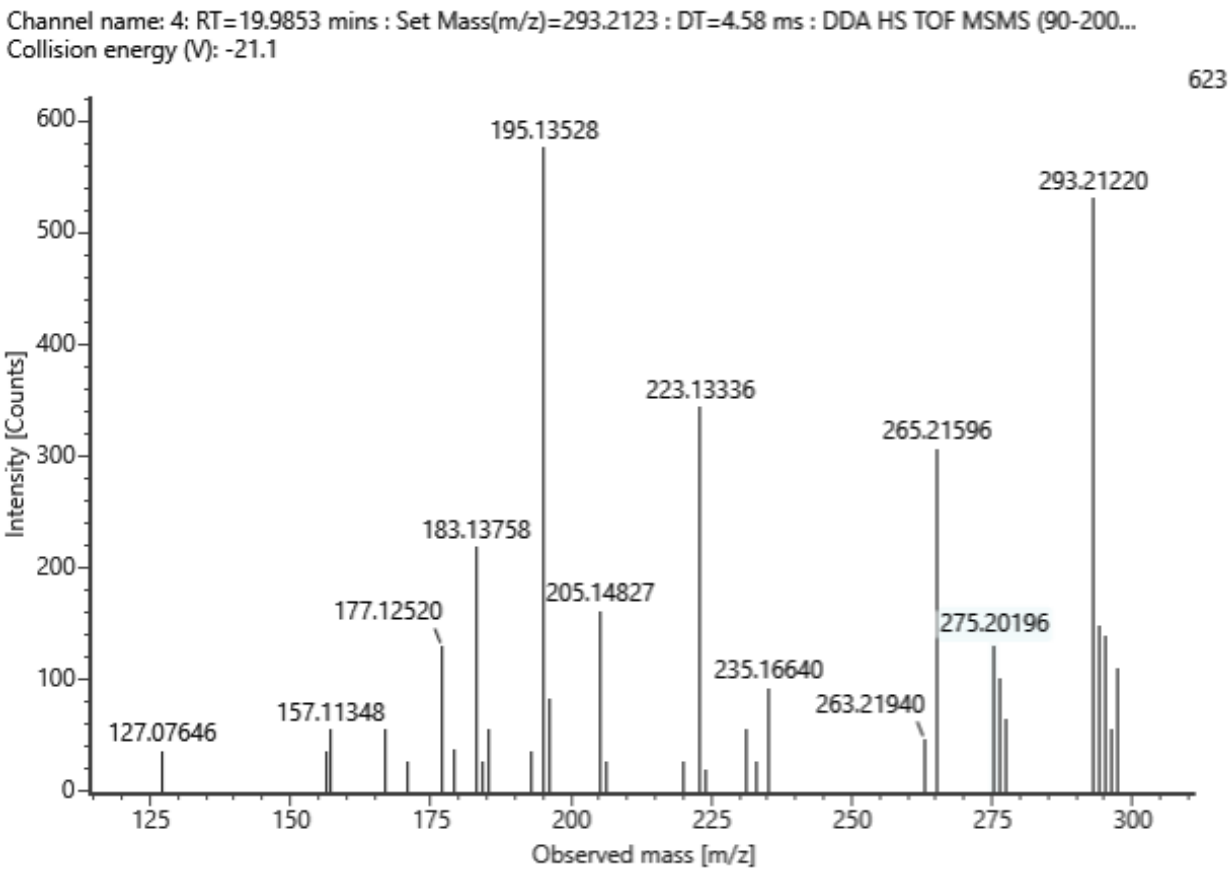

No. 84 9-hydroxy-10E,12Z-octadecadienoic acid C18H32O3 (neutral) Rt = 20.14 min

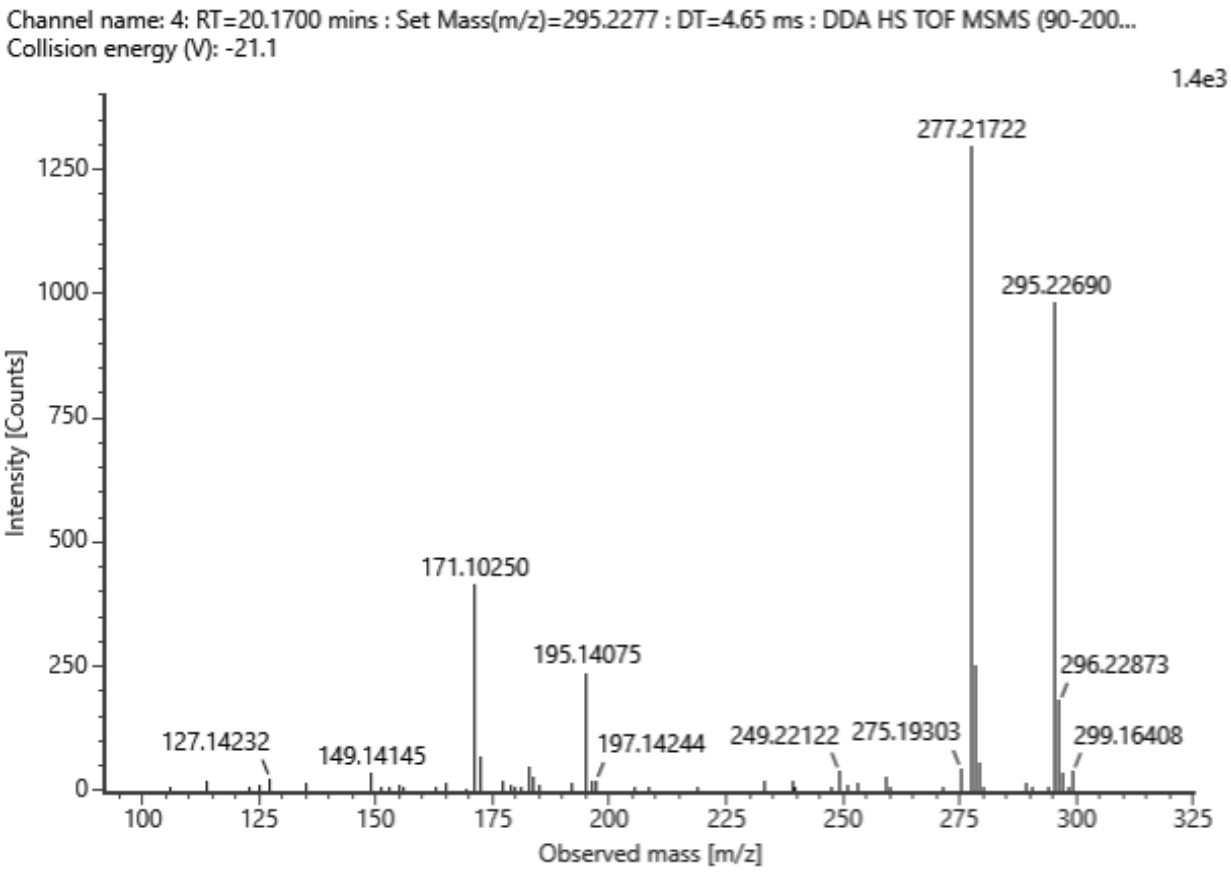

A7: Statistics

App. Table 3. List of 12 vinca alkaloids and metabolites that could be adequately separated and assigned with the UPLC-ESI-IMS-QTOF-MS setup for VIP and Games-Howell statistical analyses.

Compound	Code	Mean, cps	Std. deviation, cps	Games-Howell score
Loganic acid	1	31807	5253	ab
	2	37081	3430	b
	3	33690	3309	b
	4	37953	7364	b
	5	24231	4507	a
Strictosidine	1	1266	362	a
	2	1185	354	a
	3	1050	217	a
	4	1021	324	a
	5	922	416	a
Deacetylvindoline	1	251	52	a
	2	276	26	a
	3	183	25	a
	4	308	115	a
	5	230	42	a
Vindoline	1	44372	3916	ab
	2	46525	4070	ab
	3	38533	2223	a
	4	46933	5850	b
	5	43582	3667	ab
3’,4'-Anhydrovinblastine	1	9913	876	d
	2	1272	78	a
	3	2087	277	b
	4	1718	280	ab
	5	4397	731	c
Catharanthine	1	11651	1158	ab
	2	11569	610	b
	3	10083	293	a
	4	11120	591	ab
	5	10598	343	ab

Compound	Code	Mean, cps	Std. deviation, cps	Games-Howell score
Vincadifformine	1	1498	1011	a
	2	1062	456	a
	3	898	473	a
	4	1283	1223	a
	5	2182	836	a
Secologanin	1	57009	2008	b
	2	53310	3913	ab
	3	51261	3411	ab
	4	55362	5035	ab
	5	49599	3173	a
Vinblastine	1	5025	966	d
	2	299	34	a
	3	515	114	b
	4	416	49	b
	5	1908	599	c
Vincristine	1	641	72	d
	2	49	12	a
	3	86	14	b
	4	64	13	ab
	5	159	25	c
Vindolinine	1	20115	588	c
	2	17782	417	b
	3	17926	835	b
	4	18005	387	b
	5	15357	323	a
19-*S*-vindolinine	1	24898	566	bc
	2	23868	325	b
	3	24978	441	c
	4	24140	588	bc
	5	21714	484	a

App. Figure 4. Games-Howell statistics of the detected abundances of 12 vinca alkaloids. Error bars represent +/- 1 SD.

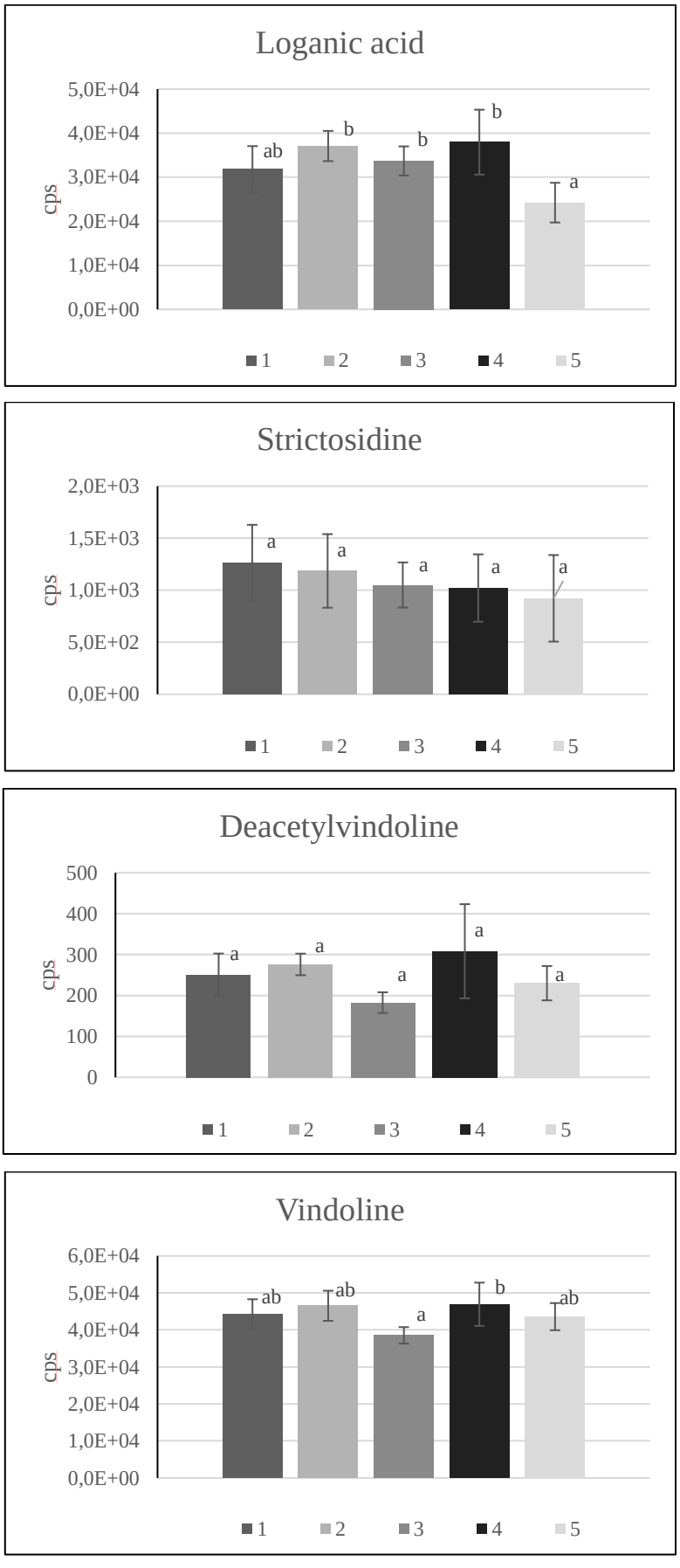

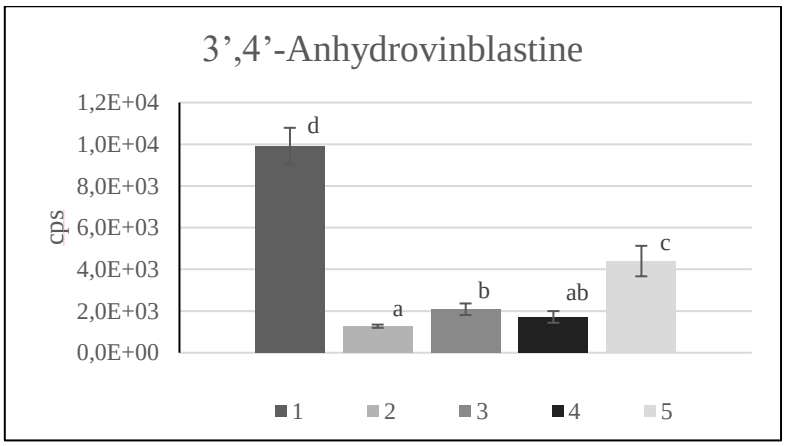
3’,4’-Anhydrovinblastine
1,2E+04
1,0E+04
8,0E+03
6,0E+03
4,0E+03
2,0E+03
0,0E+00
cps
d
a
b
ab
c
1
2
3
4
5

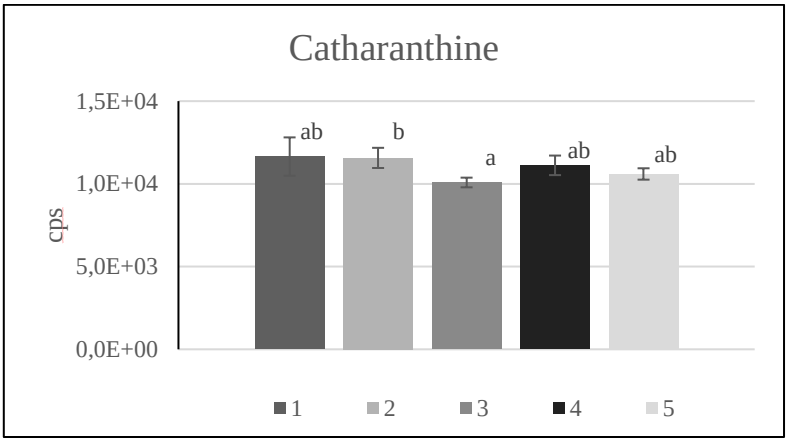
Catharanthine
1,5E+04
1,0E+04
5,0E+03
0,0E+00
cps
ab
b
a
ab
ab
1
2
3
4
5

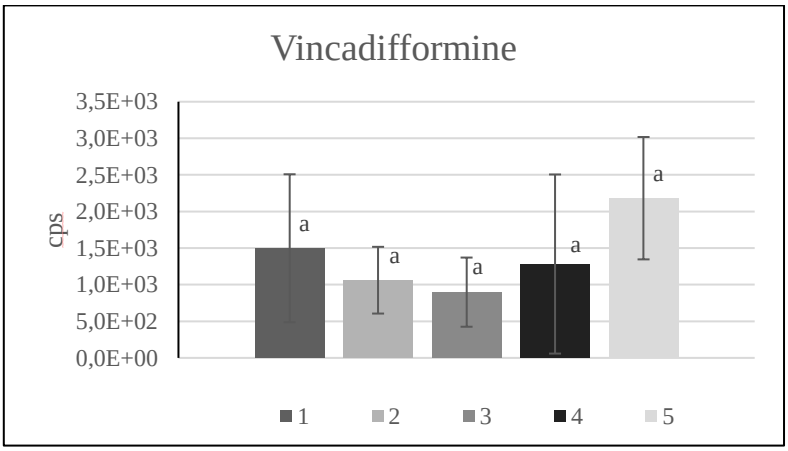
Vincadifformine
3,5E+03
3,0E+03
2,5E+03
2,0E+03
1,5E+03
1,0E+03
5,0E+02
0,0E+00
cps
a
a
a
a
a
1
2
3
4
5

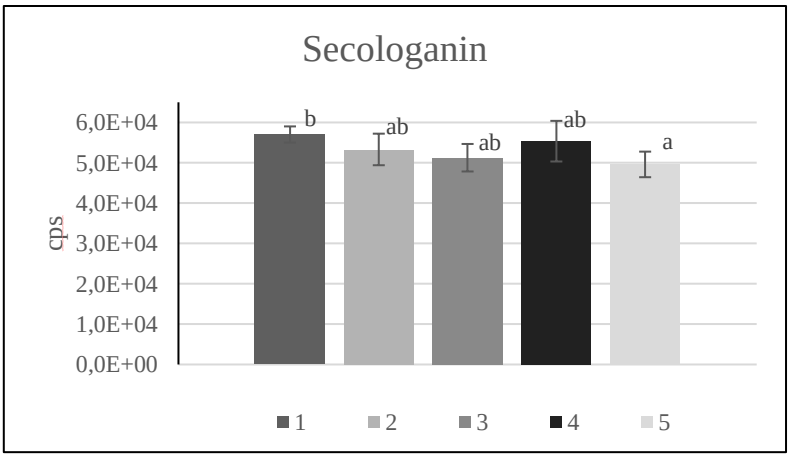
Secologanin
6,0E+04
5,0E+04
4,0E+04
3,0E+04
2,0E+04
1,0E+04
0,0E+00
cps
b
ab
ab
ab
a
1
2
3
4
5

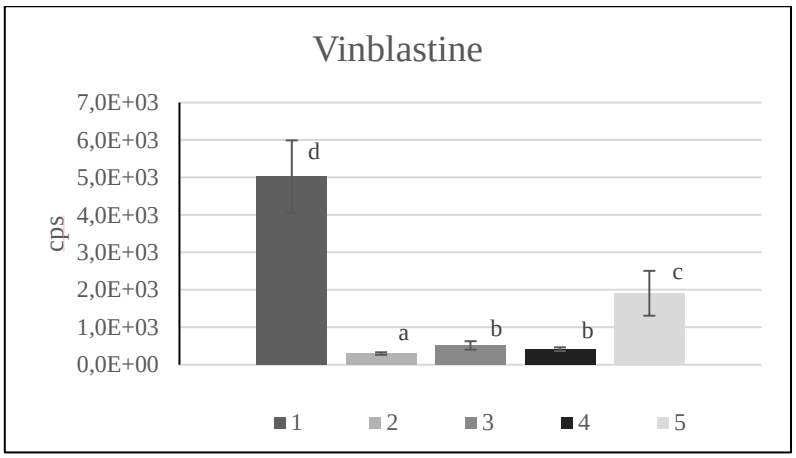
Vinblastine
7,0E+03
6,0E+03
5,0E+03
4,0E+03
3,0E+03
2,0E+03
1,0E+03
0,0E+00
cps
d
a
b
b
c
1
2
3
4
5

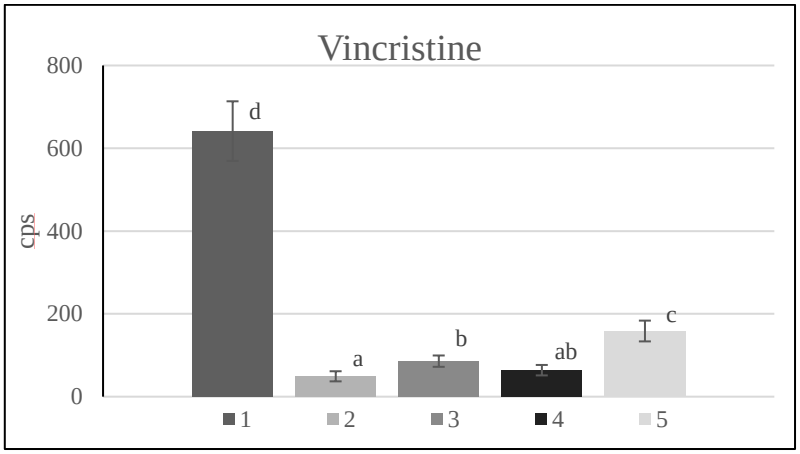
Vincristine
800
600
400
200
0
cps
d
a
b
ab
c
1
2
3
4
5

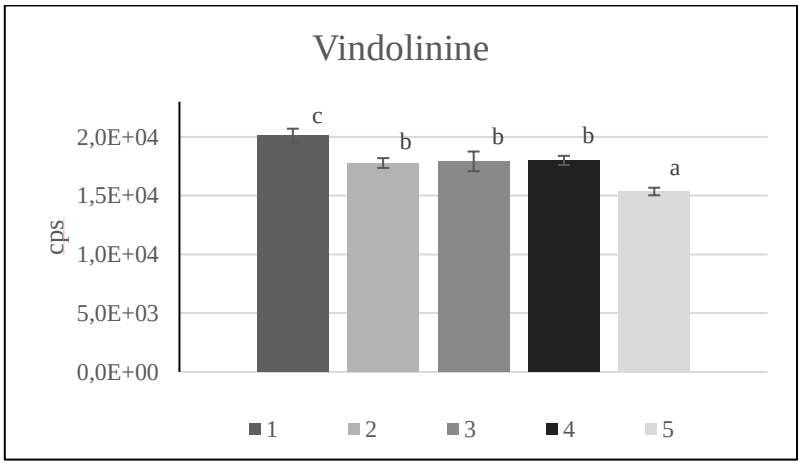
Vindolinine
2,0E+04
1,5E+04
1,0E+04
5,0E+03
0,0E+00
cps
c
b
b
b
a
1
2
3
4
5

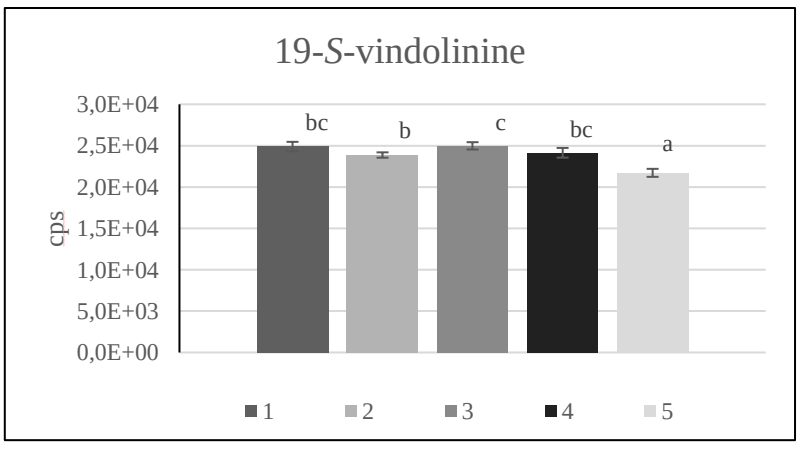
19-S-vindolinine
3,0E+04
2,5E+04
2,0E+04
1,5E+04
1,0E+04
5,0E+03
0,0E+00
cps
bc
b
c
bc
a
1
2
3
4
5

App. Table 4. Quantitative results for the 84 identified components during two months of maturation tracking in the sample batch. The sample group names indicate the date of the sampling (P.month.day.). A complete quantitative analysis was performed on the compounds of Section A. The concentrations of the compounds in section B were determined by semi-quantitative analysis (see details in the chapter Metabolomics and multivariate statistical analysis). For the compounds in section C, only normalized intensity values are shown. Mean values ± 1 SD are given (n=3). Maturation profile codes are characterized as follows: D, decreasing; R, rising; S, stable; P, peaking; V, valleying.

Section A			Concentration [mg·L^{-1}]							
No.	**Compound**	**Maturation profile**	**P.05.05.**	**P.05.12.**	**P.05.26.**	**P.06.02.**	**P.06.09.**	**P.06.16.**	**P.06.27.**	**P.07.07.**
9	Neochlorogenic acid	D	14.38±1.80	15.51±0.76	18.32±1.27	19.50±1.23	18.61±2.13	14.92±0.51	12.38±0.49	9.17±0.39
11	Esculin	D	0.47±0.00	0.14±0.01	0.07±0.02	0.07±0.00	0.08±0.01	0.07±0.01	0.08±0.00	0.11±0.02
14	Esculetin	P	6.38±0.52	8.15±0.61	10.09±0.49	14.24±0.32	14.46±1.04	10.12±1.61	9.40±0.10	7.97±0.36
15	Caffeic acid	D	65.21±4.69	73.97±1.78	90.23±3.09	84.27±1.23	70.77±2.61	34.51±5.96	19.87±0.30	8.40±0.24
17	Chryptochlorogenic acid	R	1.79±0.14	2.38±0.06	4.16±0.36	5.34±0.24	5.32±0.54	4.67±0.26	4.43±0.05	3.62±0.13
18	Daphnetin	D	1.02±0.02	1.10±0.04	1.36±0.12	0.75±0.04	0.47±0.05	0.22±0.01	<LOQ	<LOQ
21	Fraxin		<LOQ	<LOQ	<LOQ	<LOQ	<LOQ	<LOQ	<LOQ	<LOQ
31	Umbelliferone	S	1.46±0.06	1.53±0.08	1.60±0.08	1.55±0.06	1.58±0.01	1.42±0.29	1.55±0.06	1.54±0.04
34	Ferulic acid	S	3.58±0.17	3.74±0.17	4.47±0.38	5.57±0.71	5.59±0.10	4.17±0.70	3.47±0.10	<LOQ
35	Quercetin 3,4'-diglucoside		<LOQ	<LOQ	<LOQ	<LOQ	<LOQ	<LOQ	<LOQ	<LOQ
46	Robinin		<LOQ	<LOQ	<LOQ	<LOQ	<LOQ	<LOQ	<LOQ	<LOQ
48	Rutin	D	4.89±0.65	4.09±0.17	3.52±0.28	3.27±0.19	2.98±0.34	2.56±0.10	2.13±0.14	1.64±0.12
51	Luteolin 7-O-glucoside	D	15.66±1.43	4.59±0.20	1.87±0.06	1.64±0.06	1.58±0.22	1.50±0.11	1.93±0.11	2.24±0.17
56	Kaempferol 3-O-rutinoside	D	3.17±0.05	3.08±0.19	2.88±0.10	2.77±0.06	2.79±0.12	2.63±0.08	2.46±0.01	2.24±0.07
58	Quercitrin	S	0.66±0.01	0.58±0.04	0.59±0.02	0.64±0.01	0.69±0.01	0.68±0.05	0.80±0.03	0.90±0.02
60	Isorhamnetin 3-rutinoside	D	2.06±0.06	1.69±0.03	1.45±0.03	1.30±0.06	1.31±0.06	1.31±0.07	1.29±0.03	1.18±0.04
63	Rosmarinic acid		<LOQ	<LOQ	<LOQ	<LOQ	<LOQ	<LOQ	<LOQ	<LOQ
65	Hesperidin		<LOQ	<LOQ	<LOQ	<LOQ	<LOQ	<LOQ	<LOQ	<LOQ
68	Phlorizin	D	0.28±0.01	0.23±0.03	0.21±0.04	0.16±0.03	0.26±0.02	0.28±0.01	0.14±0.00	<LOQ
70	Daidzein		<LOQ	<LOQ	<LOQ	<LOQ	<LOQ	<LOQ	<LOQ	<LOQ
71	Eriodictyol	D	0.38±0.05	0.34±0.01	0.24±0.04	0.32±0.02	0.26±0.01	<LOQ	<LOQ	<LOQ
72	Sebacic acid		<LOQ	<LOQ	<LOQ	<LOQ	<LOQ	<LOQ	<LOQ	<LOQ
73	Luteolin	R	16.27±0.37	20.77±3.06	25.76±2.86	23.71±2.22	30.07±4.73	27.86±2.59	24.02±3.46	21.97±0.49
74	Ethyl caffeate	P	6.52±0.02	8.11±0.45	11.71±0.12	11.09±0.43	9.68±0.26	4.09±0.84	2.79±0.12	1.82±0.09
75	Naringenin	S	1.08±0.08	1.07±0.05	0.99±0.05	0.85±0.07	0.87±0.04	0.76±0.15	0.79±0.08	0.64±0.05
76	Apigenin	R	0.37±0.02	0.47±0.09	0.61±0.08	0.50±0.09	0.62±0.08	0.75±0.07	0.84±0.05	0.92±0.08
81	Chrysin	S	0.04±0.01	0.03±0.01	0.05±0.01	0.04±0.00	0.05±0.01	0.06±0.01	0.06±0.01	0.06±0.00
			Concentration [g·L^{-1}]							
8	Caftaric acid	D	3.45±0.38	4.11±0.18	4.82±0.27	5.25±0.46	4.97±0.65	3.27±0.12	2.37±0.26	0.86±0.10
13	Chlorogenic acid	D	0.57±0.08	0.55±0.03	0.54±0.03	0.49±0.03	0.44±0.04	0.35±0.01	0.28±0.01	0.18±0.01
42	Chicoric acid	D	4.51±0.42	4.52±0.12	4.39±0.15	4.22±0.20	3.84±0.31	3.05±0.06	2.34±0.07	1.28±0.04

Section B			Concentration [mg·L^{-1}]							
No.	**Compound**	**Maturation profile**	**P.05.05.**	**P.05.12.**	**P.05.26.**	**P.06.02.**	**P.06.09.**	**P.06.16.**	**P.06.27.**	**P.07.07.**
1	Caffeic acid glucoside_1		<LOQ	<LOQ	<LOQ	<LOQ	<LOQ	<LOQ	<LOQ	<LOQ
2	Caffeic acid derivative_1		<LOQ	<LOQ	<LOQ	<LOQ	<LOQ	<LOQ	<LOQ	<LOQ
3	Caffeic acid glucoside_2		<LOQ	<LOQ	<LOQ	<LOQ	<LOQ	<LOQ	<LOQ	<LOQ
5	Caffeic acid sulfate_1		<LOQ	<LOQ	<LOQ	<LOQ	<LOQ	<LOQ	<LOQ	<LOQ
7	Esculetin sulfate	R	0.15±0.00	0.19±0.02	0.24±0.02	0.25±0.03	0.27±0.01	0.25±0.06	0.28±0.01	0.30±0.01
10	Caffeic acid sulfate_2		<LOQ	<LOQ	<LOQ	0.97±0.03	1.12±0.11	1.10±0.19	1.13±0.10	0.98±0.10
16	1-caffeyllaminaribiose	V	19.16±2.86	14.47±2.82	11.90±0.35	9.49±0.40	11.97±0.23	9.47±1.21	12.69±0.38	<LOQ
23	Caffeoylglycerol	S	<LOQ	0.79±0.07	0.70±0.03	0.93±0.06	0.83±0.05	0.87±0.15	0.85±0.13	0.79±0.12
24	Quercetin dihexoside_1		0.27±0.03	0.12±0.03	0.05±0.00	0.05±0.00	<LOQ	<LOQ	<LOQ	<LOQ
26	Quercetin derivative_1 (pentose+hexose moiety)	D	0.67±0.03	0.26±0.03	0.12±0.02	0.06±0.01	0.06±0.01	<LOQ	<LOQ	<LOQ
27	Chicoric acid derivative	D	97.52±1.39	55.66±6.84	22.03±1.18	14.34±3.37	8.92±1.61	6.01±1.45	6.27±0.61	3.65±0.35
28	Quercetin dihexoside_2	D	0.17±0.00	0.09±0.02	<LOQ	<LOQ	<LOQ	<LOQ	<LOQ	<LOQ
32	Quercetin dihexoside_3	D	0.23±0.00	0.27±0.01	0.20±0.03	0.17±0.01	0.15±0.01	0.15±0.02	0.08±0.01	<LOQ
33	Quercetin derivative_2 (pentose+hexose moiety)	D	0.27±0.02	<LOQ	<LOQ	<LOQ	<LOQ	<LOQ	<LOQ	<LOQ
36	Schaftoside isomer_1	S	1.16±0.00	1.04±0.05	1.13±0.05	1.09±0.03	1.11±0.02	1.20±0.01	1.19±0.02	1.15±0.03
37	Quercetin hexosyl derivative	S	1.04±0.04	0.98±0.08	0.97±0.04	0.93±0.03	0.96±0.03	1.01±0.03	0.98±0.03	0.95±0.03
38	Luteolin/kaempferol dihexoside_1	D	1.45±0.01	1.16±0.06	0.96±0.03	0.90±0.04	0.89±0.01	0.81±0.01	0.77±0.03	0.66±0.01
39	Quercetin derivative_3 (pentose+hexose moiety)		<LOQ	<LOQ	<LOQ	<LOQ	<LOQ	<LOQ	<LOQ	<LOQ
41	Quercetin rutinoside	D	0.11±0.00	0.10±0.00	0.10±0.01	0.06±0.00	<LOQ	<LOQ	<LOQ	<LOQ
43	Schaftoside isomer_2	S	0.76±0.01	0.63±0.05	0.71±0.01	0.74±0.01	0.79±0.07	0.78±0.02	0.80±0.02	0.81±0.02
44	Luteolin/kaempferol dihexoside_2	D	65.39±1.43	31.71±1.92	10.67±0.03	7.74±0.20	7.09±0.27	6.33±0.05	6.77±0.20	6.85±0.16
45	Luteolin/kaempferol dihexoside_3		<LOQ	<LOQ	0.02±0.00	<LOQ	0.10±0.00	<LOQ	0.10±0.01	<LOQ
47	Quercetin pentoside_1	P	0.78±0.04	1.16±0.14	1.49±0.07	1.25±0.08	1.13±0.05	0.68±0.07	0.34±0.06	0.14±0.01
49	Quercetin glucoside	D	13.64±0.47	10.97±0.56	8.39±0.26	8.02±0.24	8.21±0.21	6.81±0.42	6.56±0.18	5.74±0.14
50	Isorhamnetin disaccharide 1	R	43.96±1.10	53.41±2.23	58.68±0.68	60.83±1.49	62.88±1.35	60.28±0.35	58.94±1.72	55.16±0.35
52	Luteolin/kaempferol rutinoside	P	90.71±1.01	99.17±4.55	98.31±2.16	97.53±2.42	89.52±15.10	85.11±15.72	84.75±3.36	79.67±0.80
53	Isorhamnetin disaccharide 2	R	14.22±0.08	17.50±1.19	19.18±0.16	19.71±0.11	20.36±0.69	17.69±3.17	18.60±0.42	17.75±0.21
54	Quercetin pentoside_2	P	0.22±0.00	0.29±0.04	0.40±0.03	0.34±0.03	0.27±0.06	0.18±0.01	0.12±0.02	0.05±0.00
55	Quercetin derivative_4	D	10.13±0.32	10.13±0.87	8.64±0.24	7.85±0.38	7.44±0.41	5.91±0.27	4.59±0.25	3.00±0.08
57	Apigenin derivative	R	6.47±0.09	8.16±0.69	8.42±0.33	8.78±0.72	9.29±0.61	8.82±0.35	8.76±0.15	8.04±0.20
59	Dicaffeoylquinic acid_1	D	213.6±1.9	217.3±5.4	199.8±3.9	191.4±3.6	183.9±3.7	141.9±21.9	122.5±5.8	81.97±4.11
61	Isorhamnetin 3-glucoside	R	18.46±0.28	17.62±1.15	19.21±0.38	20.32±0.92	20.21±3.42	22.32±0.87	23.95±0.43	26.33±0.55
62	Caffeic acid derivative_2		<LOQ	<LOQ	<LOQ	<LOQ	<LOQ	<LOQ	<LOQ	<LOQ

No.	Compound	Maturation profile	P.05.05.	P.05.12.	P.05.26.	P.06.02.	P.06.09.	P.06.16.	P.06.27.	P.07.07.
64	Chrysoeriol rutinoside		<LOQ	<LOQ	<LOQ	<LOQ	<LOQ	<LOQ	<LOQ	<LOQ
66	Dicaffeoylquinic acid_2	R	22.57±0.35	36.75±0.74	56.18±0.98	64.70±1.69	69.87±3.24	56.26±8.35	57.39±3.75	48.77±1.18
67	Luteolin/kaempferol glycoside	D	<LOQ	0.56±0.19	0.33±0.05	0.24±0.01	0.25±0.01	0.32±0.03	0.31±0.01	0.33±0.00
77	Chrysoeriol	S	12.96±0.52	15.34±1.31	17.50±0.99	15.91±0.89	19.72±0.46	24.54±1.25	25.49±4.40	32.50±2.45
			Concentration [g·L^{-1}]							
12	Caffeoylsucrose	D	2.16±0.01	2.17±0.03	2.18±0.01	2.15±0.02	2.15±0.06	2.12±0.04	2.07±0.04	2.09±0.04

Section C			Normalized detector counts [cps]							
No.	**Compound**	**Maturation profile**	**P.05.05.**	**P.05.12.**	**P.05.26.**	**P.06.02.**	**P.06.09.**	**P.06.16.**	**P.06.27.**	**P.07.07.**
4	Protocatechuoylglucose_1	D	653±3	547±14	382±3	319±10	299±9	274±2	262±6	232±2
6	Protocatechuoylglucose_2	D	1050±5	977±47	846±30	785±16	778±15	775±13	738±5	708±3
19	12-Hydroxyjasmonate sulfate_1	R	517±11	595±38	620±24	622±52	640±14	596±62	601±18	544±13
20	Taraxinositol A/B	D	2237±40	1914±50	1361±25	1042±81	967±18	736±109	637±7	458±8
22	12-Hydroxyjasmonate sulfate_2	R	3960±65	4295±257	4479±69	4609±244	4723±126	4592±408	4545±92	4375±81
25	Pyroglutamylisoleucine	R	48±0	95±5	166±9	223±13	261±4	264±14	293±3	321±1
29	Unknown1	R	20±1	18±1	20±3	21±1	22±1	24±1	30±2	36±1
30	Unknown2	R	471±0	549±27	632±37	693±20	690±106	754±9	781±7	805±9
40	Taraxinositol B/A	S	1183±13	1267±48	1294±7	1290±67	1316±5	1198±160	1179±4	1065±10
69	Abscisic acid glucose ester	S	348±7	343±17	329±9	321±18	320±8	295±35	321±17	306±9
78	Unknown3	D	1034±8	932±111	904±188	648±14	633±41	656±93	686±92	697±92
79	9,12,13-trihydroxy-10E,15Z-octadecadienoic acid	R	4791±28	6042±88	6528±155	6345±263	6650±389	6407±1033	6633±231	6523±120
80	9,12,13-trihydroxy-10E-octadecenoic acid	R	6774±159	7935±286	8272±92	8494±250	9216±280	8483±1196	8971±455	8787±256
82	9,10-dihydroxy-12Z-octadecenoic acid	S	154±21	102±13	109±18	120±3	134±16	111±21	129±14	117±5
83	Hydroxyoctadecatrienoic acid derivative	D	198±23	79±9	115±12	127±10	160±20	120±23	135±15	137±6
84	9-hydroxy-10E,12Z-octadecadienoic acid	D	106±22	30±2	38±1	35±2	39±5	27±6	26±1	26±1

<LOQ – Detector count lower than the detector count corresponding to the LOQ concentration specified for the authentic standard

A8: Authentic standards

App. Table 5. Details about the authentic standards used: CAS number; purity data; vendor; the solvent and the concentration of the stock solution.

Table 5/A: List of the authentic standards for the identified compounds in the samples

Compound name	CAS number	Purity	Vendor	Solvent	Concentration of the stock solution [mg·L^{-1}]
Apigenin	520-36-5	≥98.0%	Shanghai Shifeng Biotechnology Co.	DMSO	1000
Caffeic acid	331-39-5	98.0%	Shanghai Shifeng Biotechnology Co.	EtOH	1000
Caftaric acid	67879-58-7	99.0%	Shanghai Shifeng Biotechnology Co.	EtOH	1000
Chicoric acid	6537-80-0	98.0%	Shanghai Shifeng Biotechnology Co.	EtOH	1000
Chlorogenic acid	327-97-9	98.0%	Shanghai Shifeng Biotechnology Co.	EtOH	1000
Chrysin	480-40-0	99.0%	Merck-Sigma group	MeOH	1000
Cryptochlorogenic acid	905-99-7	≥98.0%	Shanghai Shifeng Biotechnology Co.	EtOH	1000
Daidzein	486-66-8	98.3%	Merck-Sigma group	EtOH	2000
Daphnetin	486-35-1	97.1%	Merck-Sigma group	EtOH (95 V/V%)	1000
Ethyl caffeate	102-37-4	≥99.0%	Merck-Sigma group	DMSO	3000
Eriodictyol	4049-38-1	≥99.0%	Merck-Sigma group	DMSO	2000
Esculetin	305-01-1	98.0%	Shanghai Shifeng Biotechnology Co.	EtOH	1000
Esculin	531-75-9	98.0%	Shanghai Shifeng Biotechnology Co.	EtOH	1000
Ferulic acid	1135-24-6	99.0%	Shanghai Shifeng Biotechnology Co.	EtOH	1000
Fraxin	524-30-1	98.9%	Merck-Sigma group	DMSO	2000
Hesperidin	520-26-3	≥99.0%	Merck-Sigma group	MeOH	2000
Isorhamnetin 3-rutinoside	604-80-8	99.6%	Merck-Sigma group	MeOH	1000
Kaempferol 3-O-rutinoside	17650-84-9	99.0%	Merck-Sigma group	MeOH	1000

Compound name	CAS number	Purity	Vendor	Solvent	Concentration of the stock solution [mg·L^{-1}]
Luteolin	491-70-3	≥98.0%	Shanghai Shifeng Biotechnology Co.	EtOH	1000
Luteolin 7-O-glucoside	5373-11-5	≥99.0%	Merck-Sigma group	DMSO	2000
Naringenin	480-41-1	98.0%	Merck-Sigma group	MeOH	1000
Neochlorogenic acid	906-33-2	98.0%	Shanghai Shifeng Biotechnology Co.	EtOH	1000
Phlorizin	60-81-1	≥99.0%	Merck-Sigma group	MeOH	1000
Quercetin 3,4´-diglucoside	29125-80-2	≥99.0%	Merck-Sigma group	DMSO	500
Quercitrin	522-12-3	≥99.0%	Merck-Sigma group	MeOH	1000
Robinin	301-19-9	95.1%	Merck-Sigma group	DMSO	2144
Rosmarinic acid	20283-92-5	97.0%	Shanghai Shifeng Biotechnology Co.	EtOH	1000
Rutin	153-18-4	97.2%	Merck-Sigma group	EtOH (95 V/V%)	1000
Sebacic acid	111-20-6	≥99.0%	Merck-Sigma group	MeOH	1000
Umbelliferone	93-35-6	≥99.0%	Merck-Sigma group	DMF	1000

Table 5/B: List of the authentic standards (used in the LC-MS method) for compounds not present in the samples

Compound name	CAS number	Purity	Vendor	Solvent	Concentration of the stock solution [mg·L^{-1}]
(+)-Abscisic acid	21293-29-8	98.9%	Merck-Sigma group	MeOH	1000
(+)-Catechin	154-23-4	≥99.0%	Merck-Sigma group	EtOH	1000
(-)-Epigallocatechin	970-74-1	99.5%	Merck-Sigma group	DMSO	200
(-)-Gallocatechin	3371-27-5	≥99.0%	Merck-Sigma group	DMSO	2000
(-)-Gallocatechin gallate	4233-96-9	99.6%	Merck-Sigma group	DMSO	1000
(-,-)Epicatechin	490-46-0	≥99.0%	Merck-Sigma group	DMSO	2000
2,4-Diacetyl-phloroglucinol	2161-86-6	≥99.0%	Santa Cruz Biotechnology, Inc.	EtOH	1955

Compound name	CAS number	Purity	Vendor	Solvent	Concentration of the stock solution [mg·L^{-1}]
4-Methylumbelliferone	90-33-5	≥99.0%	Merck-Sigma group	MeOH	1000
Apiin	26544-34-3	≥99.0%	Merck-Sigma group	DMF	2000
Astringin	29884-49-9	≥99.0%	Merck-Sigma group	DMSO	2000
Avenantramide A	108605-70-5	99.5%	Merck-Sigma group	EtOH (95 V/V%)	2587
Avenantramide B	108605-69-2	99.5%	Merck-Sigma group	EtOH (95 V/V%)	2487.5
Catechin gallate	130405-40-2	≥99.0%	Merck-Sigma group	MeOH	200
Daphnetin	486-35-1	97.1%	Merck-Sigma group	EtOH (95 V/V%)	1000
Epicatechin gallate	1257-08-5	97.3%	Merck-Sigma group	DMSO	2000
Epigallocatechin gallate	989-51-5	99.7%	Merck-Sigma group	DMSO	1000
Ethyl gallate	831-61-8	≥99.0%	Merck-Sigma group	MeOH	1000
Genistein	446-72-0	99.0%	Merck-Sigma group	DMSO	2000
Glucotropeolin (potassium salt)	5115-71-9	≥99.2%	Merck-Sigma group	MQ water	2000
Hesperetin	520-33-2	99.0%	Merck-Sigma group	EtOH	1000
Loganic acid	22255-40-9	98.9%	Extrasynthese	EtOH	2500
Methyl gallate	99-24-1	96.8%	Merck-Sigma group	EtOH (95 V/V%)	1000
Myricitrin	17912-87-7	≥99.0%	Merck-Sigma group	DMSO	2000
Phloretin	60-82-2	≥99.0%	Merck-Sigma group	DMSO	2000
Polydatin	65914-17-2	≥99.0%	Merck-Sigma group	EtOH	2000
Procyanidin A2	41743-41-3	≥99.0%	Merck-Sigma group	DMSO	2000
Procyanidin B1	20315-25-7	92.1%	Merck-Sigma group	EtOH	200
Procyanidin B2	29106-49-8	99.4%	Merck-Sigma group	EtOH	200
Pyoluteorin	25683-07-2	≥99.0%	Santa Cruz Biotechnology, Inc.	EtOH	500
Sakuranetin	520-29-6	≥99.0%	Merck-Sigma group	DMSO	2000
trans-Resveratrol	501-36-0	≥99.0%	Merck-Sigma group	EtOH	1000
Vitexin 7-glucoside	35109-95-6	≥99.0%	Merck-Sigma group	MeOH	1000
ε-Viniferin	62218-08-0	≥99.0%	Merck-Sigma group	DMSO	2000

Abbreviations: DMSO – dimethyl sulfoxide, EtOH – ethanol, MeOH – methanol, DMF – dimethylformamide

ACKNOWLEDGEMENT

I would like to thank my supervisors, Dr. Zsuzsanna Jókai-Szatura and Dr. Tibor Janda, for their support during my PhD. I would like to express my gratitude to Dr. Mihály Dernovics, this research could not have been accomplished without his guidance and contribution. I would also like to thank Dr. Viktória Kovács, not just her valuable insights about my work, but her support and friendship as well.

I am grateful for Dr. Márta Ladányi for her assistance in performing the statistical analyses, and József Patkós for providing the dandelion flower and liqueur samples.

I am also thankful to the members (or in some cases, formal members) of the Department of Plant Physiology and Metabolomics (HUN-REN Agricultural Institute) and the Department of Food Chemistry and Analysis (MATE Institute of Food Science and Technology), who contributed to this work. I am grateful to my former students, especially Anna Matkovits and Viktória Bernadett Balázs, for helping me develop through their supervision.

A special thanks to my mother, who always supported me and my studies, and to my friends, especially Richárd Gábor Fandel, Imre Kovács and Dr. Zoltán Horváth.

This research was supported by:

- Bilateral international research project No. NKM2022-1/2023 of the Hungarian Academy of Sciences (MTA; Hungary) and the Egyptian Academy of Scientific Research and Technology (ASRT; Egypt)
- The National Research, Development and Innovation Office, Hungary (grant No. K131907)